The effect of pH on the structure and function of α-crystallin and
Cyclodextrins as artificial molecular chaperones

Chris Hamilton Brockwell

School of Chemistry and Physics
University of Adelaide

May, 2009

Table of Contents

CHAPTER 1

INTRODUCTION AND LITERATURE REVIEW

CHAPTER 2

MATERIALS AND METHODS

CHAPTER 3

INVESTIGATING THE pH SENSITIVE CHAPERONE ABILITY OF α-CRYSTALLIN

CHAPTER 4

CHARACTERISING THE EFFECT OF pH ON THE STRUCTURE OF α-CRYSTALLIN

CHAPTER 5

CHARACTERISING THE EFFECT OF pH ON THE THERMAL STABILITY OF α-CRYSTALLIN

CHAPTER 6

THE ROLE OF HISTIDINE RESiDIUES IN THE CHAPERONE ACTIVITY OF αB-CRYSTALLIN

CHAPTER 9

CONCLUSIONS

APPENDIX A

APPENDIX B

APPENDIX C

APPENDIX D

Abstract

As the major protein of the lens, α-crystallin is a molecular chaperone that stabilises lens proteins to prevent their precipitation into solution. In this role it is vital in maintaining lens transparency. The chaperone ability of α-crystallin and its individual subunits, αA- and αB-crystallin, has been shown to be sensitive to a variety of environmental and intrinsic factors, including temperature, denaturation and post-translational modification. The effect of pH on α-crystallin chaperone ability, however, has not been thoroughly investigated. There is limited evidence to suggest that the chaperone ability of α-crystallin is pH-sensitive such that α-crystallin is a significantly worse chaperone at pH 6.0 than at pH 8.0. This is of physiological significance since in the lens there is a measurable pH gradient of pH 7.2 in outer lens cells, compared to pH 6.7 in the lens nucleus. A loss of α-crystallin chaperone function in the lens nucleus, as a consequence of decreased pH, may compromise lens transparency. Similarly, extra-lenticular fibrillar aggregation of some disease-related target proteins (Aβ-peptide, for example) is promoted by acidic pH.

This study investigates the effect of pH on the chaperone ability of α-crystallin and its subunits. Further, this study characterises the structural changes to α-crystallin accompanying pH variation in an attempt to explain the structural basis for the observed pH sensitivity. In addition, this study examines the chaperone function of cyclodextrins, a class of chemical chaperones that may act in conjunction with α-crystallin as part of a two-step protein refolding pathway.

Abstract

This study demonstrated that the chaperone activity of α-crystallin is pH sensitive between pH 6.0 and 8.0; the ability of α-crystallin to protect against temperature- and reduction-stress induced amorphous aggregation is significantly reduced at pH 6.0 and 6.5 compared to pH 7.0 and above. The decreased chaperone ability of α-crystallin at pH 6.0 and 6.5 was accompanied by partial unfolding of the protein, and a loss of secondary structure, while α-crystallin quaternary structure remained unchanged. Interestingly, α-crystallin was found to have significant chaperone ability below pH 4.0, conditions under which α-crystallin is largely unfolded. The unfolding of α-crystallin at pH 6.0 and 6.5 is comparatively minor, and it is difficult to say whether this unfolding is directly responsible for the observed pH sensitivity of α-crystallin chaperone ability. The thermal stability of α-crystallin was compromised at pH 6.0 and 6.5, which may partially explain its decreased chaperone ability at these pH values in heat-stress assays conducted at temperatures above 50°C. However, α-crystallin chaperone activity remained pH-sensitive at 37°C and 45°C, at which temperatures it is thermally stable.

Blocking exposed αB-crystallin histidine residues by chemical modification removed, to a large extent, the pH-sensitivity of its chaperone activity. This suggests that the protonation of an exposed histidine residue(s) at pH 6.0 and 6.5 is responsible for the observed pH sensitivity of α-crystallin chaperone ability. Inhibiting the protonation of a specific histidine residue, H83, by site-directed mutagenesis (H83A) did not remove the pH sensitivity of αB-crystallin chaperone activity, and suggests that protonation of this residue alone does not explain the decreased chaperone ability of α-crystallin at mildly acidic pH. This residue lies within the putative chaperone-binding region of αB-crystallin, and is highly

Abstract

conserved between species and between the human small heat shock proteins. It appears that the protonation of several histidine residues, or residues other than H83, is primarily responsible for the influence of pH on α-crystallin chaperone ability observed in this study. The observed decrease in α-crystallin chaperone function below pH 7.0 partially explains the preferential formation of age-related cataract in the lens nucleus, as the chaperone ability of α-crystallin would be compromised under the mildly acidic conditions characteristic of the nucleus. Additionally, the pH sensitivity of α-crystallin chaperone ability may be significant in the ability of extra-lenticular αB-crystallin to inhibit amyloid-related disease at sites of localised acidosis.

Cyclodextrins are a family of cyclic oligosaccharides that have been shown to function as chemical chaperones under specific protein aggregation conditions. Cyclodextrins have been demonstrated to facilitate the refolding of chemically-stressed target proteins that have already bound to synthetic nanogels, which act in a manner reminiscent of small heat shock proteins. In this study, cyclodextrins were unable to act in conjunction with α-crystallin to facilitate the refolding of thermally-stressed target proteins. β-Cyclodextrin (βCD) demonstrated little or no ability to inhibit the amorphous aggregation of target proteins, but was able to significantly inhibit the fibrillar aggregation of a number of target proteins, including the disease-related A53T α-synuclein mutant. Characterisation of the binding of βCD to target proteins during fibrillar aggregation via circular dichroism, intrinsic and extrinsic fluorescence and competitive chaperone assays provided a model of the cyclodextrin chaperone mechanism. In this model, cyclodextrins interact with already partially unfolded, pre-fibrillar protein intermediates via the insertion of aromatic residues into the cyclodextrin anulus, and by doing so inhibit intra-fibrillar

π-bonding and protofilament assembly. This suggests the potential for cyclodextrins as therapeutic molecular chaperones *in vivo* that may be able to inhibit the pathogenic aggregation of target proteins.

Declaration

This work contains no material which has been accepted for the award of any other degree or diploma in any university or other tertiary institution and, to the best of my knowledge and belief, contains no material previously published or written by another person, except where due reference has been made in the text.

I give consent to this copy of my thesis, when deposited in the university library, being made available for loan or photocopying, subject to the provisions of the Copyright Act 1968

(Signed)_____

Acknowledgements

So many people helped me get to the end of this, its impossible to know where to start (and where to finish). First of all, to Prof. John Carver, for giving me this opportunity, for being the best (and probably only) Supervisor I could have asked for, but most importantly, for being one of the most genuinely likeable people I've ever met. I doubt if I'd have done any of under anyone else. Thankyou.

     To the Carver group, the best group of researchers I'm likely to ever be a part of. To Heath, for doing so much more than should ever have been expected, and for dealing with me straight up when that's what I actually needed, and for being a good guy and an even better scientist. To Tron, for dragging me through this when I was about to go crazy, and for keeping me sane in and out of the lab. I don't have to tell you what you did. Or how much I appreciate it. To Dave, because if you're going to move interstate with someone, you could do an awful lot worse. We've come a long way with this, and you know it all would have been a lot worse without you. Thanks man, for everything. And to everyone else – to Buckley, T.K., Y.Q., Danielle, Frankie, Sean (I'm glad you're doing cyclodextrins, thanks for reading) and anyone else past or present that have made the Carver group the place it is today. Much love.

     To my friends, here and otherwise. This is it, Fat Man. Rob, it's been a long four years, I'll be home soon. And Jarod, I'll call you tonight. Thankyou for keeping me grounded when I needed it badly, all of you.

     To Scottie, for being one of the best people I've ever met – that wasn't just rhetoric, I really mean it, sonny. To mum and dad, I can't even begin to describe what you've done. Not even vaguely. Thankyou so very, very much, from the very bottom of my heart. I love you both so, so much, and I can't tell you how much you've both meant to me, or what you've done for me. Thankyou. These words don't do anything justice. I can't say any more than that. You know.

     And to Burge. This is it. I could say a whole bunch of things, but nothing is going to explain what we've done, or what we've been through, or what you mean to me. That's between us. Just know that I could never, ever, have made it through this without you, and I thank you for it every day. You're my best friend. This one's for you.

List of figures

List of figures

List of abbreviations

αCD	α-cyclodextrin
ANS	1-anilo-8-napthalene sulfonate
AS	ammonium sulphate
βCD	β-cyclodextrin
BSA	bovine serum albumin
CD	circular dichroism
Cryo-EM	cryo-electron microscopy
DEPC	diethylpyrocarbonate
DTT	dithiothreitol
ε_{240}	molar extinction coefficient at 240nm
Far UV CD	far ultra-violet circular dichroism
FPLC	fast protein liquid chromotography
γCD	γ-cyclodextrin
GuHCl	guanadinium hydrochloride
IPTG	Isopropyl β-D-1-thiogalactopyranoside
kDa	kilodalton
LB	luria broth
λ_{max}	the wavelength at which maximum fluorescence is observed
L-trp	L-tryptophan
MW	molecular weight
NMWL	nominal molecular weight limit
pKa	acid dissociation constant
PEI	polyethyleneimine

List of abbreviations

PMSF	phenylmethylsulphonyl fluoride
rcm	reduced and carboxymethylated
ThT	thioflavin T
SDS-PAGE	sodium dodecyl sulfate polyacrylamide gel electrophoreisis
SEFPLC	size exclusion fast protein liquid chromotography
sHsp	small heat shock protein
TCEP	tris (2-carboxyethyl) phosphine hydrochloride
TEM	transmission electron microscopy
tMax	the time taken to achieve maximum ThT-associated fluorescence
Tris	tris(hydroxymethyl)aminomethane

CHAPTER 1

INTRODUCTION AND LITERATURE REVIEW

Chapter 1 - Introduction

1.1 Protein folding

Correct protein folding is an essential process that underpins the very function of cellular organisms. Unfolded, non-native proteins are generally non-functional until their correct structural conformation is achieved. Consequently, the process of a protein folding to its native state is typically rapid and robust (Kim and Baldwin, 1982). Protein folding occurs as a consequence of a conformational bias towards native protein structure, brought about by the increased thermodynamic stability of the folded protein state (Anfinsen, 1973; Rossman and Argos, 1981). This is dictated by the interactions of a variety of protein structural elements; secondary structure is stabilised by multivalent hydrogen bonding across the protein backbone, facilitating the formation of α-helix and β-sheet structures, while intramolecular forces between amino acid side chains dictate secondary, tertiary and quaternary protein structure (Rossman and Argos, 1981; Murphy and Kendrick, 2007). The necessary burial of hydrophobic side chains is believed to be a decisive factor in protein folding (Chothia, 1974; 1975; Rossman and Argos, 1981), but a variety of other factors, including salt-bridges between acidic and basic side chains, disulfide bonding and dipole-ion interactions between charged side chains further influence the final native structure of a protein (Murphy and Kendrick, 2007).

While this process of folding to a native is state is necessarily rapid and precise, the complexity of intra-protein interactions required for correct folding means that comparatively simple or minor alterations can sometimes result in wildly varying

protein conformations. The correct folding of large, globular proteins, while rapid, involves the formation of a number of intermediately folded states between the unfolded polypeptide chain and the attainment of a native, functional protein. These intermediately folded proteins generally exist in a brief, transient form, but expose portions of their hydrophobic core to solution (Ellis and Hartl, 1996; Carver *et al.*, 2003). Further, the correct folding of protein intermediates to native conformation is a reversible process, and so while the protein folding pathway is indeed rapid, there is ample opportunity for vulnerable, semi-folded protein intermediates to interact unfavourably. This can result in misfolded proteins that are either non-functional or which have a potentially modified function, which can lead to a variety of problems *in vivo*.

1.2 Protein misfolding and aggregation

Protein misfolding presents serious problems for the correct functioning of cellular systems. Significant in this regard is the large scale protein aggregation arising from misfolded protein intermediates. The exposure of the hydrophobic core of semi-folded protein intermediates renders them vulnerable to hydrophobic interactions with other semi-folded proteins; such interactions can facilitate the rapid inclusion of further protein intermediates, resulting in the accumulation of large protein aggregates (Ellis and Hartl, 1996; Carver *et al.*, 2002) (Figure 1.1). It is believed that this manner of aggregation, generally referred to as amorphous aggregation, is a nucleation dependent process (Kim *et al.* 2002; Ignatova and Gierasch, 2005). Large-scale aggregation does

not occur until a suitable nucleus of misfolded protein intermediates has developed, after which further protein intermediates are added rapidly to the aggregate nucleus. This is typified by a sigmoidal relationship between time and protein aggregation; an initial lag phase as a nucleus is slowly developed, followed by a rapid increase in aggregation around the protein nucleus and concluding with a plateau region as aggregation reaches a maximal level.

Over the past 20 years protein misfolding and aggregation has been implicated in at least forty distinct diseases, of which some of the major types are listed in Table 1.1 (Chiti and Dobson, 2006). It has been suggested that protein misfolding may be implicated in as many as half of all human diseases (Bradbury, 2003), and while this conjecture may be exaggerated, the toxic effects of misfolded aggregated proteins are obvious and pronounced. Pathogenic effects can occur from a variety of causes, the most common being a loss of protein function as a consequence of misfolding (as in cystic fibrosis (Powell and Zeitlin, 2002)), or a 'gain' of toxic protein function, as in Alzheimer's and other neurodegenerative diseases (Kelly, 1996; Cohen and Kelly, 2003).

While it was initially thought that protein aggregation results solely in an unstructured, amorphous mass, research over the last 10 years has identified a stable, highly structured form of protein aggregation known as amyloid fibrils (Dobson, 1999). Amyloid fibrils are implicated in a number of neurodegenerative diseases, including Alzheimer's, Creuzfeldt-Jakob, Parkinson's and Huntington's diseases (Chiti and Dobson, 2006), and as a consequence, fibrillar protein aggregation has become a major topic of investigation.

Folding/unfolding pathway (reversible and fast)

Inc. temp.

Native Protein (N)   Ordered M.G. (I₁)   Disordered M.G. (I₂)   Unfolded Protein (U)

Aggregation

Precipitation

Off-folding pathway
(irreversible and slow)
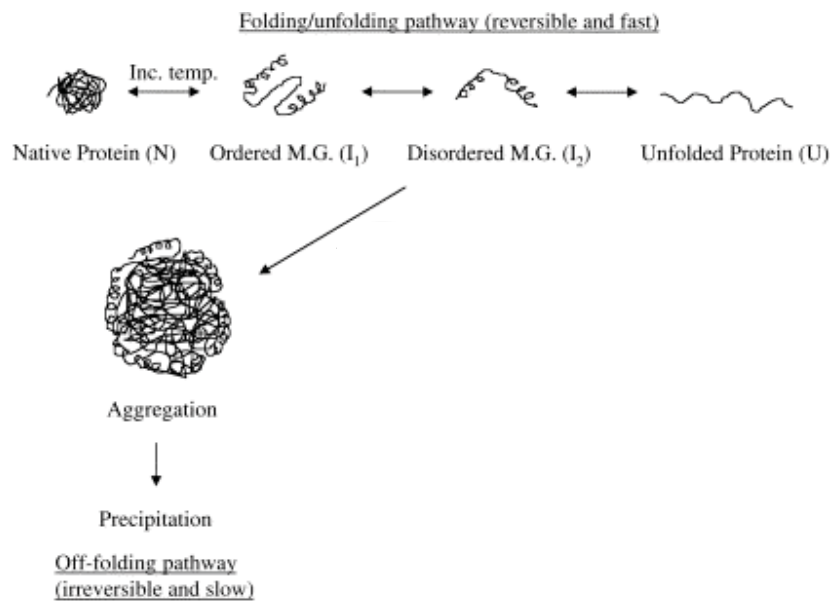
Figure 1.1 – Schematic diagram of the folding/unfolding and off-folding pathways. Newly expressed proteins adopt a number of partially-folded intermediate structures (here designated I_1 and I_2) before achieving native conformation. The folding of protein intermediates to a native conformation is reversible, particularly during cellular stress. If proteins remain intermediately folded for too long, the hydrophobic association of several intermediates can result in protein aggregation on the off-folding pathway. Aggregates can be unstructured, amorphous masses, composed of partially folded intermediate protein states; conversely, aggregates can be highly structured amyloid fibrils. Figure adapted from Carver *et al.* (2002).

Table 1.1 – A summary of the major protein-misfolding diseases *in vivo*. Table adapted from Chiti and Dobson (2006).

NOTE:
This figure is included on page 5
of the print copy of the thesis held in
the University of Adelaide Library.

1.3 Amyloid fibrils

Amyloid fibrils are highly ordered, β-sheet rich protein aggregates characterised by a common cross β-sheet core structure (Sunde and Blake, 1997; Serpell *et al.*, 2000). Amyloid fibrils are typically straight, unbranched strands of variable length, between 7 and 12nm in diameter (Sunde and Blake, 1997). These strands generally consist of a succession of tubular, β-sheet derived protofilaments arranged laterally to the fibril axis (Figure 1.2). The number of protofilaments that comprise the fibrillar superstructure varies between target proteins (Serpell *et al.*, 2000). Gross fibrillar morphology varies

significantly depending on the misfolded protein from which it is derived, with rope-like, tape-like, branched and, recently, looped fibrillar structures observed via TEM (Chiti and Dobson, 2006; Dobson, 2006). Fibril morphology appears to be directly influenced by both solvent type and the conditions under which aggregation is induced, and may also be influenced by target protein primary structure (Bauer *et al.*, 1995; Goldsbury *et al.*, 1997; Pedersen *et al.*, 2006; Porat *et al.*, 2006).

Cryo-EM and x-ray diffraction analysis have determined that fibrillar protofilaments consist of a number of closely interacting parallel β-sheets, the component β-strands of which are arranged perpendicular to the fibril axis (Blake and Serpell, 1996; Sunde and Blake, 1997). These β-strands are generally derived from small peptide regions, typically between 8 and 10 amino acids in length (Jiminez *et al.*, 2002). Accordingly, a highly ordered cross β-sheet structure is considered characteristic of amyloid fibrillar aggregates. In larger proteins and polypeptides it has been suggested that areas not contributing to the β-sheet form hydrophilic loops on the exterior of the proto-filament, and there is some evidence to suggest that these loops may influence both fibril solubility and interactions between multiple protofilaments within the gross fibril structure.

The highly ordered fibril structure is believed to be facilitated by hydrogen bonding across the protein backbone and so is generally independent of amino acid sequence (Fandrich and Dobson, 2002; Bucciantini *et al.*, 2002). The non-specific nature of these interactions and common structure of the polypeptide backbone result in morphologically similar fibrils being formed from a variety of different peptides, and suggest that fibrillar aggregation is a generic structure possible for all polypeptides

(Chiti *et al*., 1999; Dobson, 1999; Bucciantini *et al*., 2002). Despite this, recent data suggest that interactions between amino acid side chains on adjacent β-strands may be important for the formation and stability of amyloid fibrils. Analysis of Aβ-peptide derived mutants has demonstrated that side chain-side chain interactions are necessary for initiating fibrillar aggregation (Klimov and Thirumalai, 2003). π-Bonding between aromatic residues has been demonstrated to increase fibrillar aggregation propensity and stabilise cross β-sheet structure in amyloid-like structures (Makin *et al*., 2005; Gazit, 2002; Porat *et al*., 2004), and aromatic side chain interactions appear necessary for human islet amyloid polypeptide fibrillar aggregation (Zanuy *et al*., 2004). It has been suggested that aromatic residues are relatively abundant in amyloidogenic protein sequences (Gazit, 2002), and that the aromatic residues tryptophan and phenylalanine are the most amyloid-prone amino acids (Pawar *et al*., 2005). From this it has been inferred that while the ability to form fibrillar aggregates is a trait common to all proteins, the propensity to form, and stability of fibrillar aggregates is directly influenced by protein primary structure (Dobson, 1999; 2006).
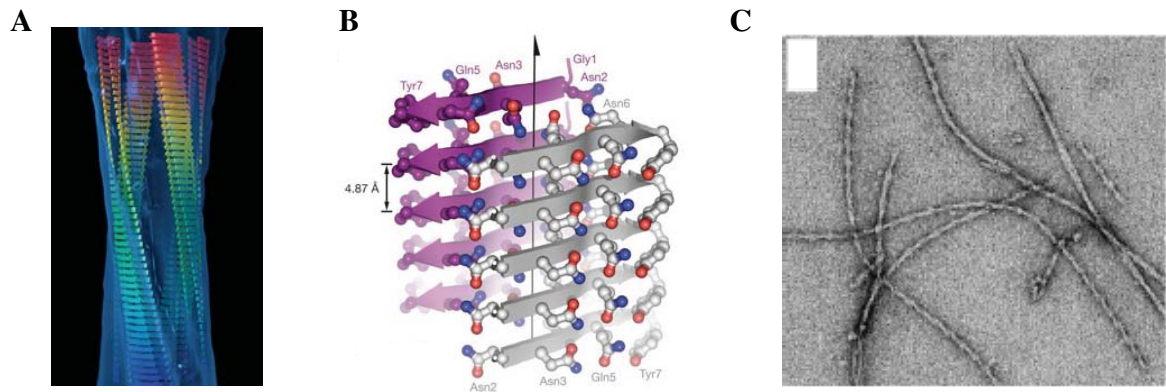
Figure 1.2 –Representations of proposed amyloid fibril structure. a) A molecular model of amyloid fibrils derived from an SH3 domain, compiled from cryo-EM data. The fibril consists of four protofilaments, each comprised of highly structured anti-parallel β-sheets (from Dobson, 1999). b) Atomic structure of fibrillar micro-crystals derived from the peptide GNNQQNY. Anti-parallel β-sheets are arranged perpendicular to the fibrillar axis, as is suggested of all fibrillar models (from Nelson *et al*., 2005). c) Aβ-peptide amyloid fibrils, observed via transmission electron microscopy (from Goldsbury *et al.*, 2000).

1.4 Mechanism of fibrillar aggregation

Like amorphous aggregation, amyloid fibril formation is believed to be a nucleation-dependent process (Jarrett and Lansbury, 1992, Jarrett *et al.*, 1993; Come *et al.*, 1993; Harper and Lansbury, 1997). Fibrillar aggregation is generally preceded by the disruption of native protein structure, in a manner similar to the initial stages of amorphous aggregation (Chiti *et al.*, 1999; Dunker *et al.*, 2002; Dobson, 2006). The resulting semi-folded, amyloidogenic protein intermediates are prone to association via

intermolecular forces, such as hydrogen bonding (Chiti *et al.*, 1999). Protein intermediates associate into large, insoluble oligomers (the fibril 'nucleus'), after which subsequent monomers are rapidly added to the growing amyloid fibril (Jarrett *et al.*, 1993; Harper and Lansbury, 1997). It has been suggested that this process is a more ordered process than that of amorphous aggregation, during which the nucleus provides a 'template' for the addition of subsequent monomers to either end of the developing amyloid fibril (Griffith, 1967; Lomakin *et al.*, 1996; Serio *et al.*, 2000) (Figure 1.3). In this model, the creation of a stable, amyloidogenic nucleus is the rate-limiting step of fibrillar aggregation, and is characterised by a pronounced lag-phase during fibrillar aggregation. Consequently, fibrillar aggregation can be sped up via the addition of pre-formed fibrils, which provide the nucleus for large-scale fibrillar aggregation (Jarret and Lansbury, 1992; Come *et al.*, 1993; Kim *et al.*, 2007).

Whilst this is the generally accepted 'generic' mechanism of fibrillar aggregation, an increasing number of exceptions are being discovered. Both HypF and acylphosphatase fibril formation can be preceded by intermediates that adopt a highly native-like structure (Plakoutsi *et al.*, 2004; Marcon *et al.*, 2005). Alzheimer's disease is characterised by plaques that are believed to form as a result of protein truncation, as opposed to stress-induced unfolding and subsequent association (Prelli *et al.*, 1988; Stefani and Dobson, 2003). Recently, a mechanism of fibrillar aggregation has been identified in which the formation of an amyloidogenic nucleus is *not* the limiting step, using reduced and carboxymethylated κ-casein as a target protein (Ecroyd *et al.*, 2008). In this system, the lag phase of fibrillar aggregation is independent of protein concentration or seeding. It is believed that this is a consequence of the structure of

monomeric κ-casein; κ-casein oligomers dissociate directly into highly amyloidogenic

monomers, removing the lag phase of fibril formation (Ecroyd *et al*., 2008).

NOTE:
This figure is included on page 10
of the print copy of the thesis held in
the University of Adelaide Library.

Figure 1.3 – A generic model of amyloid fibril formation. Natively folded proteins unfold into partially-folded amyloidogenic intermediates, which associate to form the fibrillar nucleus. Subsequent intermediates associate with the fibrillar nucleus, stacking to form protofilaments and eventual amyloid fibrils. Figure from Ecroyd *et al.* (2008).

1.5 pH influences fibrillar aggregation

Amyloid formation can be affected by a number of extrinsic factors, one of the more

significant being pH variation. Low pH has been identified as a key stress in the initial

stages of fibrillar aggregation, and provides an environment conducive to the

intermolecular interactions necessary for fibrillar aggregation (Chiti *et al*., 1999;

Dobson, 2006). Solution pH has a direct effect on the ionisable groups of amyloid-

forming peptides; consequently, the degree to which pH affects amyloid fibril

formation is influenced by the primary structure of the protein species undergoing

amyloidosis (Ma *et al*., 1999). Proteins such as HypF can be induced to form fibrils

only after a decrease in pH to 5.5 (Bucciantini *et al*., 2002), while transthyretin is

unable to adopt the necessary structural conformation for amyloid fibrils at a pH of greater than 5.0 (Lai *et al.*, 1996). α-Lactalbumin preferentially forms fibrillar aggregates at pH 2.0, and amorphous aggregates at neutral pH (Goers *et al.*, 2002). The fibrillar aggregation of β2-microglobulin, characteristic of dialysis-related amyloidosis, occurs at both acidic (pH 2.5) and neutral pH (Raman *et al.*, 2005; Sasahara *et al.*, 2008). Alzheimer's disease, characterised by Aβ-peptide amyloid plaques, coincides with localised acidosis (pH 6.0) in diseased tissue (Yates *et al.*, 1990). Significantly, Aβ-peptide is believed to adopt an amyloid-prone conformation at pH 6.0 (Khandogin and Brooks, 2007).

1.6 Molecular chaperones

The complex nature of correct protein folding means that simple modifications, such as single-point mutations, can result in significant changes to the protein structure (Murphy and Kendrick, 2007). Consequently, the cellular protein expression system has an extensive quality control system to ensure both the correct folding of expressed proteins, and the efficient removal of incorrectly folded and possibly damaging protein intermediates. This is generally understood to be a two-tiered system, controlled by both the ubiquitin-proteosome system (UPS) and a complex array of molecular chaperones (Berke and Paulson, 2003). Molecular chaperones are a variety of protein species whose key role is to inhibit the aggregation of reactive protein intermediates, and facilitate the re-folding or removal of misfolded proteins. Molecular chaperones fulfil a variety of tasks in this role; calnexin, for example, recognises and targets

abnormally folded proteins for rapid degradation via subsequent pathways (Liu *et al.*, 1999; Welch, 2003), and both calnexin and calreticulin aid the retention of misfolded proteins in the endoplasmic reticulum, to ensure that only correctly folded proteins are secreted into the cytosol (Jackson *et al.*, 1994; Pind *et al.*, 1994; Hammond and Helenius, 1995). One of the more significant roles of molecular chaperones *in vivo* is the inhibition of interactions between reactive protein intermediates by direct binding with target proteins, and by doing so inhibiting large scale protein aggregation (Derham and Harding, 1999). This can be purely protective, limiting further protein aggregation as with small heat shock proteins (Horwitz, 1992; Lee *et al.*, 1997); conversely, it may be to refold misfolded proteins, as with Hsp70 and GroEL (Hartl and Hayer-Hartl, 2002; Young *et al.*, 2004). While the exact mechanism of this protection method is still unknown, it is believed that such molecular chaperones bind to regions of hydrophobicity on misfolded protein intermediates, limiting hydrophobic interactions between multiple incorrectly folded peptides (Raman and Rao, 1994; Datta and Rao, 1999; Singh and Rao, 2002; Melkani *et al.*, 2004).

1.7 Small heat shock proteins

Small heat shock proteins (sHsps) are one of the largest and most significant families of molecular chaperones. The sHsp superfamily encompasses a widespread and diverse range of low molecular weight proteins that range in size from 15 to 42 kDa (Horwitz, 2003). There are 10 human sHsps, including αA- and αB-crystallin, Hsp27 and Hsp20 (Taylor and Benjamin, 2005). These proteins are generally found *in vivo* in large,

dynamic, heterogeneous oligomeric structures up to 1MDa in mass (Horwitz, 2003; Sun and McRae, 2005). While the overall homology between sHsp proteins is low (Plesofsky-Vig *et al.*, 1992), they share the common traits of a conserved C-terminal region of about 80 amino acids in length (dubbed the α-crystallin domain) and a low subunit molecular mass (Lindquist, 1986; Plesofsky-Vig *et al.*, 1992; Ehrnsperger *et al.,* 1998). sHsps have been detected in almost all types of organisms, and perform a variety of functions including protein stabilisation, caspase inhibition and cytoskeletal interaction (Bloemendal, 1981; Lavoie *et al.*, 1993; Mounier and Arrigo, 2002; Treweek *et al.*, 2003).

Many of the human sHsps were not classified as sHsps until comparatively recently. Several of these proteins were independently identified and characterised by disparate research groups, often within one or two years of each other, and consequently the same small heat shock protein may have several names; HspB2, for example, was independently identified as myotonic dystrophy protein kinase binding protein (MKBP), due to its role in the binding to and activation of myotonic dystrophy protein kinase (Suzuki *et al.*, 1998). Similarly, Hsp22 was initially identified as H11 kinase, due in part to its perceived similarity to the putative protein kinase domain R1 subunit of herpes simplex virus type 2 ribonucleotide reductase (Smith *et al.*, 2000). Based upon our current understanding and classification of the human sHsps, a systematic nomenclature has been proposed to 'tidy up' redundant nomenclature in the literature, designated HspB1-10 (Table 1.2) (Kappe *et al.*, 2003; Taylor and Benjamin, 2005). This nomenclature is not widely used, particularly in reference to αA- and αB-crystallin (HspB4 and 5, respectively). It does, however, provide a systematic

classification of human sHsps that is useful for database search and comparison. This study does not utilise the HspB nomenclature except during SwissProt database searching and multiple sequence alignment (Chapter 7).

Table 1.2 – The HspB classification system of sHsps, and common alternative names. The HspB classification system is infrequently used, particularly in regards to αA- and αB-crystallin (HspB4 and 5, respectively). Table adapted from Taylor and Benjamin (2005).

Name	Alternatives
HspB1	Hsp27, Hsp25
HspB2	MKBP
HspB3	HSPL27
HspB4	αA-crystallin
HspB5	αB-crystallin
HspB6	Hsp20, p20
HspB7	cvHsp
HspB8	Hsp22, H11 kinase
HspB9	-
HspB10	ODF1

1.8 sHsps as molecular chaperones

The primary role of sHsps *in vivo* is that of a molecular chaperone, to inhibit illicit interactions between misfolded or partially folded proteins (Horwitz, 1992; Jakob *et al.*, 1993; Haslbeck *et al.*, 2005). sHsps typically bind to misfolded proteins without affecting their structure, instead directly inhibiting further interactions between misfolded protein intermediates via hydrophobic binding (Horwitz, 2003; Haslbeck *et al.*, 2005). Areas of reactive, exposed hydrophobicity on partially-folded protein intermediates interact with specialised chaperone-binding regions on the sHsp, and in

so doing, protein-protein interactions leading to aggregation are avoided (Raman and Rao, 1994; Das *et al.*, 1996). In their role as molecular chaperones, sHsps do not generally refold bound target proteins, but rather sequester them into unreactive and generally stable chaperone-target protein complexes (Figure 1.4) (Horwitz, 1992; Lee *et al.*, 1997; Ehrnsperger *et al.*, 1997). This reservoir of partially folded protein intermediates will neither further aggregate nor refold, but can subsequently be acted upon by refolding chaperone proteins (Hsp70 and GroEL, for example) to facilitate the renaturation of the protein chain and correct protein folding when cellular conditions become permissive (Ehrnsperger *et al.*, 1997; Lee *et al.*, 1997; Lee and Vierling, 2000; Wang and Spector, 2000). This in turn allows for the efficient turnover and recycling of incorrectly folded proteins, which might otherwise cause complications within cells.

The function of sHsps on the off-folding pathway becomes more significant in situations of low protein turnover, such as the eye lens, where regenerative heat shock proteins are not available for the refolding of misfolded peptides (Horwitz 1992; Horwitz, 2003). In the lens, sHsps provide an indefinite reservoir of partially folded protein intermediates with no recourse for protein renaturation. A decrease in the ability of local sHsps to carry out this task may result in the accumulation of reactive, misfolded peptide species, that could in turn lead to large scale protein precipitation and possible pathological conditions (Horwitz, 1992; Horwitz, 2003).
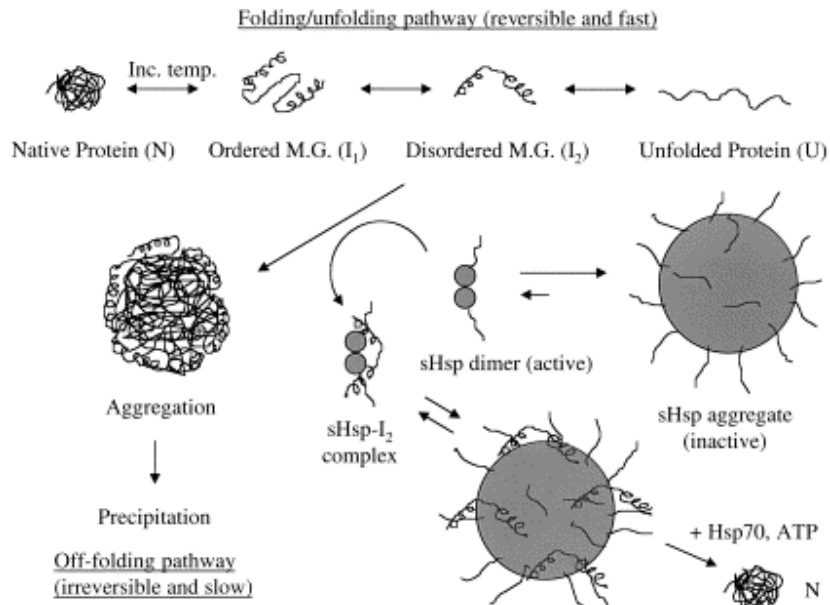
Figure 1.4 – Schematic representation of sHsps on the off-folding pathway. Functional sHsp subunits generally dissociate from un-reactive oligomeric complexes to sequester partially-folded protein intermediates, via hydrophobic interactions. While the functional sHsp unit is depicted here as dimer, this may not necessarily be the case with all sHsps. sHsps subsequently maintain protein intermediates in non-reactive complexes that can be re-folded via the action of additional molecular chaperones (Hsp70 or GroEL, for example). Figure from Carver *et al*. (2002).

1.9 Structure and function of the lens

The structure of the eye lens is inextricably linked to its key physiological function, namely the correct focusing of images onto the retina (Tardieu and Delaye, 1988). The lens structure consists of two distinct cell types, epithelial cells responsible for the generation of new lens cells, and fibre cells responsible for maintenance of the necessary transparency of the lens (Bloemendal *et al*., 2004). Epithelial cells are

arranged towards the front of the lens, aligned along the anterior capsule, while fibre cells make up the bulk of the lens structure. Younger fibre cells are arrayed at the edges of the lens, while older cells are stacked around each other at the nucleus or centre of the lens structure (Figure 1.5) (Bloemendal *et al.*, 1984). Consequently, there is no cell turn-over within the lens; aged fibre cells accumulate in the lens nucleus, while progressively younger cells are added to the extremities (Bloemendal, 1981). Cellular organelles, including those necessary for protein degradation and synthesis, are lost as lens fibre cells mature; importantly, this ensures that there is no protein turnover in mature lens cells (Bassnett and Beebe, 1992).

Accurate focusing of light onto the retina is necessary for unobstructed vision, and requires the maintenance of the correct refractive index of light passing through the lens. Consequently, incorrect scattering of light by the lens due to lens opacification results in an impaired ability to focus images (Benedek, 1971). This necessitates an exceptional degree of lens transparency; the human lens, for example, shows less than 5% light scatter (Bettelheim, 1985). Transparency is facilitated by the close packing of cell proteins within the lens cytoplasm, with essentially no fluctuation in refractive index between proteins (Benedek, 1971; Delaye and Tardieu, 1983). However, the maintenance of this refractive index within the eye lens requires an inordinately high concentration of cytoplasmic protein, with protein concentrations in excess of 450mg/ml (Fagerholm *et al.*, 1981). It was initially suggested that lens proteins were structured in a dense and highly ordered crystalline array, in order to explain both the high protein concentration and transparency of the lens (Trokel, 1962). X-ray crystallographic studies have since shown this to be false, with lens proteins instead

being arranged as a dense, freely moving liquid, with a spatial arrangement similar to that of glass. The short-range spatial order of lens proteins is responsible for lens transparency (Benedek, 1971; Delaye and Tardieu, 1983).
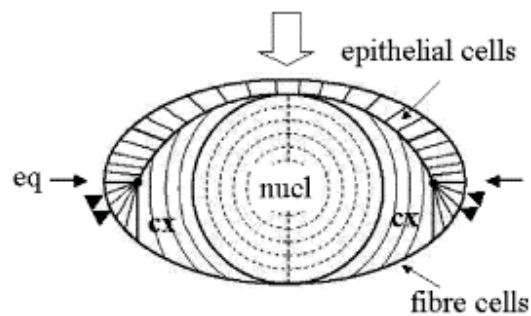
Figure 1.5 – Schematic diagram of the mammalian lens. The open arrow designates the direction of light entering the lens. Epithelial and fibre cells are arranged on the exterior of `the lens, and migrate towards the nucleus with age. 'Nucl' designates the lens nucleus, 'cx' designates the cortical region of the lens, 'eq' designates the equatorial region of the lens. Arrowheads show the region where epithelial cells differentiate into secondary fibre cells. Figure from Bloemendal *et al.* (2004).

1.10 Crystallins

The crystallins are the primary structural proteins of the lens, and account for over 90% of soluble lens protein, and up to 33% wet weight of the adult lens nucleus (Horwitz, 2003). Crystallins are generally divided into the physiologically related α-, β- and γ-families, and to date 2 α-, 7 β- and 5 γ-crystallins have been identified in the

mammalian lens (Bloemendal *et al.*, 2004). Crude lens purification typically produces five crystallin fractions, designated α_T (including αA- and αB-crystallin), β_H, β_L, γ_S and γ_T-crystallin. As the major structural proteins of the lens, crystallins facilitate lens transparency by maintaining the correct refractive index of the lens (Bloemendal, 1981). Of these, α−crystallin is the predominant crystallin species, accounting for 40% of human soluble lens protein (Horwitz, 2003). As well as maintaining lens transparency through structural interactions, lens crystallins have been implicated in a variety of physiological processes. Both β- and γ-crystallins are expressed in lens epithelial cells during cellular stress, and it has been suggested that these proteins may have a protective role in epithelial cells (Wang *et al.*, 2004). Additionally, both β- and γ-crystallins bind calcium, and are believed to play an important role in lens calcium homeostasis (Rajini *et al.*, 2001; Jobby and Sharma, 2007). Mutations in γ-crystallin structure have been implicated in both cataract and epithelial cell defects (Sinha *et al.*, 2001; Bu *et al.*, 2002). α-Crystallin has been implicated in apoptosis, cytoskeletal interactions and cell differentiation (Bennardini *et al.*, 1992; Nicholl, and Quinlan, 1999; Ito *et al.*, 2001; Kamradt *et al.*, 2005), but its most significant function appears to be that of a molecular chaperone.

1.11 α−Crystallin as an sHsp and molecular chaperone

Since its discovery as a sHsp, and subsequent identification as a molecular chaperone (Klemenz 1991; Horwitz 1992), α−crystallin has been extensively studied and characterised due to its unique role in maintaining the necessary transparency of the eye

lens. In addition to its role as an integral structural protein of the lens, α-crystallin also functions as the primary protein chaperone within the lens (Horwitz, 1992). In its capacity as a molecular chaperone, α–crystallin inhibits the aggregation of the structurally related β-crystallin and γ-crystallins, as well as a variety of minor lens components that include glyceraldehyde-3-phosphate dehydrogenase, enolase, leucine aminopeptidase and aldehyde dehydrogenase (Velasco *et al.,* 1997). By doing so, α-crystallin is believed to maintain lens transparency. Interestingly, αB-crystallin knockout mice do not display a cataractous phenotype (Brady *et al*., 2001), while αA-crystallin knockout mice show an increased propensity for cataract and cytoplasmic inclusion bodies in lens fibre cells (Brady *et al*., 1997). These inclusion bodies include aggregated γ- and αB-crystallin, as well as Hsp25, suggesting that αA-crystallin is primarily responsible for maintaining the solubility of lens proteins. The inability of α-crystallin to perform either as a soluble, structural lens protein, or as a molecular chaperone in the lens, has been argued to result in a loss of functional lens transparency. (Horwitz, 1992).

As yet, the exact nature of α–crystallin-target protein interaction is unknown. Several molecular chaperones are believed to interact with target proteins via non-specific hydrophobic interactions, including GroEL (Melkani *et al*., 2004), 70S ribosome (Singh and Rao, 2002) and mitochondrial Atp11p (Sheluho and Ackerman, 2001), and it follows that α-crystallin may interact with target proteins in a similar manner. Studies demonstrating that α-crystallin preferentially recognises non-native structures with increased surface hydrophobicity (Carver *et al.*, 1995; Das *et al*., 1996; Rajaraman *et al.*, 1998; Treweek *et al.*, 2000; Carver *et al*., 2002), and the observed

correlation between exposed hydrophobicity and enhanced chaperone ability (Raman and Rao 1994; Das and Surewicz, 1995) suggest that the α-crystallin chaperone binding mechanism may be similar to that of GroEL. Consequently, it is widely accepted that α-crystallin interacts with target proteins via non-specific interactions between hydrophobic regions on α-crystallin and areas of exposed hydrophobicity on semi-folded protein intermediates. In this manner, α-crystallin behaves as other sHsps, binding to semi-folded protein intermediates on the off-folding pathway (Carver *et al.*, 1995; Das *et al.*, 1996; Rajaraman *et al.*, 1998; Treweek *et al.*, 2000; Carver *et al.*, 2002). Putative chaperone binding regions have been identified on both αA- and αB-crystallin (Sharma *et al.*, 2000; Bhattacharyya *et al.*, 2006, Ghosh *et al.*, 2007), which lie within hydrophobic areas of β-sheet in the C-terminal ('α-crystallin') region of the protein. α–Crystallin is a relatively stable protein, and while elevated temperatures may induce thermotropic conformational changes, these appear to enhance its chaperone activity (Raman and Rao, 1994; Das and Surewicz, 1995; Datta and Rao, 1999). Additionally, both of the related αA- and αB-crystallin subunits of α–crystallin are capable of stress induced chaperone activity independently of each other (Carver, 2003). Studies have demonstrated that α–crystallin is capable of the prevention of γ-crystallin and insulin-B-chain aggregation as a consequence of chemical stress without thermal activation (Bhattacharyya and Das, 1998).

1.12 Structure of α–crystallin

Human α–crystallin consists of two similar and related subunits, the 173 residue αA–crystallin subunit and the 175 residue αB-crystallin subunit. These proteins are coded for on two distinct chromosomes (23 and 11 respectively), and share 57% sequence similarity (Bloemendal and de Jong, 1991). Primary structure is highly conserved between the two subunits, notably in the putative chaperone-binding regions (Sharma *et al*., 2000; Bhattacharyya *et al*., 2006).

In vivo, α-crystallin forms heterogenous, multimeric aggregates, which have been estimated variously to consist of between 14 and 50 α–crystallin subunits (Thomson and Augusteyn, 1988; Spector *et al*., 1971). The generally accepted molecular weight of native α-crystallin, however, lies between 700 and 800 kDa (35 – 40 subunits) (Bloemendal, 1981; Vanhoudt *et al*., 2000). In the human lens, αA- and αB-crystallin exist in a ratio of close to 3:1 (Bloemendal, 1981). αA–Crystallin appears to be lens specific, while αB-crystallin is commonly found in extra-lenticular tissue (Bhat and Nagineni, 1989; Dubin *et al*., 1989; Iwaki *et al.,* 1990; Srinivasen *et al*., 1992). Regardless of their aggregated state, it has been shown that all sHsps exist in a dynamic equilibrium between oligomeric and non-oligomeric forms (van den Oetelaar *et al*., 1990; Bova *et al*., 1997, 2000; Haley *et al*., 1998). There is substantial evidence to suggest that the dissociated subunit is the functional chaperone unit of α-crystallin, and that the dissociation of subunits from the α-crystallin oligomer facilitates the exposure of hydrophobic chaperone-binding regions of α-crystallin buried previously within the protein multimer (Plater *et al*., 1996; Bova *et al*., 1997). Accordingly,

dynamic subunit exchange between multimeric and dissociated α–crystallin has been considered a key factor in regulating chaperone function (Bova *et al.*, 1997; Avilov *et al.*, 2004; Liu *et al.*, 2006a). Studies have since suggested that the α-crystallin oligomer is a functional chaperone unit, and is capable of chaperone activity independent of subunit exchange or dissociation (Augusteyn, 2004b). It is likely that both oligomeric and dissociated α-crystallin is capable of chaperone activity, and that dissociation is not necessary for α-crystallin chaperone function.

α-Crystallin consists of three domains; the C-terminal 'α-crystallin' domain, common to all sHsps (sometimes referred to as the α–crystallin domain), the N-terminal domain and the flexible C-terminal extension. The α-crystallin domain has been extensively studied due to its commonality between sHsps, and is believed to have both a chaperone function and a role in monomer-monomer interactions within the α-crystallin oligomer (Sharma *et al.*, 2000; Ghosh and Clark, 2005; Bhattacharyya *et al.*, 2006). The α-crystallin domain is believed to consist of a complex β-sheet sandwich containing multiple β-strands (Mornon *et al.*, 1998). Putative αA- and αB-crystallin chaperone binding sites have been identified in this region, between residues 70 and 88 in αA-crystallin, and between residues 79 and 92 in αB-crystallin (Sharma *et al.*, 2000; Bhattacharyya *et al.*, 2006). Accordingly, it is believed that the hydrophobic C-terminal region of α-crystallin is important in chaperone binding and the inhibition of target protein aggregation (Saha and Das, 2004). The α-crystallin domains of Hsp27 monomers interact closely with each other within the Hsp27 multimer (Ehrnsperger *et al.*, 1997), suggesting that the α-crystallin domain may also be important in the formation and maintenance of oligomeric sHsp structures.

Despite a high degree of variation in length and amino acid sequence within sHsps, the N-terminal sHsp domain is also believed to be required for α–crystallin aggregation and monomer–monomer interaction. It has been suggested that the N-terminal domain of protein monomers is buried within the oligomeric structure, and hence that this domain is also involved in the aggregation of sHsp subunits into multimeric oligomers (Leroux *et al.*, 1997). Truncation of the N-terminal region past the first 20 residues of αA-crystallin reduces oligomer size and stability, supporting the suggestion that the N-terminal region is important for oligomeric assembly (Bova *et al.*, 2000; Sreelakshmi *et al.*, 2004; Kundu *et al.*, 2007). N-terminal deletion has been shown variously to increase α-crystallin β-sheet content, but decrease exposed hydrophobicity (Kundu *et al.*, 2007; Chaves et al., 2008). Additionally, the N-terminal region of α-crystallin has been implicated in chaperone-substrate binding, and N-terminal deletion inhibits αA-crystallin chaperone ability (Plater *et al.*, 1996; Aquilina and Watt, 2007; Kundu *et al.*, 2007). The loss of chaperone ability is particularly interesting, and is believed to be a direct consequence of the loss of αA-crystallin oligomerisation, providing further evidence for the importance of α-crystallin oligomerisation and subunit exchange in chaperone ability (Kundu *et al.*, 2007).

As determined by NMR spectroscopy, a short and highly flexible C-terminal extension extends from the α–crystallin domain of several mammalian sHsps (Carver *et al.,* 1992; Carver *et al.*, 1995a; van de Klundert *et al.*, 1998; Carver, 1999). Whilst it has been suggested that the C-terminal extension may play some role in chaperone-protein binding, this appears unlikely due to the highly hydrophilic and flexible nature of the extension. Rather, the hydrophilic nature of the C-terminal extension, and the

fact that subunit C-terminal extensions within the sHsp oligomer extend outwards into the cytosol suggest that the C-terminal extension may instead function to aid in the solubility and stability of protein oligomers and their complex with target proteins (Smulders *et al.*, 1996; Carver, 1999).

The overall secondary structure of α-crystallin has been determined by circular dichroism spectroscopy. From these studies, α-crystallin has been shown to consist primarily of β sheets (between 40 and 70%) interspersed with a minimal amount of α helical structure (Thompson and Augusteyn, 1989; Ehrnsperger *et al.*, 1997). Despite the predominance of β sheet, studies have implicated α-crystallin α–helical structure in the chaperone activity of α–crystallin (Koretz *et al.*, 1998).

A 3D model of αB-crystallin tertiary structure has recently been proposed, based upon the x-ray crystal structures of two structurally related sHsps, *Methanococcus jannaschi* Hsp16.5 and wheat Hsp16.9 (Kim *et al.*, 1998; van Montford *et al.*, 2001). A series of overlapping eight amino acid peptides, derived from αB-crystallin, were probed against αA- and αB-crystallin, to determine areas of subunit-subunit interaction. Interaction sites were then modelled onto a 3D homology model of αB-crystallin based upon Hsp 16.5 and Hsp 16.9 structures. (Ghosh and Clark, 2005) (Figure 1.6). Subunit-subunit interaction sites appear to be solvent exposed, and suggest a pattern of exposed hydrophobicity on the αB-crystallin monomer.
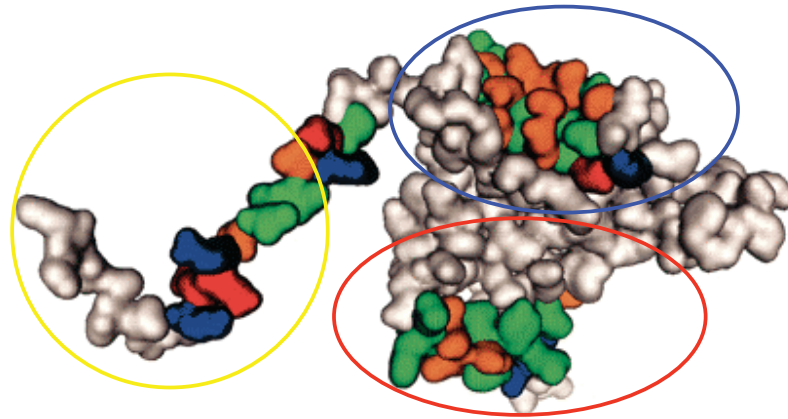
Figure 1.6 – 3D space-filling model of αB-crystallin's tertiary structure. The N-terminal α-crystallin domain (red circle) consists of a single α-helix and random coil elements; the C-terminal domain (blue circle) consists primarily of β-sheets. The C-terminal extension (yellow circle) is hydrophilic, and extends freely from the structure. Figure from Ghosh and Clark (2005).

The tertiary and quaternary structures of α–crystallin remain to be definitively established, as it has not been possible to grow crystals of the protein due to the heterogenic and dynamic nature of the α–crystallin oligomer. While NMR spectroscopy has been used to investigate the flexible C-terminal extension of the protein (Carver *et al.*, 1992, 1995a; Carver, 1999), it is not suitable for investigating further regions of the protein due to their large size. Initially, a three-layered, micelle-like association of α-crystallin subunits was proposed (Tardieu *et al.*, 1986; Augusteyn, and Koretz, 1987) based largely on the belief that α-crystallin subunits were differentially exposed to solution during oligomerisation (Figure 1.7). It was subsequently observed that αA- and αB-crystallin have broadly similar tertiary structures, and occupy equivalent positions in the α-crystallin oligomer (Hendriks *et*

al., 1990); from this, cubic and rhombic-dodecahedral oligomeric structures were proposed, in which αA- and αB-crystallin occupy equivalent positions (Wistow, 1993) (Figure 1.7b). In these models, the C-terminal regions of α-crystallin subunits are arranged externally on the oligomer, while N-terminal domains are buried within the interior of the structure. A refinement of these initial models has lead to the so-called 'pitted-flexball' model, in which α-crystallin subunits form a micelle-like association with equivalent αA- and αB-crystallin subunits. In this model, the N-terminal domains of α-crystallin subunits associate toward the interior of the oligomer, with externally facing C-terminal domains (Smulders *et al.*, 1998) (Figure 1.7c). The C-terminal extensions of α-crystallin subunits extend freely into solution, aiding oligomer solubility. This model creates a pitted oligomeric surface, in which the N-terminal regions of multiple subunits are still partially exposed to solution. Chaperone substrate binding was assumed to occur via interactions with semi-exposed N-terminal regions of α-crystallin subunits. Subsequent studies have demonstrated the importance of the C-terminal domain in α-crystallin substrate binding, and so cast some doubt on this model.

Carver *et al.* (1994) have proposed an annular oligomeric structure, in which α-crystallin subunits are arranged into a hollow cylindrical conformation reminiscent of GroEL (Figure 1.7d). Evidence for a central cavity comes from negatively-stained electron micrographs, in which the size of the α-crystallin oligomer (800kDa) can only account for roughly 50% of the average diameter of the α-crystallin oligomer (around 14nm). In this model, the N-terminal regions of subunits are arranged towards the interior of the oligomer, and are responsible for the oligomerisation of multiple

subunits. Accordingly, N-terminal domains are largely shielded from solution by larger, surface exposed C-terminal domains. C-terminal extensions extend freely into solution, and may aid solubility in a similar manner to that of the 'pitted-flexball' model. Chaperone substrate binding is believed to occur on the exterior cylindrical surface of the oligomer. Cryo-EM studies have, to an extent, supported this model, suggesting a globular α-crystallin aggregate with a large central cavity, and substrate binding on the external surface of the oligomer (Haley *et al.*, 1998) (Figure 1.8). This model of the α-crystallin oligomer is similar to x-ray crystal structures observed for Hsp16.5 and Hsp16.9; Hsp16.5 forms hollow, spherical oligomers consisting of 24 subunits (Kim *et al.*, 1998) while Hsp16.9 is formed as a similarly hollow, spherical dodecamer containing two rings each of six subunits (van Montford *et al.,* 2001) (Figure 1.9). While it is at present impossible to definitively state the quaternary structure of α-crystallin, the annular model proposed by Carver *et al.* seems the most likely of those available, and accounts for both the hollow internal cavity of α-crystallin, and the role of the C-terminal region in chaperone-substrate binding.
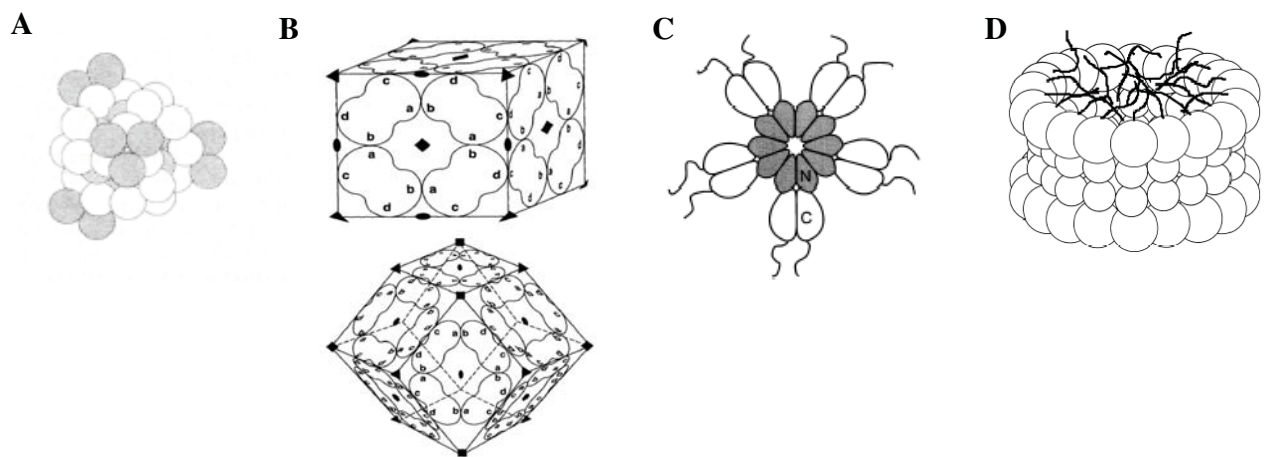
Figure 1.7 – Various suggested models for α-crystallin quaternary structure. a) a three-layered open micelle model of the α-crystallin oligomer, in which spheres designate α-crystallin subunits. Alternating grey and white spheres denote the three layers of association and accessibility of α-crystallin subunits (from Tardieu *et al.*, 1986). b) cubic and rhombic-dodecahedral quaternary structural models of α-crystallin. 'Peanut-like' shapes represent the surface-exposed C-terminal domains of α-crystallin subunits. αA- and αB-crystallin occupy equivalent positions in the oligomer. Letters denote specific association regions on each subunit; a associates with b, c associates with d (from Wistow, 1993). c) 'Pitted-flexball' quaternary structural model of α-crystallin. Grey regions denote subunit N-terminal domains, open regions indicate subunit C-terminal domains. Lines represent C-terminal extensions. Oligomerisation is achieved through the association of subunit N-terminal domains. C-terminal domains are arrayed on the external surface of the oligomer. The N-terminal domains remain surface-exposed, and provide the primary site for chaperone binding (from Smulders *et al.*, 1998). d) Annular quaternary structural model of α-crystallin. Large spheres represent subunit C-terminal domains, smaller spheres represent subunit N-terminal domains. Lines represent subunit C-terminal extensions. The oligomer contains a hollow central cavity, and substrate binding occurs on the external cylindrical surface of the oligomer (from Carver *et al.*, 1994).

A **B**
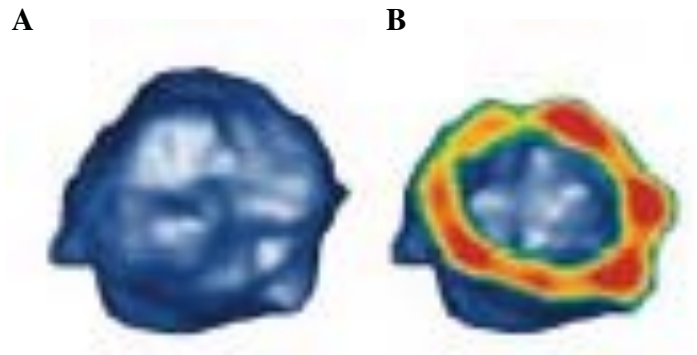
Figure 1.8 – Single resolution representation of αB-crystallin quaternary structure, based upon Cryo-EM data. b) is a cutaway of figure a). The αB-crystallin oligomer is roughly spherical in shape, and contains a large, hollow central cavity, as suggested by Carver *et al*. (1994). Figure adapted from Haley *et al*. (1998).

A **B**
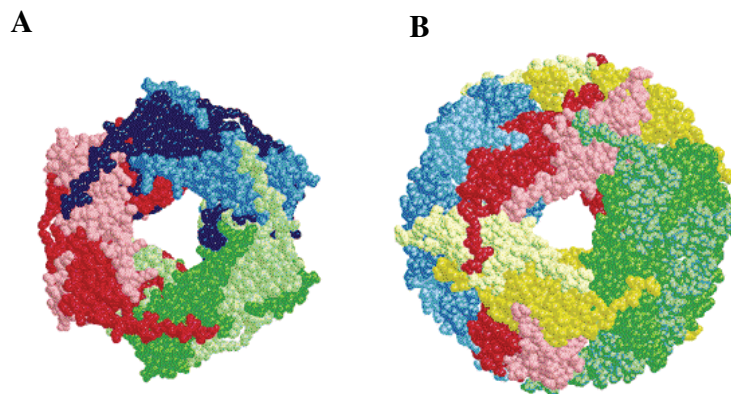
Figure 1.9 – 3D space-fill models of the quaternary structures of a) Hsp16.5 and b) Hsp16.9, derived from x-ray crystallography. Both oligomers contain a large, hollow central cavity, reminiscent of the α-crystallin oligomeric model proposed by Carver *et al*. (1994). Figure from van Montfort *et al*. (2001)

1.13 Aging within the lens

Aging within the eye lens is accompanied by a number of changes in protein structure and composition. Lens aging is characterised by the increased presence of a high molecular weight protein species, of which α- and γ-crystallin are the primary components (Liang and Rossi, 1989; Yang *et al.*, 1994); this high molecular weight protein species has significantly reduced chaperone ability compared to wild-type α-crystallin (Takemoto and Boyle, 1994; Carver *et al.*, 1996; Carver and Lindner, 1998). The relative proportions of crystallin species within the lens vary markedly with age, α-crystallin composition rising while β-crystallin remains constant, and γ-crystallin composition drops significantly (Bessems *et al.*, 1983; Bhattacharyya and Das, 1998). Soluble αA-crystallin is almost entirely absent within lenses at 60 years or older, but dominates the non-water soluble lens protein fraction (Roy and Spector, 1976; McFall-Ngai, *et al.*, 1985; Rao *et al.*, 1993).

As proteins age in the cell, they tend to become disordered and partially folded, leading to an increased degree of hydrophobicity exposed to cytosol. It is here that the significance of α-crystallin as a molecular chaperone becomes apparent, as α-crystallin is the primary chaperone responsible for the inhibition of this aggregation. This may explain the protein's elevated concentration in aged cells, as well as its absence in the free, water-soluble protein fraction of the aged lens nucleus (Rao *et al.*, 1993). As there is no significant re-folding pathway available within the lens, α-crystallin provides an indefinite reservoir of un-reactive, partially folded proteins (Horwitz, 1992; Horwitz, 2003). α-Crystallin from aged lenses demonstrates a substantial loss of chaperone

ability compared to that of juvenile lenses, which was initially attributed to age-related modifications to α-crystallin (Horwitz *et al.*, 1992; Derham and Harding, 1997). It has since been determined that the loss of chaperone ability observed in aged cells is a consequence of α-crystallin's incorporation into non-functional high molecular weight complexes with aggregating β- and γ-crystallin, which may explain the loss of soluble α-crystallin within fibre cells with age (Carver *et al.*, 1996; Carver and Lindner, 1998).

1.14 Aging and cataract formation

Cataract describes a pathological opacity of the lens, resulting in compromised transparency (Bloemendal *et al.*, 2004). It has long been known that the formation of high molecular weight protein aggregates can result in the opacification of the lens, due to light scattering (Benedek, 1971; Jedziniak, 1973), and that these high molecular weight aggregates are prevalent in cataractous lenses (Jedziniak *et al.*, 1975). The formation of these high molecular weight protein aggregates is believed to be one of the major causes of cataract formation; accordingly, cataract is widely considered to be a protein misfolding disease, in a similar manner to Alzheimer's and other neurodegenerative diseases (Benedek, 1997; Bloemendal *et al.*, 2004). Studies have demonstrated that cataractous formations are characterised by numerous modifications within the lens, including an increase in non-tryptophan fluorescence, tryptophan oxidation and de-amidation (Hoenders and Bloemendal, 1983). The role of α–crystallin in cataract formation is still not fully understood, but studies have shown cataract to be accompanied by a marked increase in α-crystallin-plasma membrane interactions

within lens fibre cells (Boyle and Takemoto, 1996). Also significant amongst these factors is the presence of increased concentrations of insoluble lens proteins, particularly within the lens nucleus (Hoenders and Bloemendal, 1983; Liang and Rossi, 1989; Yang *et al.*, 1994). The aggregation of α-crystallin into high molecular weight complexes impairs its ability to effectively chaperone other incorrectly folded proteins, leading to a situation of increased protein aggregation (Takemoto and Boyle, 1994; Carver *et al.*, 1996; Carver and Lindner, 1998). The decrease in soluble lens α-crystallin is accompanied by an observed increase in insoluble β- and γ-crystallin, which are key targets for α–crystallin chaperone activity (Hanson *et al.*, 2000). This phenomenon is aggravated by the lack of protein turnover within the lens (Bassnett and Beebe, 1992), as aging fibre cells and their compliment of high molecular weight protein are compacted towards the nucleus of the lens, and possibly jeopardise lens transparency. The loss of α-crystallin chaperone ability with age correlates with an increase in insoluble protein content in the lens, and suggests that a loss of α-crystallin chaperone function is a significant factor in cataract formation (Carver *et al.*, 1996).

1.15 α-Crystallin and cataract

Aging in the lens is accompanied by extensive post-translational modification of lens proteins, and it is believed that post-translational modification of lens α-crystallin contributes to cataract formation *in vivo* (Horwitz, 1992; Ponce *et al.*, 2006). Analysis of cataractous human lenses demonstrates significant oxidation, deamidation, acetylation and phosphorylation of lens crystallins (Hains and Truscott, 2007), and

several of these modifications have been demonstrated to impair α-crystallin chaperone ability *in vitro*. Deamidation of asparagine residues is amongst the most frequently observed post-translational modifications of α-crystallin in cataractous lenses, and in the insoluble protein fraction of aged lenses (Hains and Truscott, 2007; Hanson *et al.*, 2000); deamidation has been shown to decrease αA- and αB-crystallin chaperone ability against γ-crystallin, citrate synthase and insulin *in vitro*. (Gupta and Srivastava, 2004a,b). Oxidation of histidine, methionine and tryptophan residues in lens crystallins is considered characteristic of age-related nuclear cataract formation (Truscott, 2005), and decreases chaperone ability against β_L- and γ-crystallin aggregation *in vitro* (van Boekel *et al.*, 1996; Rajan *et al.*, 2006). Truncated α-crystallin purified from ICR/f rat lenses, a strain exhibiting hereditary cataract, demonstrates reduced chaperone ability against thermally-stressed β_L-crystallin (Takeuchi *et al.*, 2004).

Frequently, demonstrating a definitive link between post-translational modifications and decreased α-crystallin chaperone ability *in vitro* is difficult, as results can vary between target proteins and treatment conditions. Glycation of α-crystallin lysine and arginine residues, for example, is enhanced during diabetes, and is believed to be responsible for cataract formation in diabetes patients (Cherian and Abraham, 1995a). Studies have demonstrated that extensive glycation and cross-linking of human, rat and rabbit α-crystallin decreases chaperone ability against β_L-crystallin aggregation (Cherian and Abraham, 1995b); limited glycation of lysine residues, however, has no effect on chaperone ability (van Boekel *et al.*, 1996). Phosphorylation of αB-crystallin serine residues has been demonstrated to inhibit chaperone ability against ccβ-Trp peptide and α-lactalbumin aggregation, but increase chaperone ability against β_L-

crystallin, catalase, insulin, citrate synthase, alcohol dehydrogenase, α-synuclein and reduced and carboxymethylated (rcm) κ-casein (Aquilina *et al.,* 2004; Ecroyd *et al.*, 2008; Ahmad *et al.*, 2008). This is further complicated by the seemingly contradictory observation that the phosphorylation of rat αA- and αB-crystallin has no effect on the chaperone ability of either crystallin against β_L- or γ-crystallin aggregation (Wang *et al.*, 1995), and by the recent suggestion that phosphorylated αB-crystallin subunits form mixed oligomers with un-phosphorylated subunits (Ahmad *et al.*, 2008). While it is not always simple to correlate post-translational modifications to α-crystallin with decreased chaperone ability *in vitro*, the increased incidence of modified α-crystallin in cataractous deposits, and in the insoluble protein fraction of aged lenses, strongly suggests that such modifications inhibit α-crystallin solubility and/or function *in vivo*. Reduced α-crystallin function, in turn, appears to be inextricably linked with cataract formation.

Similarly, a number of αA- and αB-crystallin mutations have been isolated from cataractous human lenses, and it is believed that a loss of chaperone function accompanying these mutations is directly responsible for cataract formation *in vivo*. The αA-crystallin mutations R12C, R21W, R54C, G98R and R116G have been isolated from cataractous human lenses; of these mutations, G98R and R116C have decreased chaperone ability against γ-crystallin, insulin and alcohol dehydrogenase *in vitro* (Kumar *et al.*, 1999; Cobb and Petrash, 2000; Shroff *et al.*, 2000; Singh *et al.*, 2006), while R54C disrupts fibre and epithelial cell development (Xia *et al.*, 2006). Similarly, the αB-crystallin mutations P20S, R120G and D140N have been isolated from cataractous human lenses; of these mutations, R120G and D140N completely

remove αB-crystallin chaperone ability against α-lactalbumin, alcohol dehydrogenase and insulin *in vitro*, and promote target protein aggregation (Bova *et al.*, 1999; Kumar *et al.*, 1999; Liu *et al.*, 2006b; Simon *et al.*, 2007). R120G αB-crystallin in particular has been extensively studied, and causes desmin-related myopathy *in vivo* (Vicart *et al.*, 1998). Interestingly, there has been no investigation into the chaperone ability of P20S αB-crystallin homoaggregates *in vitro*; rather, studies have shown that the P20S αB-crystallin mutation decreased the chaperone ability of re-associated α-crystallin heteroaggregates (P20S αB-crystallin reassociated with wild type αA-crystallin) against γ-crystallin, insulin and citrate synthase (Li *et al.*, 2008). The rationale for this approach comes from the observation that αB-crystallin knock-out mice do not display a cataractous phenotype, and the assumption therefore that αB-crystallin mutations do not have a direct role in cataract formation. From this, it has been assumed that P20S αB-crystallin promotes cataract formation by influencing the subunit exchange of the α-crystallin oligomer, and specifically the chaperone ability of αA-crystallin. This interpretation seems limited, particularly in light of the decreased chaperone ability of R120G and G140A αB-crystallin *in vitro*, and the role of R120G in cataract formation and desmin-related myopathy. Mutations or post-translational modifications directly affecting the chaperone ability of α-crystallin appear to correlate with cataract formation *in vivo*. Accordingly, the removal of α-crystallin chaperone function is of physiological importance, and has significant pathological implications.

1.16 α-Crystallin and fibrillar aggregation

Of the two α–crystallin subunits, αA-crystallin is virtually non-existent in extra-lenticular tissue; conversely, non-lenticular αB-crystallin has been shown to exist in a variety of tissues, including the heart, skeletal muscle and kidney cells (Bhat and Nagineni, 1989; Dubin *et al*., 1989; Iwaki *et al.,* 1990; Srinivasan *et al*., 1992). The discovery of αB-crystallin in pathological deposits characteristic of number of neurological conditions, including Alzheimer's, Parkinson's and Creutzfeldt-Jakob disease, suggests that αB-crystallin may have a protective function against fibrillar aggregation in non-lenticular tissue (Iwaki *et al*., 1991, Lowe *et al*., 1992, Renkawek *et al*., 1992, 1994). Characteristic of these diseases is the formation of amyloid plaques; from this it appears likely that chaperone proteins may potentially combat fibrillar aggregation by inhibiting hydrophobic main-chain interactions, and as a consequence plaque formation. This idea is supported by the over-expression of αB-crystallin accompanying amyloid-induced neurological diseases (van Rijk and Bloemendal, 2000), and it has been shown *in vitro* that a variety of sHsps, including α–crystallin, have been successful in preventing the aggregation of partially folded protein chains that form fibrils (Hatters *et al*., 2001, Rekas *et al*., 2004, Lee *et al*., 2006; Wilhelmus *et al*., 2006; Ecroyd *et al*., 2008).   Importantly, αB-crystallin inhibits the fibrillar aggregation of a number of disease related proteins *in vitro,* including A53T α-synuclein (characteristic of Parkinson's disease and Lewy body dementia), Aβ-peptide (characteristic of Alzheimer's disease) and β2-microglobulin (characteristic of dialysis-related amyloidosis) (Rekas *et al*., 2004; Raman *et al*., 2005; Wilhelmus *et al*., 2006).

The implied protective role of αB-crystallin *in vivo* suggests that a loss of αB-crystallin chaperone function may have pathological implications regarding fibrillar aggregation and protein misfolding diseases.

1.17 Structural changes affecting α-crystallin as a molecular chaperone

Investigation into the relationship between α-crystallin structure and function has focused primarily on the influence that exposed hydrophobicity exerts upon α-crystallin chaperone ability. As with much of the research regarding α-crystallin chaperone ability, however, a consensus is difficult to come by. The idea that exposed hydrophobicity directly influences chaperone ability has been commonly accepted since first proposed by Raman and Rao (1994), and has been used to explain α-crystallin behaviour under a variety of conditions, including thermal stress and chemical denaturation (Raman and Rao, 1994; Datta and Rao, 1999). Accordingly, exposed hydrophobicity has been generally held to be an intrinsic function of α-crystallin chaperone activity. sHsp–target protein binding is believed to be driven by non-specific hydrophobic interactions, and α-crystallin preferentially recognises hydrophobic non-native structures for interaction and protection from aggregation (Carver *et al.*, 1995; Das *et al.*, 1996; Rajaraman *et al.*, 1998; Treweek *et al.*, 2000; Carver *et al.*, 2002). The thermally induced increase in αA- and αB-crystallin chaperone ability at higher temperatures is accompanied by large-scale protein unfolding (and consequently increased exposed hydrophobicity), and these observations provide the primary evidence for the relationship between exposed α-crystallin hydrophobicity and

chaperone ability (Raman and Rao, 1994; Das and Surewicz, 1995; Datta and Rao, 1999). Despite this, there is an increasing body of evidence to suggest that exposed hydrophobicity does not directly correlate with chaperone ability (Kumar *et al.*, 2005). An increase in exposed α-crystallin hydrophobicity has been demonstrated variously to decrease (Santhoshkumar and Sharma, 2001) or have no effect (Smulders *et al.*, 1995) on α-crystallin chaperone ability, and it has been suggested that the relationship between exposed hydrophobicity and chaperone ability is more complex than initially proposed (Reddy *et al.*, 2006). As yet there is not a consensus opinion on the role of exposed hydrophobicity regarding the chaperone ability of α-crystallin and its subunits, and research continues to attempt to clarify this relationship.

As mentioned in Section 1.12, it is long believed that oligomerisation and subunit exchange is crucial for α–crystallin's ability to inhibit the aggregation of protein species (Plater *et al.*, 1996; Bova *et al.*, 1997; Avilov *et al.*, 2004). Recent studies seem to contradict this interpretation, suggesting that the rate of subunit-exchange has little influence on α-crystallin chaperone ability (Aquilina *et al.*, 2005), and that the α-crystallin oligomer is a functional chaperone unit (Augusteyn, 2004b). This interpretation is controversial, and the role of oligomerisation and subunit exchange in α-crystallin chaperone ability is currently under debate (Haslbeck *et al.*, 2005). The fact that the α-crystallin oligomer can function as a molecular chaperone without subunit dissociation *in vitro* does not necessarily demonstrate that the oligomer is the functional chaperone unit *in vivo*; further, there has been very limited comparison of the relative chaperone abilities of oligomeric and dissociated α-crystallin. There is, however, significant anecdotal evidence to support the role of un-dissociated α-

crystallin as a functional molecular chaperone *in vitro*. The size of stable αA- and αB-crystallin oligomers does not appear to influence chaperone ability (Böde *et al.*, 2003; Saha and Das 2004, 2007), for example, yet oligomer surface hydrophobicity appears to enhance chaperone ability (Böde *et al.*, 2003; Saha and Das, 2004). Additionally, almost half of α-crystallin's histidine residues are buried within the oligomeric structure, or else otherwise protected from solution, and this has been suggested to aid chaperone activity by increasing oligomeric surface hydrophobicity (Bera and Ghosh, 1996). While it is difficult to definitively state the importance of oligomeric dissociation in the chaperone activity of α-crystallin, it would appear that oligomeric, un-dissociated α-crystallin has a more significant role as a molecular chaperone than has been previously understood.

A variety of additional structural modifications have been implicated in the chaperone ability of α-crystallin and its subunits. Decreasing pH from pH 8.0 to 6.0 is accompanied by a decrease in α-crystallin α-helical content (Koretz, 1998), which has been suggested as a possible explanation for the decreased chaperone ability of α–crystallin at pH 6.0. Similarly, decreasing pH from pH 8.0 to 6.0 inhibits the ability of α-crystallin to withstand renaturation-induced aggregation (Koretz, 1998). The significant effect of post-translational modifications and single-point mutations on α-crystallin chaperone ability has been thoroughly covered earlier in this chapter. Modification of almost all regions of α-crystallin have been variously suggested to influence the ability of the protein to inhibit target protein aggregation, and it appears that almost all regions of the protein are implicated in its chaperone activity (Augusteyn, 2004a).

1.18 Extrinsic factors affecting α–crystallin chaperone activity

A number of external factors have similarly been demonstrated to influence the chaperone ability of α-crystallin. Amongst the most thoroughly investigated is the increase in α-crystallin chaperone ability with increasing temperature. It was initially believed that α-crystallin was an exceptionally thermally stable protein (Maiti *et al*., 1988), resisting morphological change until temperatures in excess of 100°C. It has subsequently been determined that α-crystallin undergoes a major thermally induced morphological change at 62°C (Raman and Rao, 1994; Surewicz and Olesen, 1995; Gesierich and Pfeil, 1996). Evidence suggests that the 62°C unfolding event actually begins at temperatures as low as 30°C (Raman and Rao, 1994; Datta and Rao, 1999), with significant unfolding from 50°C onwards (Datta and Rao, 1999; Reddy *et al*., 2000). Regardless, α-crystallin has been demonstrated to remain functional at temperatures in excess of 65°C (Lee *et al*., 1997b), and there is significant evidence to suggest that thermally unfolded α-crystallin has enhanced chaperone ability (Raman and Rao, 1994; Das and Surewicz, 1995). It is important to note that the effect of temperature on α-crystallin chaperone ability varies between target proteins; while the ability of α-crystallin to inhibit thermally-induced β_L-crystallin aggregation is thermally sensitive up to 55°C, its ability to inhibit the reduction-induced aggregation of insulin and α-lactalbumin is only thermally sensitive up to 35°C (Raman and Rao, 1994, Datta and Rao, 1999). Further, Lee *et al*. (1997b) showed that the ability of α-crystallin to inhibit the amorphous aggregation of alcohol dehydrogenase is essentially unchanged between 48°C and 70°C.

Thermotropic conformation changes at or around 62°C cause a relaxation of the tertiary structure of α−crystallin, such that it adopts a state similar to that of a molten globule (Gesierich and Pfeil, 1996). This molten globule state is characterised by the presence of elements of secondary structure, while significant tertiary structure is absent (Horwitz, 2003). It has been hypothesised that the resulting increase in hydrophobicity exposed to solution facilitates an increased ability to bind to partially folded proteins, and hence improves the chaperone activity of α-crystallin (Raman and Rao, 1994; Das and Surewicz, 1995; Datta and Rao, 1999). This is particularly the case with αA-crystallin, the chaperone activity of which is highly temperature sensitive. While αB-crystallin is up to four times as effective a molecular chaperone as αA-crystallin at temperatures less than 40°C, depending upon the target protein, above 55°C αA-crystallin is the more effective of the two chaperones (Reddy *et. al*, 2000).

The effect of pH on the chaperone ability of α−crystallin is relatively under-investigated. Studies have shown that oligomeric aggregates of the structurally unrelated but functionally similar extracellular chaperone clusterin disassociate under mildly acidic conditions (Poon *et al.*, 2002). Concomitantly, clusterin becomes a more effective chaperone, possibly as a consequence of partial clusterin unfolding (Poon *et al.*, 2002). The same study implied a correlation between pH and α-crystallin chaperone activity, but in this case the converse was found, with α−crystallin chaperone ability decreasing significantly at low pH values (Figure 1.10a). A similar study has revealed a decrease in the ability of α−crystallin to prevent γ-crystallin aggregation accompanying a decrease in pH (Figure 1.10b), which was accompanied by a loss of α-crystallin's α-helical secondary structure (Koretz *et al.*, 1998). Investigation

into the effect of pH on Hsp20 function supported the data of Koretz *et al.* and Poon *et al.*, and suggested that α-crystallin chaperone ability was diminished at pH 6.0 (Bukach *et al.*, 2004). Hsp20 chaperone activity decreased even more significantly than that of α-crystallin at pH 6.0, as a result of the formation of unstable, dissociated Hsp20 monomers.

The reduction of α-crystallin chaperone ability has significant pathological implications, as has been noted previously with α-crystallin post-translational modifications and mutations *in vivo*. If the chaperone ability of α-crystallin is significantly pH sensitive, the mildly acidic conditions in the lens nucleus (pH 6.7) may inhibit the chaperone function of α-crystallin. Given that aged and potentially modified proteins accumulate in the lens nucleus, and that age-related cataract is most prevalent in the nucleus, the influence of pH on the chaperone ability of α-crystallin may compromise its ability to maintain the transparency of aged lenses. Similarly, extra-lenticular fibrillar aggregation of some proteins is promoted at low pH, and is in some cases accompanied by localised acidosis (Yates *et al.*, 1990; Khandogin and Brooks, 2007); decreased α-crystallin chaperone ability at low pH may accordingly compromise the suggested protective function of extra-lenticular αB-crystallin *in vivo*. Investigating the structural and functional effect of pH on α-crystallin will help to better understand the role of α-crystallin in cataract formation, lens transparency and neurodegenerative disease *in vivo*.

Interestingly, it has recently been demonstrated that α-crystallin is able to suppress the formation of amyloid fibrils formed by β2-microglubulin at pH 2.5 (Raman *et al.,* 2005). Below pH 4.0 αA- and αB-crystallin aggregate size is

significantly reduced, and both subunits are relatively unfolded (Stevens and Augusteyn, 1993). Additionally, below pH 2.5 α-crystallin dissociates into αA- and αB-crystallin homopolymers (Augusteyn *et al.*, 1988). Whilst largely unfolded below pH 2.5, αA-crystallin still retains significant secondary structural elements (Stevens and Augusteyn, 1993). Conversely, αB-crystallin is almost entirely unfolded at this pH, and exists as denatured and largely unstructured monomers (Augusteyn *et al.*, 1988; Stevens and Augusteyn, 1993). A better understanding of α-crystallin chaperone ability at acidic pH may help to clarify the effect of mildly acidic pH on α-crystallin chaperone ability, and the physiological implications of this relationship.

A

B
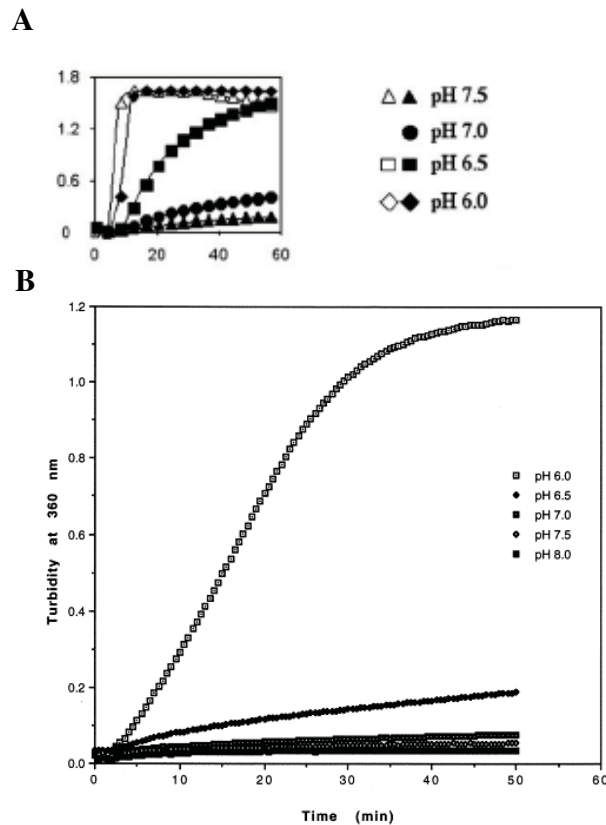
Figure 1.10 – Aggregation assays of thermally-stressed a) ovotransferrin (Poon *et al.*, 2002) and b) γ-crystallin (Koretz *et al.*, 1998) in the presence of α-crystallin, and between pH 6.0 and 8.0. In both studies, the ability of α-crystallin to inhibit protein aggregation is reduced at pH 6.0 and 6.5, compared to pH 7.0 and above. In a) Poon *et al.* (2002), open points represent aggregation in the absence of α-crystallin.

1.19 Target proteins affect α-crystallin chaperone ability

The effect of specific target proteins on the protective ability of molecular chaperones is often overlooked. This is particularly the case with α-crystallin, for which some argument exists over the effect of intrinsic and extrinsic factors on α-crystallin chaperone ability. In his now classic paper, in which α-crystallin was first determined to function as a molecular chaperone, Horwitz (1992) observed that α-crystallin

chaperone ability varied between target proteins; chaperone ability was higher for β_L- and γ- crystallin than for alcohol dehydrogenase, carbonic anhydrase B and a number of other enzymes (Horwitz, 1992). Despite this observation, investigations into α-crystallin chaperone activity frequently result in generalisations that do not take into account the nature of the target protein used for investigation. It has been observed, for example, that α-crystallin chaperone ability is thermally sensitive, and it is commonly stated that between 25°C and 60°C α-crystallin chaperone ability increases with increasing temperature (Raman and Rao, 1994; Das and Surewicz, 1995; Datta and Rao, 1999). While this is true for the thermally-induced aggregation of β_L-crystallin (Raman and Rao, 1994), the same study demonstrates that the ability of α-crystallin to inhibit the reduction-induced aggregation of insulin is only thermally sensitive between 25°C and 35°C. Similarly, studies have shown that α-crystallin's chaperone ability against alcohol dehydrogenase aggregation is essentially unchanged between 48°C and 70°C (Lee *et al.*, 1997b). In their frequently-referenced study, Das and Surewicz (1995) compared the ability of α-crystallin to inhibit the reduction-induced aggregation of α-lactalbumin at 37°C to its ability to inhibit the thermally-induced aggregation of β_L-crystallin at 60°C; from this rather indirect comparison, between differing target proteins (one of which was physiologically relevant) and stresses, it was concluded that α-crystallin chaperone ability was enhanced at 60°C compared to 37°C.

Similarly, exposed α-crystallin hydrophobicity is believed to increase α-crystallin chaperone ability (Raman and Rao, 1994; Das *et al.*, 1996); it has been observed, however, that depending upon the target protein and location of α-crystallin exposed hydrophobicity, α-crystallin chaperone ability can also be decreased

(Santhoshkumar and Sharma, 2001) or unaffected (Smulders *et al.*, 1995) by increased exposed hydrophobicity. Significantly, the rate of target protein aggregation has been shown to directly affect the chaperone ability of α-crystallin; rapid protein aggregation can outpace the binding of α-crystallin to aggregating proteins, and by doing so inhibit α-crystallin chaperone ability (Lindner *et al.*, 1997, 2001). Accordingly, α-crystallin chaperone may vary between target proteins as a consequence of aggregation rate. In a recent study, Ecroyd *et al.*, (2008) observed that phosphomimics increased the chaperone ability of αB-crystallin against β_L-crystallin, catalase, alcohol dehydrogenase and reduced and carboxymethylated (rcm) κ-casein, but decreased its chaperone ability against a ccβ-peptide mutant.

What are sometimes interpreted as conflicting results can often be explained by differences in the target proteins used between studies; consequently, it is important to take into account the target protein(s) used for investigation when making generalised statements about the chaperone ability of α-crystallin and other molecular chaperones. Ideally, investigation should canvas a number of target proteins, methods of stress and forms of aggregation, although this is obviously not always practical.

1.20 Cyclodextrins

Cyclodextrins (CDs) are a family of both naturally occurring and synthetic ring sugars, produced as a consequence of starch degradation by the enzyme CD glucosyltransferase. First identified towards the end of the 19th century (Villiers, 1891), CDs typically consist of 6 or more α 1-4 linked D-glucopyranose units arranged to

form a cyclic oligosaccharide ring. This arrangement results in a donut-like structure, with wide and narrow hydrophilic ends, and a large hydrophobic cavity lined with hydrogen molecules (Figure 1.11). The relative polarity of the wide and narrow ends of the molecule creates a preferential hydrophobic binding region within the CD annuli.

The large hydrophobic annulus of cyclodextrins facilitates the insertion of a diverse range of molecules and moieties, and it is this characteristic that makes cyclodextrins an attractive and extensive area of research. Both naturally occurring and synthetic cyclodextrins have been applied extensively to the food, cosmetic, pharmaceutical and pesticide industries (Szejtli, 1997; 1998; Easton and Lincoln, 1999), and areas of cyclodextrin research extend from physical and inorganic chemistry to biochemistry and thermodynamics (Easton and Lincoln, 1999). Cyclodextrin research is a particularly broad field; by 1997, over 15,000 papers had been printed on the topic (Szejtli, 1997), and thousands of tonnes of cyclodextrins are synthesised annually for industrial and research purposes (Szejtli, 1997; Easton and Lincoln, 1999) Insertion of a variety of moieties into the cyclodextrin cavity facilitates a variety of functions, including selectively increased or decreased reactivity, enhanced catalytic activity, molecular switching and a tentative molecular chaperone action (Camilleri *et al.*, 1994; Qin *et al.*, 2002; Danielsson *et al.*, 2004).

A

B

C
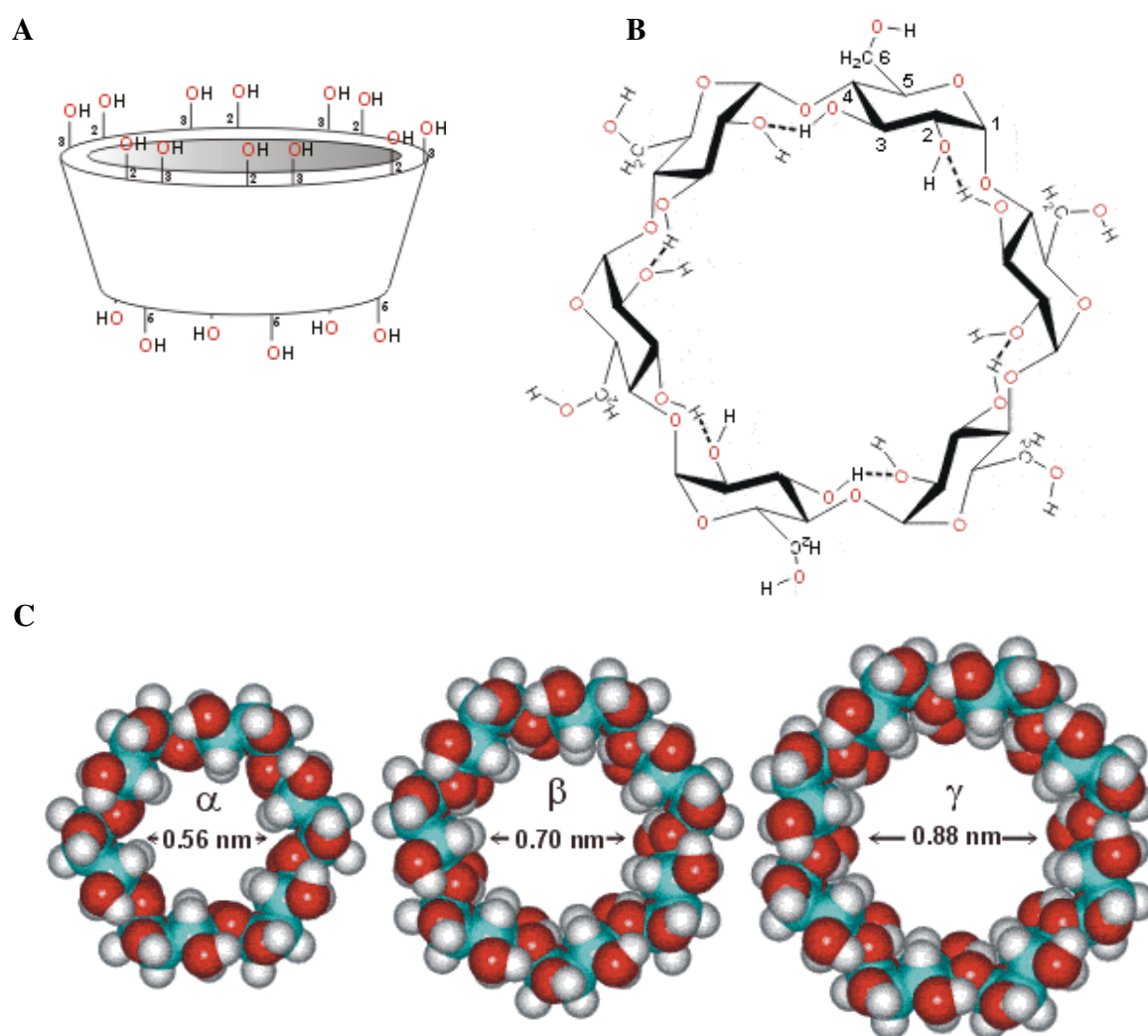
Figure 1.11 – Schematic representations of α-, β- and γ-cyclodextrin structure. a) Stylised representation of the truncated cone structure of βCD. Polar hydroxyl groups at the wide and narrow ends of the truncated cone create a relatively hydrophobic interior cavity. The hydrophobicity of this cavity is important for cyclodextrin binding to biological moieties. b) The chemical structure of βCD, consisting of 7 D-glucopyranose rings arranged around a hollow central cavity. c) 3D molecular models of α-, β and γCD, demonstrating the hollow cyclodextrin annulus and the approximate annulus widths of each cyclodextrin. The 0.7nm width of the βCD annulus is ideal for the insertion of aromatic residues.

1.21 Biological activity of cyclodextrins

Of the commonly used cyclodextrins, βCD is the most extensively utilised for biological applications. The reason for βCD's increased reactivity over αCD or γCD is not fully understood, but it has been suggested that the annulus width of βCD is the most suited to the insertion of biological moieties, particularly aromatic side-chains (Qin *et al.*, 2002). βCD has been extensively characterised as a synthetic molecular chaperone, but there is only limited evidence to suggest that βCD can effectively inhibit the aggregation of target proteins on the off-folding pathway (Tavornvipas *et al.*, 2004). Rather, the primary chaperone activity of βCD appears to be in ensuring the correct refolding of denatured proteins, in a manner similar to Hsp70 or GroEL. By this method, proteins are significantly denatured (by urea or GuHCl, for example) over an extended time frame (generally 24hrs), after which the dissociating chemical is diluted out. This facilitates refolding, but generally results in misfolding and protein aggregation; it is important to note that aggregation of this type occurs on the folding/unfolding pathway, and is distinct from aggregation on the off-folding pathway. Aggregation of carbonic anhydrase B (CAB) and insulin by this method can be inhibited by up to 90% in the presence of βCD at a 50:1 molar ratio of βCD to target protein (Karuppiah and Sharma, 1995). Additionally, chaperone protection via βCD has been shown to effectively re-fold target proteins, returning normal protein function by up to 90% (Karuppiah and Sharma, 1995). Structural and kinetic studies of βCD-protein interaction during aggregation suggest that chaperone binding requires a high level of solvent exposure of target protein binding sites (Aachmann *et al.*, 2003).

Dissociation would allow for a high degree of target protein solvent exposure prior to re-association, and so might explain why the βCD chaperone action prefers the dissociation/re-association method of protein aggregation. Studies have also demonstrated that it is primarily aromatic side chains, rather than generalised hydrophobic regions, that interact with cyclodextrin molecules via insertion into the hydrophobic annulus (Oh *et al*., 1998; Otzen *et al*., 2002; Aachmann *et al*., 2003, Danielsson *et al*., 2004).

While βCD can effectively refold unfolded or denatured proteins, research in this area has focused on a two-step artificial chaperone mechanism, utilising an additional chaperone to initially capture unfolding proteins. The additional chaperone, typically a detergent or synthetic hydrogen nanogel, sequesters stressed, molten globule protein intermediates to prevent aggregation in a manner reminiscent of sHsps *in vivo* (Rozema and Gelman, 1996; Daugherty *et al*., 1998; Kazunari *et al*., 1998; Nomura *et al*., 2003). Cyclodextrin molecules then strip the target protein from the stable nanogel-target protein complex and facilitate correct refolding and a return of protein function. CAB studies have demonstrated a return of function in excess of 85% via this two-step refolding method (Akiyoshi *et al*., 1998; Nomura *et al*., 2003).

So far, surprisingly little research has been directed towards the role of cyclodextrins in inhibiting amyloid fibril formation. A two-stage mechanism involving nanogels and βCD-refolding has been demonstrated to effectively inhibit the aggregation of Aβ-peptide (Ikeda *et al*., 2006), but more exciting is the observation that cyclodextrins can inhibit the fibrillar aggregation of Aβ-peptide on their own (Camilleri *et al*., 1994; Qin *et al*., 2002; Danielsson *et al*., 2004). βCD significantly inhibits Aβ-

peptide amyloid fibril formation, while αCD and γCD are largely ineffective (Qin *et al.*, 2002), and by doing so has been shown to diminish Aβ-peptide cytotoxicity in PC12 cells (Camilleri *et al.*, 1994). NMR spectroscopy suggests that βCD chaperone action is facilitated by the binding of aromatic side chains to the βCD annulus (Qin *et al.*, 2002; Camilleri *et al.*, 1994). βCD-Aβ-peptide interaction occurs via Phe19 and Phe20 on the Aβ-peptide, and an Aβ-peptide mutant without phenylalanine residues was completely unable to bind βCD (Danielsson *et al.*, 2004), emphasising the importance of aromatic residue binding in the chaperone action of cyclodextrins.

1.22 Project aims

This study extends investigations into the relationship between pH variance and the effectiveness of α-crystallin as a molecular chaperone, and aims to characterise any changes in the protein's structure accompanying an alteration in pH. Specifically, the effect of pH on the chaperone ability of α–crystallin and its subunits will be examined via its ability to inhibit heat-induced amorphous aggregation, reduction-induced amorphous aggregation and fibrillar aggregation. Changes to α-crystallin secondary and quaternary structure will be observed via spectrophotometric and biophysical techniques including Thioflavin T binding, intrinsic and extrinsic fluorescence, size exclusion chromatography and transmission electron microscopy. The possible pH dependence of α–crystallin's chaperone ability may have significant physiological implications with regard to the maintenance of lens transparency, due to the observed pH gradient across the lens. The nucleus of the lens is significantly more acidic than

epithelial or cortical lens cells (Mathias *et al.*, 1991; Eckert, 2001); while epithelial cells have a measurable pH of up to pH 7.2 (Bassnett and Duncan, 1985), the pH of the lens nucleus has been estimated to be as low as pH 6.7 or 6.5 (Bassnett and Duncan, 1987; Eckert, 2001). As there is no protein turnover in lens fibre cells, and aged fibre cells accumulate in the nucleus, the protein content of the nucleus consists primarily of aged and possibly modified lens proteins (Bloemendal, 1981). A reduction of α-crystallin chaperone ability in the lens nucleus, as a consequence of pH sensitivity, may significantly affect the transparency of the aging lens. The pH dependence of α-crystallin chaperone activity is similarly physiologically significant in regards to the suppression of extra-lenticular amyloid fibril formation, which for a number of proteins is promoted by acidic conditions (Lai *et al.,* 1996, You and Cheng, 2001, Khandogin and Brooks, 2007).

Additionally, the role of cyclodextrins as a possible molecular chaperone and refolding agent will be investigated. The possible co-operative relationship between cyclodextrins and α-crystallin to create a two-step refolding model will be investigated using thermally stressed molecular enzymes. Further, the ability of cyclodextrins to directly inhibit amorphous and fibrillar aggregation will be invested to determine the potential use of cyclodextrins as molecular chaperones. Cyclodextrin chaperone ability may suggest potential therapeutic applications *in vivo* as anti-amyloid molecules (Camilleri *et al.*, 1994; Qin *et al.*, 2002; Danielsson *et al.*, 2004).

The breakdown of each chapter of this thesis is as follows;

Chapter 3 - Looks at the relationship between pH and the chaperone ability of α_T- (total α-crystallin, containing both αA- and αB-crystallin subunits), αA-

and αB-crystallin between pH 6.0 and 8.0. This investigation utilises four target proteins representing three distinct forms of protein aggregation; thermal-stress amorphous aggregation (catalase and β_L-crystallin), reduction stress amorphous aggregation (α-lactalbumin) and thermal stress fibrillar aggregation (rcm κ-casein). Data demonstrate a clear correlation between pH and chaperone ability for α_T-, αA- and αB-crystallin between pH 6.0 and 8.0, whereby α-crystallin is a more effective chaperone of amorphous aggregation at pH 7.0 and above than at pH 6.0 and pH 6.5.

Chapter 4 – Characterises changes to α-crystallin structure between pH 6.0 and 8.0. Structural characterisation methods included intrinsic, ANS and ThT fluorescence, size exclusion FPLC and transmission electron microscopy. The investigation demonstrates a general loss of secondary structure and partial unfolding of α_T-, αA- and αB-crystallin as the pH decreased from pH 8.0 to 6.0. Interestingly, pH had little or no effect on the quaternary structure of α-crystallin. The extent to which these gross structural changes are responsible for the pH-sensitive chaperone ability of α-crystallin, however, is uncertain. As αA- and αB-crystallin are significantly unfolded below pH 3.5, investigation of αA- and αB-crystallin chaperone ability at this pH range was used to further understand the relationship between chaperone ability and pH-induced unfolding. Investigation demonstrated no clear relationship between pH and chaperone ability between pH 2.0 and 3.5.

Chapter 5 – Investigates the relationship between pH and α-crystallin thermal stability. The pH-sensitivity of αA- and αB-crystallin chaperone ability appears

to be more pronounced at higher temperatures, and at pH 6.0 and temperatures above 55°C α_T-, αA- and αB-crystallin form unstable complexes with aggregating target proteins. Consequently, pH-influenced thermal stability may be partially responsible for the pH-sensitivity of α-crystallin chaperone ability. Further investigation demonstrates that pH directly affects α_T-crystallin thermal stability, with lower pH resulting in an increased propensity for aggregation at elevated temperatures.

Chapter 6 – Investigates the role of histidine protonation in the chaperone activity of αB-crystallin. Histidine itself has a pKa of 6.5, and so protonation of histidine residues may be implicated in decreased αB-crystallin chaperone ability below pH 7.0. Inhibiting the protonation of exposed histidine residues largely removed the pH sensitivity of αB-crystallin chaperone ability, suggesting that histidine protonation is responsible for decreased αB-crystallin chaperone ability at pH 6.0 and 6.5. However, mutation of a single conserved histidine residue in the αB-crystallin chaperone-binding region, H83A, has no effect on αB-crystallin chaperone ability below pH 7.0, implying that the protonation of this residue is not directly responsible for the pH sensitivity of αB-crystallin chaperone ability.

Chapter 7 – Investigates the role of cyclodextrins as molecular chaperones and protein refolding agents. While βCD appears to have very limited ability to inhibit amorphous protein aggregation, and is unable to co-operate with α_T-crystallin as part of a two-step refolding mechanism, it demonstrated a significant ability to inhibit the fibrillar aggregation of rcm κ-casein, β-

lactoglobulin, α-lactalbumin and both wild-type and A53T α-synuclein. βCD was the more effective of the three cyclodextrins investigated. The ability of cyclodextrins to inhibit fibrillar, but not amorphous aggregation, suggests an amyloid-specific cyclodextrin chaperone mechanism.

Chapter 8 – Attempts to characterise the chaperone binding mechanism of βCD to target proteins, and in doing so better understand the differences between the amorphous and fibrillar aggregation of target proteins. Intrinsic fluorescence, ANS-binding, far UV circular dichroism and competitive chaperone assays enabled the development of a putative model for βCD chaperone ability, based around the insertion of exposed aromatic side chains on target proteins into the βCD cavity.

CHAPTER 2

MATERIALS AND METHODS

Chapter 2 - Materials and Methods

2.1 Reagents

A complete list of reagents suppliers used in studies described in this thesis is given in Appendix A

2.2 Chapter 3 methods

2.2.1 Purification of α_T-, and β_L- crystallin

Frozen lenses from calves less than one year old were prepared according to the method of Horwitz (1992). Lenses were thawed, decapsulated and homogenised in 3ml of 100mM Tris homogenising buffer (0.04% NaN_3, pH 7.2) per lens. The homogenised fraction was then centrifuged on a Beckman Allegra 21-R centrifuge at 12000 rpm for 15 minutes. The supernatant was extracted and separated on a HiPrep sephacryl S300 size exclusion chromatography column with dimensions 26mm x 600mm, in 50mM Tris buffer (0.04% NaN_3, pH 7.2). Protein content was detected via absorbance at 280nm using an Akta FPLC purification system. The resulting chromatograph was analysed to identify the α_T- and β_L-crystallin fractions. Other crystallin fractions not of interest to this study were discarded. Fractions were concentrated using an Amicon concentrator and a millipore regenerated cellulose membrane (NMWL <30,000) until <10ml samples were obtained. Concentrated fractions were placed in dialysis tubing and left in 3L of MilliQ water overnight with no water changes to remove excess Tris

buffer. The dialysed protein was then freeze-dried overnight in a Christ Alpha 1-4 freeze drier. The purity of the freeze-dried proteins was analysed via SDS-PAGE.

2.2.2 Purification of αA−crystallin

Human recombinant αA-crystallin was purified via a variation of the method described by Santhoshkumar and Sharma (2006). Competent BL21(DE3) *e. coli* containing the human αA-crystallin gene in a pEG23d plasmid template were plated out on ampicillin-selective agar plates and incubated overnight at 37°C. From this single colonies were grown overnight in 50ml sterile Louria Broth (LB) containing 10mM ampicillin. 20ml aliquots were transferred to 0.5L LB and grown to log phase, at which point 0.5mg/ml IPTG was added to induce αA-crystallin expression. Induction was allowed to continue for four hours.

Cell suspensions were spun down in a Beckman Allegra 21-R centrifuge at 6000rpm for 15 minutes at 4°C, and cell pellets lysed using the sequential addition of lysozyme, deoxycholic acid and DNAse I. Cell lysate was further purified via the addition of 50mM DTT and PEI. Proteins present in cell lysate were precipitated via sequential ammonium sulphate precipitation (25% and 35%), and the 35% precipitate re-dissolved in 50mM Tris buffer (0.04% NaN_3, pH 7.2). The re-suspended precipitate was purified via size exclusion chromatography over a HiPrep sephacryl S300 size exclusion chromatography column in 50mM Tris buffer (0.04% NaN_3, pH 7.2). The purified αA-crystallin peak was concentrated using an Amicon concentrator and a millipore regenerated cellulose membrane (NMWL <30,000) until <10ml samples were

obtained. Concentrated fractions were placed in dialysis tubing and left in 3L of MilliQ water overnight with no water changes to removed excess Tris buffer. The dialysed protein was then freeze-dried overnight in a Christ Alpha 1-4 freeze drier. The purity of the freeze-dried proteins was analysed via SDS-PAGE.

2.2.3 Purification of αB–crystallin

Human recombinant αB-crystallin was purified via the method described for αA-crystallin above. Competent BL21(DE3) *e. coli* containing the human αB-crystallin gene in a pET20b(+) plasmid template were plated out on kanamycin-selective agar plates and incubated overnight at 37°C. From this single colonies were grown overnight in 50ml sterile LB containing 10mM kanamycin. 20ml aliquots were transferred to 0.5L LB and grown to log phase, at which point 0.5mg/ml IPTG was added to induce αB-crystalliin expression. Induction was allowed to continue for 4 hours.

Cell suspensions were spun down in a Beckman Allegra 21-R centrifuge at 6000rpm for 15 minutes at 4°C, and cell pellets lysed using the sequential addition of lysozyme, deoxycholic acid and DNAse I. Cell lysate was further purified via the addition of 50mM DTT and PEI. Proteins present in cell lysate were precipitated via sequential ammonium sulphate precipitation (25% and 35%), and the 35% precipitate re-dissolved in 50mM Tris buffer (0.04% NaN_3, pH 7.2). The re-suspended precipitate was purified via size exclusion chromatography over a HiPrep sephacryl S300 size exclusion chromatography column in 50mM Tris buffer (0.04% NaN_3, pH 7.2). The purified αB-crystallin peak was concentrated using an Amicon concentrator and a

millipore regenerated cellulose membrane (NMWL <30,000) until <10ml samples were obtained. Concentrated fractions were placed in dialysis tubing and left in 3L of MilliQ water overnight with no water changes to removed excess Tris buffer. The dialysed protein was then freeze-dried overnight in a Christ Alpha 1-4 freeze drier. The purity of the freeze-dried proteins was analysed via SDS-PAGE.

2.2.4 Reduction and carboxymethylation of κ-casein

Reduction and carboxylation of κ-casein was undertaken via a variation of the method of Shechter *et al*., (1973). 50mg/ml κ-casein was dissolved in 5ml of 1M Tris buffer (8M urea, pH 9.0). 30mg DTT was added to κ-casein and incubated for 1hr at room temperature (with stirring) to facilitate reduction. Carboxymethylation was achieved via incubation with 150mg iodoacetic acid for 20 minutes (with stirring). Reduced and carboxmethylated (rcm) κ-casein was purified via gel filtration using a Sephadex G-75 desalting column, and eluted using 0.05M ammonium bicarbonate. Purified rcm κ-casein was freeze-dried overnight in a Christ Alpha 1-4 freeze drier. The purity of the freeze-dried proteins was analysed via SDS-PAGE.

2.2.5 SDS-PAGE of purified proteins

Samples for SDS-PAGE were dissolved at a concentration of 1mg/ml in 15 μl MilliQ water and added to 15μl SDS loading dye. The samples were heated to 100°C for 1-2 minutes to facilitate protein denaturation and loaded onto a 15% polyacrylamide gel.

Electrophoresis was run at 150 volts until the dye reached the bottom of the gel. The gel was then soaked in coomassie blue (0.025 % Coomassie Blue R-250 (w/v), 30 % methanol, 10 % glacial acetic acid) for 30 minutes to stain the protein bands, and destained by rocking overnight in destain solution (30% methanol, 10% glacial acetic acid).

2.2.6 Thermal-stress induced amorphous aggregation

The ability of α_T, αA and αB–crystallin to inhibit the aggregation of catalase and β_L-crystallin under thermal stress conditions was monitored using a FluoStar plate reader, with light scattering at 340nm measured as an indication of protein aggregation. Assays were carried out on 400μg/ml catalase samples and 600μg/ml β_L-crystallin samples in 50mM phosphate buffer (0.04% NaN$_3$) and at pH values of 6.0, 6.5, 7.0, 7.5 and 8.0. Samples were analysed in 96 well plates. α–Crystallin was added to each sample at either 0:1, 0.2:1, 0.5:1 or 1:1 molar ratio with the target protein. For catalase samples, samples were incubated at 55°C, with light scattering at 340nm measured every minute for ninety minutes. For β_L-crystallin samples, samples were incubated at 60°C, with light scattering at 340nm measured every minute for ninety minutes. Light scatter was plotted versus time to observe the effect of increased α-crystallin concentration on target protein aggregation.

2.2.7 Reduction-stress induced amorphous aggregation

The ability of α_T, αA and αB-crystallin to inhibit the amorphous aggregation of α–lactalbumin under reduction stress conditions was monitored using a FluoStar plate reader, with light scattering at 340nm measured as an indication of protein aggregation. Assays were carried out on 500μg/ml α–lactalbumin samples in 50mM phosphate buffer (0.04% NaN_3, 10mM NaCl, 10mM TCEP) and at pH values of 6.0, 6.5, 7.0, 7.5 and 8.0. Samples were analysed in 96 well plates. Crystallins was added to each sample at either 0:1, 0.2:1 or 0.5:1 molar ratio with the target protein. Samples were incubated at 37°C, with light scatter at 340nm measured every minute for 120 minutes. Light scattering was plotted versus time to observe the effect of increased crystallin concentration on protein aggregation.

2.2.8 Thermal-stress induced fibrillar aggregation

The ability of α_T, αA and αB–crystallin to inhibit the fibrillar aggregation of rcm κ-casein was monitored using a FluoStar plate reader, with thioflavin T- (ThT) associated fluorescence (440nm excitation; 490nm emission) measured as an indication of protein aggregation. Assays were carried out on 1mg/ml rcm κ-casein samples in 50mM phosphate buffer (0.04% NaN_3, 50mM ThT) and at pH values of 6.0, 7.0 and 8.0. Samples were analysed in 96 well plates. α-Crystallin was added to each sample at either 0:1 or 0.5:1 molar ratio with the target protein. Samples were incubated at 37°C, and ThT-associated fluorescence was measured *in situ* every 10 minutes for 20 hours.

ThT-associated fluorescence was plotted versus time, and change in ThT-associated fluorescence over time was plotted to observe the effect of increased α-crystallin concentration on protein aggregation.

2.3 Chapter 4 methods

2.3.1 Intrinsic tryptophan fluorescence of crystallins

Purified $α_T$, αA or αB-crystallin was dissolved in 50mM phosphate buffer (0.04% NaN_3) at pH 6.0, 6.5, 7.0, 7.5 and 8.0, and at a concentration of 200μg/ml. 2 ml samples were incubated for 1 hour at room temperature. Samples were loaded into 10mm path length glass cuvettes, and intrinsic tryptophan emission fluorescence of each sample measured at wavelengths between 300 and 450nm via Hitachi F-4500 fluorescence spectrophotometer. Excitation was at 280nm. Maximum fluorescence intensity was plotted versus wavelength for each sample pH value, as well as $λ_{max}$ versus pH.

2.3.2 ANS binding of crystallins

Purified $α_T$, αA or αB-crystallin was dissolved in 50mM phosphate buffer (0.04% NaN_3) at pH 6.0, 6.5, 7.0, 7.5 and 8.0, and at a concentration of 200μg/ml. 1.7ml samples were incubated with 300μl of 10μM 1-anilino-8-napthalene sulfonate (ANS) solution for 1 hour at room temperature. Samples were loaded into 10mm path length glass cuvettes, and ANS associated fluorescence intensity was measured between 400 and 450nm via Hitachi F-4500 fluorescence spectrophotometer. Fluorescence intensity

was plotted versus wavelength for each sample to determine λ_{max}. Following this, 30μl aliquots of 10μM ANS stock solution was titrated with fresh 2ml α-crystallin samples, and fluorescence at 450nm (λ_{max}) measured via Hitachi F-4500 fluorescence spectrophotometer after each addition of ANS. Excitation was at 387nm. Fluorescence was plotted versus ANS volume, and maximum fluorescence determined as the mean intensity of the plateau region of the plot. Mean ANS-associated fluorescence was plotted versus pH.

2.3.3 Thioflavin T binding of crystallins

Purified α_T, αA or αB-crystallin was dissolved in 150μM ThT in 50mM phosphate buffer (0.04% NaN_3) at pH 6.0, 6.5, 7.0, 7.5 and 8.0, and at a concentration of 200μg/ml protein. 2ml α-crystallin samples were loaded into 10mm path length glass cuvettes, and fluorescence intensity was measured via Hitachi F-4500 fluorescence spectrophotometer for each sample at an excitation wavelength of 440nm and emission wavelength of 490nm. Samples were acquired for thirty seconds, and fluorescence intensity measured as the average of thirty readings over this thirty-second period. Fluorescence intensity was plotted versus pH for each sample.

2.3.4 Transmission electron microscopy of crystallins

Purified α_T, αA or αB-crystallin was dissolved in 5mM phosphate buffer (0.04% NaN_3) at pH 6.0, 6.5, 7.0, 7.5 and 8.0, and at a protein concentration of 1mg/ml. 3μl samples

from each pH treatment were coated onto formvar and carbon-coated nickel TEM grids prepared previously. Grids were washed three times with 10 μl milliQ water and negatively stained with 10 μl uranyl acetate (2% w/v). Samples were viewed on a Philips CM100 transmission electron microscope under 64Kx magnification at a 100kV exceleration voltage.

2.3.5 Size exclusion fast protein liquid chromatography of crystallins

Purified α_T, αA or αB-crystallin was dissolved in 50mM phosphate buffer at pH 6.0, 7.0 and 8.0 at a protein concentration of 0.25μg/ml. 300μl samples were incubated for 1hr at room temperature. Size exclusion fast protein liquid chromatography (SEFPLC) data was acquired via an AKTA FPLC purification system using a HiPrep superose Super200 chromotography column, with dimensions 10mm by 300mm. Protein elution was monitored via absorbance at 280nm. Absorbance at 280nm was plotted versus time for each pH value.

2.3.6 The relationship between target protein aggregation rate and crystallin chaperone ability

The influence of the rate of target protein aggregation on α_T-, αA- and αB-crystallin chaperone ability was investigated by plotting percentage protection values from Sections 3.2.1-2 against the corresponding target protein aggregation rate (0:1 molar ratio crystallin : target protein). Data was plotted for α_T-, αA- and αB-crystallin against

the aggregation of catalase, β_L-crystallin and α-lactalbumin. A statistically significant relationship between the rate of target protein aggregation and percentage protection was determined by linear, logarithmic or exponential fits to the data with an r^2 value above 0.6.

2.3.7 Reduction- and thermal-stress induced amorphous aggregation at acidic pH

The ability of α_T- and αB-crystallin to inhibit the amorphous aggregation of α-lactalbumin under reduction- and thermal-stress conditions and at low pH was monitored using a FluoStar plate reader, with light scattering at 340nm measured as an indication of protein aggregation. Assays were carried out on 1.2mg/ml α–lactalbumin samples in 50mM glycine buffer (0.04% NaN$_3$, 20mM TCEP) and at pH values of 2.0, 2.5, 3.0 and 3.5. Samples were analysed in 96 well plates. Crystallins were added to each sample at either 0:1, 0.2:1 or 0.5:1 molar ratio with the target protein. Samples were incubated at 55°C, with light scatter at 340nm measured every minute for 120 minutes. Light scatter was plotted versus time to observe the effect of increased crystallin concentration on protein aggregation.

2.4 Chapter 5 methods

2.4.1 α_T-Crystallin aggregation with temperature

α_T–Crystallin thermal stability was monitored via absorbance at 340nm using a JASCO J810 circular dichroism spectrophotometer. This instrument was used instead of a UV-

vis spectrophotometer as it had the necessary software to measure absorbance with increasing temperature. 3 ml α_T-crystallin samples at pH 6.0, 7.0 and 8.0 were prepared at 0.5mg/ml. Samples were incubated for 5 minutes at 35°C for temperature equilibration. Absorbance at 340nm was read between 35°C and 90°C, with measurements taken every 0.1°C. Temperature increased at a rate of 1°C/minute. Light scattering at 340nm was plotted versus temperature, and compared between pH values.

2.4.2 α_T-Crystallin aggregation with time

α_T–Crystallin thermal stability was further monitored using a FluoStar plate reader, with light scattering at 340nm measured as an indication of protein aggregation. Assays were carried out on 200μg/ml crystallin samples in 50mM phosphate buffer (0.04% NaN$_3$) and at pH values of 6.0, 6.5, 7.0, 7.5 and 8.0. Samples were analysed in 96 well plates. Samples were incubated at 37°C, 45°C or 55°C, with light scattering at 340nm measured every minute for ninety minutes. Light scattering was plotted versus time to observe the thermal stability of α_T-crystallin at 37°C, 45°C and 55°C.

2.4.3 Thermal stress amorphous aggregation

The effect of temperature on the ability of αA- and αB–crystallin to inhibit the aggregation of catalase under thermal stress conditions was monitored using a FluoStar plate reader, with light scattering at 340nm measured as an indication of protein aggregation. Assays were carried out under conditions identical to those described in

Section 2.2.6, with the exception that assays were conducted at 45°C. Light scatter was plotted versus time and compared to data acquired in Section 3.3.1, in order to determine the effect of temperature on crystallin chaperone activity, as influenced by pH.

2.5 Chapter 6 methods

2.5.1 Modification of surface-exposed αB-crystallin histidine residues via diethylpyrocarbonate

The surface-exposed histidine residues of human αB-crystallin were modified using a variation of the method described by Pal and Ghosh (1998). Human recombinant αB-crystallin was purified via the method described in Section 2.1.3. Purified αB-crystallin (50mM phosphate buffer, 0.04% NaN_3) was incubated with a 600x molar excess of DEPC for 2hrs at room temperature to facilitate the binding of DEPC to exposed histidine residues. DEPC binding was quantified via absorbance at 240nm.

The chaperone ability of DEPC-bound αB-crystallin was immediately determined by observing its ability to suppress the thermally-induced aggregation of catalase at 55°C, as described in Section 2.2.6. Chaperone ability was investigated at pH 6.0, 6.5, 7.0, 7.5 and 8.0, and at a 0.2:1 molar ratio of chaperone to target protein. Chaperone ability was observed for unbound DEPC, αB-crystallin, and DEPC-bound αB-crystallin. The chaperone abilities of unbound DEPC and αB-crystallin were summed to create a 'theoretical' percentage protection value that was compared to the

chaperone ability of DEPC-bound αB-crystallin, to determine if DEPC-induced

modification of αB-crystallin resulted in a change in chaperone ability.

2.5.2 ClustalW sequence homology analysis of αA- and αB-crystallin

A blastp sequence similarity search of the Swiss-Prot and TrEMBL databases was run

against human αB-crystallin (primary accession number P02511), accepting the twenty

closest similarity matches. The homology of these twenty sequences was determined

using ClustalW multiple sequence alignment (opening and end gap penalty = 10,

extending and separation gap penalty = 0.05). Additionally, sequence homology of the

ten known human sHsps was determined using ClustalW multiple sequence alignment

(opening and end gap penalty = 10, extending and separation gap penalty = 0.05), with

sHsp sequences acquired from the Swiss-Prot and TrEMBL databases. For a complete

list of primary accession numbers, see Appendix B.

2.5.3 Purification of H83A αB-crystallin

Human recombinant H83A αB-crystallin was purified via the method described for

αA-crystallin in Section 2.2.2. Competent BL21(DE3) *e. coli* containing the mutant

human H83A αB-crystallin gene in a pEG23d plasmid template were plated out on

ampicillin-selective agar plates and incubated overnight at 37°C. From this single

colonies were grown overnight in 50ml sterile LB containing 10mM ampicillin. 20ml

aliquots were transferred to 0.5L LB and grown to log phase, at which point 0.5mg/ml

IPTG was added to induce H83A αB-crystallin expression. Induction was allowed to continue for 4 hours.

Cell suspensions were spun down in a Beckman Allegra 21-R centrifuge at 6000rpm for 15 minutes at 4°C, and cell pellets lysed using the sequential addition of lysozyme, deoxycholic acid and DNAse I. Cell lysate was further purified via the addition of 50mM DTT and PEI. Proteins present in cell lysate were precipitated via sequential ammonium sulphate precipitation (25% and 35%), and the 35% precipitate re-dissolved in 50mM Tris buffer (0.04% NaN_3, pH 7.2). The re-suspended precipitate was purified via size exclusion chromatography over a HiPrep sephacryl S300 size exclusion chromatography column in 50mM Tris buffer (0.04% NaN_3, pH 7.2). The purified H83A αB-crystallin peak was concentrated using an Amicon concentrator and a millipore regenerated cellulose membrane (NMWL <30,000) until <10ml samples were obtained. Concentrated fractions were placed in dialysis tubing and left in 3L of MilliQ water overnight with no water changes to removed excess Tris buffer. The dialysed protein was then freeze-dried overnight in a Christ Alpha 1-4 freeze drier. The purity of the freeze-dried proteins was analysed via SDS-PAGE.

2.5.4 Thermal-stress induced amorphous aggregation

The ability of H83A αB-crystallin to inhibit the aggregation of catalase under thermal-stress conditions was monitored using a FluoStar plate reader, with light scattering at 340nm measured as an indication of protein aggregation. Assays were carried out on 400μg/ml catalase samples in 50mM phosphate buffer (0.04% NaN_3) and at pH values

of 6.0, 6.5, 7.0, 7.5 and 8.0. Samples were analysed in 96 well plates. H83A αB-crystallin was added to each sample at either 0:1, 0.2:1 or 0.5:1 molar ratio with the target protein. Samples were incubated at 45°C, with light scattering at 340nm measured every minute for ninety minutes. Light scattering was plotted versus time to observe the effect of increased α-crystallin concentration on protein aggregation.

2.5.5 Reduction-stress induced amorphous aggregation

The ability of H83A αB-crystallin to inhibit the amorphous aggregation of α–lactalbumin under reduction stress conditions of was monitored using a FluoStar plate reader, with light scattering at 340nm measured as an indication of protein aggregation. Assays were carried out on 500μg/ml α–lactalbumin samples in 50mM phosphate buffer (0.04% NaN_3) and at pH values of 6.0, 6.5, 7.0, 7.5 and 8.0. Samples were analysed in 96 well plates. H83A αB-crystallin was added to each sample at either 0:1, 0.2:1 or 0.5:1 molar ratio with the target protein. Samples were incubated at 37°C, with light scattering at 340nm measured every minute for 120 minutes. Light scattering was plotted versus time to observe the effect of increased crystallin concentration on protein aggregation.

2.6 Chapter 7 methods

2.6.1 βCD-induced refolding of catalase

The ability of βCD to refold thermally denatured catalase in conjunction with α_T-crystallin was monitored via the return of catalase enzymatic activity after thermal-stress. Thermally-induced catalase aggregation was monitored via light scattering at 340nm as described in Section 2.2.6. α_T-Crystallin was added to aggregating catalase at a 1:1 molar ratio to entirely inhibit catalase aggregation, and samples were incubated for 120 minutes to ensure the complete aggregation of α_T-crystallin-free catalase. After incubation, βCD was added to both α_T-crystallin bound and α_T-crystallin free catalase samples at a 100x molar excess, and incubated for 24hrs via the method described by Akiyoshi *et al*. (1999). Catalase enzymatic activity was monitored via the degradation of hydrogen peroxide (H_2O_2). H_2O_2 degradation was measured via light scattering at 240nm on a FluoStar plate reader. Enzymatic activity was compared between native catalase, thermally-stressed catalase (with or without incubation with βCD) and catalase thermally stressed in the presence of α_T-crystallin (with or without incubation with βCD), to determine if a combination of α_T-crystallin and βCD could facilitate the refolding of thermally-stressed catalase.

2.6.2 βCD and amorphous aggregation

The ability of βCD to inhibit the aggregation of catalase under thermal stress conditions and insulin under reduction stress conditions was monitored using a FluoStar plate

reader, with light scattering at 340nm measured as an indication of protein aggregation. Catalase assays were carried out at a concentration of 400μg/ml in 50mM phosphate buffer (0.04% NaN_3, pH 7.5). Insulin assays were carried out at a concentration of 500μg/ml in 50mM phosphate buffer (0.04% NaN_3, 20mM DTT, pH 7.5). Samples were analysed in 96 well plates. βCD was added to each sample at either 0:1, 5:1, 10:1, 25:1 or 50:1 molar ratio with the target protein. For catalase aggregation, samples were incubated at 55°C, with light scattering at 340nm measured every minute for ninety minutes. For insulin samples, samples were incubated at 37°C, with light scattering at 340nm measured every minute for sixty minutes. Light scattering was plotted versus time to observe the effect of increased βCD concentration on protein aggregation.

2.6.3 Cyclodextrins and rcm κ-casein fibrillar aggregation

The ability of αCD, βCD and γCD to inhibit the fibrillar aggregation of rcm κ-casein was undertaken using a variation of the method outlined in Section 2.2.8. The ability of cyclodextrins to inhibit rcm κ-casein fibrillar aggregation was monitored using a FluoStar plate reader, with ThT-associated fluorescence (excitation 440nm, emission 490nm) measured as an indication of protein aggregation. Cyclodextrins were added to aggregating 1mg/ml rcm κ-casein (50mM phosphate buffer, 0.04% NaN_3, pH 7.5) at a 5:1 or 25:1molar ratio. ThT fluorescence was measured every 10 minutes for twenty hours, with fluorescence plotted versus time. The change in ThT-associated fluorescence with time was plotted between cyclodextrins samples to observe the effect of cyclodextrins on fibrillar protein aggregation.

2.6.4 βCD and fibrillar aggregation

The ability of βCD to inhibit the fibrillar aggregation of rcm κ-casein was investigated using the method described in section 2.6.3, with the exception that a dose-dependant response was observed by adding βCD at a 5:1, 10:1, 25:1, 50:1 and 100:1 molar ratios.

The ability of βCD to inhibit α-lactalbumin and β-lactoglobulin fibrillar aggregation under reduction stress conditions was monitored using a FluoStar plate reader, with ThT-associated fluorescence (excitation 440nm, emission 490nm) measured as an indication of protein aggregation. α-Lactalbumin assays were carried out at a concentration of 3mg/ml in 50mM phosphate buffer (0.04% NaN_3, 20mM DTT, 12.5mM ThT, pH 7.5). β-lactoglobulin assays were carried out at a concentration of 2mg/ml in 50mM phosphate buffer (0.04% NaN_3, 20mM DTT, 12.5 mM ThT, pH 7.5). βCD was added to each sample at a 50:1 molar ratio with the target protein.

The ability of βCD to inhibit wild-type and A53T mutant α-synuclein fibrillar aggregation under thermal stress conditions was similarly monitored using a FluoStar plate reader, with ThT-associated fluorescence (440nm excitation, 490nm emission) measured as an indication of protein aggregation. Samples were incubated in a ThermoStar plate shaker at 37°C, and time point measurements taken at 8 or 16 hour timepoints for 160 hours. Assays were carried out at a concentration of 2mg/ml in 50mM phosphate buffer (0.04% NaN_3, 12.5mM ThT, pH 7.5). βCD was added to each sample at a 12:1, 25:1 or 50:1 molar ratio with target protein. For all samples, ThT-associated fluorescence was plotted versus time, and change in ThT-fluorescence over

time plotted to observe the effect of increased βCD concentration on protein

aggregation.

2.7 Chapter 8 methods

2.7.1 Intrinsic fluorescence of aggregating proteins

The effect of βCD on protein structure during fibrillar aggregation was observed via

intrinsic tryptophan fluorescence intensity over time. β-lactalbumin and rcm κ-casein

were dissolved in 50mM phosphate buffer (0.04% NaN$_3$, pH 7.4), and at a

concentration of 2mg/ml protein. 20mM DTT was added to the β-lactoglobulin sample.

2 ml samples were incubated for 1 hour at room temperature. Samples were loaded into

1cm path length glass cuvettes, with βCD added to each protein sample at 0:1 and 50:1

molar ratios. Intrinsic tryptophan emission fluorescence of each sample was measured

at wavelengths between 300 and 400nm via a Cary Eclipse fluorescence

spectrophotometer, with excitation at 280nm. Wavelength scans were taken every 20

minutes for twelve hours for each target protein and βCD concentration. Fluorescence

intensity was plotted versus wavelength for each time point, as well as λ_{max} versus time

and maximum fluorescence intensity versus time.

2.7.2 Circular dichroism spectrophotometry of aggregating proteins

The effect of βCD on the structure of fibrillar aggregating proteins was further

investigated via CD spectrophotometry over time. βCD was added to 2ml 1mg/ml rcm

κ-casein samples in 5mM phosphate buffer (0.04% NaN_3, pH 7.4) at 0:1 and 25:1

molar ratios to target protein. Samples were incubated in a 37°C waterbath for 20hrs,

with 200ml samples taken at 1, 2, 3, 6, 8, 10, 12, 18 and 24 hrs. Far UV CD spectra for

time point samples were acquired on a JASCO J810 circular dichroism

spectrophotometer at 37°C and at wavelengths between 250 and 190nm using 1mm

path length glass cuvettes. Molar ellipticity was plotted versus wavelength for each

sample and timepoint, as well as ellipticity at 205nm versus time and at 216nm versus

time.

2.7.3 Competitive ANS binding

The nature of βCD-protein interaction during fibrillar aggregation was observed via

competitive ANS binding over time. rcm κ-Casein (1mg/ml) or β-lactalbumin (2mg/ml)

samples were dissolved in 50mM phosphate buffer (0.04% NaN_3, pH 7.5). 20mM DTT

was added to the β-lactoglobulin sample. 1.4 ml samples were added to 600μl of 10μM

ANS solution, and βCD was added to each protein sample at either a 0:1 or 50:1 molar

ratio with target protein. ANS-associated fluorescence of each sample was measured

via Cary Eclipse fluorescence spectrophotometer (excitation 280nm, emission 387nm).

Measurements were taken every 20 minutes for twelve hours for each target protein and

βCD concentration. Fluorescence intensity was plotted versus time for each target

protein and βCD concentration.

     This was further observed via competitive chaperone assays against aggregating

rcm κ-casein. ANS, βCD, or a combination of the two were added to aggregating rcm

κ-casein at 0:1 and 50:1 molar ratios. ThT-associated fluorescence was measured at 0, 1, 2, 6, 12 and 20 hour timepoints, with fluorescence plotted versus time. The chaperone activity of the βCD/ANS combination was compared to the activity of independent βCD and ANS samples, to investigate a possible additive effect of the two chaperones, and consequently if their protein binding mechanisms were in direct competition.

2.7.4 Co-operative chaperone activity of βCD with α_T-crystallin

The possible additive effect of sHsp and cyclodextrin chaperone abilites was investigated using a variation of the method described in section 2.6.4. βCD, α_T-crystallin, or a combination of both was added to aggregating rcm κ-casein at molar ratios of 25:1 (βCD) and 0.5:1 (α_T-crystallin). ThT fluorescence was measured every 10 minutes for twenty hours, with fluorescence plotted versus time. The chaperone activity of the βCD/α_T-crystallin combination was compared to the activity of βCD and α_T-crystallin on their own to investigate a possible additive effect of the two chaperones, and consequently if their protein binding mechanisms were in direct competition.

2.7.5 The relationship between protein aggregation rate and βCD chaperone ability

The relationship between the rate of target protein aggregation and βCD chaperone ability was investigated using a similar method to that described in Section 2.3.7. Percentage protection values for βCD against the fibrillar aggregation of α-lactalbumin, β-lactoglobulin, rcm κ-casein, wild-type α-synuclein and A53T α-synuclein were plotted against the corresponding time taken to achieve maximum ThT fluorescence (tMax) at a 0:1 molar ratio of βCD to target protein. A statistically significant relationship between tMax and βCD percentage protection was determined by linear, logarithmic or exponential fits to the data with an r^2 value above 0.6.

2.8 Statistics

The statistical significance of any differences observed between group means was determined by analysis of variance. Post-hoc testing of differences between groups was accomplished using Student's t-test assuming unequal variance, with $p \leq 0.05$ considered statistically significant. Where appropriate, data are presented as means ± SD.

CHAPTER 3

INVESTIAGTING THE pH SENSITIVE CHAPERONE MECHANISM
OF α-CRYSTALLIN

Chapter 3 – Investigating the pH-sensitive chaperone ability of α-crystallin

3.1 Introduction

As the primary molecular chaperone of the mammalian lens, α-crystallin is essential for stabilizing lens proteins and maintaining lens transparency (Horwitz, 1992; Bloemendal *et al*., 2004). The high protein concentration of the lens, coupled with the constant accumulation of aged cells in the nucleus, places unusual pressure on the lens chaperone system (Bloemendal *et al*., 2004). As lens cells age, the ability of α-crystallin to protect against target protein aggregation becomes compromised, presumably as the concentration of available, functional α-crystallin becomes diminished (Horwitz, 1992; Carver *et al*., 1996; Derham and Harding, 1999). As a consequence, the frequency of cataract development increases markedly with age, and aging is considered to be the key risk factor for nuclear cataract development (Truscott, 2005).

There is evidence to suggest that α-crystallin is a more effective chaperone at pH 7.5 and 8.0 than at pH 6.0 (Koretz *et al*., 1998; Poon *et al*., 2002). As yet, the reasons for this apparent pH-sensitivity are not known. Lens pH varies from pH 7.2 at the cortex to pH 6.7 in the lens nucleus (Bassnett and Duncan, 1985; 1987), and so the influence of mildly acidic pH on α-crystallin chaperone ability may be physiologically significant in the lens. As aged and modified proteins accumulate in the lens nucleus, the ability of α-crystallin to function as a molecular chaperone becomes imperative in the maintenance of lens transparency. If α-crystallin chaperone ability is significantly decreased at lower pH, then the ability of α-crystallin to inhibit protein aggregation in the lens nucleus would almost certainly be compromised. This in turn may result in increased protein aggregation, reduced lens transparency and potentially an increased likelihood of cataract formation. An increase in insoluble, high molecular weight protein content has been identified as characteristic of lens aging (Liang and Rossi, 1989; Yang *et al*., 1994), and

the build up of high molecular weight protein species in aged lens nuclei has been well observed (Stauffer *et al.*, 1974; Jedziniak *et al.*, 1975). This suggests a reduced chaperone capability of α-crystallin in the lens nucleus, characterised by an inability to inhibit the aggregation and precipitation of lens proteins.

Extra-lenticular αB-crystallin is up-regulated in response to a number of clinical disorders, including Alzheimer's and Parkinson's disease, that are characterised by fibrillar aggregation (Clark and Muchowski, 2000; Sun and McRae, 2005). Accordingly, αB-crystallin is believed to play a protective role in the prevention of fibrillar aggregation characteristic of a variety of disorders *in vivo* (Clark and Muchowski, 2000). Amyloid fibril formation of a number of proteins is promoted by acidic conditions, including α-lactalbumin (Goers *et al.*, 2002), HypF (Bucciantini *et al.*, 2002), transthyretin (Lai *et al.,* 1996) and β2-microglobulin (Raman *et al.*, 2005). Additionally, Alzheimer's disease has been demonstrated to coincide with localized acidosis in infected brain tissue, wherein pH drops below pH 6.0 (Yates *et al.*, 1990). Recent investigation suggests that fibrillar aggregation of Aβ-peptide, characteristic of Alzheimer's disease, is promoted at pH 6.0 (Khandogin and Brooks, 2007). If the chaperone ability of α-crystallin is reduced under acidic conditions, the ability of αB-crystallin to effectively inhibit extra-lenticular fibrillar aggregation and protect against clinical disorders may be compromised in mildly acidic environments *in vivo*.

Chapter 3 – Chaperone ability of α-crystallin

Rationale for work presented in this chapter

The effect of pH on the chaperone ability of α_T-crystallin and its subunits, αA- and αB-crystallin, was investigated between pH 6.0 and pH 8.0, to determine if α-crystallin chaperone ability is pH sensitive. Characterisation was carried out using four *in vitro* target proteins; the thermal-stress induced amorphous aggregation of a physiologically relevant target protein (β_L-crystallin, a structural lens protein and physiological target for α-crystallin), thermal-stress induced amorphous aggregation of a physiologically un-related target protein (catalase), reduction-stress induced amorphous aggregation of α-lactalbumin and the thermal-stress induced fibrillar aggregation of reduced and carboxymethylated (rcm) κ-casein. The variety of target proteins and stress conditions investigated in this study were selected to encompass a broad range of aggregation conditions.

3.2 Results

3.2.1 Thermal-stress induced amorphous aggregation

Light scattering at 340nm is indicative of protein aggregation; an increase in light scattering with time is characteristic of amorphous protein aggregation. The ability of α_T-, αA- and αB-crystallin to prevent thermal-stress amorphous aggregation was determined by observing the light scattering at 340nm of heat stressed β_L-crystallin and catalase. Profiles were measured at pH 6.0, 6.5, 7.0, 7.5 and 8.0, and at varying molar subunit ratios of α_T-, αA- or αB-crystallin (See appendix C, Figures C1-2).

At pH 6.5 and above, the rate of both catalase and β_L-crystallin aggregation showed a dose-dependent decrease with the addition of increasing amounts of α_T-, αA- or αB-crystallin, indicating the inhibition of target protein aggregation. The ability of α_T-, αA- and αB-crystallin to suppress target protein aggregation decreased below pH 7.0. At pH 6.0, maximum light scattering at 340nm for both target protein samples increased slightly with the addition of chaperone protein. This suggests that the target protein-chaperone complex is inherently unstable at low pH, and that these conditions promoted aggregation.

For all aggregation curves, the pH sensitivity of chaperone ability was quantified via the comparison of percentage protection values. Percentage protection was determined using a modified version of the method of Raman and Rao (1994), according to the equation;

$$\text{percentage protection} = ((R_0 - R_{0.5})/R_0) * 100$$

where R_0 and $R_{0.5}$ are the rate of light scatter increase in the absence (0:1 molar subunit ratio with target protein) and presence (0.5:1 molar subunit ratio with target protein) of chaperone respectively. Calculations were based upon the initial rate of protein aggregation. Higher percentage protection values demonstrate an increase in

chaperone ability. Percentage protection values were plotted versus pH for each chaperone and target protein (Figure 3.1-2). Percentage protection was lowest at pH 6.0, and increased significantly between pH 6.0 and pH 7.0 for each chaperone with either target protein. There was no significant variation in percentage protection between pH 7.0 and 8.0 for α_T- or αA-crystallin with either target protein, or for αB-crystallin with catalase. αB-crystallin percentage protection against β_L-crystallin aggregation increased significantly between pH 7.0 and 7.5, but did not vary significantly between pH 7.5 and 8.0.
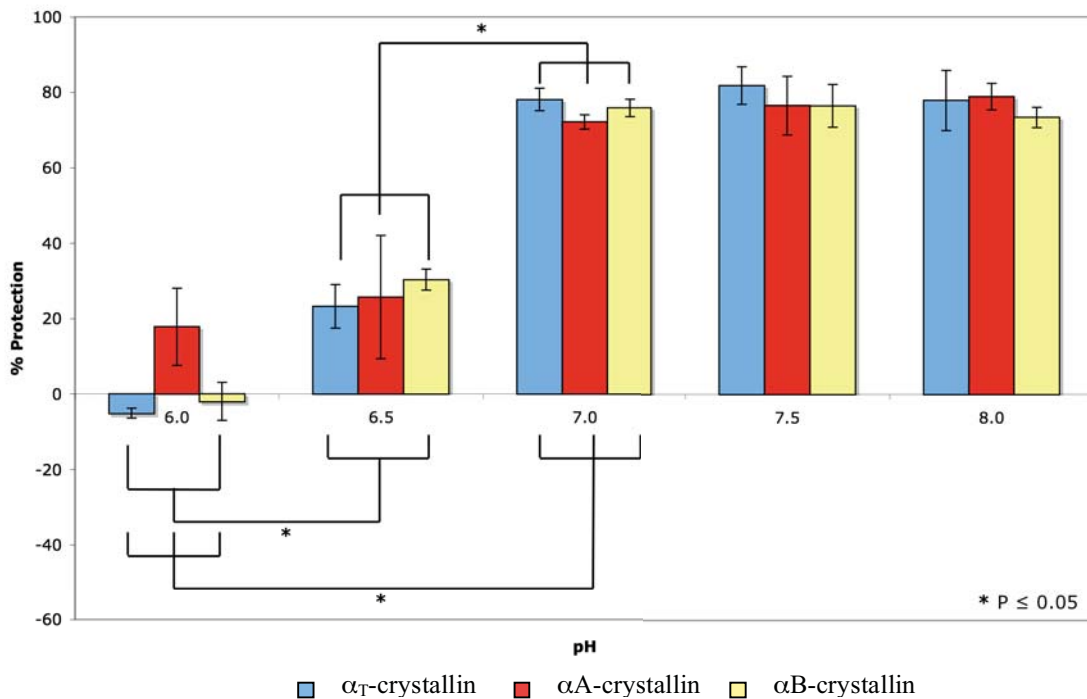
Figure 3.1 – Percentage protection, calculated from light scattering assays, of α_T-, αA- and αB-crystallin against the thermally-induced amorphous aggregation of catalase (55°C). Percentage protection increased significantly between pH 6.0 and pH 7.0, but showed no significant variation between pH 7.0 and pH 8.0. * Indicates significant difference in the mean percentage protection ($p \leq 0.05$).
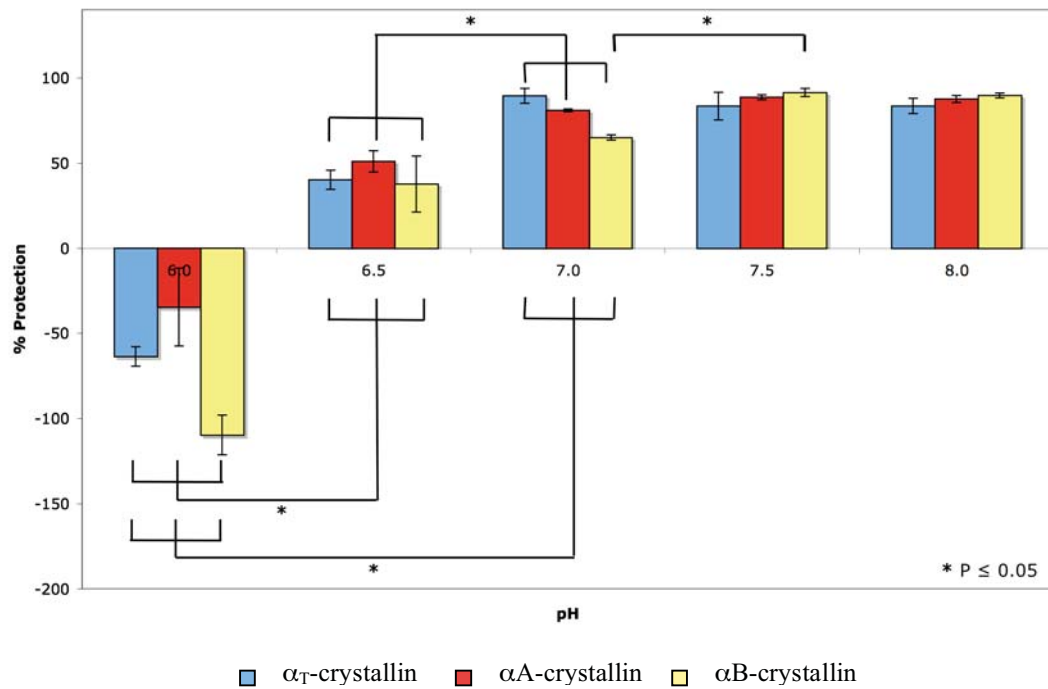
Figure 3.2 - Percentage protection, calculated from light scattering assays, of α_T-, αA- and αB-crystallin against the thermally-induced amorphous aggregation of β_L-crystallin (60°C). Percentage protection increased significantly between pH 6.0 and 7.0. α_T- and αA-crystallin percentage protection showed no significant variation between pH 7.0 and pH 8.0. αB-Crystallin percentage protection increased significantly between pH 7.0 and 7.5, but showed no significant variation between pH 7.5 and 8.0 * Indicates significant difference in the mean percentage protection (p ≤ 0.05).

3.2.2 Reduction-stress induced amorphous aggregation

The ability of α_T-, αA- and αB-crystallin to prevent the reduction-stress induced amorphous aggregation of α-lactalbumin was determined using the same method described in Section 3.2.1. Reduction of disulphide bonds between cysteine residues can disrupt the native conformation of target proteins and induce aggregation. Dithiothreitol (DTT)-induced reduction has been demonstrated extensively to induce the aggregation of α-lactalbumin under physiological conditions (37°C, pH 7.4) (Magnuson and Magnuson, 1971; Lindner *et al.*, 1997; Rajaraman *et al.*, 1998; Carver *et al.*, 2002). TCEP was chosen over DTT as a reducing agent due to its broader effective pH range, and its ability to reduce disulphide bonds in a non pH-sensitive manner between pH 6.0 and 8.0 (Han and Han, 1994).

TECP-induced α-lactalbumin aggregation was measured via light scattering at 340nm. α-lactalbumin aggregation was measured at pH 6.0, 6.5, 7.0, 7.5 and 8.0, and at varying molar ratios of α_T-, αA- or αB-crystallin. As with thermal-stress amorphous aggregation (Section 3.2.1), α-lactalbumin aggregation decreased in a dose-dependent fashion with the addition of increasing amounts of chaperone, suggesting the inhibition of α-lactalbumin aggregation (See appendix C, Figure C3). α_T- , αA- and αB-crystallin percentage protection was lowest at pH 6.0, and increased significantly between pH 6.0 and pH 7.0 (Figure 3.3). There was no significant change in αA-crystallin percentage protection between pH 7.0 and pH 7.5. αA-crystallin percentage protection increased significantly between pH 7.5 and 8.0. There was no significant difference in either α_T- or αB-crystallin percentage protection between pH 7.0 and 8.0. This is largely consistent with data from Section 3.2.1.
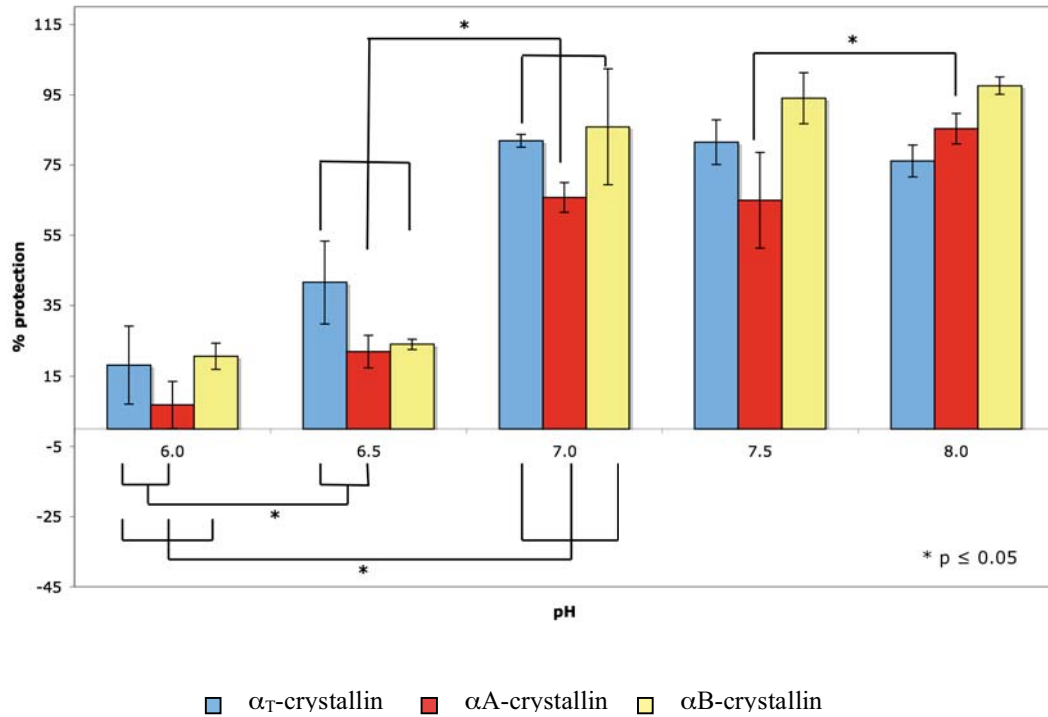
Figure 3.3 - Percentage protection, calculated from light scattering assays, of α_T-, αA- and αB-crystallin against the reduction-induced amorphous aggregation of α-lactalbumin (37°C). Percentage protection values increased significantly between pH 6.0 and pH 7.0. There was no significant variation in α_T- or αB-crystallin percentage protection between pH 7.0 and pH 8.0. There was no significant difference in αA-crystallin percentage protection between pH 7.0 and 7.5, but percentage protection increased significantly between pH 7.5 and 8.0. * Indicates significant difference in the mean percentage protection ($p \leq 0.05$).

3.2.3 Thermal-stress induced fibrillar aggregation of rcm κ-casein

The ability of α_T-, αA- and αB-crystallin to prevent the fibrillar aggregation of rcm κ-casein was determined using a similar method to that described in Section 3.2.1. Thioflavin T (ThT) is a fluorescent dye that binds strongly to regions of stacked β-sheets, in particular those associated with the formation of amyloid fibrils. Fluorescence at 490nm is characteristic of ThT-protein binding (LeVine, 1999). As a highly ordered cross β-sheet structure is characteristic of amyloid fibrils, an increase in β-sheet content over time, as observed by ThT fluorescence, is representative of fibrillar aggregation (LeVine, 1999, Khurana *et al*., 2005). ThT-associated fluorescence of reduced, carboxymethylated (rcm) κ-casein at an emission wavelength of 490nm (440nm excitation wavelength) was measured at pH 6.0, 7.0 and 8.0, and at varying molar ratios of α_T-, αA- or αB-crystallin (Figure 3.4). ThT fluorescence assays were undertaken *in situ*.

ThT fluorescence associated with rcm κ-casein aggregation decreased with the addition of α_T-, αA- or αB-crystallin. The chaperone ability of α_T-, αA- and αB-crystallin against rcm κ-casein aggregation was quantified by comparison of the change in ThT-associated fluorescence after 20 hours, by the equation;

$$\text{percentage protection} = ((\Delta F_0 - \Delta F_{0.5}) / \Delta F_0) * 100$$

where ΔF_0 and $\Delta F_{0.5}$ are the change in ThT-associated fluorescence in the absence (0:1 ratio with rcm κ-casein) and presence (0.5:1 molar ratio with rcm κ-casein) of chaperone, respectively (Figure 3.4). Unlike data observed in Sections 3.2.1-2, in general there was no significant change in either α_T-, αA- or αB-crystallin percentage protection against rcm κ-casein aggregation between pH 6.0 and 8.0. The only exception to this was α_T-crystallin chaperone ability, which demonstrated a

significant difference between pH 7.0 and 8.0. This appears to be a consequence of the particularly low percentage protection observed for α_T-crystallin against rcm κ-casein aggregation at pH 7.0, and is not representative of the data set. In contrast to the data for the inhibition of amorphous target protein aggregation (Sections 3.2.1-2), the ability of α-crystallin to inhibit rcm κ-casein fibrillar aggregation does not appear to be pH sensitive.
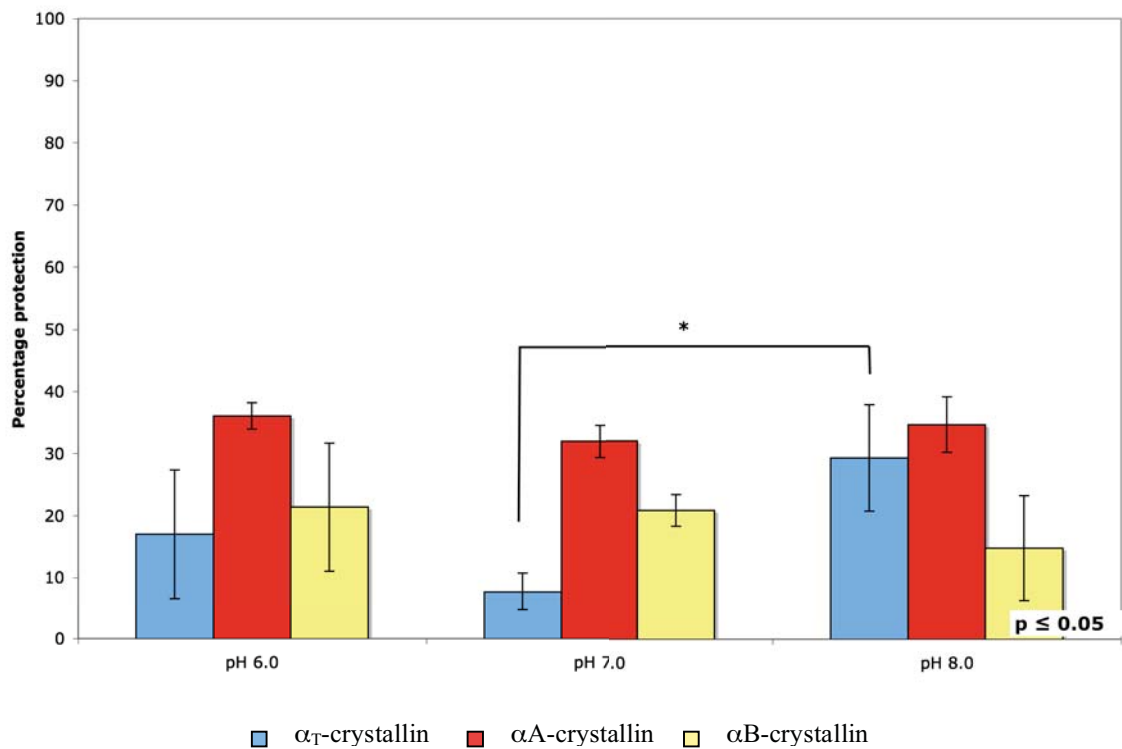
Figure 3.4 –Percentage protection, calculated from the change in ThT-fluorescence, of α_T-, αA- and αB-crystallin against the fibrillar aggregation of rcm κ-casein. Percentage protection did not vary significantly with pH, except with α_T-crystallin between pH 7.0 and 8.0.

3.3 Discussion

Investigation into the effect of pH on molecular chaperone activity has to date been limited. Mildly acidic pH (pH 6.0) has been demonstrated to enhance the dissociation and chaperone ability of clusterin, an extra-cellular protein with chaperone-like qualities (Poon *et al.*, 2002). It is believed that acidic pH increases exposed clusterin hydrophobicity, and by doing so facilitates enhanced chaperone ability, in a manner reminiscent of α-crystallin at elevated temperatures (Poon *et al.*, 2002). Conversely, Hsp20 chaperone ability decreases from pH 7.5 to 6.0 in a manner reminiscent of α-crystallin (Bukach *et al.*, 2004). Interestingly, direct comparison suggests that Hsp20 is a significantly less effective chaperone at pH 6.0 than α-crystallin (Bukach *et al.*, 2004). Koretz *et al.* (1998) have demonstrated that $α_T$-crystallin is less able to inhibit the thermal-stress induced aggregation of γ-crystallin at mildly acidic pH (pH 6.0), possibly as a consequence of decreased α-helical content.

In this study, $α_T$-, αA- and αB-crystallin percentage protection increased significantly as pH increased from pH 6.0 to 7.0 for three of the target proteins investigated (catalase, $β_L$-crystallin and α-lactalbumin). For these target proteins, there is a clear correlation between pH and α-crystallin chaperone ability in this pH range, demonstrating that $α_T$-crystallin and its subunits are pH-sensitive molecular chaperones. The decreased chaperone ability of $α_T$-crystallin at pH 6.0 and pH 6.5 observed in this study is in agreement with the results of others (Koretz *et al.,* 1998; Poon *et al.,* 2002; Bukach *et al.*, 2004). Similarly, the results observed for the αA- and

αB-crystallin subunits support investigations by Koteiche and Mchaourab (2003), who showed a marked increase in the affinity of αA- and αB-crystallin for T4 lysozyme mutants as pH increased from pH 6.0 to 8.0. Interestingly, it appears that there is no significant difference between the pH sensitivity of α_T-, αA- and αB-crystallin across the pH range investigated; that is, all three crystallins demonstrated significantly decreased chaperone ability below pH 7.0. The fact that the observed pH sensitivity of chaperone ability was common to three target proteins suggests that pH affects the ability of α-crystallin to inhibit both thermal- and reduction-stressed amorphous aggregation, and that the observed pH-sensitive trend appears to be an intrinsic function of α-crystallin and its individual subunits.

Interestingly, the pH-sensitive chaperone ability of α-crystallin observed against catalase, β_L-crystallin and α-lactalbumin amorphous aggregation was not seen against the fibrillar aggregation of rcm κ-casein. κ-Casein has recently been shown to aggregate via a unique mechanism, whereby the unfolding of native κ-casein to an amyloidogenic precursor conformation (which is believed to be typical of many forms of fibrillar aggregation) does not occur prior to fibrillar aggregation (Ecroyd *et al.*, 2008). Rather, κ-casein monomers or dimers that have dissociated from the κ-casein oligomer are believed to exist as amyloidogenic precursors that do not require unfolding to adopt an amyloidogenic conformation; accordingly, fibrillar aggregation can commence immediately upon dissociation. It has been suggested that this aggregation mechanism limits the ability of sHsps, particularly αB-crystallin to interact with aggregating κ-

casein, due to the transient presence of the amyloidogenic fibrillar precursor (Ecroyd *et al.*, 2008). αB-Crystallin selectively interacts with partially-folded protein intermediates on the off-folding pathway, and largely ignores natively folded proteins, or partially-folded protein intermediates in a structurally stable conformation that are not prone to aggregation (Carver *et al.*, 1995; Rajaraman *et al.*, 1998; Treweek *et al.*, 2000; Carver *et al.*, 2002). This chaperone mechanism is considered characteristic of sHsps, and of aggregation on the off-folding pathway. The aggregation of rcm κ-casein, which is facilitated by dissociation, and is not characterized by the formation of partially-folded protein intermediates, would not allow for such interactions. α-Crystallin has been shown previously to be a poor molecular chaperone of rcm κ-casein, supporting this theory (Rekas *et al.*, 2007; Ecroyd *et al.*, 2007; Ecroyd and Carver, 2008). Similarly, in this study both α_T-, αA- and αB-crystallin showed reduced chaperone ability against rcm κ-casein, compared to the other target proteins investigated. The atypical nature of rcm κ-casein aggregation leads to inefficient interactions between α-crystallin and rcm κ-casein, which most likely explains the unexpected results observed in this study. In light of this, the data observed for rcm κ-casein aggregation in this study do not necessarily contradict the data observed for catalase, β_L-crystallin or α-lactalbumin aggregation.

A further explanation for the results observed for rcm κ-casein aggregation in this study may involve possible differences in the α-crystallin chaperone mechanism of action for amorphous versus fibrillar aggregation. The proposed 'generic' mechanism of fibrillar aggregation on the off-folding pathway involves the unfolding of target

proteins into a relaxed, partially-folded conformation that contains elements of secondary structure; hydrophobic interactions between these precursor intermediates are believed to facilitate subsequent protein aggregation (Dobson 1999; Chiti, 1999; Chiti and Dobson, 2006). As sHsps are believed to inhibit protein aggregation via their interaction with areas of exposed hydrophobicity on misfolded protein intermediates (Das *et al.*, 1996; Singh and Rao, 2002; Melkani *et al.*, 2004), it is commonly assumed that sHsps and other molecular chaperones can effectively inhibit both amorphous and fibrillar target protein aggregation. Several molecular chaperones have been shown to be capable of inhibiting both amorphous and fibrillar aggregation, including α-crystallin (Horwitz, 1992; Wilhelmus *et al.*, 2006) and clusterin (Poon *et al.*, 2002; Kumita *et al.*, 2007), which supports this assumption.

It may be, however, that the specifics of the sHsp chaperone mechanism vary against amorphous versus fibrillar aggregation. While there has so far been little research into characterizing any differences between the mechanisms of amorphous and fibrillar aggregation, there is circumstantial evidence to suggest subtle differences exist between the respective chaperone mechanisms. Ecroyd *et al.* (2007) demonstrated that mimicking the phosphorylation of serine residues of αB-crystallin increased its chaperone ability against the amorphous aggregation of catalase, $β_L$-crystallin, insulin and α-lactalbumin, but decreased its chaperone ability against the fibrillar aggregation of ccβ-peptide. Similarly, the addition of lysine-HCl to αB-crystallin increased its chaperone ability against the fibrillar aggregation of α-synuclein, but either decreased or had no effect on αB-crystallin chaperone ability against the amorphous aggregation of catalase, insulin or α-lactalbumin (Ecroyd and Carver, 2008). Although the current

evidence is as yet limited, it may help to explain the aberrant results observed in this study for the aggregation of rcm κ-casein.

Importantly, the observed pH-sensitive chaperone trend was consistent between lens-purified α_T-crystallin and recombinant, bacterially expressed αA- and αB-crystallin. This rules out the possibility of post-translational modifications to α-crystallin influencing the pH sensitivity of its chaperone ability. A number of post-translational modifications to α-crystallin have been observed *in vivo*; of these, phosphorylation of lens α-crystallin serine residues is the most commonly observed (Ito *et al.*, 1997; Kato *et al.*, 1998). Both oxidation and phosphorylation of α-crystallin have been shown to reduce its chaperone ability against specific target proteins (Aquilina *et al.*, 2004; Rajan *et al.*, 2006; Ecroyd *et al.*, 2007). As the recombinant (and consequently unmodified) αA- and αB-crystallin subunits exhibited the same pH-sensitive trend as the lens-purified (and possibly modified) α_T-crystallin, post translational modification of α-crystallin appears to have little or no effect on the relationship between pH and chaperone ability.

Almost all elements of the secondary, tertiary and quaternary structure of α_T-crystallin are believed to influence its ability to inhibit target protein aggregation (Horwitz, 2003; Augusteyn, 2004a). Unfolding and exposed hydrophobicity may play an important role in regulating α-crystallin chaperone ability (Raman and Rao, 1994; Das and Surewicz, 1995), although the exact nature of this relationship is currently under debate (Reddy *et al.*, 2006). Previous investigation has demonstrated that pH-induced modifications to α-crystallin secondary structure may affect its chaperone

ability (Koretz *et al.*, 1998), and while α-crystallin oligomer size appears to have little effect on its chaperone ability (Saha and Das 2004; 2007), oligomer hydrophobicity is believed to directly influence and facilitate α-crystallin chaperone ability (Saha and Das 2007; Augusteyn, 2004b). It seems likely then that pH-induced modifications of α-crystallin structure may be responsible for the pH-sensitive chaperone ability observed in Section 3.2. Consequently, gross structural characterisation of α-crystallin with pH may help to understand the reasons behind its observed pH-sensitive chaperone ability.

A final factor effecting α-crystallin's pH-sensitive chaperone ability may be the kinetic relationship between the rate of target protein aggregation and chaperone-target protein interaction.   It has been suggested that at fast aggregation rates, target protein nucleation outpaces, and consequently overwhelms, the rate of chaperone-protein interaction (Lindner *et al.*, 2001). As aggregation occurs via hydrophobic interactions between target proteins, similar to those implicated in chaperone-target protein binding, rapid protein aggregation may inhibit the ability of α-crystallin to successfully bind target proteins. Aggregating target protein intermediates may 'out-compete' α-crystallin for hydrophobic binding sites, and by doing so decrease α-crystallin chaperone ability. This has been demonstrated previously with α-crystallin's inhibition of both α-lactalbumin (Lindner *et al.*, 2001) and rcm κ-casein aggregation at low temperatures (Rekas *et al.*, 2007). Catalase, β_L-crystallin and α-lactalbumin each aggregated more rapidly at pH 6.0 and 6.5 than at pH 8.0, which may have influenced the ability of α-crystallin to inhibit their aggregation. Accordingly, the observed pH-sensitivity of α-

crystallin chaperone ability may be, in part, a consequence of target protein aggregation

kinetics.

CHAPTER 4

CHARACTERISING THE EFFECT OF pH ON THE STRUCTURE OF α-CRYSTALLIN

Chapter 4 – Characterising the effect of pH on the structure of α-crystallin

4.1 Introduction

α-Crystallin acts as a molecular chaperone under a variety of conditions, both *in vivo* and *in vitro*. The exact mechanism of its chaperone ability is currently unknown. The structure of α-crystallin is believed to be a key determinant of its chaperone ability; dissociation, oligomerisation and the rate of subunit exchange have each been argued to influence the chaperone activity of α-crystallin (Bova *et al.*, 1997; Avilov *et al.*, 2004; Liu *et al.*, 2006), but the precise effect of these factors is still open to interpretation (Augusteyn 2004b; Aquilina *et al.*, 2005). Similarly, the exposed hydrophobicity of both dissociated and oligomeric α-crystallin is also believed to be a decisive factor in determining the chaperone activity of α-crystallin (Raman and Rao, 1994; Das *et al.*, 1996; Saha and Das, 2004; Augusteyn 2004b). It has been generally accepted that exposed hydrophobicity facilitates the binding of α-crystallin to semi-folded protein intermediates, and consequently that increased exposed hydrophobicity enhances α-crystallin chaperone activity, (Raman and Rao, 1994; Das and Surewicz, 1995, Datta and Rao, 1999). However, in recent years studies have indicated that increased α-crystallin hydrophobicity can either inhibit (Santhoshkumar and Sharma, 2001) or have no effect (Smulders *et al.*, 1996) on α-crystallin chaperone activity. Consequently, the relationship between exposed hydrophobicity and α-crystallin chaperone activity is currently the subject of debate (Kumar *et al.*, 2005; Reddy *et al.*, 2006)

The rate of nucleation-dependent target protein aggregation also appears to influence sHsp chaperone activity; target protein aggregation has been observed to outpace chaperone-target protein interaction in situations of high aggregation rate,

and consequently overwhelm potential chaperone activity (Lindner *et al.*, 2001). Three of the four target proteins discussed in Section 3.2 (catalase, β_L-crystallin, α-lactalbumin) appeared to aggregate more rapidly as pH decreased from pH 8.0 to 6.0, which correlated with a decrease in the chaperone activity of α-crystallin and its subunits.

Characterising the structural modifications to α-crystallin and its subunits accompanying pH variation should assist in explaining the pH-sensitive chaperone activity observed in Section 3.2. Additionally, investigating the relationship between protein aggregation rate and crystallin percentage protection will determine if nucleation rate, as opposed to exposed hydrophobicity or other intrinsic structural factors, is primarily responsible for the pH sensitive chaperone activity of α_T-, αA- and αB-crystallin.

Rationale for work presented in this chapter

Characterisation of α_T- , αA- and αB-crystallin protein structure over the pH range observed in Sections 3.2.1-3 (pH 6.0 – 8.0) was used to gain a greater understanding of their pH-dependent chaperone activity. pH-induced structural changes to α_T-, αA- and αB-crystallin were observed via intrinsic tryptophan fluorescence, ANS binding, ThT-associated fluorescence, size exclusion fast protein chromatography and transmission electron microscopy. This structural characterisation suggested that α-crystallin is partially unfolded at pH 6.0 and 6.5, compared to pH 7.0 and above. Additionally, the effect of the rate of target protein aggregation on the activity of α_T-, αA- and αB- crystallin to protect against target protein aggregation was investigated by observing the relationship between percentage protection and

target protein aggregation rate for each crystallin and target protein investigated in Sections 3.2.1-2. A strong statistical relationship between protein aggregation rate and percentage protection would imply that aggregation rates may contribute to the pH sensitivity of α-crystallin chaperone activity observed in Sections 3.2.1-2. Finally, the ability of α_T- and αB-crystallin to inhibit the amorphous aggregation of α-lactalbumin was investigated between pH 2.0 and 3.5. At acidic pH, α_T-crystallin separates into αA-crystallin homopolymers and denatured αB-crystallin monomers, and both αA- and αB-crystallin are significantly unfolded and less structured than at pH 6.0 and 6.5 (Augusteyn *et al.,* 1988; Stevens and Augusteyn, 1993); comparison of α_T- and αB-crystallin chaperone ability between mildly acidic (pH 6.0 and 6.5) and acidic pH (pH 2.0 – 3.5) may help to determine the functional significance of the partial α-crystallin unfolding observed in this chapter.

4.2 Results

4.2.1 Intrinsic tryptophan fluorescence of α_T-, αA- and αB-crystallin

Tryptophan fluorescence is highly sensitive to environmental conditions, and can be used to investigate changes in the environment surrounding tryptophan residues (Freifelder, 1982). A decrease in fluorescence intensity suggests quenching of tryptophan fluorescence, generally by adjacent amino acids, whilst a red-shift in λ_{max} demonstrates a decrease in the exposure of tryptophan to a polar environment; this can generally be interpreted as representative of protein unfolding. Intrinsic tryptophan fluorescence profiles in this study for αA- and αB-crystallin at pH 7.0 were in agreement with those of Sun *et al.*, (1997), with a λ_{max} around 340nm and significantly higher maximum fluorescence for αB-crystallin than αA-crystallin. This is most likely a consequence of αB-crystallin's two tryptophan residues (W9, W60), as opposed to αA-crystallin's one (W9). Intrinsic fluorescence profiles demonstrated neither a shift in α-crystallin λ_{max} (340nm) or an observable trend in maximum fluorescence as pH increased from pH 6.0 to 8.0 (Figure 4.1). This suggests that as pH increased there was no significant change in the exposure of α-crystallin tryptophan residues to solution. The single N-terminal tryptophan residue of αA-crystallin, and two tryptophan residues of αB-crystallin are believed to lie buried within the overall crystallin multimer (van den Oetelaar *et al.*, 1990, Carver *et al.*, 1994). Consequently, they would be largely sheltered from solution. The insensitivity of α-crystallin tryptophan fluorescence to pH change between pH 6.0 and 8.0 suggests that this change in pH does not result in enough protein unfolding to significantly alter either the N-terminal region of α_T-, αA- or αB-crystallin, or the multimeric assemblies of these proteins.
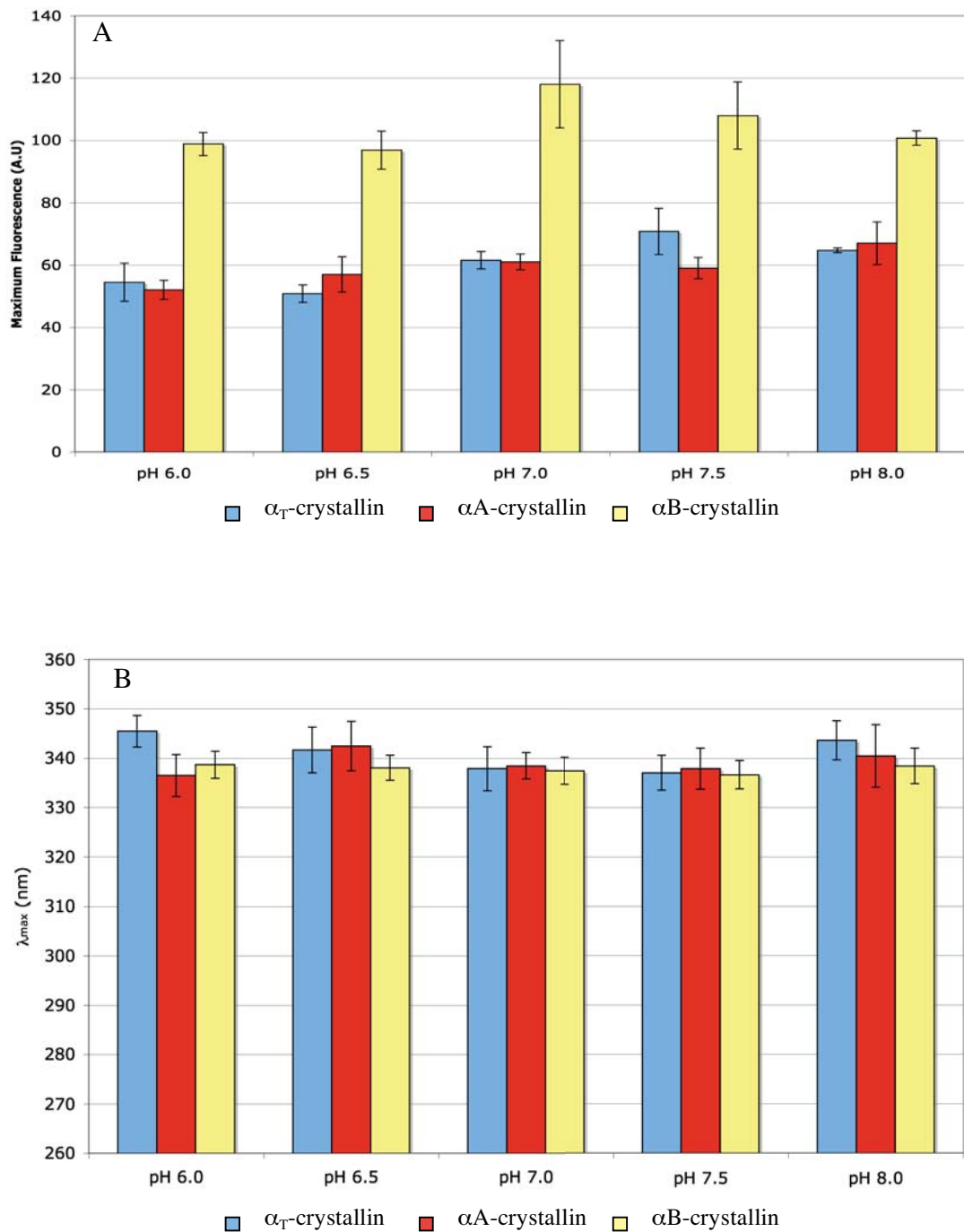
Figure 4.1 – (a) Maximum intrinsic tryptophan fluorescence and (b) λ_{max} of α_T-, αA- and αB-crystallin between pH 6.0 and pH 8.0. There was no trend in maximum fluorescence or λ_{max} for either α_T-, αA- or αB-crystallin, suggesting that α-crystallin tryptophan fluorescence is unaffected by pH changes within this pH range.

4.2.2 ANS-associated fluorescence of α_T-, αA- and αB-crystallin

1-anilino-8-napthalene sulfonate (ANS) is a fluorescent dye that binds strongly to areas of exposed, clustered hydrophobicity. When bound to a protein, ANS has a characteristic λ_{max} between 400 and 500nm, at an excitation wavelength of 387nm. Accordingly, ANS fluorescence in this range can be used as an indication of exposed hydrophobicity on the particular protein (Freifelder, 1982). Alteration in fluorescence intensity is representative of changing surface hydrophobicity. In the present study, ANS λ_{max} remained constant at 450nm for α_T-, αA- and αB-crystallin between pH 6.0 and 8.0. α_T-Crystallin maximum ANS-associated fluorescence at 450nm decreased significantly between pH 6.0 and pH 7.0, but remained constant between pH 7.0 and pH 8.0. αA- and αB-crystallin maximum ANS-associated fluorescence at 450nm decreased significantly between pH 6.0 and 6.5, but remained constant between pH 6.5 and 8.0 (Figure 4.2). ANS in phosphate buffer, used as a negative control, did not change significantly between pH 6.0 and 8.0, demonstrating that ANS-associated fluorescence is not pH sensitive in this pH range.

α_T-Crystallin bound significantly less ANS as pH increased from pH 6.0 to 7.0, which suggests a decrease in exposed protein hydrophobicity. There appeared to be no change in the exposed hydrophobicity of α_T-crystallin above pH 7.0. Similarly, as pH increased from 6.0 to 6.5, αA- and αB-crystallin bound significantly less ANS, suggesting decreased exposed hydrophobicity. There was no change in the exposed hydrophobicity of αA- or αB-crystallin above pH 6.5. Increased surface hydrophobicity is suggestive of partial protein unfolding, as a loss of tertiary structure results in the exposure of hydrophobic protein regions

previously buried within the native protein structure. Consequently, the ANS-binding data implies the partial unfolding of α_T-crystallin as pH decreased from pH 7.0 to pH 6.0, and of αA- and αB-crystallin as pH decreased from pH 6.5 to 6.0. This unfolding correlates, in part, with the decrease in α_T-, αA- and αB-crystallin chaperone ability observed below pH 7.0 in Sections 3.2.1-2.
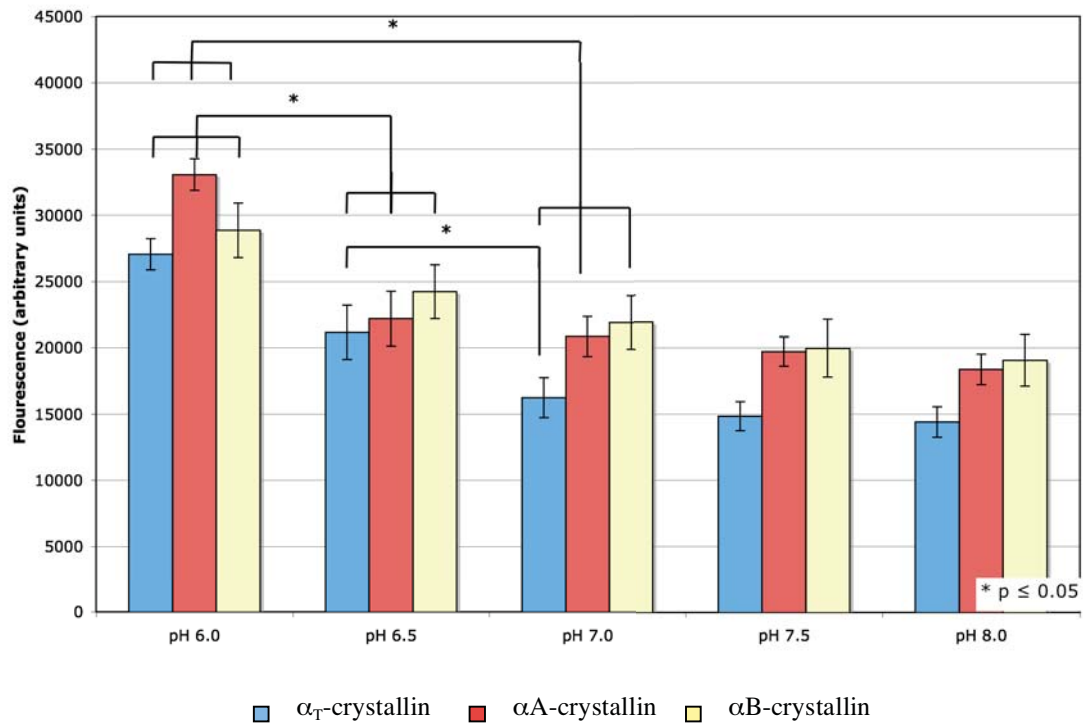
Figure 4.2 – ANS-associated fluorescence of α_T-, αA- and αB-crystallin between pH 6.0 and 8.0. ANS-associated fluorescence decreased significantly between pH 6.0 and 7.0 for α_T-crystallin, and between pH 6.0 and 6.5 for αA- and αB-crystallin. * denotes significant difference in the mean maximum fluorescence ($p \leq 0.05$).

4.2.3 Thioflavin T-associated fluorescence of α_T-, αA- and αB-crystallin

 ThT binds strongly to areas of stacked β-sheet within a protein, and is particularly sensitive to the cross β-sheet structure characteristic of amyloid fibrils (LeVine, 1999, Khurana *et al.*, 2005). Bound ThT fluoresces at 490nm (with an excitation of 440nm), and so ThT fluorescence at this wavelength can be measured as an indication of stacked β-sheet content. α-Crystallin has a high native β-sheet content (between 40 and 70% secondary structure) (Thompson and Augusteyn, 1989; Ehrnsperger *et al.*, 1997), and so a loss of β-sheet can be interpreted as a loss of secondary structure, and hence as an indication of partial protein unfolding. ThT-associated fluorescence increased significantly between pH 6.0 and 6.5 for α_T-, αA- and αB-crystallin, and increased significantly between pH 6.5 and 7.0 for α_T- and αA-crystallin (Figure 4.3). There was no significant change in ThT fluorescence for any of the three crystallins between pH 7.0 and 8.0, or for αB-crystallin between pH 6.5 and 8.0.

The decreased ThT-fluorescence of α_T-, αA- and αB-crystallin below pH 7.0 demonstrates a loss of β-sheet. As β-sheet is the primary structural element of native α-crystallin, the loss of β-sheet at pH 6.0 suggests that α_T-, αA- and αB-crystallin are less structured below pH 7.0. The observed loss of protein structure suggests the partial unfolding of α_T-, αA- and αB-crystallin between pH 7.0 and 6.0, which is largely in agreement with the previously observed ANS-binding data (Section 4.2.2).
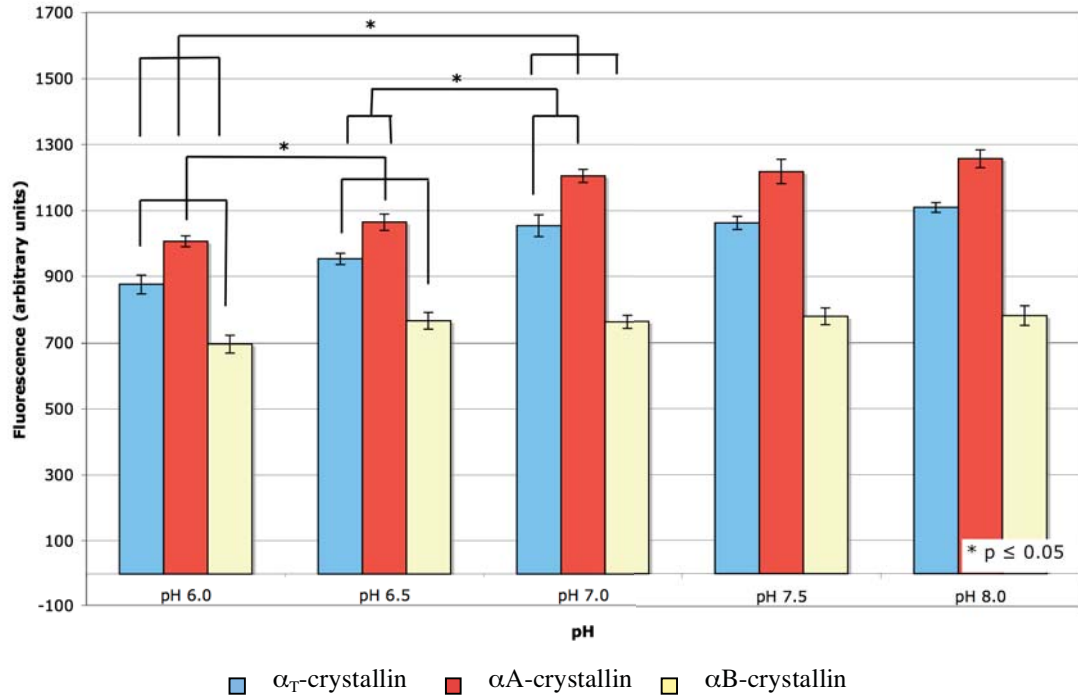
Figure 4.3 – ThT-associated fluorescence of α_T-, αA- and αB-crystallin between pH 6.0 and 8.0. ThT-associated fluorescence increased significantly between pH 6.0 and 6.5 for α_T-, αA- and αB-crystallin, and increased significantly between pH 6.5 and 7.0 for α_T- and αA-crystallin. There was no significant difference in ThT-associated fluorescence between pH 7.0 and 8.0 for any of the three crystallins. * denotes significant difference in the mean fluorescence intensity ($p \leq 0.05$).

4.2.4 Transmission electron microscopy of α_T-, αA- and αB-crystallin

Transmission electron microscopy (TEM) can be used to visualise any gross changes to the shape of α_T, αA- or αB-crystallin aggregates occurring due to changes in pH. Transmission electron micrographs showed a constant aggregate shape between pH 6.0 and 8.0 for both α_T, αA- and αB-crystallin (Figure 4.4). Aggregates retained the roughly spherical shape expected of α-crystallin multimers (Burgio *et al.*, 2000; Meehan *et al.*, 2004). Changing pH had no visible effect on the gross shape of α_T-, αA- or αB-crystallin aggregates, which suggests that the quaternary structure of α-crystallin is unaffected by pH changes between pH 6.0 and 8.0.
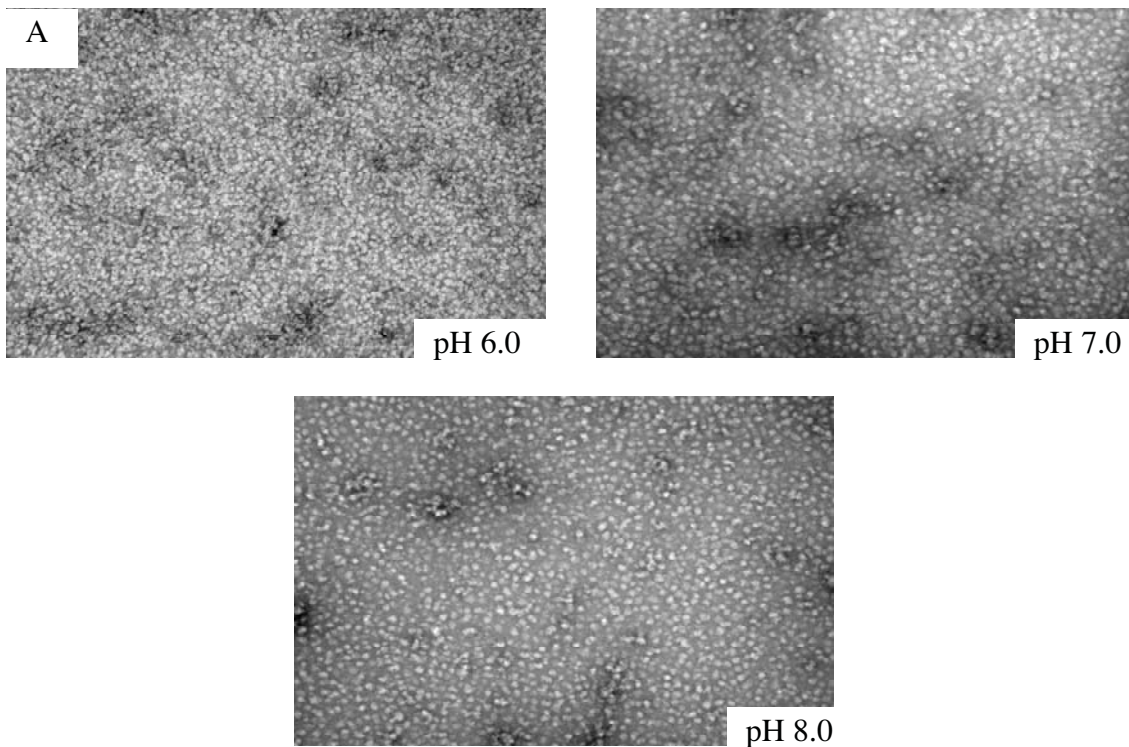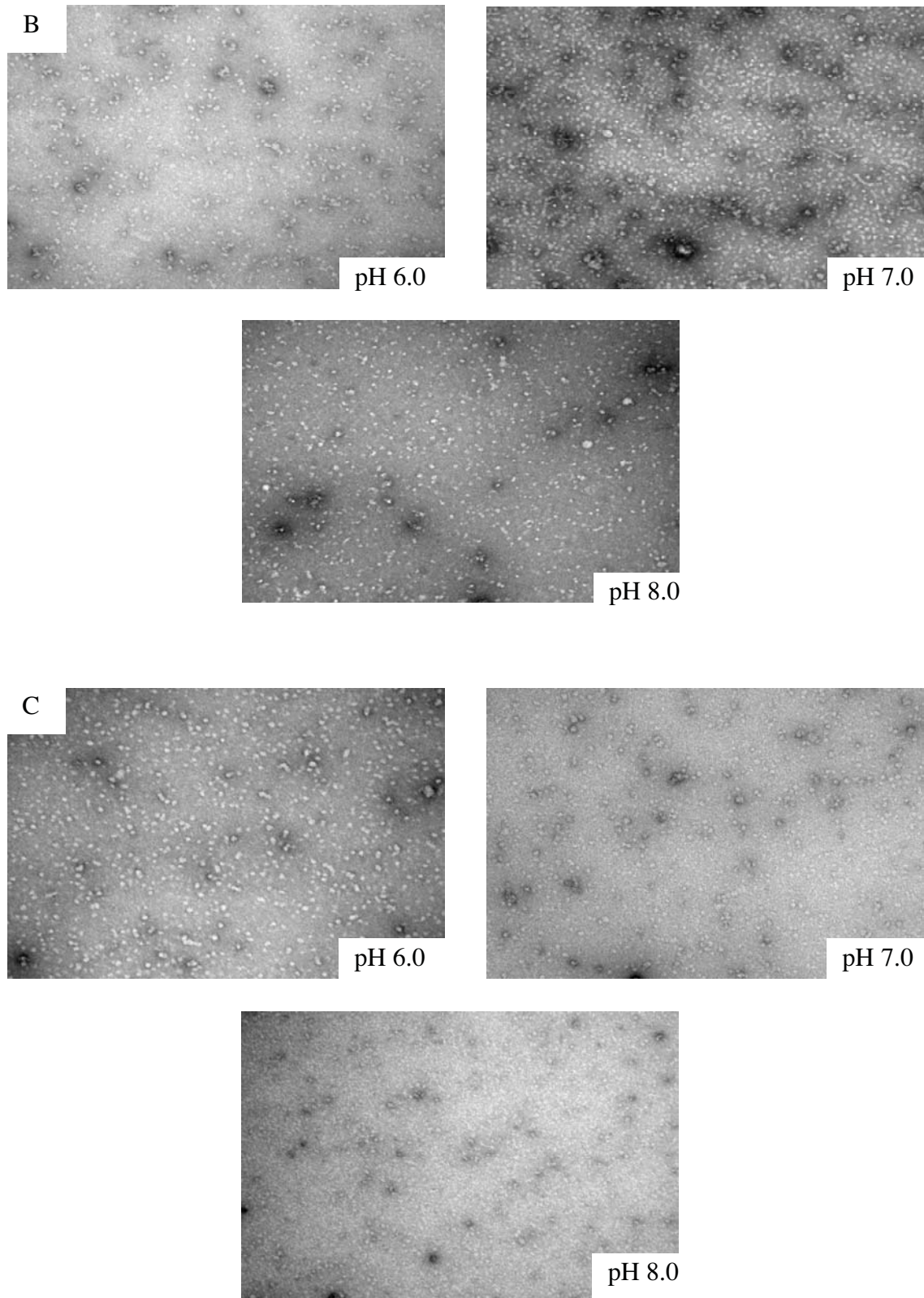
Figure 4.4 – Transmission electron micrographs of (a) α_T-, (b), αA- and (c) αB-crystallin between pH 6.0 and 8.0. Crystallin aggregates demonstrated a roughly spherical shape characteristic of α-crystallin aggregates regardless of pH, suggesting that pH has little effect on α_T-, αA- or αB-crystallin quaternary structure.

4.2.5 Size exclusion fast protein chromatography of α_T-, αA- and αB-crystallin

Size exclusion gel chromatography separates molecules by size, with larger molecules passing more rapidly through the gel bed. Comparison of protein elution times can therefore give an indication of protein aggregate size, and variations in elution time are suggestive of a change in aggregate size. The elution times of α_T-, αA- and αB-crystallin did not vary significantly with pH between pH 6.0 and 8.0 (Figure 4.5). It appears that pH has no effect on α_T-, αA- or αB-crystallin aggregate size between pH 6.0 and 8.0. While peak intensity varied between pH samples, there was no trend in this variation, and it can be attributed changes in protein sample concentration during chromatography. This would arise from variations in sample load volume during the injection of samples onto the chromatography column. The α_T-crystallin samples had an additional minor peak prior to the major α_T-crystallin peak, which can be attributed to high molecular weight α_T-crystallin aggregates commonly isolated from calf lenses. As with TEM data discussed previously (Section 4.2.4), the constant aggregate size between pH 6.0 and 8.0 supports the conclusion that pH has no effect on the quaternary structure of α-crystallin between pH 6.0 and 8.0.
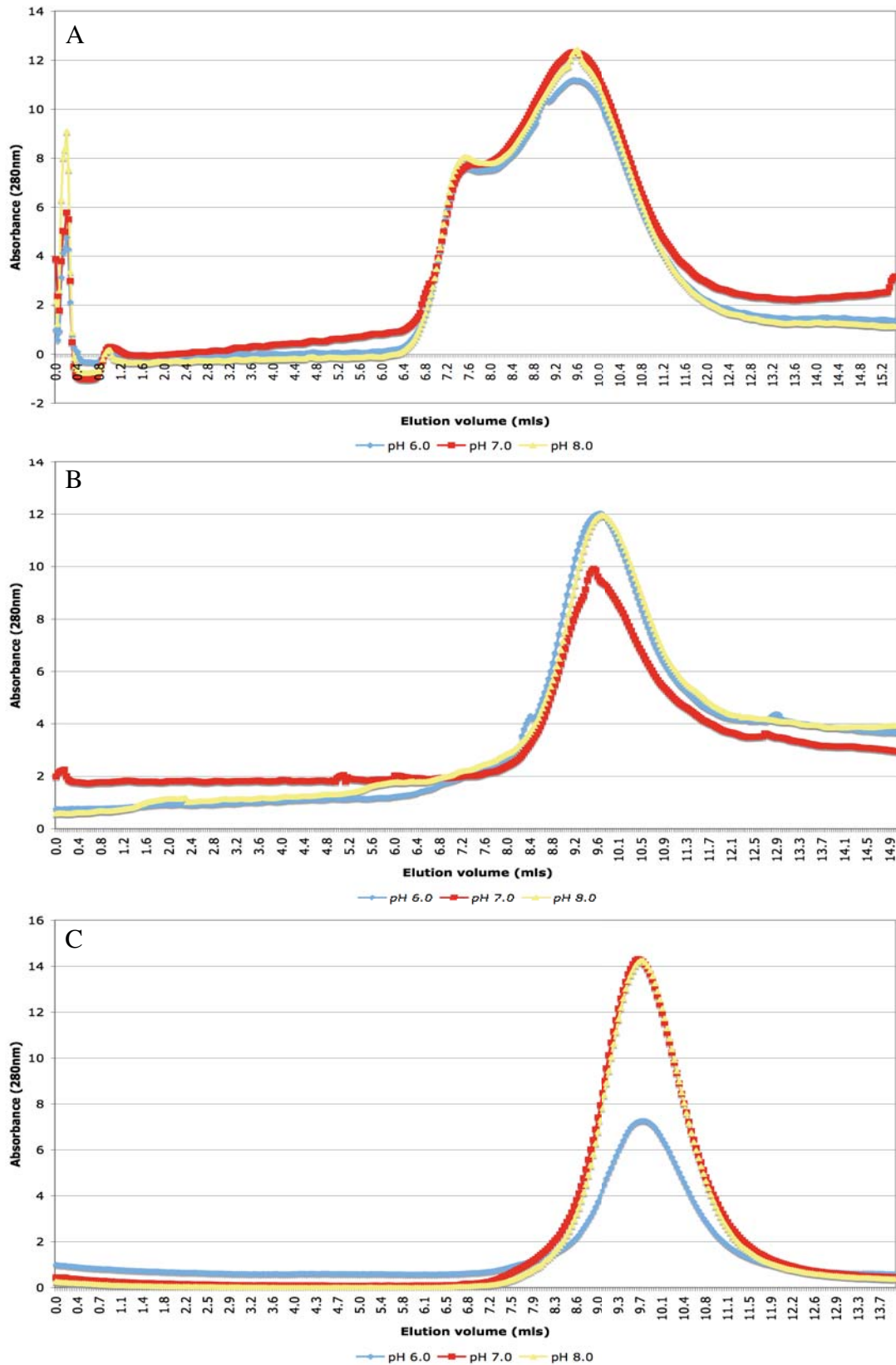
Figure 4.5 – SEFPLC of (a) α_T-, (b) αA- and αB- (c) crystallin between pH 6.0 and 8.0. Elution times remained constant for α_T-, αA- and αB-crystallin with increasing pH, suggesting that pH changes in this range have little effect on α-crystallin aggregate size, and consequently that α-crystallin quaternary structure is unaffected by pH between pH 6.0 and 8.0.

4.2.6 The relationship between target protein aggregation rate and crystallin chaperone ability

It has been demonstrated previously that the rate of protein aggregation may influence the chaperone ability of sHsps (Lindner *et al.*, 2001). It is believed that sHsp-target protein interactions occur predominantly via hydrophobic interactions, similar to those that drive nucleation-dependent protein aggregation (Das *et al.*, 1996; Singh and Rao, 2002). Consequently, rapid protein aggregation may 'outpace' the rate of sHsp binding with target-proteins. This may lead to misfolded target proteins interacting with each other at the expense of the prospective chaperone molecule (Lindner *et al.,* 2001). In the amorphous aggregation studies discussed in Sections 3.2.1-2, catalase, β_L-crystallin and α-lactalbumin aggregated more rapidly at pH 6.0 and pH 6.5 than at pH 7.0 and above. The increased aggregation rate of catalase, β_L-crystallin and α-lactalbumin coincides with a decrease in the ability of α_T-, αA- and αB-crystallin to protect against target protein aggregation. It could be argued that the rate of target protein aggregation is influencing the chaperone ability of α_T-, αA- and αB-crystallin below pH 7.0. If true, this may help explain the pH-sensitive chaperone ability of α-crystallin and its subunits.

To assess this, the rate of target protein aggregation (0:1 molar ratio chaperone to target protein) was plotted versus percentage protection for each crystallin and each target protein investigated in Sections 3.2.1-2 (Figure 4.6). All pH values were included. A statistically significant relationship between aggregation rate and percentage protection, indicated by r^2 values over 0.6, would suggest that the chaperone ability of α_T-, αA- or αB-crystallin was directly influenced by the rate of target protein aggregation.

Thermally stressed catalase and β_L-crystallin (55°C and 60°C, respectively) demonstrated no significant exponential, linear or logarithmic relationship between α_T-, αA- or αB-crystallin percentage protection and target protein aggregation rate (Table 4.1); the rate of catalase or β_L-crystallin aggregation appeared to have no direct influence on the observed chaperone ability of α_T-, αA- or αB-crystallin, irrespective of pH.

Contrary to the findings for catalase or β_L-crystallin, reduction-stressed α-lactalbumin aggregation (37°C) demonstrated a correlation between chaperone activity and target protein aggregation. Strong linear and logarithmic relationships between α_T-, αA- and αB-crystallin percentage protection and target protein aggregation rate were observed (Table 4.1). Percentage protection decreased proportionately to increased α-lactalbumin aggregation rate. There appears to be a strong correlation between α-lactalbumin aggregation rate and α-crystallin percentage protection, which is in agreement with previous studies (Lindner *et al.*, 2001)
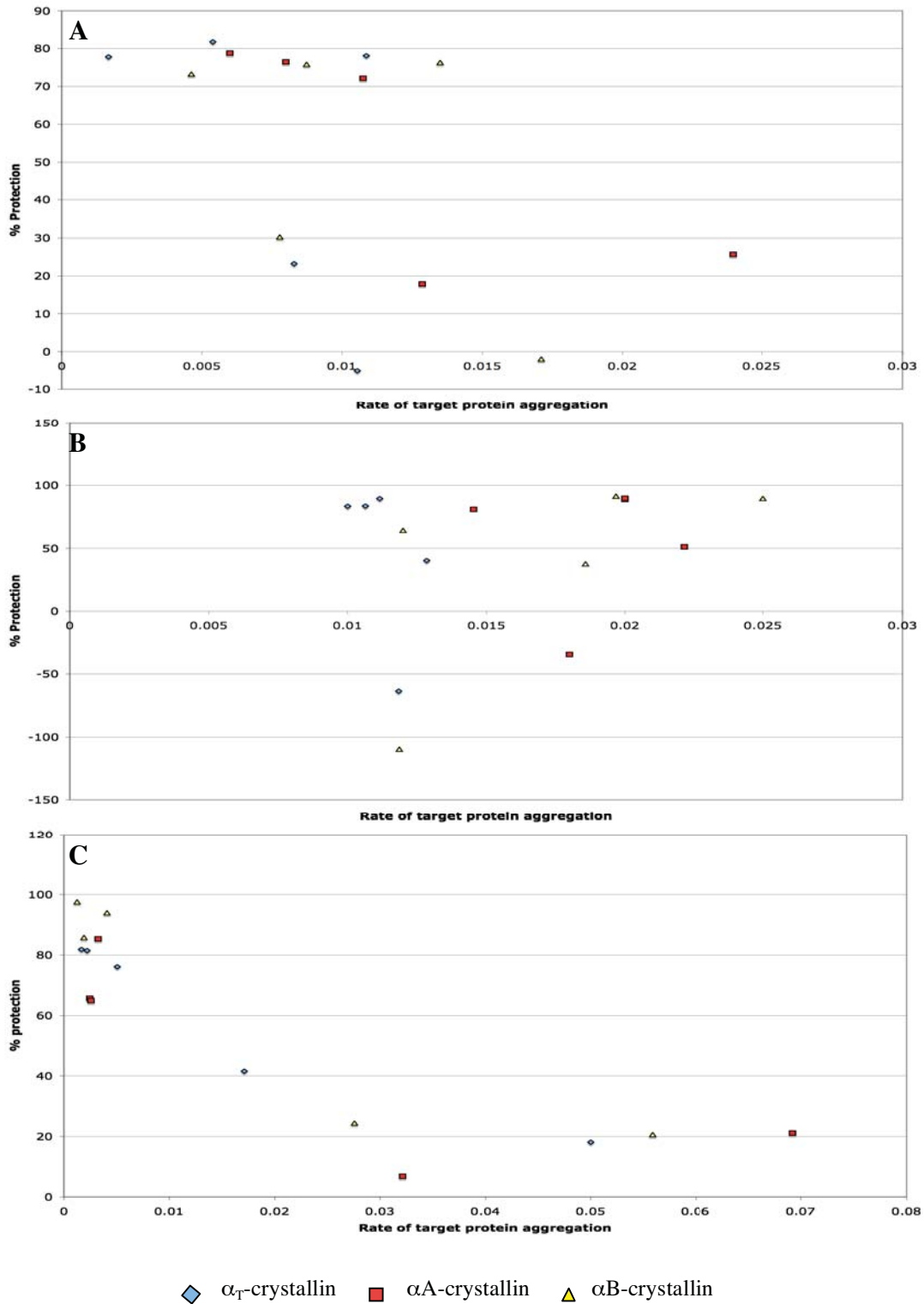
Figure 4.6 – Plots of the rate of a) catalase, b) β_L-crystallin and c) α-lactalbumin aggregation versus the corresponding α_T-, αA- or αB-crystallin percentage protection values determined in Sections 3.2.1-2. There was no statistically significant linear, logarithmic or exponential relationship between the rates of catalase or β_L-crystallin aggregation and the corresponding percentage protection values of α_T-, αA- or αB-crystallin (data from Section 3.2.1). There were, however, strong linear and logarithmic relationships between the rate of α-lactalbumin aggregation and the corresponding percentage protection values of α_T-, αA- and αB-crystallin (data from section 3.2.2). This suggests that the rate of α-lactalbumin aggregation directly influences the chaperone ability of α_T-, αA- and αB-crystallin in assays from section 3.2.2.

111

Table 4.1 – r^2 Values of linear, logarithmic and exponential trendlines from Figure 4.6. r^2 Values above 0.6 suggest a statistical relationship between the rate of protein aggregation and α-crystallin chaperone ability. There were strong linear and logarithmic relationships between the rate of α-lactalbumin aggregation and $α_T$-, αA- and αB-crystallin chaperone ability observed in Section 3.2.2. This suggests that the rate of aggregation directly influences the ability of $α_T$-, αA- and αB-crystallin to inhibit α-lactalbumin aggregation; as aggregation rate increases, chaperone ability decreases. A '-' demonstrates that no fit was possible.

	Linear	Logarithmic	Exponential
With catalase			
$α_T$-crystallin	0.2774	0.2527	-
αA-crystallin	0.5683	0.5459	0.4717
αB-crystallin	0.3168	0.2551	-
With $β_L$-crystallin			
$α_T$-crystallin	0.2685	0.2729	-
αA-crystallin	0.0025	0.0006	-
αB-crystallin	0.4081	0.4269	-
With α-lactalbumin			
$α_T$-crystallin	0.9055	0.9553	0.9798
αA-crystallin	0.6174	0.8073	0.4277
αB-crystallin	0.8367	0.9180	0.8726

4.2.7 $α_T$- and αB-crystallin chaperone ability at acidic pH

The structural characterization undertaken in this chapter suggests that $α_T$-, αA- and αB-crystallin are partially unfolded at pH 6.0 and 6.5, compared to pH 7.0 and above. This partial protein unfolding corresponds with decreased chaperone ability at pH 6.0 and 6.5 against the amorphous aggregation of catalase, $β_L$-crystallin and α-lactalbumin (Sections 3.2.1-2). The precise effect of α-crystallin unfolding and exposed hydrophobicity on its chaperone ability is currently unclear (Reddy *et al.*, 2006), and consequently it is difficult to determine the extent to which the observed

partial unfolding of α-crystallin below pH 7.0 is responsible for its corresponding decrease in chaperone ability. Previous investigation by Stevens and Augusteyn (1993) has shown that both αA- and αB-crystallin are significantly unfolded below pH 4.0, and are less structured at this pH range than at pH 6.0. At pH 2.5 $α_T$-crystallin separates into αA- and αB-crystallin homoaggregates. Below this pH value, αB-crystallin is entirely unfolded, and exists in solution as dissociated monomers, while αA-crystallin is largely unfolded and forms significantly smaller homoaggregates than at neutral pH (Stevens and Augusteyn, 1993)**.** Investigating the chaperone ability of $α_T$- and αB-crystallin at acidic pH (pH 2.0 – 3.5), under which conditions these proteins are significantly unfolded, may help to understand the relationship between partial protein unfolding and decreased chaperone ability observed at pH 6.0 and 6.5 in this study.

The reduction of protein disulphide bonds is promoted by alkaline pH, and is inhibited by acidic pH (Stryer, 1995). DTT, the most commonly used reducing agent for biological assays, has an effective reduction range of pH 6.5 to 9.5, and is most effective above pH 7.0 (Zahler and Cleland, 1968; Jocelyn, 1987). Thus, it is an ineffective reducing agent at acidic pH, and so DTT-induced protein reduction was unsuitable for the pH range used in this study (pH 2.0 - 3.5). By contrast, TCEP is more stable at acidic pH than DTT, and is an effective reduction agent at pH 1.5 (Han and Han, 1994). TCEP is limited in its ability to interact with disulphide protein bonds buried within strongly hydrophobic protein regions at neutral pH, but under denaturing conditions (including thermal denaturation or acidic pH) is up to twice as efficient a reducing agent than DTT (Han and Han, 1994). A

combination of reduction- (TCEP) and thermal-stress (55°C) was capable of inducing the amorphous aggregation of α-lactalbumin between pH 2.0 and 3.5.

The ability of α_T- and αB-crystallin to prevent the reduction- and thermal-stress induced amorphous aggregation of α-lactalbumin at acidic pH was determined by observing light scatter at 340nm of α-lactalbumin (55°C). Aggregation profiles were compared between pH 2.0 and 3.5, with the addition of increasing concentrations of α_T- and αB-crystallin. As with aggregation profiles of α-lactalbumin between pH 6.0 and pH 8.0 (Section 3.2.2), α-lactalbumin aggregation showed a dose-dependant decrease with the addition of increasing amount of α_T- or αB-crystallin between pH 2.0 and 3.5. There was no change in α_T- or αB-crystallin percentage protection between pH 2.0 and 3.5, or between α_T- and αB-crystallin (Figure 4.7). This is particularly interesting for the α_T-crystallin samples, which would consist of a mixture of semi-folded αA-crystallin homoaggregates and denatured αB-crystallin monomers at pH 2.0 and 2.5. Percentage protection values were uniformly high, and higher than at pH 6.0 or 6.5.
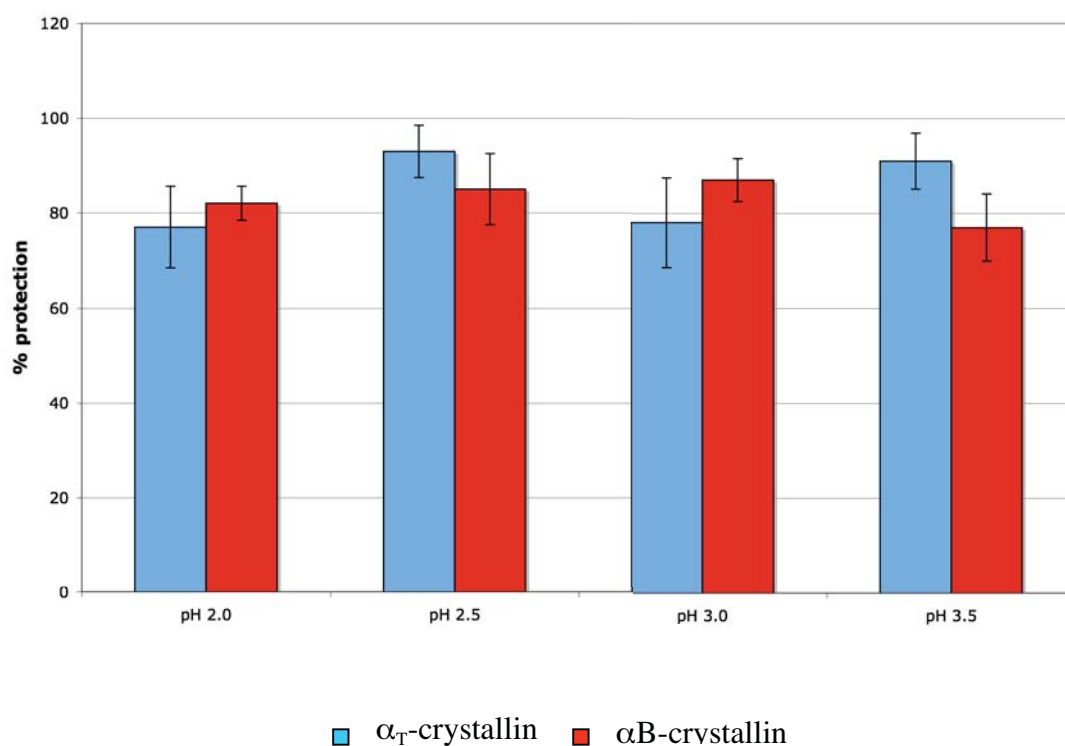
Figure 4.7 – Percentage protection values for α_T- and αB-crystallin against the amorphous aggregation of α-lactalbumin between pH 2.0 and 3.5, and at 55°C. Percentage protection was calculated from light scattering assays, and did not vary between pH 2.0 and 3.5 for either α_T- or αB-crystallin.

4.3 Discussion

Neither α_T-, αA- nor αB-crystallin aggregate size alters as pH changes from pH 6.0 to pH 8.0. Size exclusion FPLC data showed no change in the elution time of the α_T-, αA- and αB-crystallin aggregate peak as pH increased from pH 6.0 to 8.0, suggesting that there was no significant change in protein aggregate size. These data are supported by transmission electron microscopy, which showed no observable change in protein aggregate morphology as pH increased from pH 6.0 to 8.0. Constant aggregate size with pH suggests that changes in α-crystallin quaternary structure play little or no role in the pH dependence of the chaperone ability of α-crystallin over the observed pH range.

The tryptophan residues of αA- and αB-crystallin (αA-crystallin; W9, αB-crystallin; W9, W60) are located within their N-terminal regions, which are most likely buried within the interior of the α-crystallin multimer (Augusteyn and Koretz, 1987; van den Oetelaars *et al.*, 1990; Carver *et al.*, 1994). The increased maximum tryptophan fluorescence of αB-crystallin over that of αA-crystallin is in agreement with others (Sun *et al.*, 1997), and is probably a consequence of αB-crystallin's two tryptophan residues, as opposed to one residue in αA-crystallin. The lack of an observable trend in intrinsic fluorescence suggests that α-crystallin tryptophan residues are insensitive to environmental changes resulting from pH variation between pH 6.0 and 8.0. This is in agreement with previous studies (Stevens and Augusteyn, 1993). It appears that between pH 6.0 and 8.0 neither α-crystallin nor its subunits undergo significant structural change to further expose the N-terminal region of the protein to solution.

The significant increase in ANS-associated fluorescence intensity of α_T-crystallin below pH 7.0 demonstrates an increase in clustered, exposed α_T-crystallin hydrophobicity at pH 6.0 and 6.5. Similarly, the ANS-associated fluorescence of αA- and αB-crystallin demonstrates an increase in clustered, exposed hydrophobicity at pH 6.0 compared to pH 6.5 and above. Increased exposed hydrophobicity is characteristic of partial protein unfolding, as previously buried hydrophobic regions of the protein become exposed to solution. The increase in exposed α_T, αA- and αB-crystallin hydrophobicity at pH 6.0 coincides with decreased chaperone activity, as observed in Sections 3.2.1-2

The observed increase in ThT binding of α_T-, αA- and αB-crystallin as pH increased from pH 6.0 to 7.0 implies an increase in stacked β-sheet content. As previously discussed, ThT binds strongly to regions of stacked β-sheet, and consequently ThT fluorescence can be directly correlated with β-sheet content. α-Crystallin contains between 40 and 70% native β-sheet structure (Thompson and Augusteyn, 1989; Ehrnsperger *et al.*, 1997), and consequently the decrease in ThT-fluorescence below pH 7.0 (and hence decrease in β-sheet content) can be interpreted as a loss of protein secondary structure. A loss of secondary structure in this manner suggests partial protein unfolding below pH 7.0, which is largely in support of the ANS-binding data from Section 4.2.2. As with ANS binding, ThT-associated fluorescence data suggest that a partial loss of protein secondary structure coincides with a decrease in chaperone ability below pH 7.0.

The demonstrated pH-sensitive chaperone ability of α_T-, αA- and αB-crystallin does not appear to be directly related to the rate of protein aggregation in either of the thermal stress amorphous aggregation models investigated (catalase and β_L-crystallin). Plots of the rate of target protein aggregation versus percentage

protection for thermally-stressed catalase and β_L-crystallin demonstrated no suitable linear, exponential or logarithmic fit. The lack of a strong relationship between the rate of target protein aggregation and percentage protection for catalase and β_L-crystallin with either α_T-, αA- or αB-crystallin suggests that the rate of target protein aggregation did not directly influence the ability of α_T-, αA- or αB-crystallin to interact with aggregating target proteins, and is not responsible for the pH-sensitive chaperone ability observed in Section 3.2.1.

The reduction-stress induced amorphous aggregation of α-lactalbumin, however, showed strong linear and logarithmic relationships between the rate of protein aggregation and crystallin percentage protection. This suggests that for α-lactalbumin, under these conditions, aggregation rate directly influenced α-crystallin chaperone ability. As aggregation rate increased, the ability of α_T-, αA- or αB-crystallin to inhibit target protein aggregation decreased proportionally, which suggests that the rate of α-lactalbumin aggregation directly affects the chaperone ability of α_T-, αA- and αB-crystallin This has been shown previously for αB-crystallin chaperone ability against α-lactalbumin aggregation (Lindner *et al.,* 2001), and implies that below pH 7.0 the increased rate of α-lactalbumin aggregation is partially responsible for the corresponding decreased chaperone ability of α_T-, αA- or αB-crystallin, as observed in Section 3.2.2. However, the fact that target protein aggregation rate was only relevant for one target protein studied suggests that rate considerations are only one of several variables that may be responsible for the pH-sensitive chaperone activity of α-crystallin.

The structure of α-crystallin has been partially characterised between pH 2.0 and 4.0 (Augusteyn *et al.,* 1988; Stevens and Augusteyn, 1993). Below pH 2.5 α_T-crystallin dissociates into homogeneous αA-crystallin homopolymers and entirely

denatured αB-crystallin monomeric chains. Circular dichroism suggests that αA-crystallin polypeptides experience a 12% loss of secondary structure between pH 4.0 and 2.0, accompanied by an increase in random coil protein structure. Intrinsic tryptophan fluorescence red-shifts significantly for both αA- and αB-crystallin between pH 7.0 and pH 3.5, suggesting significant protein unfolding (Stevens and Augusteyn, 1993). The implication, therefore, is that between pH 2.0 and 4.0, the pH range used in Section 4.2.7, αB-crystallin exists in an entirely denatured, unfolded monomeric form, while αA-crystallin exists in unfolded, semi-structured homogeneous aggregates.

A combination of reduction- and thermal-stress induced the amorphous aggregation of α-lactalbumin between pH 2.0 and 3.5. Aggregation profiles of α-lactalbumin with $α_T$- and αB-crystallin between pH 2.0 and 3.5 showed that both crystallins are capable of chaperone activity at this pH range. α-Lactalbumin aggregation decreased in a dose-dependent fashion with the addition of increasing concentrations of either $α_T$- or αB-crystallin. This agrees with the investigation of Raman *et al.* (2005), who showed that both αA- and αB-crystallin are able to inhibit the fibrillar aggregation of β2-microglobulin at pH 2.5. It is possible that the chaperone ability of $α_T$- and αB-crystallin observed in Section 4.2.7 may be a partial consequence of the presence of a highly unfolded protein during α-lactalbumin aggregation, as opposed to a specific chaperone action (such as that observed for $α_T$- and αB-crystallin at neutral pH). Bovine serum albumin (BSA), for example, is significantly unfolded at acidic pH (Estey *et al.*, 2006), and has been demonstrated to inhibit β2-microglobulin aggregation at pH 2.5, but not at pH 7.4 (Raman *et al.*, 2005). While possible, this explanation does not adequately account for the high α-crystallin chaperone ability observed in this study; in the study of

Raman *et al.* (2005), the 'chaperone ability' of BSA was noticeably less than that of αB-crystallin under the same conditions, suggesting that the chaperone activity observed was at least partially representative of a specific chaperone mechanism.

Comparison of percentage protection data for both α_T- and αB-crystallin showed no change in chaperone ability between pH 2.0 and 3.5. This was particularly interesting for α_T-crystallin samples; above pH 2.5 the α_T-crystallin samples would consist of α_T-crystallin heteroaggregates, while below pH 2.5 α_T-crystallin samples would consist of a mixture of semi-folded αA-crystallin homopolymers and denatured αB-crystallin monomers (Stevens and Augusteyn, 1993). Accordingly, there appears to be no direct correlation between pH-induced protein unfolding or dissociation between pH 2.0 and 3.5 and subsequent α_T- or αB-crystallin chaperone ability.

Comparison of α-crystallin chaperone ability between pH 2.0 and 8.0 does not show a clear correlation between pH and chaperone ability. Between pH 2.0 and 3.5 α_T- and αB-crystallin chaperone ability against amorphous α-lactalbumin aggregation is similar to that observed at pH 7.0 and above. However, both α_T- and αB-crystallin chaperone ability is significantly lowered at pH 6.0 and 6.5. While α-crystallin chaperone ability is clearly pH-sensitive under mildly acidic conditions, the correlation between decreasing pH and decreased chaperone ability observed between pH 6.0 and 8.0 (Section 3.2.1-2) is not applicable at low pH (pH 2.0 to 3.5).

The relationship between α-crystallin exposed hydrophobicity (as a consequence of protein unfolding) and corresponding chaperone ability is currently the subject of debate. It was initially believed that an increase in exposed α-crystallin hydrophobicity correlated with an increase in chaperone ability; evidence

for this comes primarily from investigation into the effect of increasing temperature on αA- and αB-crystallin chaperone ability, in which thermally-induced α-crystallin unfolding corresponded with an increase in chaperone ability at higher temperatures (Raman and Rao, 1994; Datta and Rao, 1999). As the α-crystallin chaperone mechanism is believed to be based primarily upon hydrophobic interactions between partially-folded protein intermediates and the chaperone binding region of α-crystallin (Raman and Rao, 1994; Das *et al.*, 1996), it was assumed that an increase in exposed hydrophobicity (as a result of unfolding) would improve α-crystallin-target protein interactions, and facilitate greater chaperone ability. It has been demonstrated, however, that this is an over-simplification, and that under a variety of conditions an increase in exposed hydrophobicity has no influence on chaperone ability (Smulders *et al.*, 1995), and in some cases correlates with a *decrease* in chaperone ability (Santhoshkumar and Sharma, 2001). A recent isothermic titration calorimetry study suggests that there is no general correlation between exposed α-crystallin hydrophobicity and chaperone ability; rather, it appears that exposed hydrophobicity is only one of a number of factors that can influence α-crystallin's ability to inhibit target protein aggregation (Kumar *et al.*, 2005). Accordingly, while α-crystallin unfolding and exposed hydrophobicity may in some cases directly influence the chaperone ability of α-crystallin, it seems likely that in other cases further (possibly subtle) intrinsic factors are equally important in dictating the interaction of α-crystallin with aggregating target proteins.

Structural characterisation in this chapter demonstrated that the pH-induced decrease in chaperone ability of αT-, αA- and αB-crystallin between pH 8.0 and 6.0 corresponded with partial α-crystallin unfolding and increased exposed, clustered hydrophobicity. The partial unfolding of α-crystallin between pH 8.0 and 6.0 was,

however, comparatively minor, and the structural modifications observed are less

extensive than those between pH 2.0 and 4.0 (Stevens and Augusteyn, 1993).

Further, the data from Sections 4.2.1-5 agree with infrared spectroscopy

investigation, which has demonstrated that while α-crystallin becomes partially

denatured as pH decreases from pH 8.0 to 6.0, at pH 6.0 α-crystallin still retains

many of the structural elements present at pH 8.0 (Lin *et al.*, 1999). It is difficult to

say whether these minor changes to α-crystallin secondary structure influence its

chaperone ability to the extent observed in Sections 3.2.1-2.

There has been comparatively little investigation into the effect of pH on the

ability of molecular chaperones to inhibit protein aggregation. The decreased

chaperone ability of α-crystallin at pH 6.0 has been reported previously (Koretz *et

al.*, 1998), and was attributed to a decrease in α-helical content, rather than changes

in exposed hydrophobicity. Clusterin chaperone ability is enhanced at mildly acidic

pH, apparently as a consequence of partial protein unfolding similar to that

observed for α-crystallin in Section 4.2 (Poon *et al.*, 2002). This is in direct contrast

to the correlation between partial unfolding and decreased chaperone ability

observed for α-crystallin in this study. Hsp20 chaperone ability is compromised at

pH 6.0 in a manner similar to that of α-crystallin, and appears to be an even more

pH-sensitive chaperone than α-crystallin (Bukach *et al.*, 2004). Interestingly,

Bukach *et al.* did not report a correlation between partial protein unfolding and

Hsp20's decreased chaperone ability. Rather, Hsp20 appeared to form dissociated,

semi-folded monomers at pH 6.0 that were unstable when binding to target proteins,

resulting in decreased chaperone ability. It is unlikely, however, that this

explanation can explain the pH-sensitivity of α-crystallin chaperone ability

observed in this study; below pH 2.5 αB-crystallin exists as dissociated, unfolded

monomers (Stevens and Augusteyn, 1993) that are both soluble and efficient molecular chaperones. Based on previous data, it is difficult to attribute the pH-sensitive chaperone ability of α-crystallin observed in Sections 3.2.1-2 to partial protein unfolding. This is made even more difficult because significant αA- and αB-crystallin unfolding below pH 4.0 does not correlate with a decrease in chaperone ability. While pH-induced changes to α-crystallin structure and function have been extensively characterised in this study, none of the observed structural changes adequately explain the pH-sensitive chaperone ability of α-crystallin as seen in Sections 3.2.1-2.

Below pH 4.0, αA- and αB-crystallin homopolymers decrease in size to an average of 250kDa (αA-crystallin) and 140kDa (αB-crystallin); more significantly, below pH 2.5 αA-crystallin exists in homogenous aggregates of 160 kDa (8 subunits) while αB-crystallin is monomeric and entirely denatured (Stevens and Augusteyn, 1993). It is unlikely that these changes to αA- and αB-crystallin oligomerisation or aggregate size influence chaperone ability at low pH. At neutral pH α_T-crystallin exists in large heterogenous multimers of varying sizes, the most thorough estimate placing the α-crystallin oligomer at 700kDa (Vanhoudt *et al.,* 2000). Oligomer formation and subsequent dissociation have been identified as important factors in dictating the chaperone ability of α-crystallin (Avilov *et al.*, 2004), but recent data suggests that oligomer dissociation and subunit exchange rate do not necessarily directly correlate with chaperone ability (Augusteyn, 2004b; Aquilina *et al.*, 2005). Between pH 2.0 and 4.0 there appeared to be no difference in the chaperone ability of α_T- or αB-crystallin, despite differences in oligomer size, the dissociation of α_T-crystallin into αA- and αB-crystallin homoaggregates, and the dissociation of αB-crystallin into monomers below pH 2.5. This suggests that

oligomer size does not influence α_T- or αB-crystallin chaperone ability across this pH range, which is in agreement with previous investigation at neutral pH (Saha and Das 2004; 2007). Further, the similar chaperone ability of α_T- and αB-crystallin below pH 2.5 suggests there is little difference between the chaperone ability of monomeric and oligomeric α-crystallin at acidic pH. Interestingly, tryptic digest studies characterising α-crystallin oligomer size demonstrated that the presence of exposed hydrophobic clefts on the α-crystallin multimer is more important for effective chaperone ability than the actual oligomer size (Saha and Das, 2004; 2007).

Given the relatively tight pH range across which α-crystallin chaperone ability appears to be altered, it is possible that electrostatic interactions may be at least partially responsible for the pH sensitivity observed in Sections 3.2.1-2. Protonation of an ionisable amino acid residue (or residues) with a pKa value between pH 6.0 and 7.0 may lead to electrostatic repulsion between the chaperone molecule and target protein. This in turn may affect α-crystallin's ability to interact with, and consequently sequester target proteins. Histidine has a pKa value of 6.5 (Stryer, 1995), and so would be protonated at pH 6.5 and below. Interestingly, there is a highly conserved histidine residue (H83) within the putative chaperone-binding regions of both αA- and αB-crystallin (Sharma *et al*., 2000; Bhattacharyya *et al*., 2006). Replacement of this histidine with an alanine residue in αB-crystallin results in increased chaperone ability and molar mass, but little change to αB-crystallin secondary structure (Santhoshkumar and Sharma, 2006). Protonation of H83 at around pH 6.5 would add an additional positive charge to the chaperone-binding region of α-crystallin, and might compromise the hydrophobic interactions necessary for α-crystallin chaperone binding.

The data observed suggest three possible factors which may be responsible for the pH dependent chaperone ability of α-crystallin;

1. Gross structural changes, as characterised in this chapter. These include protein unfolding, loss of secondary structure and an increase in exposed hydrophobicity as pH decreases. It is difficult to evaluate the significance of these structural changes towards α-crystallin chaperone ability, particularly in light of the increased chaperone ability of significantly unfolded αA- and αB-crystallin at acidic pH.

2. Temperature sensitivity. The trend towards decreased percentage protection at pH 6.0 and 6.5 appears to be less pronounced at 37°C than at 55°C, which may imply that the inherent thermal stability of α-crystallin may be affected by pH (Sections 3.2.1-2). Further, α_T and αB-crystallin-target protein complexes appear unstable at pH 6.0 and pH 6.5 at 55°C (section 3.2.1), but not at 37°C (Section 3.2.2). Finally, α_T-, αA- and αB-crystallin chaperone function appears independent of the rate of target protein aggregation at 55°C and 60°C, but not always so at 37°C (Section 4.2.7).

3. Protein primary structure. The fact that pH is the variable investigated in this study implies that the surface charge of the chaperone binding region of the protein may affect its chaperone ability. αA- and αB-crystallin each have a highly conserved histidine residue in their chaperone binding regions (H83), which if solvent exposed would have a pKa value of 6.5, and so would be protonated at pH 6.0.

These factors each need investigation in greater detail. Whilst α-crystallin is a reasonably thermally stable protein, data from Sections 3.2.1-2 suggest that at

mildly acidic pH the chaperone-target protein complex was unstable at 55°C (but not so at 37°C). Accordingly, the thermal stability of α-crystallin and its subunits may be pH-sensitive in a similar manner to chaperone ability. Previous studies have suggested that α-crystallin is less able to resist re-naturation induced aggregation at pH 6.0 than at pH 8.0 (Koretz *et al*., 1998), suggesting that the inherent structural stability of α-crystallin may be compromised at pH 6.0. α-Crystallin thermal stability between pH 6.0 and 8.0 was characterised to determine whether thermal stability is pH sensitive, and in turn whether this thermal stability influences the chaperone ability of α-crystallin (Chapter 5). If α-crystallin is thermally unstable at temperatures at which thermal-aggregation assays were undertaken in Section 3.2.1, it seems likely that reduced protein stability may be partially responsible for the impaired chaperone ability of α-crystallin below pH 7.0.

The effect of amino-acid protonation on α-crystallin chaperone ability, as discussed above, was investigated using site-directed αB-crystallin mutagenesis and the chemically-induced masking of exposed histidine residues. Diethylpyrocarbonate was used to chemically mask exposed αB-crystallin histidine residues, to determine if histidine residues might be responsible for the pH sensitive chaperone ability of αB-crystallin observed in Sections 3.2.1-2 (Chapter 6). Additionally, the chaperone ability of a histidine -> alanine αB-crystallin mutant (H83A) under the conditions described in sections 3.2.1-2 (thermally-stressed catalase aggregation, reduction-stressed α-lactalbumin aggregation) was compared to that of wild-type αB-crystallin, to determine whether electrostatic interactions between charged amino acids, as affected by pH variation, might influence the chaperone ability of α-crystallin.

CHAPTER 5

CHARACTERISING THE EFFECT OF pH ON THE THERMAL
STABILITY OF α-CRYSTALLIN

Chapter 5 – The effect of pH on the thermal stability of α-crystallin

5.1 Introduction

α-Crystallin is relatively resistant to thermal modification at physiological pH, and is structurally stable at temperatures up to 62°C (Gesierich and Pfeil, 1996). Despite this stability, significant α-crystallin unfolding may begin at temperatures as low as 30°C (Raman and Rao, 1994), and between 45°C and 60°C α-crystallin undergoes a large-scale structural transition to a relaxed, molten-globule like conformation (Surewicz and Olesen, 1995; Gesierich and Pfeil, 1996). The ability of α-crystallin to inhibit β_L-crystallin aggregation increases with temperature between 30°C and 60°C, and this enhanced chaperone ability corresponds with partial α-crystallin unfolding (Raman and Rao, 1994). Accordingly, it is believed that the increased chaperone ability of α-crystallin at elevated temperatures is a direct result of increased exposed hydrophobicity, resulting from the partial unfolding of α-crystallin (Raman and Rao, 1994; Das and Surewicz, 1995). Both αA- and αB-crystallin homoaggregates have been shown to be susceptible to thermally-induced unfolding between 50°C and 60°C (Surewicz and Olesen, 1995; Gesierich and Pfeil, 1996; Datta and Rao, 1999; Reddy *et al.*, 2000). While increased temperature enhances α-crystallin chaperone ability at neutral pH, data from Section 3.2 suggest that increased temperature may inhibit chaperone ability below pH 7.0; at pH 6.0 α_T- and αB-crystallin appeared to form unstable complexes with catalase and β_L-crystallin at 55°C and 60°C, resulting in negative percentage protection as the unstable chaperone-target protein complex precipitated out of solution. At 37°C, however, the chaperone-target protein complex (α-lactalbumin or rcm κ-casein) appeared to remain stable and soluble at pH 6.0. It seems reasonable then that pH

might influence the thermal stability of α-crystallin and its subunits below pH 7.0, and that thermal stability might help to explain the variation in chaperone ability observed in Sections 3.2.1-2.

Rationale for work presented in this chapter

α_T-Crystallin aggregation with temperature was compared between pH 6.0 and pH 8.0, demonstrating that α_T-crystallin is less thermally stable at pH 6.0 than at pH 7.0 or above. Catalase chaperone assays identical to those undertaken in Section 3.2.1 were repeated at reduced temperature (45°C), at which temperature α_T-crystallin is largely thermally stable between pH 6.0 and 8.0. Percentage protection values were compared to those at 55°C, in order to observe the effect of temperature on α-crystallin chaperone ability. From these data, the effect of pH on the thermal stability of α-crystallin could be characterised, to determine what role this might have on the observed pH dependence of the chaperone ability of α-crystallin.

5.2 Results

5.2.1 The influence of pH on the thermal stability of α_T-crystallin

The effect of pH on the ability of α_T-crystallin to withstand thermal stress was monitored via light scattering at 340nm with increasing temperature. Light scatter at 340nm was measured as an indicator of protein aggregation. α_T-Crystallin samples at pH 6.0, 7.0 and 8.0 were heated from 30°C to 80°C, with light scattering compared between pH values (Figure 5.1). At pH 6.0 α_T-crystallin light scatter increased from 40°C onwards. However, at pH 7.0 and pH 8.0 light scatter did not increase noticeably until above 55°C. Maximum light scatter was higher at pH 6.0 than at pH 7.0 or pH 8.0. pH appears to directly influence the thermal stability of α_T-crystallin; α_T-crystallin is prone to thermal aggregation at lower temperatures at pH 6.0 than at pH 7.0 and above. Importantly, at pH 6.0 α_T-crystallin aggregated extensively at temperatures below those used to investigate the thermally-induced aggregation of catalase and β_L-crystallin in Section 3.2.1. The thermal instability of α_T-crystallin at pH 6.0 may partially explain the decreased chaperone ability of α_T-, αA- and αB-crystallin under thermal stress observed below pH 7.0.
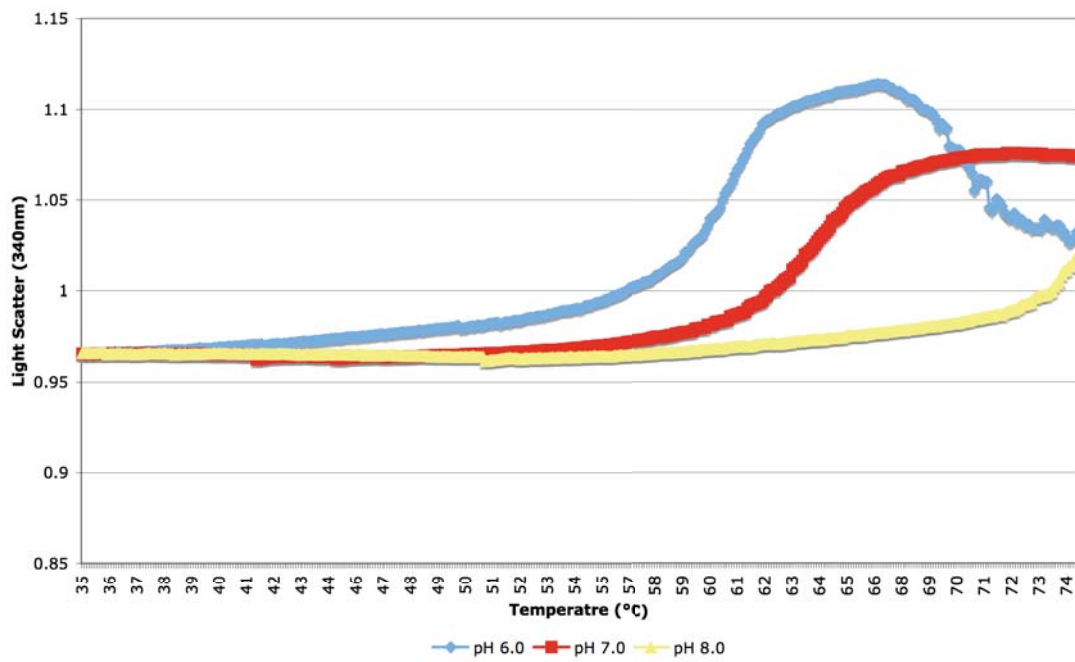
Figure 5.1 - Light scattering at 340nm of α_T-crystallin with increasing temperature between pH 6.0 and 8.0. Light scattering increased with temperature at all pH values. Light scattering at pH 6.0 increased from 40°C onwards. Light scattering at pH 7.0 and 8.0 increased from 57°C onwards.

α_T-Crystallin thermal stability was investigated in greater detail under the conditions used in Section 3.2.1, but in the absence of target protein. Light scattering (340nm) at pH 6.0, 6.5, 7.0, 7.5 and 8.0 was monitored at 37°C, 45°C and at 55°C over 2hrs, and at concentrations representative of a 1:1 molar ratio of α_T-crystallin with β_L-crystallin (0.03μM) (Figure 5.2). This concentration is in excess of that used for catalase thermal-stress aggregation assays in Section 3.2.1, and so encompasses both thermal-stress amorphous aggregation models from Section 3.2.1. At pH 7.0 or above, there was no increase in light scatter at 37°C, 45°C or 55°C. At pH 6.5, light scattering increased slightly at 55°C, but did not increase at 37°C or 45°C. At pH 6.0, light scattering increased noticeably with time at 55°C, and increased very slightly at 45°C, but did not increase at 37°C. While the rate of α_T-crystallin aggregation was low, and aggregation was comparatively slight, these data suggest that under the conditions used for catalase and β_L-crystallin thermal-stress amorphous aggregation in Section 3.2.1 α_T-crystallin was thermally unstable and prone to aggregation. At 37°C and 45°C, however, α_T-crystallin was largely thermally stable. The thermal instability of α_T-crystallin under the conditions used in Section 3.2.1 may partially explain the pH-sensitivity of α-crystallin, particularly at elevated temperatures.
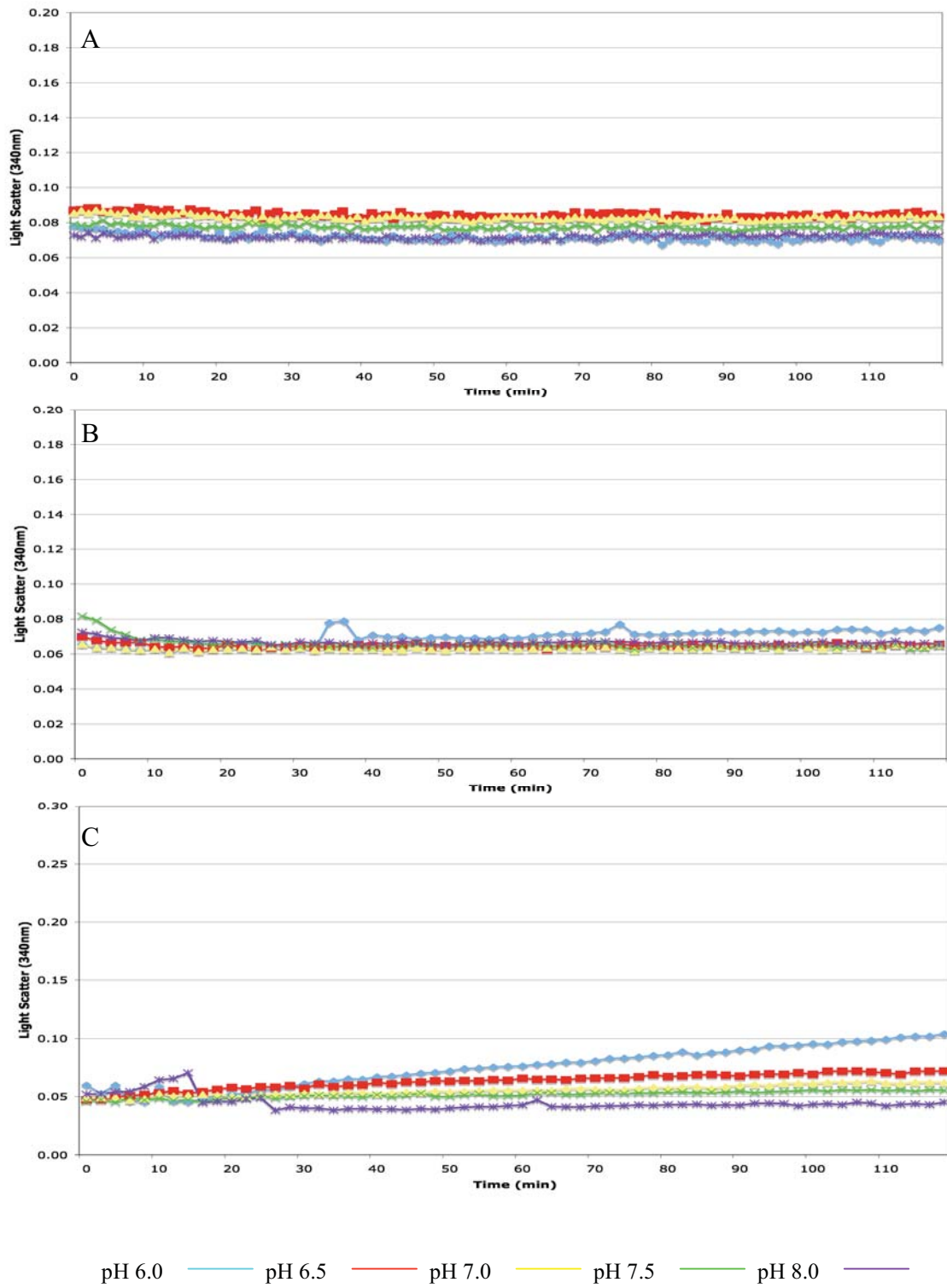
Figure 5.2 - Light scattering at 340nm of α_T-crystallin between pH 6.0 and 8.0 at (a) 37°C, (b) 45°C and (c) 55°C. At 37°C, 45°C and 55°C there was no increase in α_T-crystallin light scatter between pH 7.0 and 8.0. At 45°C α_T-crystallin light scatter increased slightly at pH 6.0. At 55°C α_T-crystallin light scatter increased at both pH 6.0 and 6.5.

5.2.2 Thermal-stress amorphous aggregation with temperature

Data from Section 5.2.1 suggest that at 55°C and pH 6.0 (and to a lesser extent, pH 6.5), α_T-crystallin is thermally unstable, and prone to thermally induced aggregation. Two of the four aggregation assays used to investigate α-crystallin chaperone ability in Section 3.2.1 were conducted at or above 55°C (catalase and β_L-crystallin); if α-crystallin aggregates under the conditions used in these assays, this would presumably affect α-crystallin chaperone ability. To examine the effect of α-crystallin's thermal stability on its chaperone ability between pH 6.0 and 8.0, the ability of αA- and αB-crystallin to prevent the thermal-stress amorphous aggregation of catalase was compared between 45°C and 55°C, and between pH 6.0 and 8.0. Whilst data from Section 5.2.1 suggests that α_T-crystallin aggregates very slightly at pH 6.0 and at 45°C, this aggregation is less extensive than that observed at 55°C; further, α_T-crystallin is very thermally stable at pH 6.5 and 45°C, but aggregates slightly at pH 6.5 and 55°C. A significant decrease in the chaperone ability of α-crystallin below pH 7.0 at 55°C compared to 45°C would suggest that the thermal stability of α-crystallin is directly influencing its chaperone ability.

Thermal stress aggregation assays were conducted with catalase as a target protein using the method described in Section 3.2.1, and using the same protein stocks for assays at 45°C and 55°C. Data were acquired at pH 6.0, 6.5, 7.0, 7.5 and 8.0. The ability of αA- and αB-crystallin to inhibit thermal-stress induced catalase aggregation at 45°C demonstrated a pH dependence similar to that observed at 55°C. For each chaperone, target protein aggregation showed a dose-dependant decrease with the addition of increasing amount of αA- or αB-crystallin. As at 55°C, percentage protection was lowest at pH 6.0, and increased significantly

between pH 6.0 and pH 7.0. There was no significant variation in percentage protection between pH 7.0 and pH 8.0.

Percentage protection values for αA- and αB-crystallin with catalase were compared between 45°C and 55°C (Figure 5.3). Comparison of percentage protection values at 45°C and 55°C across the observed pH range showed a significant increase in αA- and αB-crystallin percentage protection at 45°C and at pH 6.0 and 6.5. Interestingly, above pH 7.0, there was no significant difference in either αA- or αB-crystallin percentage protection between 55°C and 45°C. Below pH 7.0, αA- and αB-crystallin are more effective chaperones of catalase at 45°C than at 55°C. Conversely, above pH 7.0 neither αA- or αB-crystallin chaperone ability appeared to be significantly effected by temperature.
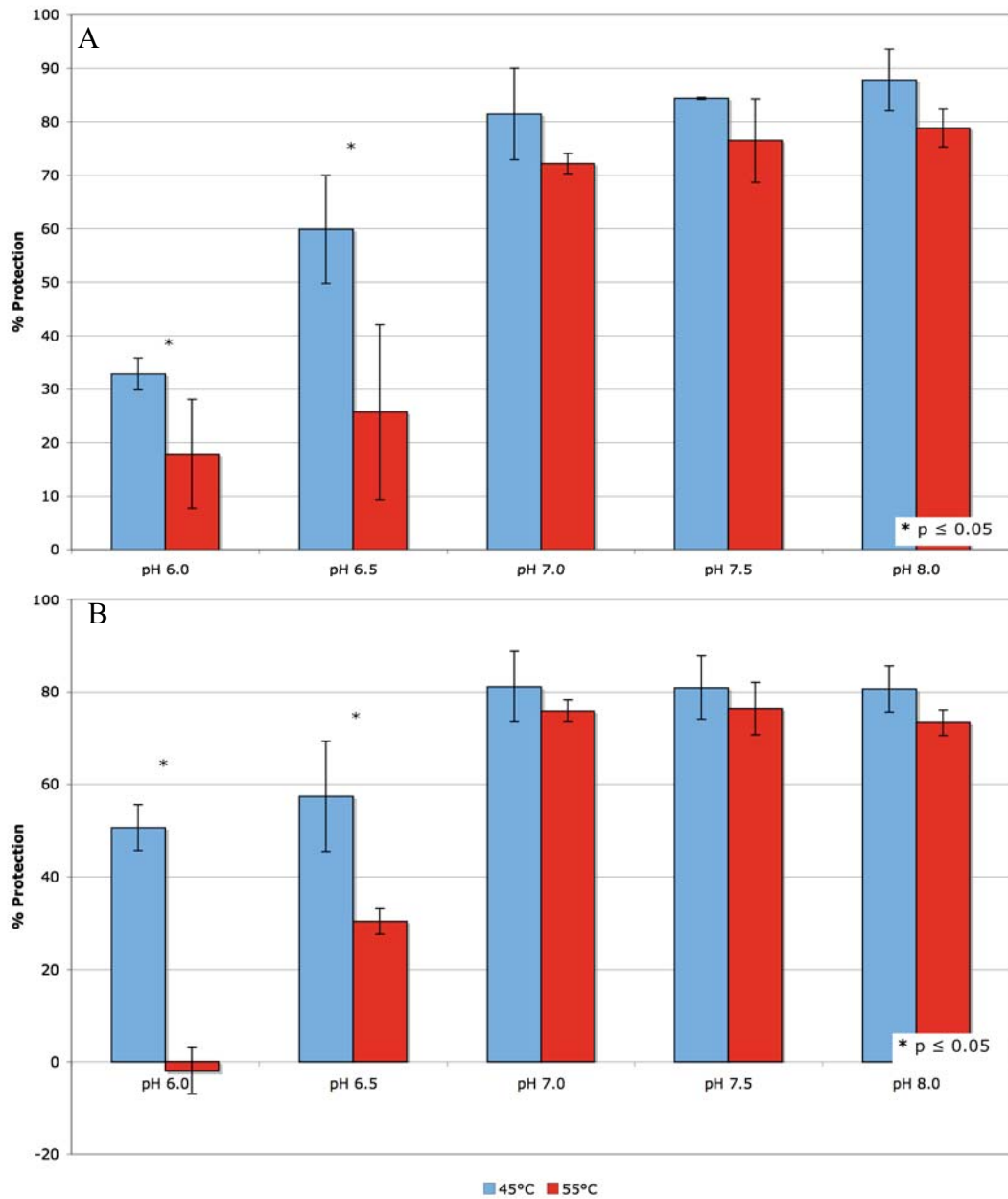
Figure 5.3 -.Comparison of percentage protection values of a) αA- and b) αB-crystallin against catalase aggregation between pH 6.0 and 8.0, and at 45°C and 55°C. At pH 6.0 and 6.5, percentage protection for αA- and αB-crystallin was significantly increased at 45°C compared to 55°C. At pH 7.0 and above there was no significant difference in percentage protection for either α_T- or αB-crystallin between 45°C and 55°C. * indicates significant difference in the mean percentage protection between 45°C and 55°C at each pH value ($p \leq 0.05$).

5.3 Discussion

Light scattering at 340nm demonstrated that α_T-crystallin is unstable, and slightly prone to thermal-stress induced aggregation at elevated temperatures and at lower pH values. At pH 7.0 and 8.0, thermal-stress induced α_T-crystallin aggregation began at approximately 60°C. Interestingly, at pH 6.0 α_T-crystallin aggregation occurred at temperatures as low as 40°C, which is significantly lower than at pH 7.0 or above. Mildly acidic pH appears to compromise the thermal stability of α_T-crystallin. Importantly, the temperature of α_T-crystallin aggregation at pH 6.0 is below that used in a number of chaperone assays in this study, including the thermal-stress induced aggregation of catalase and β_L-crystallin (55°C, Section 3.2.1). It would appear that α_T-crystallin (and presumably αA- and αB-crystallin) would be prone to aggregation at pH 6.0 and 6.5 during some of the aggregation assays used in this study; accordingly, this aggregation would inhibit α-crystallin chaperone ability.

Time-course aggregation assays of α_T-crystallin between pH 6.0 and 8.0 for 2 hrs at 55°C showed that α_T-crystallin aggregation occurred at pH 6.0 and 6.5, but not at pH 7.0 or above (Figure 5.2). There was little or no α_T-crystallin aggregation observed at 37°C or 45°C. Consequently, it appears that α_T-crystallin is thermally unstable under the conditions used for catalase and β_L-crystallin aggregation assays in Section 3.2.1. The chaperone ability of α-crystallin would be compromised under these conditions, due to its aggregation, and so the effect of pH on the thermal stability of α-crystallin may help to explain the pH-sensitivity of α-crystallin chaperone ability.

Increased temperature directly affects αA- and αB-crystallin chaperone ability. Previously, increased temperature has been demonstrated to enhance α-crystallin chaperone ability at neutral pH (Raman and Rao, 1994; Das and Surewicz, 1995; Datta and Rao, 1999). However, the relationship between increased temperature and α-crystallin chaperone ability is not necessarily a straightforward one; Raman and Rao (1994) saw no difference in the ability of α-crystallin to inhibit the reduction-stress induced aggregation of insulin above 35°C, while Lee *et al.* (1997b) found that the ability of α-crystallin to inhibit the thermal-stress induced aggregation of alcohol dehydrogenase was essentially unchanged between 48°C and 70°C. Above pH 7.0, this study showed no significant difference in αA- or αB-crystallin percentage protection values against thermally-stressed catalase at 45°C and 55°C. These data do not necessarily contradict that of previous researchers, as it is likely that a number of factors require consideration in discussing the effect of temperature on α-crystallin chaperone ability. Rekas *et al.* (2007) identified that while the ability of α-crystallin to inhibit rcm κ-casein aggregation is thermally sensitive, investigation becomes complicated by the increased aggregation rate of rcm κ-casein at elevated temperatures. It may be the case in this study that the increased aggregation rate of catalase at 55°C compared to 45°C mitigates, to an extent, the chaperone ability of αA- and αB-crystallin, as has been seen for α-lactalbumin aggregation (Lindner *et al.*, 2001). This would mask any effect of increased temperature on the chaperone ability of α-crystallin.

At pH 6.0 and 6.5, increased temperature inhibited αA- and αB-crystallin chaperone ability; percentage protection was significantly lower for both αA- and αB-crystallin with thermally-stressed catalase at 55°C than at 45°C. It may be the case, as discussed above, that the decreased rate of catalase aggregation at 45°C

enhances the chaperone ability of αA- and αB-crystallin, and that this may explain the increased percentage protection values observed for αA- and αB-crystallin at 45°C compared to 55°C. This explanation appears insufficient, however, when considered in light of the lack of a significant difference in αA- and αB-crystallin percentage protection values between 45°C and 55°C above pH 7.0. Rather, these data suggest that the thermal stability of α-crystallin, as investigated in this study, directly influences its chaperone ability between pH 6.0 and 7.0. Accordingly, the decreased thermal stability of α-crystallin at pH 6.0 and 6.5, compared to pH 7.0 and above, may be partially responsible for the pH sensitive chaperone ability observed in Section 3.2. It is important to note, however, that the ability of αA- and αB-crystallin to inhibit the thermally-induced aggregation of catalase at 45°C is still pH sensitive; that is, at 45°C αA- and αB-crystallin are more efficient chaperones against catalase aggregation at pH 7.0 and above than at pH 6.0 or 6.5. Similarly, the ability of α_T-, αA- and αB-crystallin to inhibit the reduction-stress induced aggregation of α-lactalbumin at 37°C (Section 3.2.2) is pH sensitive in a manner reminiscent of aggregation assays conducted at higher temperatures (i.e, catalase or β_L-crystallin at 55°C). While higher temperatures appear to exacerbate the inability of αA- and αB-crystallin to efficiently chaperone aggregating catalase below pH 7.0, α-crystallin chaperone ability below pH 7.0 is still significantly compromised at temperatures as low as 37°C.

Koretz *et al.* (1998) have described a variety of effects that pH has on the quaternary structure of α_T-crystallin, including an increased susceptibility to renaturation-induced aggregation at pH 6.0 compared to pH 8.0. (Koretz *et al.*, 1998). The protonation of an ionisable amino acid, such as histidine (as discussed in section 4.3), might help to explain the pH-dependent thermal stability of α-

crystallin. Modification of a single histidine residue (H83) results in a two-fold increase in αB-crystallin aggregate size upon reassociation (Santhoshkumar and Sharma, 2006), and the chemical modification of surface histidine residues by diethylpyrocarbonate (DEPC) increases α_T-crystallin aggregate size and modifies subunit re-assembly and oligomeric re-organisation after protein denaturation (Pal and Ghosh, 1998). As roughly 43% of α-crystallin histidine residues are buried within the α-crystallin oligomer (Bera and Ghosh, 1996), it has been suggested that the differential accessibility of α-crystallin histidine residues may be significant in stabilising α-crystallin quaternary structure and maintaining surface hydrophobicity. Were this the case, protonation of histidine residues at pH 6.5 may affect the stability or solubility of the α-crystallin aggregate, and in turn be responsible for the compromised thermal stability observed in this study.

Previous investigations suggest that the flexibility of the C-terminal extension is necessary for retaining protein solubility and thermal stability (Carver and Lindner, 1998). NMR analysis of tryptophan and alanine αA-crystallin C-terminal mutants demonstrated that reduction of C-terminal extension flexibility, by introducing a hydrophobic tryptophan residue to the largely polar C-terminal extension, had no effect on the temperature of protein unfolding of α-crystallin. Despite this, the less flexible tryptophan mutant aggregated and precipitated out of solution at 52°C while the alanine mutant remained soluble (Smulders *et al.*, 1996). Accordingly, pH-induced modification of the α-crystallin C-terminal extension may result in compromised flexibility, may be further cause for the observed pH sensitivity of α-crystallin thermal stability.

It appears then that the pH sensitivity of α-crystallin chaperone ability observed in Section 3.2 can, in part, be explained by the influence of pH on the

thermal stability of the protein. At pH 6.0 and 6.5, α_T-crystallin is prone to thermally induced aggregation at temperatures above 50°C, while at pH 7.0 and above α_T-crystallin remains thermally stable. This differential thermal stability may be a consequence of decreased C-terminal extension flexibility or electrostatic instability, and results in the chaperone forming unstable complexes with aggregating target proteins. These unstable complexes aggregate and precipitate out of solution, resulting in negative percentage protection and increased target protein aggregation at pH 6.0. However, at temperatures as low as 37°C, at which α-crystallin has been demonstrated to be thermally stable, percentage protection is still dependent upon pH and mirrors the trend observed at higher temperatures. Thermal stability on its own does not adequately explain the pH sensitive chaperone ability of α-crystallin; a variety of factors appear to be responsible for the decreased chaperone ability of α-crystallin under mildly acidic conditions.

CHAPTER 6

THE ROLE OF HISTIDINE RESIDUES IN THE CHAPERONE
ACTIVITY OF αB-CRYSTALLIN

Chapter 6 – The role of histidine residues in the chaperone action of αB-crystallin

6.1 Introduction

A variety of factors have been investigated so far in this study to explain the pH sensitivity of α-crystallin chaperone ability against amorphous aggregation, as described in Sections 3.2.1-2. Partial unfolding of α-crystallin as pH decreases from pH 7.0 to 6.0 appears to have only a limited influence on the ability of α-crystallin to inhibit target protein aggregation. Further, significant α-crystallin unfolding below pH 4.0 appears to enhance α-crystallin chaperone ability with α-lactalbumin. While the effect of pH on α-crystallin thermal stability appears to partially influence the chaperone ability of α-crystallin at 55°C and 60°C, this does not explain the pH sensitive chaperone ability observed at 37°C and 45°C (at which temperatures α-crystallin is largely thermally stable). A relationship between percentage protection and target protein aggregation rate may help to explain the effect of pH on α-crystallin chaperone ability against the amorphous aggregation of α-lactalbumin at 37°C, but not the effect of pH on α-crystallin chaperone ability at 45°C, 55°C or 60°C. It appears that other intrinsic factors are influencing the chaperone ability of α-crystallin and its subunits at pH 6.0 and 6.5.

The putative chaperone binding regions of both αA- and αB-crystallin have been characterised previously (Sharma *et al.*, 2000; Bhattacharyya *et al.*, 2006). There is significant overlap between these chaperone binding regions in αA- and αB-crystallin, and both αA- and αB-crystallin have a highly conserved histidine residue within their chaperone-binding region (αA-crystallin H79; αB-crystallin H83). Protonation of this histidine residue, which would occur when the pH is

lowered from pH 7.0 to 6.0, may result in electrostatic repulsion between α-crystallin and misfolded target proteins, and thereby interfere with hydrophobic interactions between α-crystallin and aggregating, partially folded target proteins. The significant decrease in chaperone ability between pH 7.0 and 6.0 suggests that protonation of a histidine residue may be partially responsible for the decreased chaperone ability of α-crystallin below pH 7.0.

The effect of histidine residues on α-crystallin structure and chaperone activity has been characterised previously, but not in relation to pH. Modification of exposed αB-crystallin histidine residues using diethylpyrocarbonate (DEPC), a histidine masking molecule, demonstrated no significant effect on chaperone ability at pH 7.4 (Bera and Ghosh, 1996; Pal and Ghosh, 1998). Conversely, studies using an H83A αB-crystallin mutant demonstrated a two-fold increase in molar mass, and showed a 15 - 20% increase in chaperone ability against alcohol dehydrogenase and insulin aggregation at pH 7.2 (Santhoshkumar and Sharma, 2006). Chaperone assays using both DEPC-modified and H83A mutant αB-crystallin between pH 6.0 and pH 8.0 may help to determine what effect, if any, protonation of histidine residues has on the chaperone ability of α-crystallin.

Rationale for work presented in this chapter

The protonation of exposed histidine residues on αB-crystallin can be blocked via the binding of DEPC. Characterising the ability of DEPC-bound αB-crystallin to inhibit the aggregation of thermally-stressed catalase between pH 6.0 and 8.0 will clarify the influence of exposed histidine residues on the chaperone ability of αB-crystallin; if protonation of histidine residues is responsible for the decreased

chaperone ability of αB-crystallin below pH 7.0, DEPC binding to αB-crystallin should enhance chaperone ability at pH 6.0 and 6.5 compared to unmodified αB-crystallin. Similarly, substituting mutant H83A αB-crystallin into the thermal- and reduction-stress aggregation assays described in Sections 3.2.1-2 will clarify the influence of a specific histidine residue, His83, on the chaperone ability of αB-crystallin. If blocking the protonation of one or more histidine residues improves the chaperone ability of αB-crystallin at pH 6.5 and below, it would suggest that histidine protonation is at least partially responsible for the pH sensitive chaperone ability of αB-crystallin observed in Sections 3.2.1-2.

6.2 Results

6.2.1 Modification of surface-exposed histidine residues on αB-crystallin

Diethylpyrocarbonate (DEPC) binds covalently to a number of nucleophiles, including amines and imidazoles (Ovadi and Keleti, 1969; Tawfik, 1996). The binding of DEPC to a histidyl residue results in the formation of N-carbethoxyhistidyl product (Figure 6.1), and this reaction has been shown to inhibit histidine protonation (Dietz *et al.*, 1992). N-carbethoxyhistidine has a characteristic absorbance at 240nm (ε_{240} = 3200 M^{-1} cm^{-1}) (Miles, 1977; Tawfik, 1996), and so the binding of DEPC to histidine residues can be followed spectrophotometrically. Consequently, the binding of DEPC is commonly used to inhibit histidine protonation *in vitro*, and to probe the role of histidine residues in protein function (Dietz *et al.*, 1992; Carneiro *et al.*, 2003; Kawai *et al.*, 2005). The binding of DEPC to α_T-crystallin has been well characterised previously (Bera and Ghosh, 1996; Pal and Ghosh, 1998), demonstrating that approximately 57% of α_T-crystallin histidine residues are available for binding with DEPC (Bera and Ghosh, 1996). In that study, the binding of DEPC to α_T-crystallin increased α_T-crystallin aggregate size upon subunit re-assembly, but had no effect on α_T-crystallin chaperone ability at pH 7.4 (Pal and Ghosh, 1998).
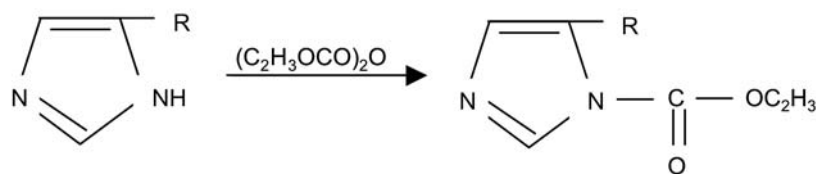
Figure 6.1 – The reaction of diethylpyrocarbonate with a histidyl residue, resulting in the formation of N-carbethoxyhistidyl derivative.

The modification of surface-exposed αB-crystallin histidine residues was achieved via DEPC binding, using a variation of the method described by Bera and Ghosh (1996). αB-crystallin in phosphate buffer was incubated with a 600-fold molar excess of DEPC for 2 hrs at room temperature. These have been identified as the optimal conditions for DEPC binding to α-crystallin (Bera and Ghosh, 1996). DEPC binding was monitored by absorbance at 240nm. The binding of DEPC to αB-crystallin was quantified on a molar subunit basis using the extinction coefficient of N-carbethoxyhistidine ($\varepsilon_{240} = 3200$ M^{-1} cm^{-1}). At 2 hours four moles of N-carbethoxyhistidine were observed per mole of αB-crystallin, demonstrating that four of a possible seven histidine residues were modified per αB-crystallin subunit (56%) (Figure 6.2). This is in agreement with the findings of Bera and Ghosh (1996).

Chaperone assays were conducted under conditions identical to those described in Section 3.2.1. Light scattering at 340nm of heat-stressed catalase was measured at pH 6.0, 6.5, 7.0, 7.5 and 8.0, and in the presence of DEPC-modified αB-crystallin (see appendix D, Figure D1). Dialysis disrupts the binding of DEPC to histidine residues, and unbound DEPC rapidly hydrolyses to ethanol and carbonate;

consequently, it is common practice to conduct activity assays involving DEPC-modified proteins without removing excess DEPC from solution (Tawfik, 1996). However, control experiments demonstrated that unbound DEPC in solution significantly inhibited catalase aggregation. Presumably, not all unbound DEPC was hydrolysed during incubation with αB-crystallin, and interacted with catalase to stabilise it against unfolding. To quantify the effect of DEPC binding on αB-crystallin chaperone ability, and account for the added influence of DEPC-induced inhibition of catalase aggregation, percentage protection was compared between DEPC, unmodified αB-crystallin, and DEPC-modified αB-crystallin. The percentage protection values of unbound DEPC and unmodified αB-crystallin were summed to create a 'theoretical' percentage protection value that accounted for the cumulative effect of both αB-crystallin and unbound DEPC on catalase aggregation. The calculation of theoretical percentage protection as a control value was considered the most suitable method of control (as opposed to using a combination of DEPC and αB-crystallin prepared immediately prior to analysis, for example), as this method eliminated the possibility of DEPC interacting with αB-crystallin in the control sample over the course of the aggregation assays. The theoretical value was compared to the observed percentage protection value of DEPC-modified αB-crystallin to determine whether binding DEPC to αB-crystallin had any effect on αB-crystallin chaperone ability (Figure 6.3). If the theoretical percentage protection value matched that of the DEPC-bound αB-crystallin, it would suggest that any effect on αB-crystallin chaperone ability observed after the addition of DEPC was an artefact of the inherent protein-stabilising ability of DEPC, and not a consequence of structural modifications to αB-crystallin resulting from DEPC binding.

Theoretical percentage protection values were significantly lower than that of DEPC-modified αB-crystallin at pH 6.0 and 6.5, suggesting that binding DEPC to αB-crystallin increases its chaperone ability. At pH 7.0 and 7.5 there was no significant difference between the theoretical percentage protection value and that of DEPC-modified αB-crystallin. At pH 8.0 the theoretical percentage protection value was in excess of 100%, as a result of the significant chaperone ability of DEPC at pH 8.0. As percentage protection values cannot in reality exceed 100%, theoretical percentage protection was 'capped' at 100% at pH 8.0, to enable comparison with DEPC-modified αB-crystallin. When analysed in this way, there was no significant difference between the theoretical percentage protection value and that of DEPC-bound αB-crystallin; that is, binding DEPC to αB-crystallin enhances αB-crystallin chaperone ability at pH 6.0 and 6.5, but has no effect on chaperone ability at pH 7.0 or above. This suggests that blocking surface-exposed histidine residues on αB-crystallin enhances its chaperone ability at pH 6.5 and below. Whilst binding DEPC to αB-crystallin enhanced chaperone ability at pH 6.0, the percentage protection value for DEPC-bound αB-crystallin at pH 6.0 was still significantly lower than that at pH 6.5 and above. There was no significant difference in percentage protection for DEPC-modified αB-crystallin at pH 6.5 and above. Modifying surface-exposed histidine residues via DEPC binding removes, to a large extent, the pH-sensitivity of αB-crystallin.
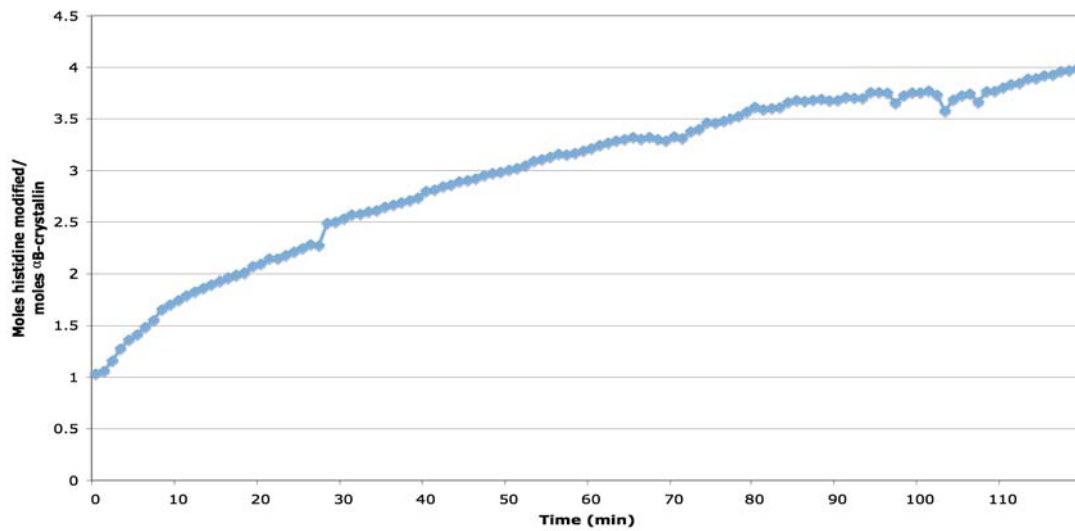
Figure 6.2 – Moles of DEPC bound to histidine per mole of αB-crystallin (with time), as calculated from absorbance at 240nm. After a two hour incubation, approximately four moles of DEPC were bound to histidine per mole of αB-crystallin, demonstrating that four DEPC molecules were bound to each molecule of αB-crystallin, and hence that four histidine residues were modified per αB-crystallin monomer.
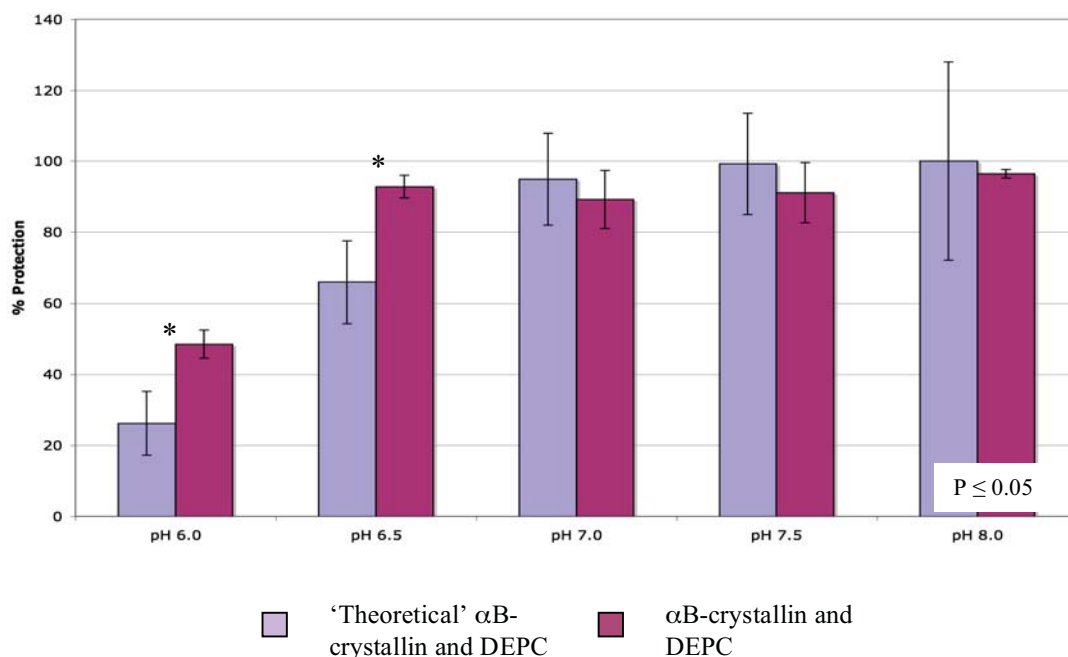
Figure 6.3 – Comparison of percentage protection values between αB-crystallin, and αB-crystallin modified by DEPC, against catalase aggregation. As unbound DEPC stabilises catalase against aggregation, it was necessary to compare the percentage protection values of unbound DEPC, αB-crystallin, and DEPC-bound αB-crystallin; percentage protection was summed for unbound DEPC and αB-crystallin, to provide a 'theoretical' percentage protection value that accounts for the chaperone effect of unbound DEPC. 'Theoretical' percentage protection values were compared to those for DEPC-bound αB-crystallin. Percentage protection values were higher for DEPC-bound αB-crystallin than the corresponding theoretical percentage protection values values at pH 6.0 and 6.5, but there was no statistical difference between theoretical and observed percentage protection values at pH 7.0 and above. * denotes significant difference in the mean between 'theoretical' and observed percentage protection values at a given pH (p ≤ 0.05).

6.2.2 Sequence similarity search and multiple sequence alignment of conserved histidine residues in αA- and αB-crystallin

Blastp is a similarity search algorithm that can be used to compare a number of protein sequences within the Swiss-Prot and TrEMBL protein databases, and rank them in terms of sequence similarity. Multiple protein sequences can be subsequently aligned using ClustalW2, which aligns divergent protein sequences and allows for comparison of residues between numerous protein sequences.

A blastp sequence similarity search of the Swiss-Prot and TrEMBL protein databases against human αB-crystallin resulted in twenty αA- and αB-crystallin sequences from a variety of organisms. ClustalW2 multiple sequence alignment suggested highly conserved αA- and αB-crystallin primary structures amongst the twenty proteins obtained via sequence similarity search. The previously characterised human αA- and αB-crystallin putative chaperone-binding regions (αA-crystallin residues 54-113; αB-crystallin residues 58-117) (Sharma *et al.*, 2000; Bhattacharyya *et al.*, 2006) were highly conserved between species for both αA- and αB-crystallin, and there was significant overlap between the chaperone binding regions of αA- and αB-crystallin (Figure 6.4). Both subunits contained a highly conserved histidine residue within the chaperone-binding region (αB-crystallin H83; αA-crystallin H79).

A clustalW2 multiple sequence alignment of the ten known human sHsps demonstrated that the histidine residue at H83 of αB-crystallin is reasonably conserved between human sHsps, and is the consensus residue at this location (HspB1 H103; HspB2 H82; HspB6 H82) (Figure 6.5). The HspB- classification of human sHsps was used for clustalW2 multiple sequence alignment, due to its

systematic nomenclature. The conserved nature of this histidine residue, and its location within the putative chaperone binding regions of αA- and αB-crystallin, suggests that it may have a role in the chaperone activity of α-crystallin and other human sHsps. Protonation of this residue at mildly acidic pH may explain the decreased chaperone ability of both α_T, αA- and αB-crystallin observed in this study (Sections 3.2.1-2).

```
CRYAA_TAMME     RTALDSGISEVRSDRDRFVILLDVKHFSPEDLTVKVLDDFVEIHGKHNERQDDHGYISRE     113
CRYAA_BRAVA     RTALDSGISEVRSDRDKFVIFLDVKHFSPEDLTVKVLGDFVEIHGKHNERQDDHGYISRE     113
CRYAA_CHOHO     RTVLDSGISEVRSDRDKFVIFLDVKHFSPEDLTVKVLDDFVEIHGKHNERQDDHGYISRE     113
CRYAA_HUMAN     RTVLDSGISEVRSDRDKFVIFLDVKHFSPEDLTVKVQDDFVEIHGKHNERQDDHGYISRE     113
CRYAA_MACMU     RTVLDSGISEVRSDRDKFVIFLDVKHFSPEDLTVKVQDDFVEIHGKHNERQDDHGYISRE     113
CRYAA_MERUN     RTVLDSGISEVRSDRDKFVIFLDVKHFSPEDLTVKVLEDFVEIHGKHNERQDDHGYISRE     113
CRYAA_TUPGL     RTVLDSGISEVRSDRDKFVIFLDVKHFSPEDLTVKVLEDFVEIHGKHNERQDDHGYISRE     113
CRYAA_CAVPO     RTVLDSGISEVRSDRDKFVIFLDVKHFSPEDLTVKVQEDFVEIHGKHNERQDDHGYISRE     113
CRYAA_PEDCA     RTVLDSGISEVRSDRDKFVIFLDVKHFSPEDLTVKVQEDFVEIHGKHNERQDDHGYISRE     113
CRYAA_RABIT     RTVLDSGISEVRSDRDKFVIFLDVKHFSPEDLTVKVQEDFVEIHGKHNERQDDHGYISRE     113
CRYAA_HORSE     RTVLDSGISEVRSDRDKFVIFLDVKHFSPEDLTVKVQEDFVEIHGKHNERQDDHGYISRE     113
CRYAA_CERSI     RSVLDSGVSEVRSDRDKFVIFLDVKHFSPEDLTVKVQEDFVEIHGKHNERQDDHGYISRE     113
CRYAA_TAPIN     RTVLDSGISEVRSDRDKFVIFLDVKHFSPEDLTVKVQEDFVEIHGKHNERQDDHGYISRE     113
CRYAA_BOVIN     RTVLDSGISEVRSDRDKFVIFLDVKHFSPEDLTVKVQEDFVEIHGKHNERQDDHGYISRE     113
CRYAA_SHEEP     RTVLDSGISEVRSDRDKFVIFLDVKHFSPEDLTVKVQEDFVEIHGKHNERQDDHGYISRE     113
CRYAA_PIG       RTVLDSGVSEVRSDRDKFVIFLDVKHFSPEDLTVKVQEDFVEIHGKHNERQDDHGYISRE     113
CRYAA_ARTJA     RTVLDSGISEVRSDRDKFVIFLDVKHFSPEDLTVKVQEDFVEIHGKHNERQDDHGYISRE     113
CRYAA_LOXAF     RTVLDSGISEVRSDRDQFVILLDVKHFSPEDLTVKVQDDFVEIHGKHNERQDDHGYISRE     113
CRYAA_PROCA     RTVLDSGISEVRSDRDQFLILLDVKHFSPEDLTVKVLDDFVEIHGKHNERQDDHGYISRE     113
CRYAA_TUPTE     RTVLESGISEVRSDRDKFTIFLDVKHFSPEDLSVKVIEDFVEIHGKHNERQDDHGYISRE     113
CRYAB_HUMAN     PSWFDTGLSEMRLEKDRFSVNLDVKHFSPEELKVKVLGDVIEVHGKHEERQDEHGFISRE     117
CRYAB_PONPY     PSWFDTGLSEMRLEKDRFSVNLDVKHFSPEELKVKVLGDVIEVHGKHEERQDEHGFISRE     117
CRYAB_MACFA     PSWFDTGLSEMRLEKDRFSVNLDVKHFSPEELKVKVLGDVIEVHGKHEERQDEHGFISRE     117
CRYAB_RABIT     PSWIDTGLSEMRLEKDRFSVNLDVKHFSPEELKVKVLGDVIEVHGKHEERQDEHGFISRE     117
CRYAB_MESAU     PSWIDTGLSEMRMEKDRFSVNLDVKHFSPEELKVKVLGDVVEVHGKHEERQDEHGFISRE     117
CRYAB_RAT       PSWIDTGLSEMRMEKDRFSVNLDVKHFSPEELKVKVLGDVIEVHGKHEERQDEHGFISRE     117
CRYAB_SPAJD     PSWIDTGLSEMRMEKDRLSVNLDVKHFSPEELKVKVLGDVIEVHGKHEERQDEHGFISRE     117
CRYAB_MOUSE     PSWIDTGLSEMRLEKDRFSVNLDVKHFSPEELKVKVLGDVIEVHGKHEERQDEHGFISRE     117
CRYAB_SHEEP     PSWIDTGLSEVRLEKDRFSVNLDVKHFSPEELKVKVLGDVIEVHGKHEERQDEHGFISRE     117
CRYAB_BOVIN     PSWIDTGLSEMRLEKDRFSVNLDVKHFSPEELKVKVLGDVIEVHGKHEERQDEHGFISRE     117
CRYAB_CHICK     PSWLETGLSEMRLEKDKFSVNLDVKHFSPEELKVKVLGDMIEIHGKHEERQDEHGFIARE     116
CRYAB_ANAPL     PSWLETGLSEMRLEKDKFSVNLDVKHFSPEELKVKVLGDMVEIHGKHEERQDEHGFIARE     116
CRYAB_RANCA     PSWIESGLSEMRLEKDKFSINLDVKHFSPEELKVKVSGDFIEIHGKHEERQDEHGYVSRD     115
CRYAB_SQUAC     PSWAQTGLSELRLDKDKFAIHLDVKHFTPEELRVKILGDFIEVQAQHEERQDEHGYVSRE     119
```

Figure 6.4 – A section of the clustalW2 multiple sequence alignment of αA- and αB-crystallin (αA-crystallin residues 54-113; αB-crystallin residues 58-117), from a variety of species. Previously characterised chaperone-binding regions (αA-crystallin residues 70 – 88; αB-crystallin residues 79-92) within human αA- and αB-crystallin are in blue (Sharma *et al.*, 2000; Bhattacharyya *et al.*, 2006). Conserved histidine residues within these regions (αA-crystallin H79; αB-crystallin H83) are in red. For an explanation of Swiss-Prot entry names, see Appendix B.

```
CRYAA_HUMAN    KFVIF----------LDVKHFSPEDLTVKVQDDFVEIHGKHNERQDDHGYISREFHRRYR--    119
CRYAB_HUMAN    RFSVN----------LDVKHFSPEELKVKVLGDVIEVHGKHEERQDEHGFISREFHRKYR--    123
HSPB6_HUMAN    HFSVL----------LDVKHFSPEEIAVKVVGEHVEVHARHEERPDEHGFVAREFHRRYR--    122
HSPB1_HUMAN    RWRVS----------LDVNHFAPDELTVKTKDGVVEITGKHEERQDEHGYISRCFTRKYT--    143
HSPB8_HUMAN    PWKVC----------VNVHSFKPEELMVKTKDGYVEVSGKHEEKQQEGGIVSKNFTKKIQ--    144
HSPB2_HUMAN    KFQAF----------LDVSHFTPDEVTVRTVDNLLEVSARHPQRLDRHGFVSREFCRTYV--    122
HSPB3_HUMAN    HFQIL----------LDVVQFLPEDIIIQTFEGWLLIKAQHGTRMDEHGFISRSFTRQYK--    119
HSPB7_HUMAN    AYEFA----------VDVRDFSPEDIIVTTSNNHIEVR---AEKLAADGTVMNTFAHKCQ--    127
HSPB9_HUMAN    GFQMK---------LDAHGFAPEELVVQVDGQWLMVTGQQQLDVRDPERVSYRMSQKVHRK    104
ODFP1_HUMAN    RILASSCCSSNILGSVNVCGFEPDQVKVRVKDGKVCVSAERENRYDCLGSKKYSYMNICKEF    175
```

Figure 6.5 – A section of the clustalW2 multiple sequence alignment of the ten human sHsps. Previously characterised chaperone-binding regions (αA-crystallin residues 70 – 88; αB-crystallin residues 79-92) are in blue (Sharma *et al.*, 2000; Bhattacharyya *et al.*, 2006). Conserved histidine residues within these regions (αA-crystallin H79; αB-crystallin H83; HspB1 H103; HspB2 H82; HspB6 82) are in red. For an explanation of Swiss-Prot entry names, see appendix B.

6.2.3 Chaperone ability of H83A αB-crystallin

The plasmid for a histidine 83 to alanine mutant of αB-crystallin was acquired from Prof. K. Krishna Sharma (University of Missouri-Columbia, U.S.A), who has previously characterized this mutant (Santhoshkumar and Sharma, 2006). It was hoped that by substituting the ionisable histidine residue for an alanine residue, the chaperone ability of mutant H83A αB-crystallin would be less pH-sensitive than that of unmodified αB-crystallin; that is, H83A αB-crystallin chaperone ability would not be significantly inhibited at pH 6.0 and 6.5, compared to pH 7.0 and above. This would imply that the residue H83 is intimately involved in the pH sensitivity of αB-crystallin chaperone ability. The ability of H83A αB-crystallin to prevent the amorphous aggregation of thermally stressed catalase was determined by the method described in Section 3.2.1. Light scattering at 340nm of heat-stressed catalase was measured between pH 6.0 and 8.0, and at 0:1, 0.2:1 and 0.5:1 molar ratios of H83A

αB-crystallin to catalase. Aggregation assays were conducted at 45°C (Figure 6.7a). Chaperone ability was quantified via percentage protection values calculated as described in Section 3.2.1. H83A αB-crystallin percentage protection was lowest at pH 6.0, and increased significantly between pH 6.0 and pH 7.0. There was, however, no significant change in H83A αB-crystallin chaperone ability between pH 7.0 and pH 8.0. H83A αB-crystallin chaperone ability was pH sensitive in the same manner as unmodified αB-crystallin.

The ability of H83A αB-crystallin to prevent the reduction-stress induced aggregation of α-lactalbumin was determined by the method described in Section 3.2.2. As with the thermal-stress induced aggregation of catalase described above, H83A αB-crystallin percentage protection was lowest at pH 6.0, and increased significantly between pH 6.0 and pH 7.0 (Figure 6.6b). There was, however, no significant change in percentage protection between pH 7.0 and pH 8.0. Thus, substitution of H83 with an alanine residue had little effect on the pH sensitivity of αB-crystallin chaperone ability against catalase.

There was no significant difference in the ability of H83A αB-crystallin to inhibit α-lactalbumin aggregation between pH 6.0 and 6.5. Additionally, the ability of H83A αB-crystallin to inhibit α-lactalbumin aggregation appeared to be more pH sensitive than that of wild-type αB-crystallin (Section 3.2.2); that is, the change in percentage protection between pH 6.5 and 7.0 for H83A αB-crystallin was larger than that of wild-type αB-crystallin (H83A αB-crystallin; 68%, wild-type αB-crystallin; 27%). Thus, it appears that substituting the ionisable H83 residue for alanine slightly increases the pH-sensitivity of αB-crystallin chaperone ability against α-lactalbumin.
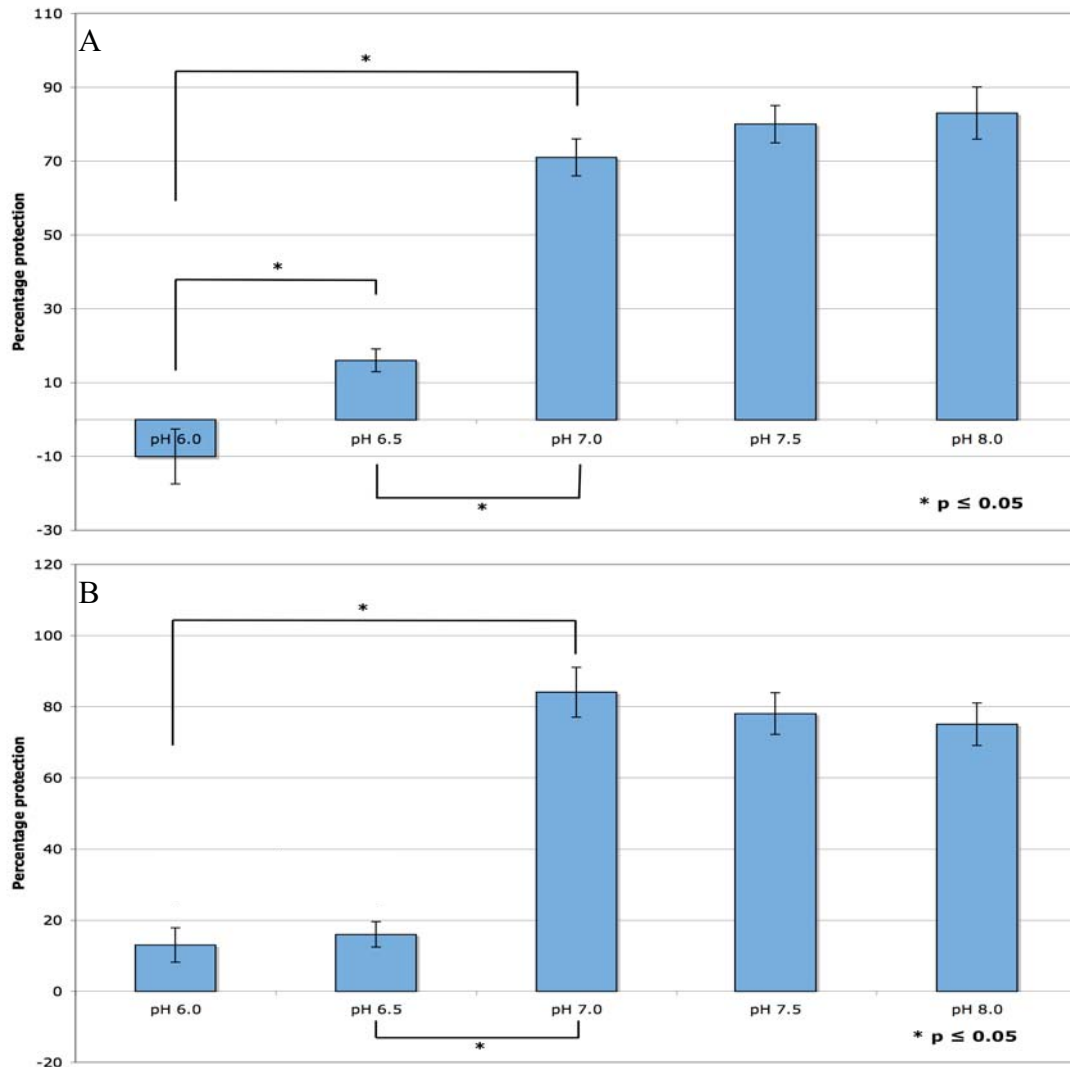
Figure 6.6 - Percentage protection calculated from light scattering assays for H83A αB-crystallin with a) catalase at 45°C and b) α-lactalbumin at 37°C. Percentage protection increased significantly between pH 6.5 and 7.0 for H83A αB-crystallin with both α-lactalbumin and catalase. There was no significant variation in H83A αB-crystallin chaperone ability between pH 7.0 and pH 8.0 for either of the target proteins investigated. * indicates significant difference in the mean percentage protection ($p \leq 0.05$).

6.3 Discussion

The pH sensitivity of α_T-, αA- and αB-crystallin chaperone ability against amorphous aggregation has been well characterised in this study; both α-crystallin and its subunits are less effective chaperones at pH 6.0 and 6.5 than at pH 7.0 and above (Section 3.2.1-2). Characterising the structural changes to α_T-, αA- and αB-crystallin accompanying pH variation does not adequately explain their observed pH-sensitive chaperone ability (Section 4.2); further, investigation into α_T- and αB-crystallin chaperone ability at acidic pH (pH 2.0 – 3.5) showed that significant protein unfolding increased chaperone ability, and made a correlation between pH-induced protein unfolding and decreased chaperone ability difficult. This study demonstrated that α_T-crystallin is less thermally stable at pH 6.0 and 6.5 than at pH 7.0 and above, which correlates with decreased chaperone ability below pH 7.0; at 55°C and 60°C, α_T-crystallin aggregates at pH 6.0 and 6.5 (Section 5.2), but not at pH 7.0 and above. Decreased thermal stability may partially explain the decreased chaperone ability of α-crystallin below pH 7.0. However, the ability of α_T-, αA- and αB-crystallin to inhibit α-lactalbumin aggregation at 37°C, and of αA- and αB-crystallin to inhibit catalase aggregation at 45°C, was shown to be pH sensitive in the same manner as their ability to inhibit catalase and β_L-crystallin aggregation at 55°C and 60°C. Thus, despite significant investigation in this study, the cause of the observed pH sensitive chaperone ability of α_T-, αA- and αB-crystallin remains unclear.

The ionisation of amino acids, particularly histidine, accompanying pH change has been implicated in the biochemical activity of many proteins. For example, protonation of histidine resides enhances the catalytic activity of

homoserine kinase (Huo and Viola, 1996), the chaperone activity of GroEL

(Gibbons and Horowitz, 1995), and the fusion of *Vesicular stomatitis* virus and

cytochrome C to cellular and mitochondrial membranes respectively (Carneiro *et al.*, 2003; Kawai *et al.*, 2005); conversely, histidine protonation has been

demonstrated to inhibit the catalytic activity of xylose isomerase (Lee *et al.*, 1990).

Protonation of histidine residues is also partially responsible for the Bohr effect in

Haemoglobin, which promotes the release of haemoglobin-bound O_2 into acidic

tissue (Stryer, 1995). Histidine protonation is commonly inhibited via the binding

of DEPC to exposed histidine residues (Dietz *et al.*, 1992; Carneiro *et al.*, 2003;

Kawai *et al.*, 2005). The isolated histidine amino acid has a pKa value of 6.5, which

can vary with regards to its local environment (Lodi and Knowles, 1991, 1993; Lin

et al., 1998); this pKa value corresponds with the pH range in which α-crystallin

chaperone ability was observed to decrease significantly (pH 6.0 - 7.0) (Section

3.2.1). Solvent-exposed histidine residues in α-crystallin would be predominantly

protonated at pH 6.0 and 6.5, and hence positively charged, but would be generally

neutrally charged at pH 7.0 and above. A positive charge on histidine residues may

disrupt hydrophobic interactions between α-crystallin and aggregating target

proteins. The protonation of an exposed histidine residue (or residues) between pH

6.0 and 6.5 may provide a possible explanation for the decreased chaperone ability

of α_T-, αA- and αB-crystallin at mildly acidic pH, as observed in this study.

Blocking histidine protonation via DEPC binding increased the ability of

αB-crystallin to inhibit temperature-induced catalase aggregation at pH 6.0 and 6.5

(by 48% and 23% respectively). DEPC binding had no statistical effect on αB-

crystallin chaperone ability at pH 7.0 and above, which is in agreement with

previous work by Pal and Ghosh (1998), who saw no effect on α-crystallin

chaperone ability against γ-crystallin aggregation at pH 7.0. Binding of DEPC has been reported to only modify surface-exposed histidine residues, which account for 57% of α_T-crystallin histidine residues (Bera and Ghosh, 1996). Absorbance at 240nm from the current study supports this conclusion for αB-crystallin, suggesting that four of a possible seven (56%) αB-crystallin histidine residues were modified via DEPC binding.

While DEPC binding at pH 6.0 increased the chaperone ability of αB-crystallin by 48% against thermal-stress aggregation, DEPC-bound αB-crystallin was still a significantly worse chaperone at pH 6.0 than at pH 6.5 and above. It appears that factors other than protonation of histidine residues may be contributing to the decreased chaperone ability of αB-crystallin at pH 6.0; these may include the previously identified thermal stability of αB-crystallin, which is significantly reduced at pH 6.0. The chaperone ability of DEPC-modified αB-crystallin at pH 6.5 was, however, statistically identical to that at pH 7.0 and above; blocking histidine protonation at pH 6.5 completely removed the pH sensitivity of αB-crystallin chaperone ability.

While a number of regions of αB-crystallin have been implicated in chaperone-target protein binding, the most well-characterised is a fourteen amino acid sequence in the αB-crystallin C-terminal domain (79-92) (Bhattacharyya *et al.*, 2006). This region contains a single histidine residue (H83), and clustalW2 multiple sequence alignment demonstrates that this residue is highly conserved amongst different species, and between αA- and αB-crystallin, and is relatively conserved amongst human sHsps. Its position in the putative chaperone-binding region of αB-crystallin suggests that H83 may be implicated in the chaperone binding of αB-crystallin, and that protonation of this residue could result in the decrease in αB-

crystallin chaperone ability observed at pH 6.0 and 6.5. A His83-Ala αB-crystallin mutant has previously been expressed and well characterised by Santhoshkumar and Sharma (2006). In their study, Santhoshkumar and Sharma reported little change to the secondary structure of H83A αB-crystallin, but did see increased oligomer size, and a 15-20% increase in chaperone ability against alcohol dehydrogenase and insulin aggregation at pH 7.2 (Santhoshkumar and Sharma, 2006).

The current study demonstrated that H83A αB-crystallin's chaperone ability was pH sensitive in a manner similar to that of wild type αB-crystallin; H83A αB-crystallin was less able to inhibit the thermal-stress induced aggregation of catalase (45°C), and the reduction-stress induced aggregation of α-lactalbumin (37°C), at pH 6.0 and 6.5 than at pH 7.0 and above. Percentage protection values of H83A αB-crystallin with thermally-stressed catalase at 45°C were comparable to those of wild type αB-crystallin. Interestingly, H83A αB-crystallin appeared to be less able to inhibit the reduction-stress induced aggregation of α-lactalbumin at pH 6.5 than wild type αB-crystallin at the same pH value. Modifying H83 in αB-crystallin had no effect on the pH sensitivity of αB-crystallin chaperone ability, suggesting that the protonation of H83 is not directly implicated in the pH sensitivity of αB-crystallin chaperone ability, and/or that the protonation of several histidine residues is responsible for the decreased chaperone ability of αB-crystallin at pH 6.0 and 6.5.

As the structure of αB-crystallin is not yet known, it is impossible to know whether H83 is solvent exposed in the αB-crystallin oligomer. Quaternary structural models of α-crystallin place the C-terminal domain, in which H83 lies, on the outside of the α-crystallin oligomer (Carver *et al.*, 1994). H83 lies one residue outside of one of the regions identified by Ghosh and Clark (2005a,b) as responsible for both subunit-subunit and chaperone-target protein interactions, and studies have placed it within the putative chaperone-binding region of αB-crystallin (Bhattacharyya *et al.*,

2006). It therefore seems likely that H83 interacts with DEPC. If H83 does prove to be accessible for DEPC binding, it would suggest that the protonation of several histidine residues is responsible for the pH-sensitive chaperone ability of αB-crystallin observed in this study.

In summary, the chaperone activity of α-crystallin against amorphous aggregation is pH sensitive between pH 6.0 and 8.0. The decreased chaperone ability of α-crystallin at pH 6.0 and 6.5 is accompanied by partial protein unfolding, and a slight loss of α-crystallin secondary structure, while α-crystallin quaternary structure remains unchanged. The relationship between partial α-crystallin unfolding and chaperone ability does not extend below pH 4.0, and it is doubtful whether a correlation between partial unfolding and α-crystallin chaperone ability is responsible for the decreased chaperone ability of α-crystallin at mildly acidic pH. The thermal stability of α-crystallin is compromised at pH 6.0 and 6.5, which may partially explain the decreased α-crystallin chaperone ability at these pH. However, α-crystallin chaperone ability is significantly pH-sensitive at 37°C and 45°C, at which temperatures α-crystallin is largely thermally stable. This suggests that other factors are responsible for the decreased chaperone ability of α-crystallin at pH 6.0 and 6.5. Blocking exposed αB-crystallin histidine residues by chemical modification removes, to a large extent, the pH-sensitivity of its chaperone activity, and suggests that the protonation of exposed histidine residues at pH 6.0 and 6.5 is at least partially responsible for the observed pH sensitivity of α-crystallin chaperone ability. Inhibiting the possibility of the protonation of a specific histidine residue, H83, does not remove the pH sensitivity of αB-crystallin chaperone activity, and suggests that protonation of this residue alone does not explain the decreased chaperone ability of α-crystallin at pH 6.0 and 6.5. Thus, it appears that

the protonation of several histidine residues, or residues other than H83, is

responsible for the decreased chaperone ability of α-crystallin at mildly acidic pH.

CHAPTER 7

CYCLODEXTRINS AS MOLECULAR CHAPERONES

Chapter 7 – Cyclodextrins as molecular chaperones

7.1 Introduction

α-Crystallin is effective in inhibiting protein aggregation and precipitation, but has only a limited ability to facilitate protein refolding (Horwitz, 1992; Muchowski and Clark, 1998). It is believed that sHsps, α-crystallin included, retain misfolded proteins indefinitely in a semi-folded state, and in doing so create a reservoir of unreactive but 're-foldable' protein intermediates (Horwitz, 1992; Ehrensperger *et al.*, 1997; Lee *et al.*, 1997). The subsequent interaction of sHsp-bound protein intermediates with further chaperones, such as Hsp70, is believed to facilitate protein re-folding to a native conformation (Ehrensperger *et al.*, 1997; Lee *et al.*, 1997; Horwitz, 2003).

Cyclodextrins have been extensively studied and characterised due to the unique functional properties afforded by their annular structure. The comparatively hydrophobic cyclodextrin annulus allows for the insertion of a variety of hydrophobic moieties, which in turn facilitates a variety of enzymatic, physical-chemical and nano-technological applications (Szjetli, 1997; 1998). Despite this, there has been comparatively little research into potential biochemical applications of cyclodextrins. Studies have focused primarily on the ability of βCD to re-fold semi-folded target proteins captured either by detergents (Rozema and Gellman, 1996a,b; Daugherty *et al.*, 1998; Yazdanparast *et al.*, 2005) or synthetic nanogels (Akiyoshi *et al.*, 1999; Nomura *et al.*, 2003; Ikeda *et al.*, 2006; Asayama *et al.*, 2008) during aggregation. Hydrogen nanogels mimic sHsp chaperone activity, binding to thermally unfolded target proteins via hydrophobic interactions (Akiyoshi *et al.*, 1999). It seems plausible that this research might be extended to

include biological molecular chaperones, substituting α-crystallin for carbon nanogels to facilitate an sHsp-βCD two-step refolding pathway.

Studies suggest that cyclodextrins can also act individually as molecular chaperones. Research has concentrated on the ability of cyclodextrins to inhibit amorphous aggregation upon protein re-naturation, whereby cyclodextrins (particularly βCD) are able to inhibit the aggregation of already denatured (and therefore largely unfolded) target proteins that are induced to misfold by the removal of denaturant (Karuppiah and Sharma, 1995; Sharma and Sharma, 2001; Desai *et al.*, 2006). There is increasing evidence to suggest that cyclodextrins, βCD in particular, can also effectively inhibit fibrillar aggregation (Qin *et al.*, 2002; Danielsson *et al.*, 2004). Amyloid plaques are characteristic of a number of neurodegenerative diseases, including Cruzfeldt-Jacob's, Alzheimer's and Parkinson's disease (Chiti and Dobson, 2006). Cyclodextrins, as molecular chaperones, may have potential therapeutic applications towards the inhibition of amyloid plaques, but their use is limited by the large molar excesses of cyclodextrin necessary for significant protection from aggregation (up to 20:1 molar ratio of cyclodextrin to target protein) (Qin *et al.*, 2002). If these ratios could be lowered, and cyclodextrins demonstrated to be more efficient molecular chaperones, therapeutic applications of cyclodextrins may become more practical.

Rationale for work presented in this chapter

The ability of α_T-crystallin to replace synthetic hydrogen nanogels in a two-step βCD refolding system was investigated via catalase aggregation and return of enzymatic activity. It became clear that α_T-crystallin was unable to function with

βCD to facilitate protein refolding. The ability of βCD to inhibit amorphous aggregation was investigated using catalase and insulin aggregation assays, which demonstrated that βCD had no effect on amorphous protein aggregation. The inability of βCD to inhibit amorphous protein aggregation was surprising, particularly in light of the demonstrated ability of βCD to inhibit fibrillar aggregation. Consequently, the ability of βCD (and other cyclodextrins) to inhibit fibrillar aggregation was investigated in-depth using rcm κ-casein, β-lactoglobulin, α-lactalbumin and α-synuclein (both wild type and the disease-related A53T mutant) to further clarify if βCD chaperone ability was specific to fibrillar aggregation.

7.2 Results

7.2.1 βCD and α$_T$-crystallin induced refolding of catalase

In Section 3.2.1, α$_T$-crystallin was demonstrated to inhibit the thermally-induced aggregation of catalase at 55°C. The ability of βCD to act in conjunction with α$_T$-crystallin to facilitate protein refolding was investigated under conditions similar to those described in Section 3.2.1. Catalase was thermally stressed at 55°C in the presence of α$_T$-crystallin (1:1 molar ratio), and at pH 7.5 for 90 minutes. Light scattering was monitored at 340nm to ensure α$_T$-crystallin binding to aggregating catalase (Figure 7.1a). After heating, βCD was added to the α$_T$-crystallin/catalase complex and incubated for 24hrs at 37°C to facilitate the interaction of βCD molecules with chaperone-bound catalase, using a variation of the method described by Akiyoshi *et al.* (1999). Catalase refolding was determined via the return of catalase enzyme activity. Catalase catalyses the decomposition of hydrogen peroxide (H_2O_2) into water and oxygen. H_2O_2 degradation can be measured by its absorbance between wavelengths of 200 and 300nm (Beers and Sizer, 1951). As only natively folded catalase degrades H_2O_2, a return of catalase activity is representative of catalase refolding to a native conformation. Catalase activity was monitored at 240nm (Figure 7.1b), and quantified by expressing α$_T$-crystallin- and βCD- influence on catalase activity as a percentage of that of native, unstressed catalase (Figure 7.1c).

There was less than 10% return of catalase activity after the addition of α$_T$-crystallin and βCD to aggregating catalase at 55°C. There was no significant difference in the catalytic activity of thermally-stressed catalase incubated with or without α$_T$-crystallin and βCD, suggesting that a combination of α$_T$-crystallin and

βCD is unable to facilitate the refolding of catalase via the proposed two-step refolding pathway. As α_T-crystallin was demonstrated to efficiently inhibit the thermally induced aggregation of catalase, it appears that βCD was unable to free α_T-crystallin-bound catalase molecules to facilitate further refolding. Accordingly, α_T-crystallin is not a viable substitute for hydrogen nanogels as part of a two-step refolding pathway. Interestingly, negative controls demonstrated that βCD was unable to inhibit catalase aggregation on its own (Figure 7.1a).
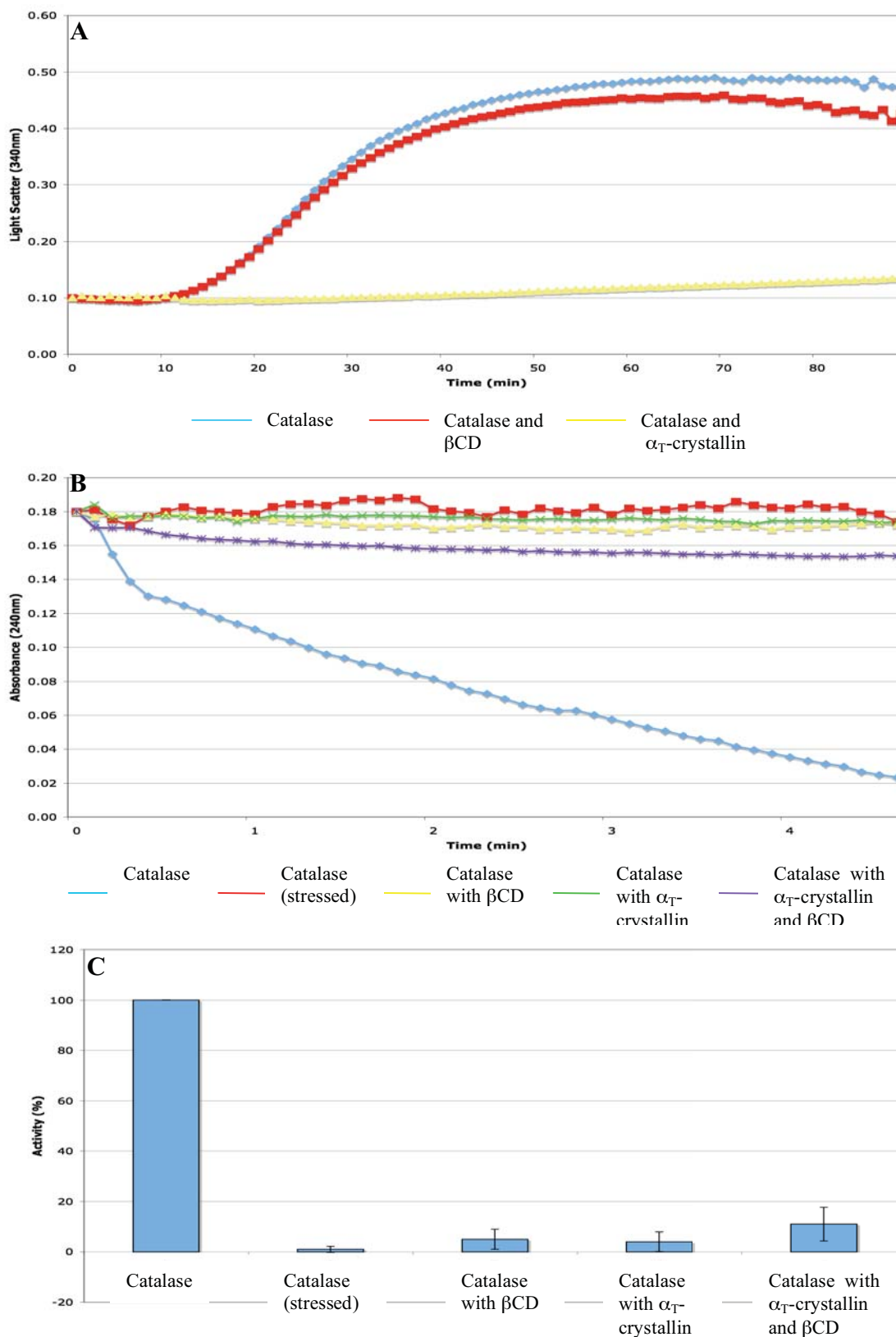
Figure 7.1 – βCD-induced refolding of thermally-stressed catalase. (a) Light scattering at 340nm demonstrated that α_T-crystallin inhibited the aggregation of thermally-stressed catalase (55°C). (b) Light scattering at 240nm demonstrated that thermally-stressed catalase was unable to catalyse the degradation of H_2O_2 in either the presence or absence of βCD. Conversely, non-stressed catalase facilitated H_2O_2 degradation. (c) Catalase refolding was quantified by return of activity, and demonstrated that the α_T-crystallin/βCD refolding mechanism was unable to facilitate the refolding of thermally-stressed catalase.

7.2.2 βCD and amorphous aggregation

There is only limited evidence to suggest that cyclodextrins can inhibit the amorphous aggregation of thermally-stressed target proteins on the off-folding pathway (Tavornvipas, 2004). Rather, cyclodextrin chaperone ability appears limited to re-naturation induced protein aggregation on the folding-unfolding pathway (Karuppiah and Sharma, 1995; Sharma and Sharma, 2001). Negative controls from Section 7.2.1 suggest that βCD is unable to inhibit the thermally induced aggregation of catalase at 55°C (Figure 7.1a). The ability of βCD to inhibit the amorphous aggregation of thermally-stressed catalase and reduction-stressed insulin was observed in a manner similar to that described in Sections 3.2.1-2. Catalase and insulin aggregation was measured via light scattering at 340nm, with the addition of increasing concentrations of βCD. βCD concentration ranged from 5:1 to 50:1 molar ratios of βCD:target protein.

βCD concentration had no effect on the amorphous aggregation of catalase at 55°C, or insulin at 37°C. Chaperone activity was quantified by percentage protection, calculated by the method described in Section 3.2.1 (Figure 7.2). βCD was unable to inhibit amorphous aggregation by any more than 11% at a 50:1 molar ratio to target protein, consistent with the negative controls from Section 7.2.1, and demonstrating that βCD was unable to significantly inhibit the amorphous aggregation of catalase or insulin.
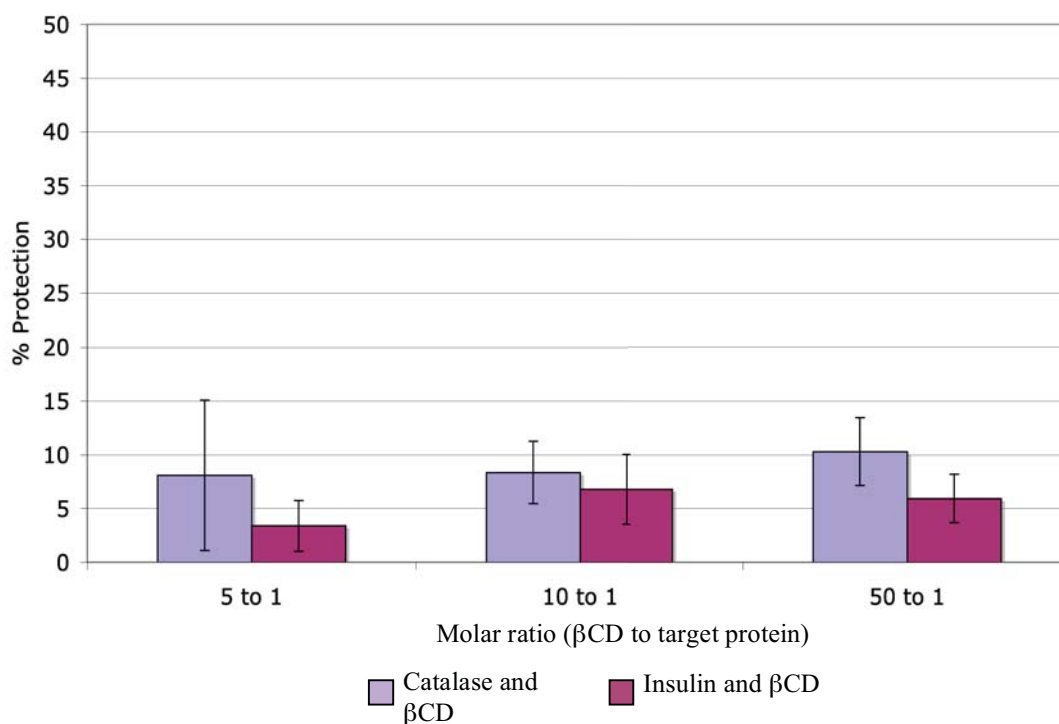
Figure 7.2 – Percentage protection values for βCD against the amorphous aggregation of catalase and insulin. βCD had little to no effect on either catalase or insulin aggregation, as quantified by percentage protection calculations.

7.2.3 Cyclodextrins and fibrillar aggregation

The ability of cyclodextrins to inhibit the fibrillar aggregation of rcm κ-casein was determined using the method described in Section 3.2.3. ThT-associated fluorescence of aggregating rcm κ-casein was monitored in the presence of two concentrations of α, β and γCD (5:1 and 25:1 molar ratios with target protein) for 20 hours and at 37°C (Figure 7.3). ThT-associated fluorescence of rcm κ-casein decreased in a dose-dependent manner with the addition of α, β and γCD, demonstrating the inhibition of fibrillar aggregation by each of the cyclodextrins investigated. Chaperone ability was quantified by percentage protection, calculated

by the method described in Section 3.2.1. There was little difference in chaperone ability between α, β or γCD at a 5:1 molar ratio with target protein. βCD was significantly more effective at inhibiting amyloid fibril formation than either α or γCD at a 25:1 molar ratio with target protein (53% compared to 12% and 22%). This is in agreement with the inhibition of Aβ-peptide aggregation (Qin *et al.*, 2002). Consequently, βCD was selected as the cyclodextrin species for all further fibrillar inhibition investigation.

βCD demonstrated a dose-dependent ability to inhibit rcm κ-casein fibrillar aggregation at 37°C (Figure 7.4). ThT-fluorescence decreased with increasing concentrations of βCD, up to a 50:1 molar ratio with the target protein. There was little difference in βCD chaperone ability at a 50:1 and 100:1 molar ratio with rcm κ-casein.

βCD showed a comparable ability to inhibit amyloid fibril formation from three distinct target proteins; rcm κ-casein (by heating), β-lactoglobulin (by reduction) and α-lactalbumin (by reduction) (Figure 7.5). Fibrillar aggregation was monitored by ThT-associated fluorescence as described in Section 3.2.3. The ability of βCD to inhibit the fibrillar aggregation of rcm κ-casein, β-lactoglobulin and α-lactalbumin implies that fibrillar aggregation inhibition by βCD is a generalised characteristic, and not limited to a specific target protein (e.g. rcm κ-casein). It appears that cyclodextrins selectively inhibit fibrillar, but not amorphous, protein aggregation. Characterisation of the cyclodextrin chaperone mechanism may help to understand the preferential chaperone ability of cyclodextrins towards fibrillar aggregation.
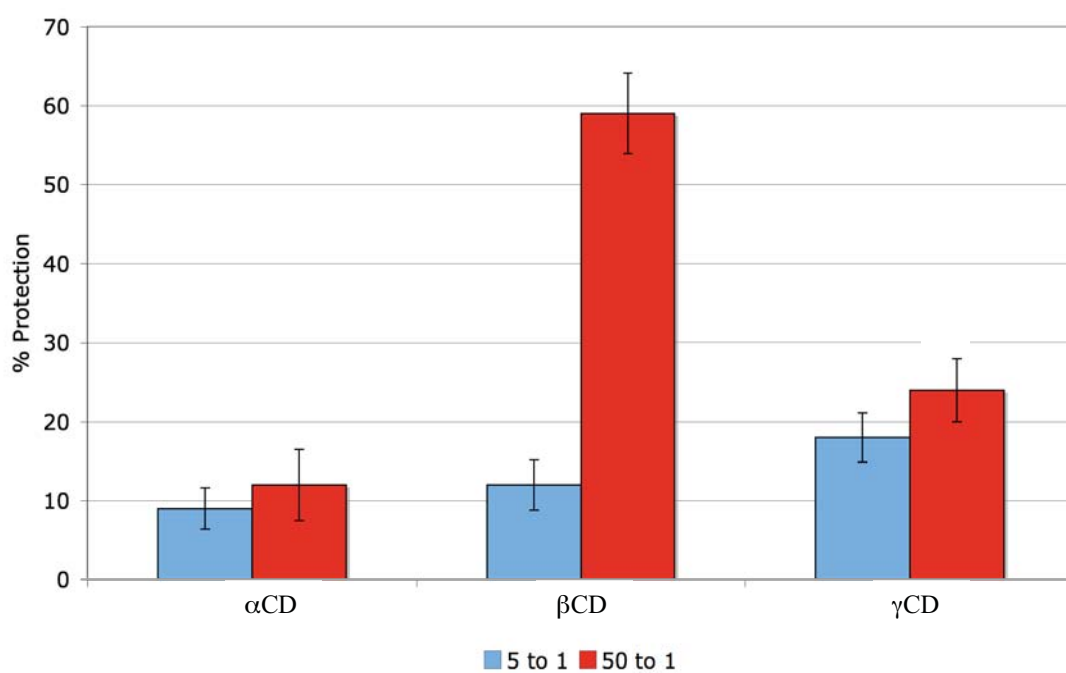
Figure 7.3 –Percentage protection calculated from change in ThT fluorescence of α,β and γCD with aggregating rcm κ-casein at 5:1 and 25:1 molar ratios (cyclodextrin : rcm κ-casein). βCD is a more effective molecular chaperone at higher concentrations than either αCD or γCD.
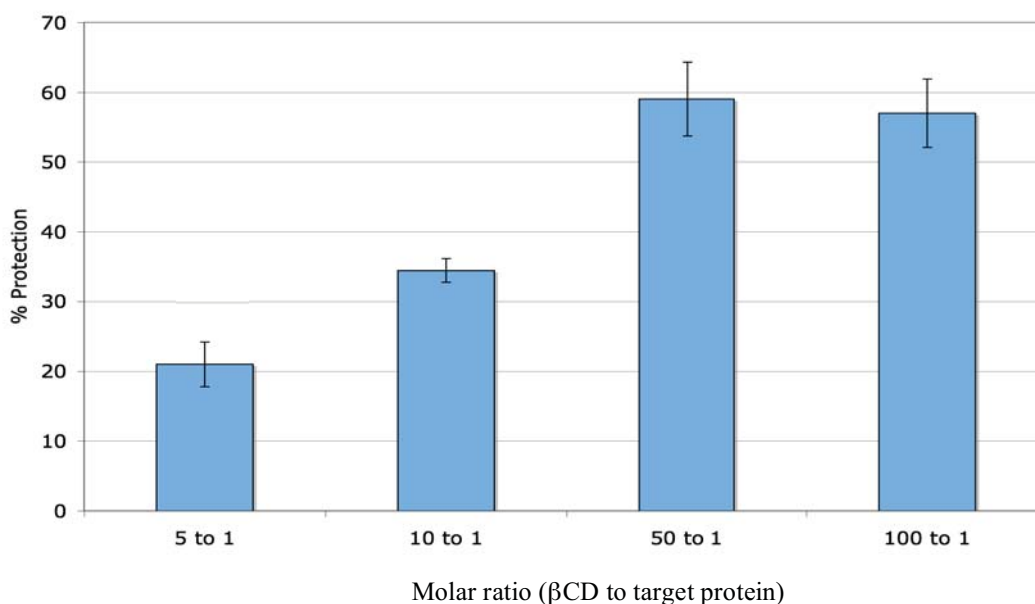
Figure 7.4 –Percentage protection, calculated from change in ThT-associated fluorescence, of rcm κ-casein in the presence of increasing concentrations of βCD. βCD chaperone ability increases significantly with concentration up to a 50:1 molar ratio.

Figure 7.5 –Percentage protection, calculated from change in ThT-associated fluorescence, of α-lactalbumin, β-lactoglobulin and rcm κ-casein fibrillar aggregation in the presence of βCD (25:1 and 50:1 molar ratios βCD : target protein. βCD was able to effectively inhibit the fibrillar aggregation of all target proteins. βCD percentage protection was similar for rcm κ-casein, α-lactalbumin and β-lactoglobulin.

7.2.4 A53T α-synuclein as a physiologically significant target for βCD chaperone action

The neurodegenerative diseases Parkinson's disease and Lewy body dementia are characterised by the build up of protein aggregates, known as Lewy bodies, in the substantia nigra (Forno, 1996). Lewy bodies consist primarily of fibrillar aggregates of α-synuclein (Spillantini *et al.*, 1998), and A53T and A30P α-synuclein mutations have been implicated in Parkinson's disease (Polymeropoulos *et al.*, 1997; Kruger *et al.*, 1998; Tofaris and Spillantini, 2005). While a direct correlation between α-synuclein mutation, fibrillar aggregation and Parkinson's disease is still speculative (Tofaris and Spillantini, 2007), A53T α-synuclein transgenic mice demonstrate a build up of α-synuclein in cell bodies, dystrophic neurons and impaired motor function reminiscent of Parkinson's disease (Giasson *et al.*, 2002). *In vitro*, the fibrillar aggregation of A53T α-synuclein is accelerated over wild-type or A30P α-synuclein (Kotzbauer *et al.*, 2004), and consequently A53T α-synuclein is the more attractive target protein for fibrillar aggregation studies.

The ability of βCD to inhibit the fibrillar aggregation of wild-type and A53T α-synuclein was monitored via time-point ThT fluorescence assays in the presence of increasing concentrations of βCD. α-Synuclein ThT fluorescence was monitored over 160 hrs at 37°C at 0:1, 25:1 and 50:1 molar ratios with βCD, to determine the ability of βCD to inhibit α-synuclein fibrillar aggregation. βCD chaperone ability was quantified via percentage protection, calculated by the method described in Section 3.2.1 (Figure 7.6). βCD was more efficient at inhibiting the fibrillar aggregation of both wild-type and A53T α-synuclein than of rcm κ-casein, β-lactoglobulin or α-lactoglobulin.
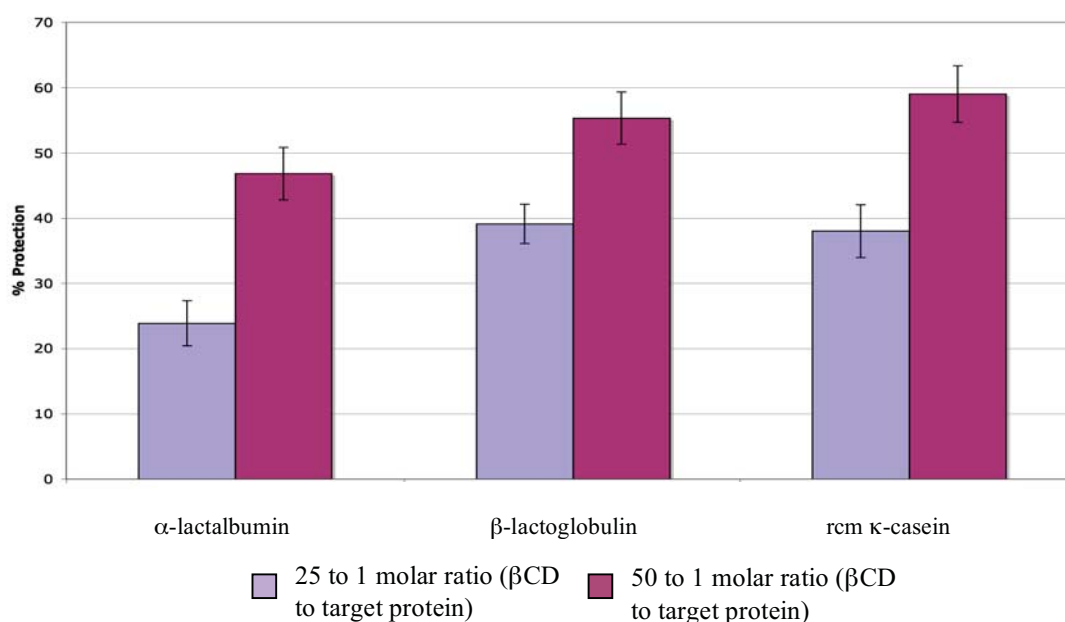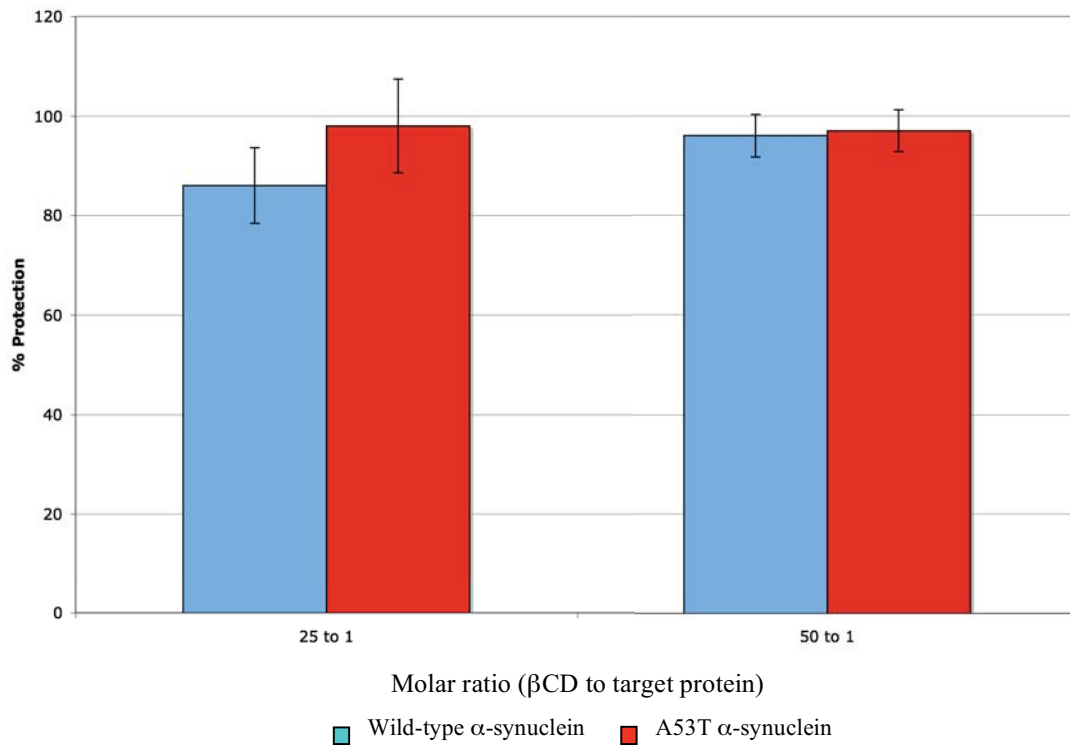
Figure 7.6 – Percentage protection, calculated from change in ThT-associated fluorescence, of wild-type and A53T α-synuclein fibrillar aggregation in the presence of βCD. Percentage protection calculations demonstrate that βCD is a particularly efficient molecular chaperone of both wild-type and A53T α-synuclein.

7.3 Discussion

Cyclodextrins have been demonstrated extensively to function in conjunction with an initial synthetic molecular chaperone (either detergents or synthetic hydrogen nanogels) to facilitate the refolding of thermally stressed target proteins (Rozema and Gelman, 1996; Daugherty *et al.*, 1998; Akiyoshi *et al.*, 1999; Nomura *et al.*, 2003). The refolding mechanism is believed to occur in two distinct stages; firstly, aggregating, semi-folded target proteins are captured on the surface of nanogel molecules by non-specific hydrophobic interactions, and in doing so are rendered incapable of further protein-protein interactions that would lead to large-scale aggregation. In this regard, the hydrogen nanogel functions in a manner similar to that of sHsps. Second, βCD molecules are added to solution and dissociate the synthetic chaperone from weakly bound semi-folded protein intermediates. This is achieved either by stripping detergent molecules from the protein intermediate (Daugherty *et al.*, 1998), or by destroying the gel nanoparticles, and in doing so freeing bound protein intermediates (Akiyoshi *et al.*, 1999). The freeing of bound protein in this manner then allows for effective protein refolding, although the degree to which cyclodextrin molecules interact with the refolding target protein is unclear. This method has been demonstrated to be particularly efficient, and has resulted in the return of carbonic anhydrase B and citrate synthase activity (an indicator of protein refolding to a native conformation) in excess of 70% (Nomura *et al.*, 2003). Similarities between the role of hydrogen nanogels in this process and that of sHsps, particularly α-crystallin, *in vivo* suggested that α_T-crystallin might be an effective (and more physiologically significant) replacement for nanogels as part of a βCD-facilitated two-step protein refolding system. Further investigation,

however, demonstrated this assumption to be incorrect; α_T-crystallin was unable to co-operate with βCD to enable the correct refolding of thermal-stressed catalase. Light scatter at 340nm demonstrated that α_T-crystallin was binding as expected to aggregating catalase, and in doing so inhibiting large-scale protein aggregation. Accordingly, it appears that the ability of βCD to meaningfully interact with α_T-crystallin-bound catalase is inhibited in this system.

While α_T-crystallin effectively inhibits the aggregation of catalase in a manner reminiscent of hydrogen nanogels and other synthetic chaperones, it would seem impossible for βCD molecules to cause the dissociation of the α_T-crystallin-catalase complex. Dissociation of bound protein intermediates from hydrogen nanogels in previous studies was facilitated by destruction of the functional hydrogel nanoparticle (Akiyoshi *et al.*, 1999). Binding of βCD to accessible cholesterol moieties on hydrogen nanogels disrupts cross-linking within nanoparticles, which results in the destruction of the nanoparticle, and the subsequent freeing of bound protein intermediates (Akiyoshi *et al.*, 1999). This would be impossible with α_T-crystallin, and so βCD not be able to free α_T-crystallin bound catalase intermediates for subsequent refolding.

Interestingly, negative controls from Section 7.2.1 demonstrated little or no ability for βCD to inhibit catalase aggregation on its own. Cyclodextrins have been demonstrated previously to be efficient molecular chaperones (Karuppiah and Sharma, 1995; Sharma and Sharma, 2001), although studies have generally concentrated on the refolding of target proteins during renaturation-induced protein aggregation, a process that is distinct from aggregation on the off-folding pathway. Amorphous aggregation assays from Section 7.2.2 supported the controls from Section 7.2.1, demonstrating that βCD was unable to inhibit the aggregation of

catalase or insulin at a 50:1 molar ratio to target protein. There appeared to be little or no correlation between βCD concentration and percentage protection for either insulin or catalase aggregation, and percentage protection was never better than 11%.

βCD has been shown to inhibit the fibrillar aggregation of a variety of target proteins, including Aβ-peptide (Qin *et al.*, 2002; Danielsson *et al.*, 2004). This study is in agreement with previous studies, and demonstrated that βCD has significant chaperone ability against the fibrillar aggregation of rcm κ-casein, β-lactoglobulin, α-lactalbumin and both wild-type and A53T α-synuclein. The significantly greater chaperone ability of βCD than either αCD or γCD was in agreement with previous Aβ-peptide aggregation studies (Qin *et al.*, 2002).

βCD is a far more efficient chaperone of A53T and wild-type α-synuclein aggregation than of rcm κ-casein, β-lactoglobulin or α-lactalbumin; at a 25:1 molar ratio βCD inhibited both wild type and A53T α-synuclein aggregation by over 85%, compared to between 20 and 40% for the other target proteins studied. The structure of α-synuclein may in part explain the observed differential chaperone ability of βCD with various target proteins; native α-synuclein is largely un-structured *in vitro* (Weinreb *et al.*, 1996), which would provide a high degree of solvent accessibility for binding sites on the target protein. While it is true that rcm κ-casein has a similarly relaxed structure, κ-casein exists in a multimeric state that requires dissociation into dimeric or monomeric protein intermediates before fibrillar aggregation can begin (Ecroyd *et al.*, 2008). Consequently, βCD would be more able to bind extensively with α-synuclein, and in doing so facilitate a higher degree of chaperone protection. Also requiring consideration is the time-frame over which aggregation occurs; α-synuclein aggregation requires an incubation period

approaching 180 hrs, while rcm κ-casein, α-lactalbumin and β-lactoglobulin aggregate over 20 hrs (and amorphous aggregation occurs in 2 hrs or less). Cyclodextrins generally require extended incubation periods and a high degree of solvent exposure to inhibit protein aggregation (Aachmann *et al*, 2003). Consequently, a high rate of target protein aggregation may affect the ability of βCD to interact with target proteins and inhibit protein aggregation.

It is significant that in this study βCD demonstrates little or no ability to inhibit amorphous protein aggregation, but can effectively inhibit fibrillar aggregation. Despite their structural and mechanistic differences, it is believed that both amorphous and fibrillar aggregates occur as a result of non-specific hydrophobic interactions (Das *et al.*, 1996; Chiti *et al.*, 1999; Singh and Rao, 2002; Chiti and Dobson, 2006). Molecular chaperones are believed to inhibit aggregation via the interaction of hydrophobic binding regions with areas of exposed hydrophobicity on misfolded protein intermediates (Das *et al.*, 1996; Singh and Rao, 2002; Melkani *et al.*, 2004). A number of molecular chaperones have been shown to inhibit both fibrillar and amorphous aggregation, including α-crystallin (Horwitz, 1992; Wilhelmus *et al.*, 2006) and clusterin (Poon *et al.*, 2002; Kumita *et al.*, 2007); this may be a consequence of the role of non-specific hydrophobic interactions in both amorphous and fibrillar aggregation. The fact that cyclodextrins demonstrate differential chaperone ability between amorphous and fibrillar aggregation suggests that there may be some intrinsic characteristic of the cyclodextrin chaperone mechanism that favours interaction with fibrillar aggregation rather than amorphous aggregation. Characterisation of the βCD chaperone mechanism may help to further understand the differences between amorphous and fibrillar aggregation.

CHAPTER 8

CHARACTERISING THE CYCLODEXTRIN CHAPERONE
MECHANISM

Chapter 8 – Characterising the mechanism of cyclodextrin chaperone activity

8.1 Introduction

In Section 7.2, it was demonstrated that cyclodextrins can effectively inhibit the fibrillar aggregation of a variety of proteins, including A53T and wild-type α-synuclein. Conversely, βCD was unable to inhibit amorphous protein aggregation on the off-folding pathway. The observed inhibition of fibrillar aggregation by cyclodextrins, βCD in particular, is in agreement with previous studies (Qin *et al.*, 2002). While there is extensive evidence to suggest that cyclodextrins are capable of inhibiting protein aggregation (Karuppiah and Sharma, 1995; Sharma and Sharma, 2001), studies have focused specifically on the misfolding of denatured proteins. Aggregation of this kind is distinct from the amorphous aggregation of semi-folded protein intermediates on the off-folding pathway.

Both fibrillar and amorphous aggregation are believed to result from non-specific hydrophobic interactions between intermediately folded proteins (Chiti *et al.*, 1999; Chiti and Dobson, 2006); consequently, molecular chaperones are often able to inhibit both forms of protein aggregation. Clusterin, for example, inhibits the amorphous aggregation of α-lactalbumin and γ-crystallin (Poon *et al.*, 2002) as well as the fibrillar aggregation of lysozyme (Poon *et al.*, 2002; Kumita *et al.*, 2007), and α-crystallin inhibits the amorphous aggregation of insulin, alcohol dehydrogenase and α-lactalbumin (Horwitz, 1992; Datta and Rao, 1999), as well as the fibrillar aggregation of

apoliprotein C-II, κ-casein and Aβ-peptide (Hatters *et al.*, 2001; Wilhelmus *et al.*, 2006; Ecroyd *et al.*, 2007, 2008). The specificity of cyclodextrin chaperone activity towards fibrillar aggregation provides an important opportunity to better understand the differences between the mechanisms of amorphous and fibrillar aggregation. Characterising the specifics of βCD-target protein interactions during fibrillar aggregation may provide insight into the factors that dictate the binding of target proteins to molecular chaperones, and help elucidate the still speculative mechanism of molecular chaperone activity.

Rationale for work presented in this chapter

Intrinsic fluorescence, ANS binding, competitive chaperone binding and circular dichroism were used to provide a thorough insight into the nature of βCD interactions with fibril forming proteins. Based upon these data, a speculative model of the cyclodextrin chaperone mechanism is proposed. The proposed cyclodextrin chaperone mechanism may provide an important starting point for further investigation into the intrinsic factors driving fibrillar aggregation, as opposed to amorphous aggregation.

8.2 Results

8.2.1 Intrinsic tryptophan fluorescence characterisation of fibrillar aggregation in the presence of βCD

Intrinsic tryptophan fluorescence can be used to monitor protein structure and unfolding *in situ* (as described in Section 4.1). Fibrillar aggregation is believed to be preceded by the unfolding and dissociation of the target protein into a relaxed, amyloidogenic conformation (Chiti *et al.*, 1999; Chiti and Dobson, 2006). Consequently, intrinsic tryptophan fluorescence was used to investigate the initial stages of the cyclodextrin chaperone mechanism. As both rcm κ-casein and β-lactoglobulin contain tryptophan residues (κ-casein, W155; β-lactoglobulin, W19, W61), a shift in tryptophan fluorescence with time may be suggestive of protein unfolding around these tryptophan residues prior to fibrillar aggregation.

Real-time intrinsic fluorescence was monitored over the course of rcm κ-casein and β-lactoglobulin fibrillar aggregation, in both the presence and absence of βCD as a chaperone. There was no significant change in λ_{max} over the course of rcm κ-casein fibrillation, while maximum fluorescence, decreased steadily (Figure 8.1). It is believed that rcm κ-casein does not undergo significant unfolding prior to fibrillar aggregation; rather, it appears that the κ-casein multimer dissociates directly into already highly amyloidogenic fibrillar precursors, allowing for immediate association into fibrillar aggregates (Ecroyd *et al.*, 2008). The lack of a shift in rcm κ-casein intrinsic fluorescence agrees with this assumption, and suggests no significant unfolding of rcm κ-casein prior to or during fibrillar aggregation. The presence of βCD increased maximum rcm κ-casein intrinsic fluorescence, slightly, but controls suggest that βCD increases L-trp fluorescence

proportionally. βCD had no effect on rcm κ-casein λ_{max}, and the rate of maximum fluorescence decrease was identical in the presence and absence of βCD. Consequently, it appears that βCD had no effect on the dissociation of rcm κ-casein.

      With β-lactoglobulin as a target protein, however, a decrease in maximum tryptophan fluorescence after 5 hours was accompanied by a red shift in λ_{max} (Figure 8.2). A red-shift in λ_{max} indicates exposure of tryptophan residues to a more polar environment, and so is suggestive of protein unfolding around tryptophan residues. Accordingly, intrinsic tryptophan fluorescence data suggest β-lactoglobulin unfolding in the environment of residues W19 and W61 during the initial stages of fibrillar aggregation. The addition of βCD to aggregating β-lactoglobulin increased maximum β-lactoglobulin tryptophan fluorescence, but L-trp controls demonstrate that βCD increased L-trp fluorescence proportionally. The addition of βCD to aggregating β-lactoglobulin had no effect on β-lactoglobulin λ_{max}, or on the rate of maximum fluorescence decrease with time. Consequently, it appears that βCD has no influence on the unfolding of β-lactoglobulin prior to fibrillar aggregation.
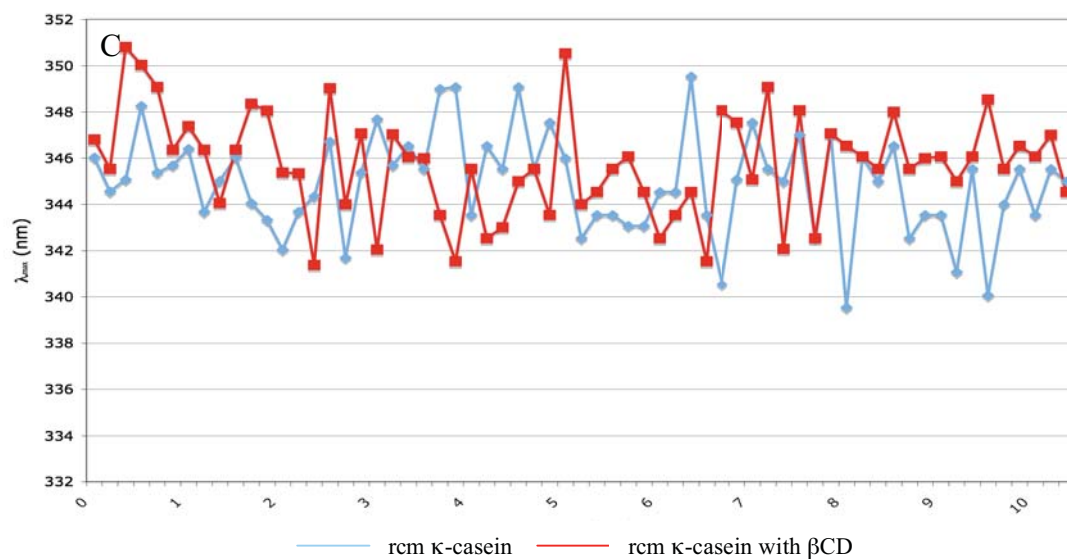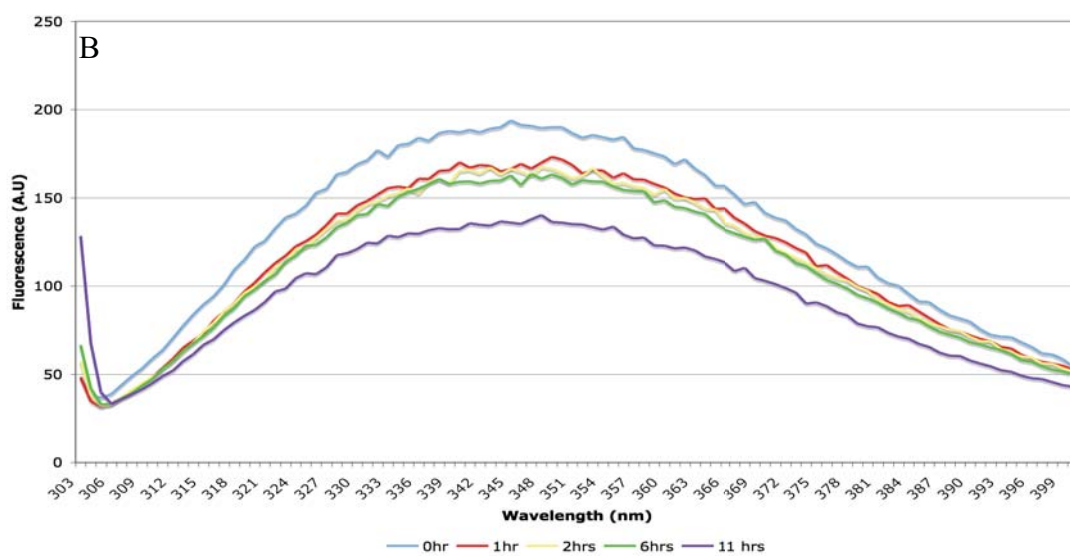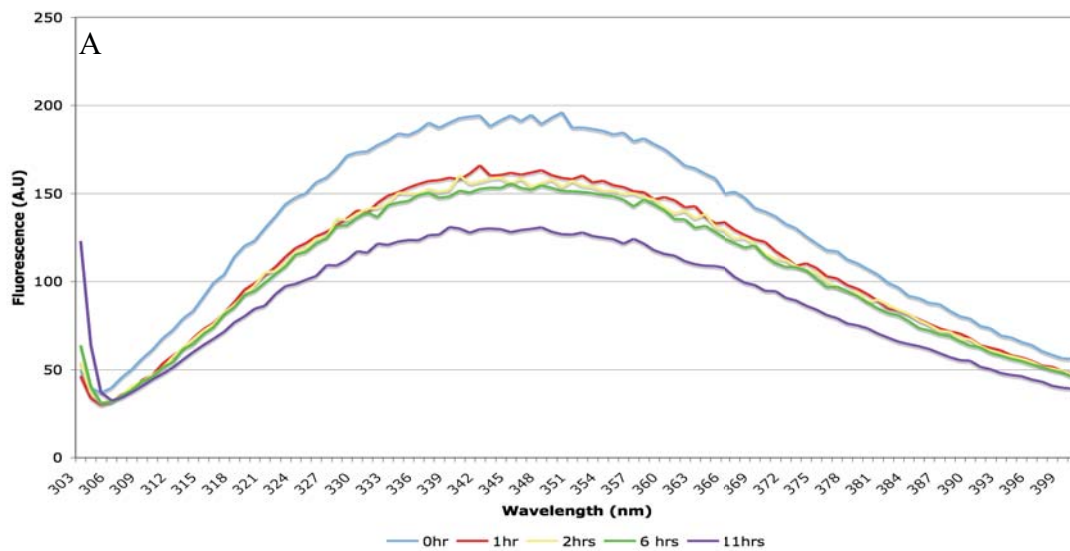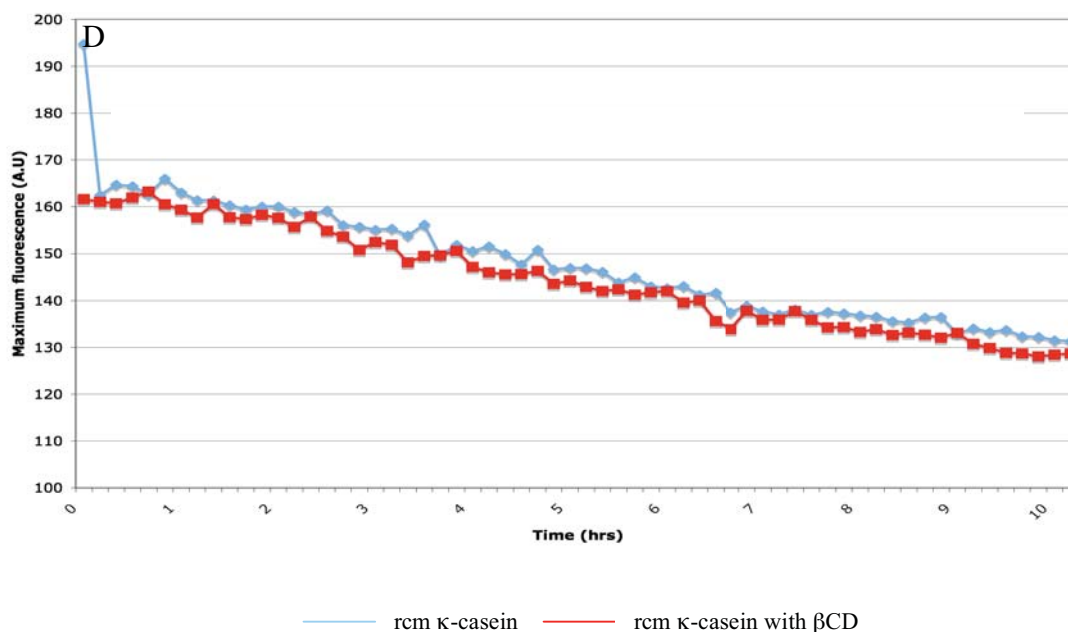
Figure 8.1 – Real-time intrinsic tryptophan fluorescence of rcm κ-casein fibril formation in the presence (25:1 molar ratio) and absence of βCD. Wavelength scans of intrinsic tryptophan fluorescence during rcm κ-casein aggregation in the (a) absence and (b) presence of βCD show a decrease in overall fluorescence intensity with time. (c) λ_{max} does not change over the course of protein fibrillation, and is unaffected by the presence of βCD. (d) Maximum fluorescence decreases steadily over the course of protein aggregation, probably as a consequence of fluorescence quenching during aggregation. βCD has little effect on the rate of decrease.
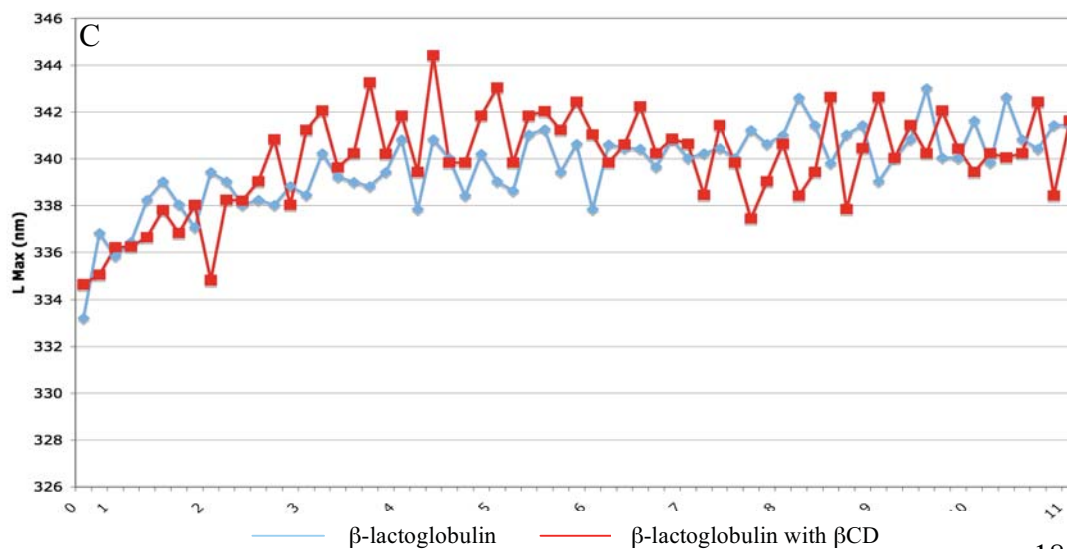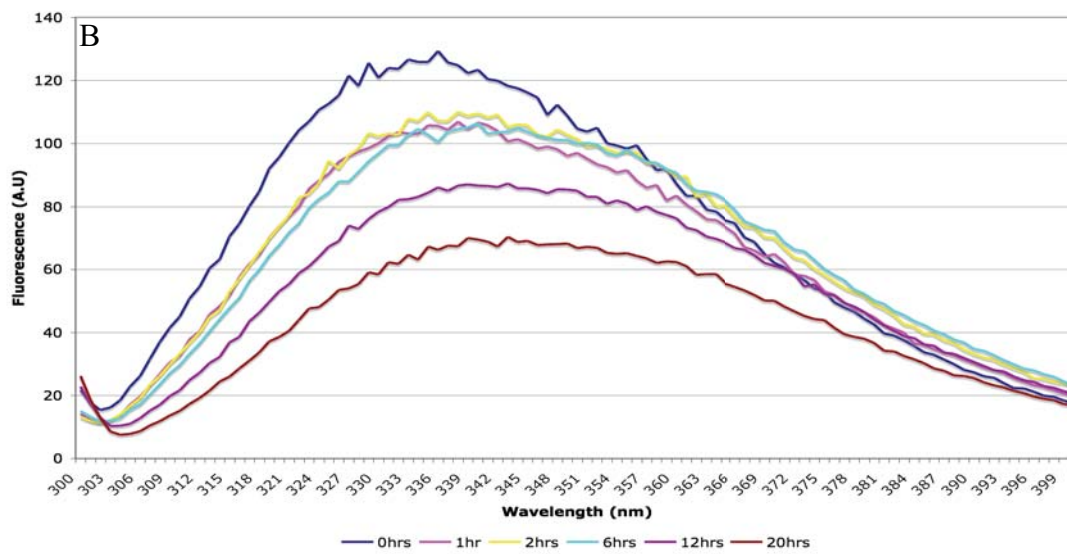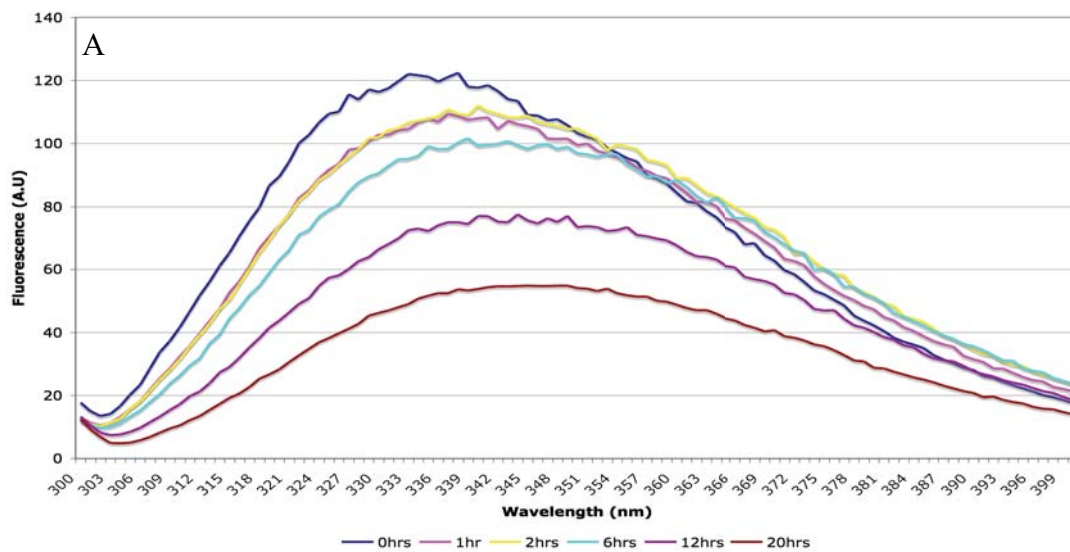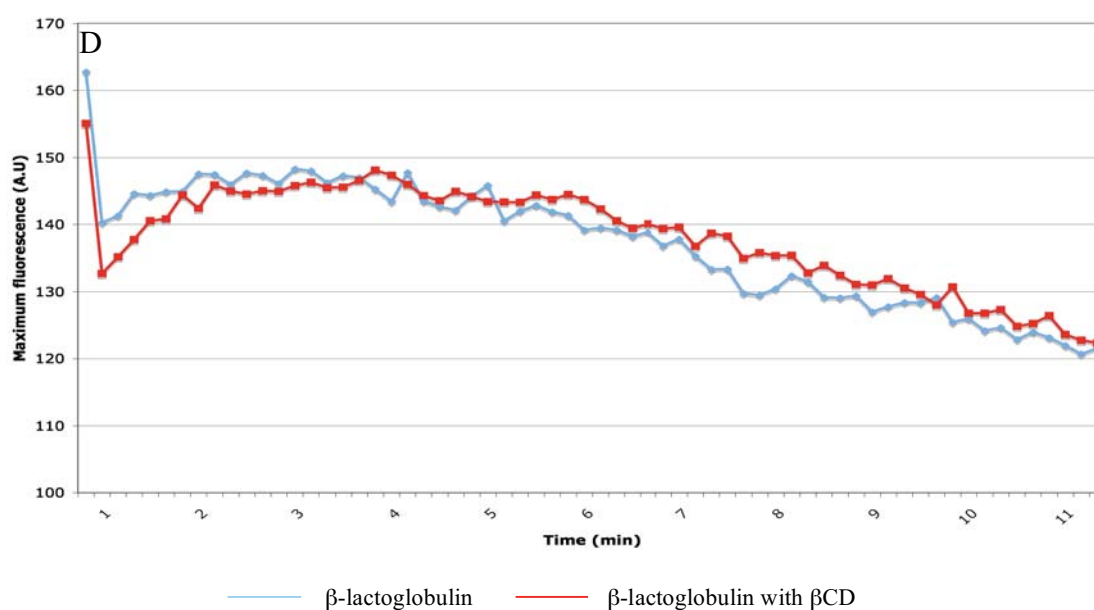
Figure 8.2 – Real-time intrinsic tryptophan fluorescence of β-lactoglobulin fibril formation in the presence (25:1 molar ratio) and absence of βCD. Wavelength scans of intrinsic tryptophan fluorescence during β-lactoglobulin aggregation in the (a) absence and (b) presence of βCD show a decrease in overall fluorescence intensity with time. (c) λ_{max} shifts to the red during the initial five hours of protein fibrillation, suggesting significant protein unfolding during the initial stages of β-lactoglobulin aggregation. The shift in λ_{max} is unaffected by the presence of βCD. (d) Maximum fluorescence decreases steadily after 5 hours, probably as a consequence of fluorescence quenching during aggregation. βCD has little effect on the rate of decrease.

8.2.2 Far UV circular dichroism spectroscopy of fibrillar aggregation in the presence of βCD

Far UV Circular dichroism spectroscopy was used to monitor structural modifications accompanying the fibrillar aggregation of rcm κ-casein, and in the presence of βCD. Fibrillar aggregation can be observed via ellipticity at both 205 nm and 216nm; Fibrillar aggregation is characterised by an increase in β-sheet content, which is indicated by a decrease in ellipticity at 216nm over time. Additionally, fibrillar aggregation is generally preceded by partial protein unfolding, which is indicated by decreased ellipticity at 205nm during the initial stages of aggregation.

Far UV CD spectra were observed for aggregating rcm κ-casein in the presence and absence of βCD at 0, 1, 2, 3, 6, 12, 18, 20 and 24hrs (Figure 8.3). Aggregating rcm κ-casein showed no significant change in ellipticity at 205nm (characteristic of random coil structure) until after 18 hours. Random coil content decreased substantially after 18 hours, suggesting that the majority of rcm κ-casein in solution was involved in structured, presumably fibrillar aggregates. Ellipticity at 216nm decreased slightly from 0-12 hrs, before a dramatic decrease between 12 and 24hrs. This implies a gradual increase in β-sheet structure up to 12 hrs followed by a significant increase in β-sheet between 12 and 24hrs. β-Sheet is the primary structural element of amyloid fibrils, and so it appears that fibril assembly occurs at a steady rate for the first 12 hours of aggregation before a rapid period of β-sheet stacking and fibril assembly after 12 hours.

The presence of βCD had no effect on aggregating rcm κ-casein ellipticity at 205nm. Between 3 and 18 hours, ellipticity at 216nm remained significantly higher

in the presence of βCD compared to the rcm κ-casein control, demonstrating that βCD inhibited rcm κ-casein β-sheet formation in this time period. After 18 hours, ellipticity at 216nm decreased in a similar fashion to the rcm κ-casein control. Significant β-sheet stacking appeared to be inhibited by βCD during the initial stages of fibrillar aggregation, after which fibril assembly continued as in the absence of βCD. The delay and inhibition of fibrillar assembly observed in the presence of βCD supports the conclusions suggested by intrinsic fluorescence; that is, βCD does not appear to influence the initial unfolding or dissociation of aggregating proteins. Rather, βCD inhibits the formation of β-sheet rich structures (presumably protofilaments) from already unfolded and dissociated protein intermediates.
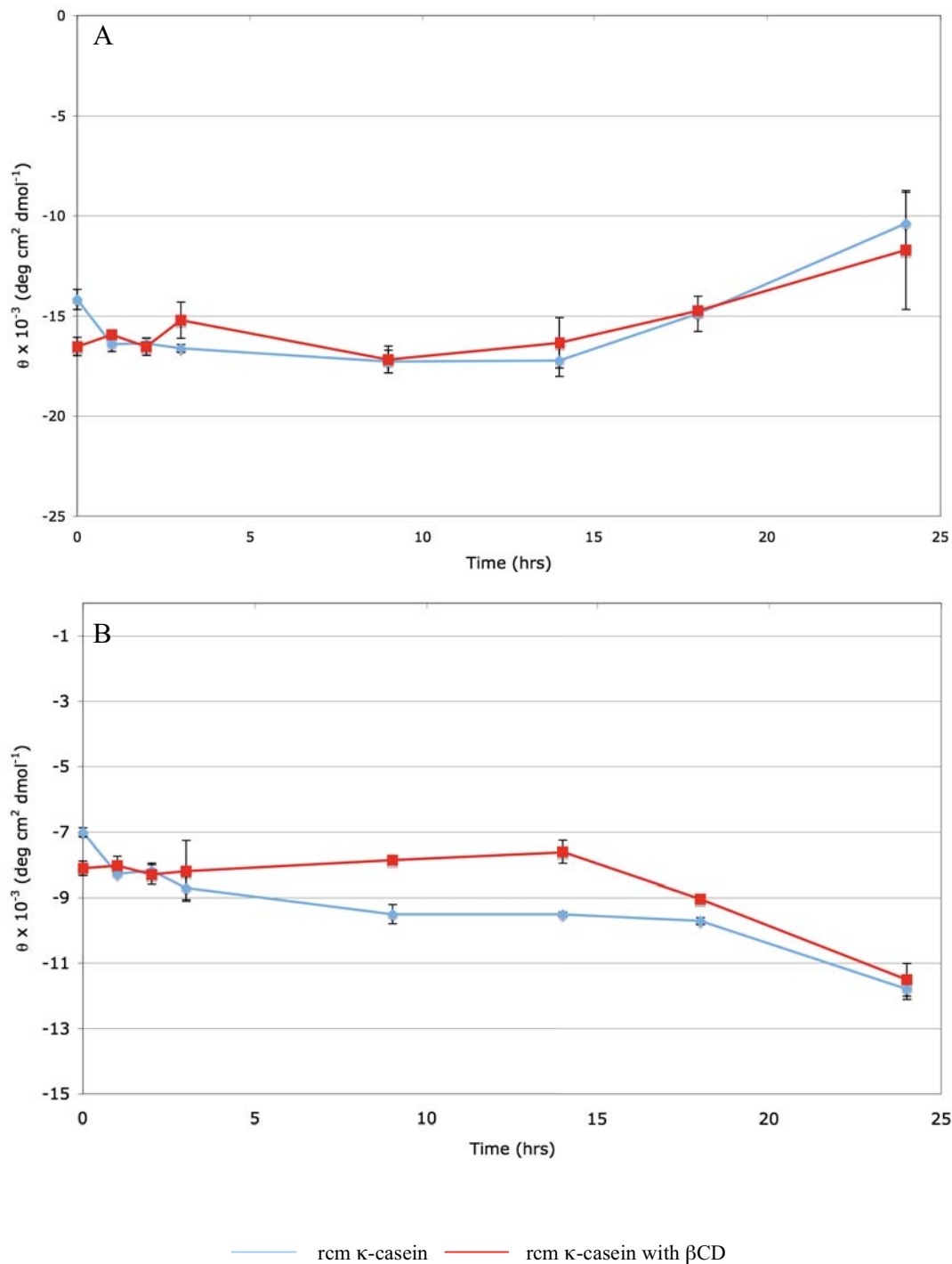
Figure 8.3 – Ellipticity at a) 205nm and b) 216nm derived from far UV CD spectra of aggregating rcm κ-casein, in the absence and presence (25:1 molar ratio) of βCD. Ellipticity at 205nm of aggregating rcm κ-casein remained constant up to 18 hours. The presence of βCD had no effect on ellipticity at 205nm. In the absence of βCD, ellipticity at 216nm of aggregating rcm κ-casein decreased slightly over the first 12 hours before decreasing significantly after 12 hours. The presence of βCD increased ellipticity at 216nm over that of the rcm κ-casein control between 3 and 18 hours. βCD appears to inhibit β-sheet stacking (and hence fibril formation) over the first 18 hours of aggregation.

8.2.3 Competitive binding of ANS and βCD to aggregating proteins

βCD does not appear to influence the initial unfolding of fibril forming proteins, but somehow disrupts the ordering and stacking of β-sheets. Competitive ANS binding was used to determine if βCD binds in a generalised fashion to exposed hydrophobic regions on the already partially unfolded target protein, in much the same manner as α-crystallin and other sHsps (Raman and Rao, 1994; Das *et al.*, 1996). As previously described (Section 4.2), ANS binds to areas of exposed, clustered hydrophobicity on molecules *in vitro*. Further, it has been reported that in its capacity to bind to exposed hydrophobicity on aggregating proteins, ANS can act as a molecular chaperone and inhibit protein aggregation (Fu *et al.*, 2005). ANS-associated fluorescence of aggregating rcm κ-casein and β-lactoglobulin was measured in the presence and absence of βCD (Figure 8.4). ANS-associated fluorescence should increase slightly during the initial stages of fibrillar aggregation, as target proteins dissociate (rcm κ-casein) or unfold (β-lactoglobulin) into amyloidogenic fibrillar precursors that exhibit a high degree of exposed hydrophobicity. If βCD inhibits protein aggregation by reducing protein unfolding or dissociation during the initial stages of fibrillar aggregation, the addition of βCD to aggregating target proteins should result in little to no increase in ANS fluorescence over time. Additionally, if βCD binds non-specifically to regions of exposed hydrophobicity on the target protein during fibrillar aggregation, competitive binding would occur between ANS and βCD, which would decrease ANS fluorescence against target proteins aggregating in the absence of βCD.

ANS-associated fluorescence increased over the first ten hours of both rcm κ-casein and β-lactoglobulin fibrillar aggregation. This suggests the increasing

exposure of hydrophobic intermediates during the initial stages of fibrillar aggregation, either as a result of protein unfolding or oligomer dissociation into amyloidogenic, hydrophobic precursors. ANS-associated fluorescence levelled off after 10 hours for both target proteins. The addition of βCD to either rcm κ-casein or β-lactoglobulin during fibrillar aggregation had no effect on ANS-associated fluorescence. This supports intrinsic fluorescence data from Section 8.2.1, and demonstrates that βCD does not inhibit fibrillar aggregation by influencing the unfolding or dissociation of target proteins into amyloidogenic precursors. Additionally, it appears that ANS and βCD bind to unfolded proteins via significantly disparate mechanisms to avoid competition for binding sites.

It may, however, be the case that ANS has a significantly increased binding affinity to the unfolded target proteins over that of βCD, and consequently out-competes βCD for binding sites. Were this true, βCD would have no influence on ANS-associated fluorescence, as was seen in Figure 8.4. To investigate this, aggregation profiles of rcm κ-casein (monitored via ThT-associated fluorescence) with a 50:1 molar excess of either ANS or βCD, as well as a combination of ANS and βCD, were compared. It was assumed that if ANS was entirely out-competing βCD for binding sites on κ-casein, the percentage protection of ANS against rcm κ-casein aggregation would be identical to the percentage protection of an ANS-βCD combination. While there did not appear to be an entirely additive effect between ANS and βCD, the combination of both chaperones had a larger percentage protection than the sum of the individual percentage protection values of ANS and βCD (labelled 'theoretical') (Figure 8.5). This implies that the two molecules bound to aggregating rcm κ-casein in a significantly separate manner to avoid competitive binding. Consequently, it appears that βCD is not necessarily inhibiting protein

fibril formation by binding non-specifically to areas of exposed hydrophobicity on
the aggregating target proteins.
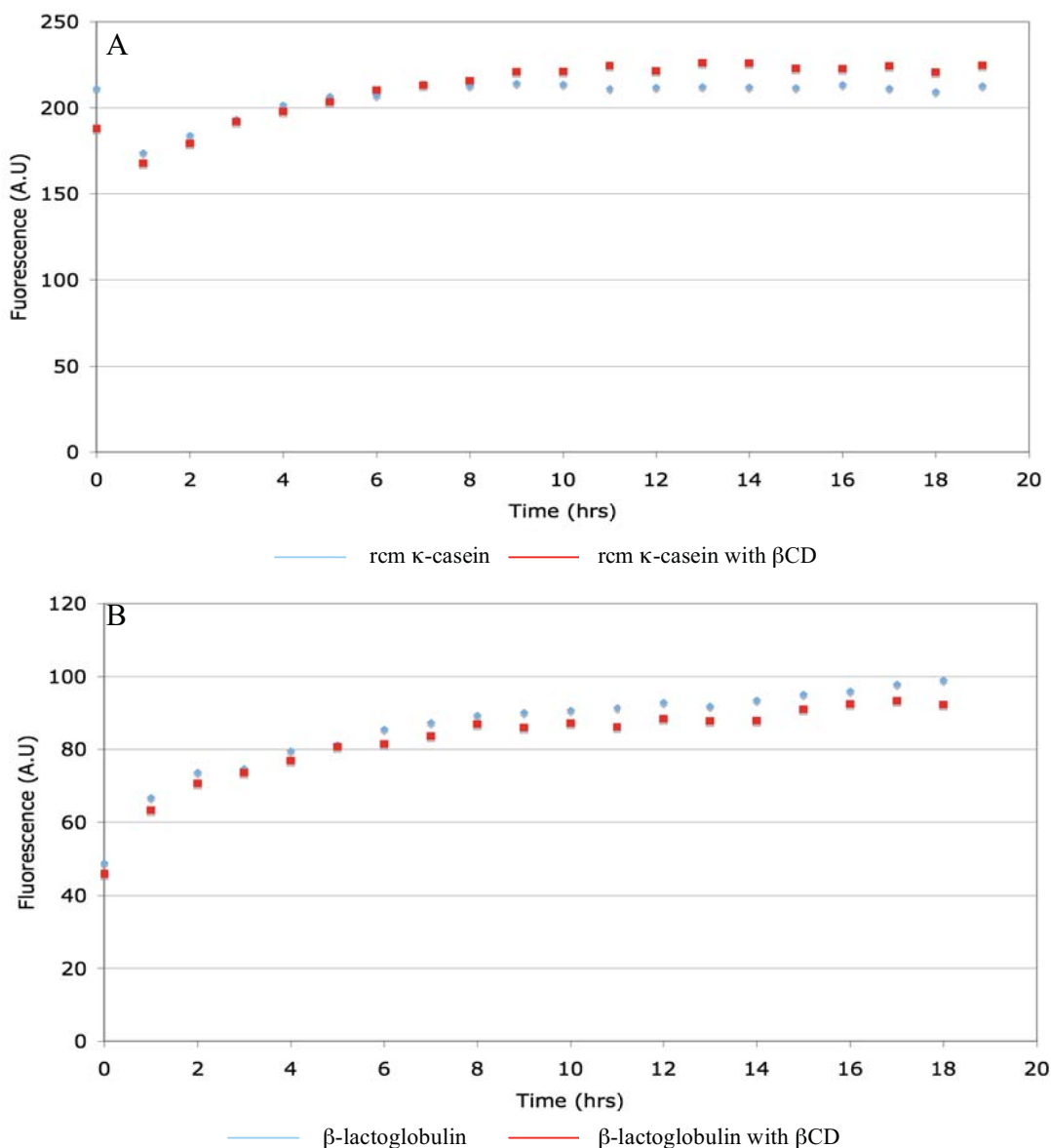
Figure 8.4 – ANS binding with (a) rcm κ-casein and (b) β-lactoglobulin during fibrillar
aggregation in the presence of βCD. ANS-associated fluorescence increased over the first 8
- 10 hours for both rcm κ-casein and β-lactoglobulin, suggesting dissociation or unfolding
into a relaxed, amyloidogenic precursor conformation with increased exposed
hydrophobicity. The presence of βCD had no effect on ANS binding to either rcm κ-casein
or β-lactoglobulin during fibrillar aggregation. There was no competition for binding sites
between βCD and ANS.
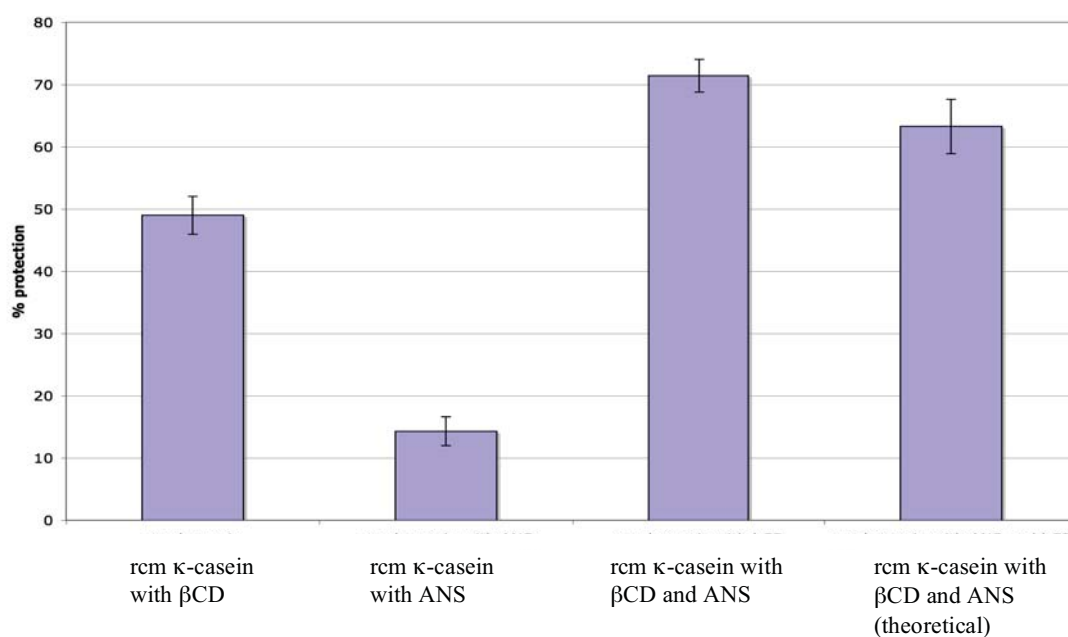
Figure 8.5 – Percentage protection values from rcm κ-casein fibrillar aggregation in the presence of excess ANS and/or βCD. ANS, βCD and a combination of ANS and βCD inhibited fibrillar aggregation. Percentage protection calculations demonstrate that chaperone ability of the βCD and ANS combination was higher than sum of βCD and ANS individually (labelled 'theoretical'). ANS and βCD did not appear to compete for binding sites on aggregating rcm κ-casein.

8.2.4 Competitive binding of α_T-crystallin and βCD to aggregating proteins

To further investigate the nature of hydrophobic interactions between βCD and aggregating target proteins, competitive binding of α_T-crystallin and βCD was monitored via ThT fluorescence chaperone assays. It is believed that during its chaperone action, α_T-crystallin binds to aggregating proteins via hydrophobic interactions (Raman and Rao, 1994; Das *et al.*, 1996). If βCD binds to target proteins via a similar non-specific hydrophobic mechanism, binding of βCD to target proteins should preclude the binding of α_T-crystallin (or vice-versa). ThT-associated fluorescence assays demonstrated that α_T-crystallin (at a 1:1 molar ratio of chaperone to target protein), βCD (at a 25:1 molar ratio of chaperone to target protein), and a combination of both α_T-crystallin and βCD each effectively inhibited rcm κ-casein aggregation (Figure 8.6). Percentage protection of the βCD/α_T-crystallin combination was comparable to the sum of the percentage protection values of individual α_T-crystallin and βCD (labelled 'theoretical', as in Section 8.2.3). There appeared to be no competition between the chaperone mechanisms of α_T-crystallin and βCD; the ability of βCD to inhibit target protein aggregation was not compromised by the addition of α_T-crystallin, and vice versa. βCD does not appear to compete with α_T-crystallin for binding sites on aggregating rcm κ-casein and β-lactoglobulin, which suggests that the two molecules bind to target proteins by significantly disparate mechanisms. This supports ANS data from Section 8.2.3, suggesting that βCD does not bind to target proteins via non-specific hydrophobic interactions.
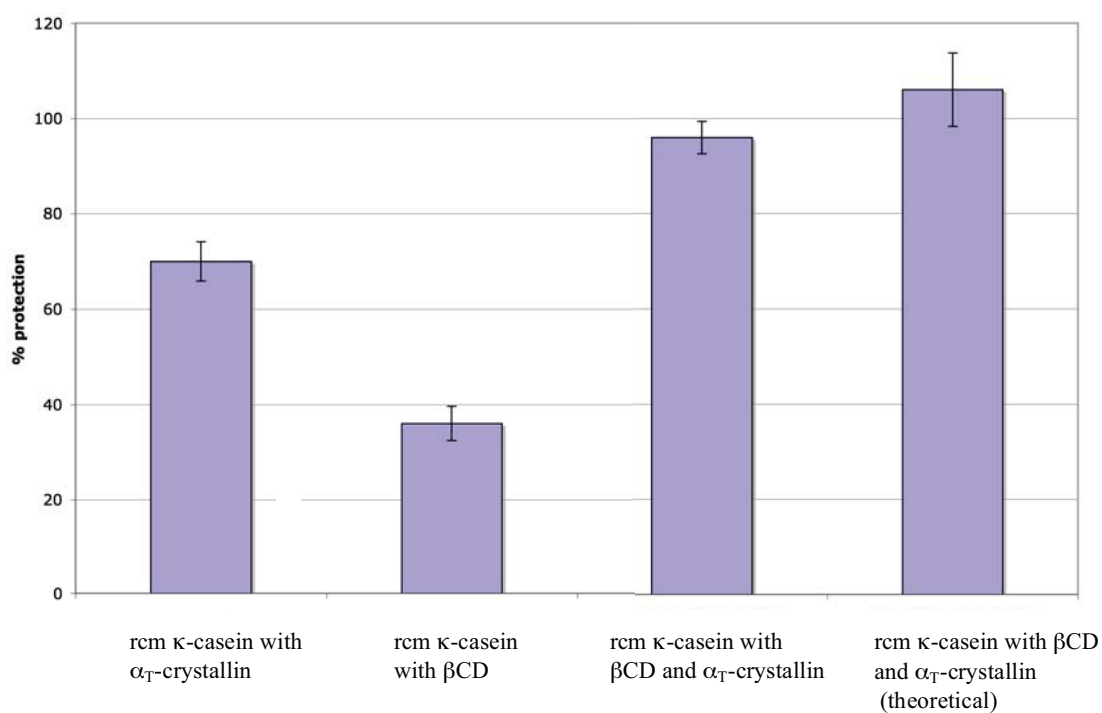
Figure 8.6 – Percentage protection values from rcm κ-casein fibrillar aggregation in the presence of α_T-crystallin and/or βCD. α_T-Crystallin, βCD and a combination of α_T-crystallin and βCD inhibited the fibrillar aggregation of rcm κ-casein. Percentage protection calculations demonstrate that the chaperone ability of the α_T-crystallin and βCD combination was comparable to the sum of α_T-crystallin and βCD individually (labelled 'theoretical'). α_T-crystallin and βCD did not appear to compete for binding sites on aggregating rcm κ-casein.

8.2.5 The relationship between target protein aggregation rate and βCD chaperone ability

Data from Section 7.2 show that βCD is better able to inhibit the fibrillar aggregation of wild-type and A53T α-synuclein than of α-lactalbumin, β-lactoglobulin or rcm κ-casein. Importantly, both wild-type and A53T α-synuclein aggregated at a much slower rate than either α-lactalbumin, β-lactoglobulin or rcm κ-casein; this may help explain the enhanced chaperone ability of βCD against wild-type and A53T α-synuclein. Previous studies have shown that cyclodextrins require highly solvent exposed binding sites for interactions with target proteins, and preferentially interact with significantly unfolded proteins (Aachmann *et al*, 2003). Slowly aggregating target proteins would facilitate more accessible binding sites for βCD-target protein interaction, as target proteins remain in a semi-folded state for a greater period of time. This, in turn, may enhance βCD chaperone ability.

The relationship between the rate of target protein aggregation and βCD chaperone ability was investigated using a similar method to that described in Section 4.2.7. The analysis used α-lactalbumin, β-lactoglobulin, rcm κ-casein, wild-type α-synuclein and A53T α-synuclein fibrillar aggregation data from Section 7.2. The aggregation data compared for investigation involved differing target proteins and protein concentrations, as well as different ThT stocks. These factors could result in differing ThT fluorescence intensities between data sets, irrespective of protein aggregation; consequently, comparing the rate of ThT-fluorescence increase over time was not considered an accurate method of investigation. To accommodate for the differences in aggregation conditions between data sets, the time taken to maximum fluorescence (tMax) was used as an indicator of the rate of target protein

aggregation. Percentage protection values (at a 25:1 molar ratio of βCD to target protein) were plotted against tMax in each assay (Figure 8.7). As with data from Section 4.2.7, a statistically significant relationship between tMax and percentage protection values (as determined by r^2 values) suggests that the rate of target protein aggregation directly influences βCD chaperone ability.

There were strong linear, logarithmic and exponential relationships between βCD percentage protection and the time to maximum ThT-fluorescence for aggregation assays from Section 7.2. βCD chaperone ability increased proportionally as the rate of fibrillar aggregation decreased (linear fit $r^2 = 0.9482$, exponential fit $r^2 = 0.9172$, linear fit $r^2 = 0.8698$). This demonstrates a direct relationship between the rate of target protein aggregation and βCD chaperone ability, and suggests that the rate of target protein aggregation directly influences the chaperone ability of βCD.
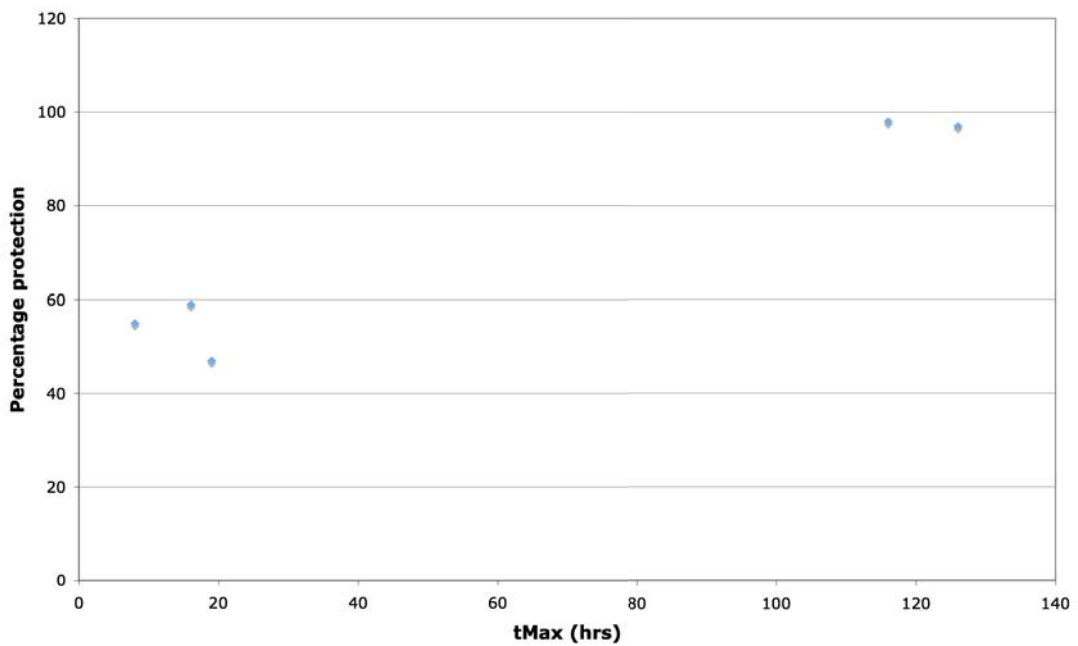
Figure 8.7 - Percentage protection versus the time taken to maximum ThT fluorescence (tMax) for data from Section 7.2. There were strong linear, logarithmic and exponential relationships between βCD percentage protection and the time taken to maximum ThT fluorescence (r^2 = 0.9482, 0.8698 and 0.9172, respectively). The rate of target protein aggregation directly influences the chaperone ability of βCD.

8.3 Discussion

Intrinsic fluorescence data demonstrated that βCD did not significantly affect the unfolding (β-lactoglobulin) or dissociation (rcm κ-casein) of proteins during the initial stages of fibrillar aggregation. It appears that cyclodextrins prevent fibrillar aggregation by interacting with already unfolded, sometimes dissociated target proteins. Previous studies support this conclusion; it has been demonstrated that cyclodextrins preferentially interact with highly unfolded target proteins (Karrupiah and Sharma, 1995; Aachmann *et al*, 2003), and require binding sites on target proteins with a high degree of solvent exposure to enable cyclodextrin/target protein interaction (Aachmann *et al*, 2003).

Circular dichroism spectroscopy from this study further supports this conclusion, demonstrating that βCD had little effect on the dissociation of rcm κ-casein prior to fibrillar aggregation. It appeared that βCD had little effect on rcm κ-casein random coil content, but significantly delayed the emergence of β-sheet structure of aggregating rcm κ-casein for up to 18 hours. After this time, βCD appeared to have no influence on rcm κ-casein aggregation, and fibrillar aggregation (as implied by increasing β-sheet content) continued as in the control sample.

βCD had no effect on the ANS-associated fluorescence of β-lactoglobulin or rcm κ-casein during the initial stages of fibrillar aggregation, demonstrating that βCD did not influence the exposed hydrophobicity of either target protein during fibrillar aggregation. An increase in exposed hydrophobicity can be interpreted as partial protein unfolding (in the case of β-lactoglobulin) or dissociation into semi-folded monomers or dimers (in the case of rcm κ-casein), as would occur prior to

fibril assembly; accordingly, these data support the intrinsic tryptophan fluorescence and circular dichroism data, and suggest that the presence of βCD has no effect on the initial unfolding (β-lactoglobulin) or dissociation (rcm κ-casein) of target proteins prior to fibril assembly. Competitive binding of ANS and βCD to aggregating rcm κ-casein showed that there was little or no competition for binding sites between ANS and βCD. ANS fluorescence was constant in the presence and absence of βCD, suggesting that ANS binding was not inhibited by the presence of βCD. Additionally, neither βCD's, nor ANS's ability to protect against fibrillar aggregation was affected by the presence of the other molecule. The non-competitive binding of ANS and βCD to rcm κ-casein suggests distinct binding mechanisms, or regions of binding, for ANS and βCD. ANS binds non-specifically to areas of exposed, clustered hydrophobicity on target proteins (Freifelder, 1982), and is believed to inhibit fibrillar aggregation as a consequence of non-specific hydrophobic interactions with aggregating target proteins (Fu *et al.*, 2005). The lack of competition between βCD and ANS for binding sites on aggregating rcm κ-casein implies that βCD does not interact with target proteins in a non-specific hydrophobic manner, and consequently that the βCD chaperone mechanism is not driven by non-specific hydrophobic interactions with target proteins.

Competitive chaperone assays of α_T-crystallin and βCD with aggregating rcm κ-casein support this conclusion. As an sHsp, α_T-crystallin is believed to bind to exposed hydrophobic regions on misfolded protein intermediates (Raman and Rao, 1994; Das *et al.*, 1996). βCD chaperone ability was unaffected by the presence of α_T-crystallin, and likewise α_T-crystallin chaperone ability was unaffected by the presence of βCD. From this it can be inferred that βCD and α_T-crystallin bind to

aggregating target proteins via sufficiently distinct mechanisms, which allows for the simultaneous binding of both molecules to target proteins.

Previous studies have shown that the annulus of the cyclodextrin ring preferentially accepts the insertion of aromatic amino acid side-chains from target proteins (Oh *et al.*, 1998; Otzen *et al.*, 2002; Aachmann *et al.*, 2003; Danielsson *et al.*, 2004). NMR spectroscopy has shown that aromatic side-chains are inserted into the βCD cavity during the inhibition of fibrillar aggregation (Qin *et al.*, 2002; Danielsson *et al.*, 2004), and that βCD is unable to interact with phenylalanine-free Aβ-peptide mutants (Danielsson *et al.*, 2004) This may help to explain the observed lack of competition for target protein binding sites between βCD and either ANS or α_T-crystallin. While both ANS and α_T-crystallin bind non-specifically to areas of exposed hydrophobicity on target proteins, it appears that βCD may instead bind specifically to aromatic amino acid side-chains. Interaction in this manner would allow for the simultaneous binding of βCD and either ANS or α_T-crystallin to aggregating target proteins. Further, this may help to explain the observed dependency of cyclodextrin binding on high levels of target protein solvent exposure (Aachmann *et al*, 2003), and the observation that cyclodextrins are most able to chaperone denatured and significantly unfolded target proteins (Karrupiah and Sharma, 1995; Sharma and Sharma, 2001); the highly specific cyclodextrin binding sites on target proteins would necessitate a comparatively high degree of accessibility, and would favour significantly unfolded target proteins. This idea is supported by the observed intrinsic tryptophan fluorescence, ANS fluorescence and CD data, which demonstrated that βCD has little or no influence on target protein unfolding, but delays and decreases the formation of stacked β-sheet structure in aggregating rcm κ-casein.

Recent data suggest that side chain interactions, particularly π-bonding between aromatic residues on adjacent β-sheet strands, may be necessary for the stacking and stabilisation of amyloid protofilaments (Gazit, 2002; Porat *et al.*, 2004; Zanuy *et al.*, 2004; Makin *et al.*, 2005). Aromatic residues, particularly tryptophan and phenylalanine, have been identified to be amongst the most 'amyloid-prone' amino acid residues (Pawar *et al.*, 2005). The disruption of π-bonding between aromatic residues has been suggested as an explanation for the anti-amyloid properties of aromatic-binding molecules, polyphenols in particular (Ono *et al.*, 2003, 2004; Taniguchi *et al.*, 2005; Porat *et al.*, 2006). This theory is supported by the observed insertion of aromatic amino acid residues into the annuli of βCD molecules during the inhibition of Aβ peptide aggregation (Qin *et al.*, 2002; Danielsson *et al.*, 2004).

Our data, coupled with previous findings, suggest a mechanism for βCD chaperone activity based upon βCD binding to exposed aromatic residues on unfolded or partially folded target proteins (Figure 8.8). Prior to fibrillar aggregation, natively folded target proteins unfold or dissociate into a relaxed conformation that acts as a precursor to fibrillar aggregation (Chiti *et al.*, 1999; Chiti and Dobson, 2006). Hydrophobic regions on these amyloidogenic protein intermediates associate into β-sheet stacks, forming protofilaments that arrange themselves to form amyloid fibrils (Chiti *et al.*, 1999; Chiti and Dobson, 2006). This is a simplified explanation of the fibrillar aggregation mechanism, but is representative of a general model describing amyloid fibril formation. Exceptions to this model have been reported; rcm κ-casein, for example, dissociates directly into partially folded, highly amyloidogenic monomers that can immediately associate into fibrillar aggregates (Ecroyd *et al.*, 2008). Protein unfolding (or dissociation)

into amyloidogenic monomers is unaffected by the presence of βCD; βCD molecules are instead able to interact with solvent accessible aromatic amino acid residues on relaxed target protein intermediates. The insertion of aromatic side chains into the annulus of cyclodextrin molecules inhibits the correct stacking of adjacent β-sheets on developing protofilaments by disrupting π-bonding, and destabilises the developing protofibrils. This in turn inhibits the formation of amyloid fibrils.
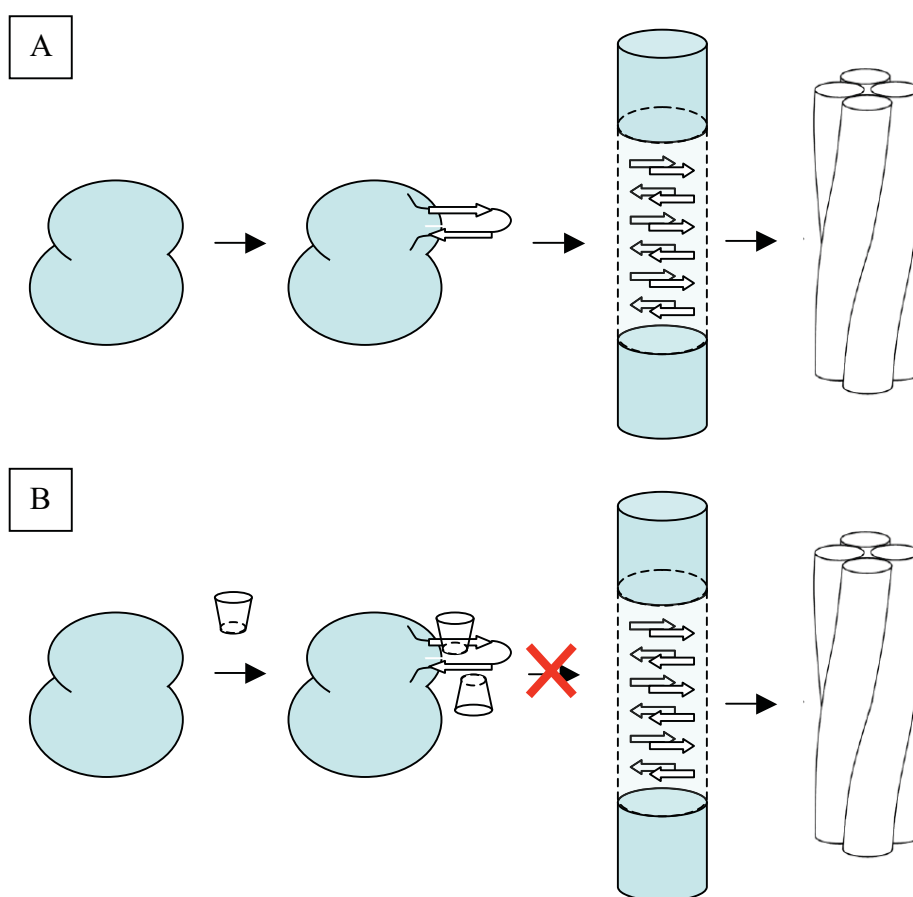
Figure 8.8 – Schematic representation of fibrillar aggregation in the (a) absence and (b) presence of βCD. The aggregation mechanism is by necessity simplified, but provides a general representation of fibrillar aggregation. Native proteins unfold (or dissociate) into an amyloidogenic precursor conformation, which facilitates β-sheet stacking and the assembly of protofilaments. These protofilaments then arrange into fibrillar aggregates. In the presence of βCD (b), natively folded proteins unfold or dissociate as normal. The relaxed conformation of amyloidogenic proteins allows βCD molecules to interact with exposed aromatic residues of the target protein. Insertion of aromatic side chains into βCD molecules inhibits β-sheet stacking and disrupts π-bonding that stabilises protofilaments. This, in turn, inhibts amyloid fibril formation.

Recently, the fibril-forming cores of rcm κ-casein (Ecroyd *et al.*, 2008) and α-synuclein (Qin *et al.*, 2007) have been determined via a combination of mass spectroscopy and NMR spectroscopy. The fibril-forming core of κ-casein contains eleven aromatic residues; three phenylalanine (F38, F39 and F76) and eight tyrosines (Y56, Y59, Y63, Y64, Y79, Y81, Y82 and Y91), which account for 18% of residues in the fibril-forming region. α-Synuclein has two aromatic residues in its fibril-forming core; one phenylalanine (F94) and one tyrosine (Y39). These residues could provide binding sites for βCD molecules during amyloid fibril formation, and to an extent support the aromatic residue-binding model proposed above. Importantly, both of the amorphous aggregation target proteins used in this study contain a significant number of aromatic side chains (58 in catalase, 8 in insulin). Assuming that the proposed βCD binding model is feasible, it appears that there are adequate aromatic binding sites available for βCD-target protein interactions for amorphously aggregating catalase and insulin, but that the rapid nature of amorphous aggregation does not allow for significant interaction between βCD and aggregating target proteins. Similarly, the conformation of intermediately folded protein monomers may vary between the initial stages of amorphous and fibrillar aggregation, such that protein intermediates preceding amorphous aggregation do not significantly expose aromatic residues for βCD binding.

There has so far been limited investigation into the correlation between target-protein aromatic residue content and cyclodextrin chaperone ability. As discussed previously, Aβ-peptide studies have demonstrated that βCD interacts with F19 and F20 during chaperone activity, and that βCD is unable to bind to a phenylalanine-free Aβ-derived peptide or prevent aggregation (Danielsson *et al.*, 2004). Further investigation into a possible differential βCD chaperone ability

between aromatic-rich and aromatic-poor target proteins may provide definitive evidence as to the veracity of the βCD chaperone mechanism proposed in this study.

If verified, this binding model suggests a number of exciting physiological implications. Cyclodextrins, as naturally occurring molecules, provide an excellent opportunity to investigate the therapeutic inhibition of disease-related fibrillar aggregation. βCD has now been demonstrated to inhibit the fibrillar aggregation of Aβ-peptide (Qin *et al.*, 2002; Danielsson *et al.*, 2004) and A53T α-synuclein (Section 7.2). These proteins are implicated in two of the most prevalent neurodegenerative diseases, Alzheimer's and Parkinson's disease. Both α and γCD have been approved for use as novel foods by the Australia New Zealand Food Authority (ANZFA), and βCD has been approved as a processing agent. Further characterisation and analysis of this mechanism may provide important applications for the inhibition of disease-causing protein misfolding *in vivo*.

CHAPTER 9

CONCLUSIONS

Chapter 9 – Conclusions

9.1 α-Crystallin chaperone ability is pH sensitive

The results presented in this thesis show conclusively that the chaperone ability of α-crystallin and its subunits is pH dependent against amorphous aggregation. Amorphous target protein aggregation, resulting from both thermal and reduction stress, demonstrates that α_T-, αA- and αB-crystallin are all significantly better chaperones at pH 7.0 and above compared to at pH 6.0 and pH 6.5. This pH sensitivity is of particular relevance in the lens, where αA-crystallin is the primary molecular chaperone. The nucleus of the lens, where aged cells accumulate, is significantly more acidic (pH 6.7) than the exterior epithelial or cortical cells of the lens (pH 7.2) (Bassnett and Duncan, 1985; 1987). The lack of protein turnover in the lens ensures that the oldest lens crystallins accumulate in the nucleus, and these crystallins are more prone to modification and consequential aggregation; reduced pH in the nucleus may further compromise the chaperone function of α-crystallin as the lens ages, and help explain the preferential development of age-related cataract in the lens nucleus (Truscott, 2005). Additionally, the observed pH-sensitive chaperone ability may compromise the ability of extra-lenticular αB-crystallin to inhibit fibrillar aggregation in low pH environments, for example at sites of localised acidosis. αB-crystallin expression is elevated in response to extra-lenticular amyloidosis in what is believed to be an extra-cellular protection mechanism (Shinohara *et al.*, 1993; Renkawek *et al.*, 1994), and has been isolated from low-pH exclusion bodies characteristic of Parkinson's disease (Lowe *et al.*, 1990; Lowe *et al.*, 1992; Mizutani *et al.*, 1998). Aβ-peptide aggregation,

characteristic of Alzheimer's disease, is accompanied by localised acidosis, and is promoted at pH 6.0 (Khandogin and Brooks, 2007).

The pH-sensitive chaperone ability of α-crystallin observed against amorphous aggregation was not seen against the fibrillar aggregation of rcm κ-casein. This may result from inherent differences between the aggregation mechanisms of amorphous and fibrillar aggregation, but may equally be a consequence of the atypical aggregation method of rcm κ-casein, as identified by Ecroyd *et al.* (2008). Support for this latter interpretation comes from the significantly reduced chaperone ability of α_T-, αA- and αB-crystallin against rcm κ-casein aggregation, reported here and in the work of others (Rekas *et al.*, 2007; Ecroyd *et al.*, 2007; Ecroyd and Carver, 2008). Accordingly, it is entirely possible that the data presented here for rcm κ-casein aggregation are not typical of α-crystallin chaperone ability against fibrillar aggregation, and that the ability of αB-crystallin to inhibit extra-lenticular fibrillar aggregation *in vivo* is pH-sensitive in the same manner as its ability to inhibit amorphous aggregation *in vitro*. If this is the case, the ability of αB-crystallin to function as an effective chaperone under conditions of localised amyloidosis may be compromised *in vivo*.

There appears to be no clear structural correlation between pH and chaperone ability of α-crystallin. Whilst all three crystallins are partially unfolded at pH 6.0 and pH 6.5, compared to pH 7.0 and above, and demonstrate a higher degree of exposed hydrophobicity, this does not appear to directly influence their ability to inhibit target protein aggregation. At pH 3.5 and below, where αA- and αB-crystallin are highly unfolded, chaperone ability is significantly heightened over that of pH 6.0, or even pH 8.0. These observations are reminiscent of the thermally-

enhanced chaperone ability of α-crystallin observed by Raman and Rao (1994), amongst others (Das and Surewicz, 1995; Datta and Rao, 1999, Reddy *et al.*, 2000). A thorough reading of the available literature suggests that increasing exposed hydrophobicity can both increase (Das and Surewicz, 1995; Datta and Rao, 1999) and decrease (Smulders *et al.*, 1995) chaperone ability, and so whilst surface hydrophobicity probably plays some role in dictating chaperone ability, it does not directly correlate with the ability of α-crystallin and its subunits to protect against target protein aggregation.

A kinetic relationship between the rate of target protein aggregation and the ability of α-crystallin to inhibit target protein aggregation does not appear to be a sufficient explanation for the pH sensitive chaperone ability of α-crystallin observed in this thesis. Reduction-stress induced aggregation of α-lactalbumin at 37°C demonstrated a strong correlation between the rate of protein aggregation and α-crystallin percentage protection; as the rate of α-lactalbumin aggregation increased, α_T-, αA- and αB-crystallin chaperone ability decreased. For all other target proteins and aggregation conditions, however, no such relationship was evident. It has been demonstrated previously that when the rate of target protein aggregation significantly outpaces the subunit exchange between α-crystallin and target proteins, chaperone ability is compromised (Lindner *et al.*, 2001); consequently, α-crystallin is believed to be a better chaperone of slowly aggregating target proteins. In this study, however, the relationship between target protein aggregation rate and α-crystallin chaperone ability does not appear to be a significant factor in explaining the observed pH sensitivity of α-crystallin chaperone ability.

The relative thermal stability of both α-crystallin and its subunits may have a more direct effect on chaperone ability with varying pH, particularly at pH 6.0.

Initial chaperone assays (Section 3.2.1) were undertaken at elevated temperatures (55°C or 60°C), at which α-crystallin has been previously shown to begin to unfold (Surewicz and Olesen, 1995; Gesierich and Pfeil, 1996). At these temperatures, α-crystallin has been shown to retain a high degree of both stability and solubility, and function effectively as a molecular chaperone (Raman and Rao, 1994; Raman *et al.*, 1995; Das and Surewicz, 1995; Datta and Rao, 1999). However, the solubility and thermal stability of α_T-crystallin appears to be directly influenced by pH, and α_T-crystallin is unable to form stable complexes with target proteins at 55°C and pH 6.0 (and to a lesser extent at pH 6.5). This corresponds with decreased chaperone ability for both α_T-crystallin and its subunits, and so provides a possible explanation for the influence pH has on the chaperone ability of these proteins. However, even at lower temperatures, where α_T-crystallin is demonstrated to be neither unfolded nor structurally unstable at pH 6.0 and 6.5, there remains a clear correlation between pH and chaperone ability. It appears therefore that while the relative thermal stability of α-crystallin may exacerbate the influence of pH on the ability of α-crystallin to inhibit target protein aggregation, it is not necessarily the sole cause of this phenomenon.

Chemical modification of exposed histidine residues largely removed the pH sensitivity of αB-crystallin chaperone ability. DEPC modification of histidine residues significantly increased the chaperone ability of αB-crystallin at pH 6.0 and 6.5, but had no effect on the chaperone ability of αB-crystallin between pH 7.0 and 8.0. While the chaperone ability of DEPC-bound αB-crystallin was still significantly lower at pH 6.0 than at pH 6.5 and above, there was no significant difference in DEPC-bound αB-crystallin chaperone ability between pH 6.5 and 8.0. DEPC binding to exposed histidine residues inhibits histidine protonation (Dietz *et*

al., 1992; Carneiro *et al.*, 2003; Kawai *et al.*, 2005); consequently, protonation of an exposed histidine residue or residues appears to be primarily responsible for the decreased chaperone ability of αB-crystallin (and most likely also α_T- and αA-crystallin) at pH 6.0 and 6.5. Interestingly, site-directed mutagenesis of a specific histidine residue, H83, in the chaperone-binding region of αB-crystallin, did not improve the chaperone ability of αB-crystallin at pH 6.0 and 6.5 relative to wild-type αB-crystallin. It would appear that protonation of H83 is not involved in the pH-sensitivity of αB-crystallin chaperone ability, or else that protonation of several histidine residues is responsible for the decreased chaperone ability of α-crystallin at pH 6.0 and 6.5, compared to at pH 7.0 and above.

9.2 Cyclodextrins are effective molecular chaperones of fibrillar aggregation

Whilst it is commonly stated that cyclodextrins are efficient molecular chaperones, an appraisal of the literature shows that this is predominantly the case in situations of renaturation-induced aggregation. During this type of aggregation, the target protein is significantly, if not totally unfolded for extended periods of time in the presence of a denaturant (for example, urea or guanadinium hydrochloride), and then induced to refold via the removal of the initial denaturant (Karuppiah and Sharma, 1995; Sharma and Sharma, 2001). Aggregation of this type is distinct from that of the off-folding pathway, in which semi-folded protein intermediates aggregate via hydrophobic interactions between multiple intermediates. In the dynamic, intermediate-derived aggregation characteristic of the off-folding pathway, there is only limited evidence to suggest that cyclodextrins function as efficient chaperones (Tavornvipas *et al.*, 2004), and instead function as the second

stage of a two-step refolding pathway; this mechanism necessitates an additional molecular chaperone, acting in much the same manner as an sHsp, to capture aggregating target proteins (Rozema and Gelman, 1996; Daugherty *et al.*, 1998; Akiyoshi *et al.*, 1999; Nomura *et al.*, 2003).

As shown in this thesis cyclodextrins do, however, efficiently inhibit the fibrillar aggregation of target proteins under a variety of conditions. βCD is more efficient in this capacity than either αCD or γCD, and favours slower rates of protein aggregation. The relationship between protein aggregation rate and percentage protection suggests that kinetic considerations are a significant factor in the βCD chaperone mechanism, and might be explained by the high specificity of βCD-target protein binding. Both the available literature and data presented here suggests that βCD does not bind to aggregating target proteins in a non-specific hydrophobic manner, and is unable to prevent the initial unfolding of target proteins. Rather, βCD appears to interact with fibril-forming proteins during the assembly of protofilaments, and thereby delays the onset of β-sheet stacking. This most probably occurs via interactions with aromatic residues (Qin *et al.*, 2002; Aachman *et al.*, 2003; Danielsson *et al.*, 2004), which are increasingly demonstrated to play a significant role in fibrillar aggregation (Gazit, 2002; Porat *et al.*, 2004; Zanuy *et al.*, 2004; Makin *et al.*, 2005). This highly specific mode of interaction would require both significant solvent exposure and a relatively slow rate of protein aggregation, both of which are suggested to be key factors in enabling βCD-protein interaction (Aachman *et al.*, 2003). More significantly, βCD has been shown to be unable to interact with phenylalanine-free mutants of the Aβ-peptide, a peptide that βCD normally binds strongly to (Danielsson *et al.*, 2004). The weight of data suggests a putative chaperone mechanism reliant upon the insertion of aromatic

side-chains into the central βCD cavity, inhibiting π-bonding between β-strands in fibrillar protofilaments, and consequently delaying or inhibiting fibril formation. Polyphenols have recently been demonstrated to inhibit fibril formation via a similar method, and this provides an exciting insight into potential anti-amyloid applications (Ono *et al.*, 2003, 2004; Taniguchi *et al.*, 2005; Porat *et al.*, 2006). The data presented here are particularly pertinent in light of the inhibition by βCD of A53T α-synuclein fibrillar aggregation, a protein characteristic of Parkinson's disease (Tofaris and Spillantini, 2005, 2007). An approximately 2:1 weight to weight ratio of βCD with A53T α-synuclein was able to inhibit target protein aggregation in excess of 90%, suggesting a possible therapeutic role for cyclodextrins in inhibiting amyloidosis *in* vivo. The ability of small, aromatic-binding compounds such as cyclodextrins to inhibit fibrillar aggregation demands further research into their use for inhibiting amyloid formation *in vivo*, and thereby combating neurodegenerative diseases such as Alzheimer's and Parkinson's disease.

9.3 Future directions

The pH sensitivity of α-crystallin chaperone ability has been shown conclusively in this study, except in regards to rcm κ-casein fibrillar aggregation. It is possible that the unexpected results observed for rcm κ-casein aggregation are a consequence of the atypical mechanism of κ-casein fibril formation, and not necessarily representative of differences between the mechanisms of fibrillar and amorphous aggregation. To determine whether the ability of α-crystallin to inhibit fibrillar aggregation is pH sensitive, in the same manner as against amorphous aggregation, it would be necessary to repeat the experiments from Section 3.2.3 with two or more

target proteins that form amyloid fibrils between pH 6.0 and 8.0. Most fibrillary aggregating species require very specific solution conditions for fibrillar aggregation, and it is difficult to identify target proteins that will aggregate satisfactorily at both pH 6.0 and 8.0; possible exceptions include ccβ-peptide and Aβ-peptide, which aggregate under a variety of solution conditions and may help to clarify the relationship between pH and α-crystallin chaperone ability against fibrillar aggregation.

It is likely that the protonation of histidine residues influences the chaperone ability of α_T- and αA-crystallin, as has been observed in this thesis for αB-crystallin. This cannot be definitively stated, however, until both αA- and α_T-crystallin have been similarly investigated. Repetition of the DEPC-binding studies from section 7.2.1 utilising α_T- and αA-crystallin as molecular chaperones will provide an overall picture of the role of histidine residues in the chaperone ability of α-crystallin.

While this study involved a thorough investigation into the causes of α-crystallin's pH sensitive chaperone ability, the exact role of histidine protonation is not yet clear. It appears that an exposed histidine residue or residues, of which αB-crystallin has four, is implicated in the chaperone ability of αB-crystallin. It is unclear whether the protonation of a single or several histidine residues results in the decreased chaperone ability of αB-crystallin at pH 6.0 and 6.5, based upon the current data. Data show that protonation of H83 on its own does not result in decreased αB-crystallin chaperone ability below pH 7.0, and so it would appear that several other histidine residues are implicated in the pH-sensitivity of αB-crystallin chaperone ability. Characterising the specific histidine residues involved in αB-crystallin chaperone action would be difficult; mass spectroscopy of DEPC-bound

αB-crystallin would be unhelpful in determining which histidine residues are modified by DEPC, as the ethoxyformyl product is inherently unstable (Tawfik, 1996). Synthesis of a series of his -> ala mutants, focusing on the C-terminal domain of αB-crystallin, would be necessary to determine which specific histidine residues are implicated in the pH-sensitivity of αB-crystallin chaperone ability.

The demonstrated ability of cyclodextrins to inhibit fibrillar aggregation provides a wealth of future research options and potential clinical applications. In relation to this study, however, there are still a number of experiments that would help clarify the proposed βCD-target protein binding mechanism. So far, very little has been done to investigate the differential binding and chaperone ability of βCD to target peptides with a high and low proportion of aromatic residues. Whilst βCD binds to and inhibits the aggregation of Aβ-peptide, the demonstrated inability of βCD to bind to aggregating phenylalanine-free Aβ-peptide mutants suggests that βCD will preferentially bind to, and consequently inhibit, the aggregation of aromatic residue-rich peptides and proteins (Danielsson *et al.*, 2004). To quantify this it would be both necessary and helpful to investigate the ability of βCD to inhibit the aggregation of a variety of fibril forming peptides with varying aromatic residue content. This in turn would support the βCD-target protein binding mechanism suggested in this study.

βCD facilitates the refolding of aggregating target proteins, either individually or as part of a two-step refolding pathway (Karuppiah and Sharma, 1995; Rozema and Gelman, 1996; Daugherty *et al.*, 1998; Sharma and Sharma, 2001). From this it seems possible that, in addition to inhibiting fibrillar aggregation, βCD might be able to facilitate the refolding and return of function of aggregating target proteins. Currently, there are few enzymatically active proteins

for which fibrillar aggregation has been extensively characterised. Lysozyme

fibrillar aggregation has been characterised under a variety of conditions, and two

lysozyme mutants (I56T, D67H) are characteristic of amyloidosis *in vivo* (Pepys *et al.*, 1993; Booth *et al.*, 1997; Kumita *et al.*, 2007). Further, the commonly used

lysozyme functionality assay is simple and rapid, and so lysozyme provides a

perfect model for investigating the refolding ability of βCD during the inhibition of

fibrillar aggregation. A return of function of βCD-bound aggregating lysozyme, as

determined by the breakdown of bacterial cell membrane, would suggest return of

correct folding and definitively demonstrate the refolding ability of βCD.

APPENDICES

Appendix A – Reagents, suppliers and materials

A.1 Reagents and suppliers

Reagent	Supplier
α-lactalbumin	Sigma-Aldrich, MO, U.S.A
ammonium hydrogen carbonate	Ajax Finechem, N.S.W., Australia
ammonium persulphate	Merck Scientific, Vic., Australia
ammonium sulphate	Merck Scientific, Vic., Australia
ampicillin	Sigma-Aldrich, MO, U.S.A
ANS	Sigma-Aldrich, MO, U.S.A
β-lactoglobulin	Sigma-Aldrich, MO, U.S.A
β-mercaptoethanol	Amresco Pty. Ltd., OH, U.S.A
bis-acrylimide (40%)	Amresco Pty. Ltd., OH, U.S.A
catalase	Sigma-Aldrich, MO, U.S.A
coomassie blue	MP Biochemicals, OH, U.S.A
deoxycholic acid	Astral Scientific, N.S.W., Australia
DEPC	Sigma-Aldrich, MO, U.S.A
DMSO	Ajax Finechem, N.S.W., Australia
DNAse I	Sigma-Aldrich, MO, U.S.A
DTT	Astral Scientific, N.S.W., Australia
Ethanol	Ajax Finechem, N.S.W., Australia
glacial acetic acid	Merck Scientific, Vic., Australia
glycine	Amresco Pty. Ltd. OH, U.S.A
hydrochloric acid	Ajax Finechem, N.S.W., Australia
hydrogen peroxide	Ajax Finechem, N.S.W., Australia
insulin	Sigma-Aldrich, MO, U.S.A
iodoacetic acid	Sigma-Aldrich, MO, U.S.A
IPTG	Astral Scientific, N.S.W., Australia
κ-casein	Sigma-Aldrich, MO, U.S.A
kanamycin	Sigma-Aldrich, MO, U.S.A
L-trp	BDH Laboratory Supplies Ltd., U.K
Lysozyme	Sigma-Aldrich, MO, U.S.A
Methanol	Ajax Finechem, N.S.W., Australia

PEI	Sigma-Aldrich, MO, U.S.A
PMSF	Sigma-Aldrich, MO, U.S.A
sodium azide	Sigma-Aldrich, MO, U.S.A
sodium chloride	Amresco Pty. Ltd., OH, U.S.A
SDS	BDH Laboratory Supplies Ltd., U.K
sodium diphosphate	Merck Scientific, Vic., Australia
sodium hydroxide	Ajax Finechem, N.S.W, Australia
sodium monophosphate	Merck Scientific, Vic., Australia
TCEP	Sigma-Aldrich, MO, U.S.A
TEMED	Amresco Pty. Ltd., OH, U.S.A
ThT	Sigma-Aldrich, MO, U.S.A
Tris HCl	Amresco Pty. Ltd., OH, U.S.A
Tris base	Amresco Pty. Ltd., OH, U.S.A

A.2 Materials

Material	Supplier
regenerated cellulose membranes	Adelab Scientific, S.A., Australia
snakeskin dialysis tubing	Pierce Scientific, IL, U.S.A
TEM grids	ProSciTech, Qld., Australia
96 well clear plates	Greiner BioOne, Germany
96 well black clear-bottom plates	Greiner BioOne, Germany
10mm path length quartz cuvettes	Starna Pty. Ltd., N.S.W., Australia
10mm path length glass cuvettes	Starna Pty. Ltd., N.S.W., Australia
1mm path length glass cuvettes	Starna Pty. Ltd., N.S.W., Australia

Appendix B – Explanation of Swiss-Prot entry names from Chapter 7

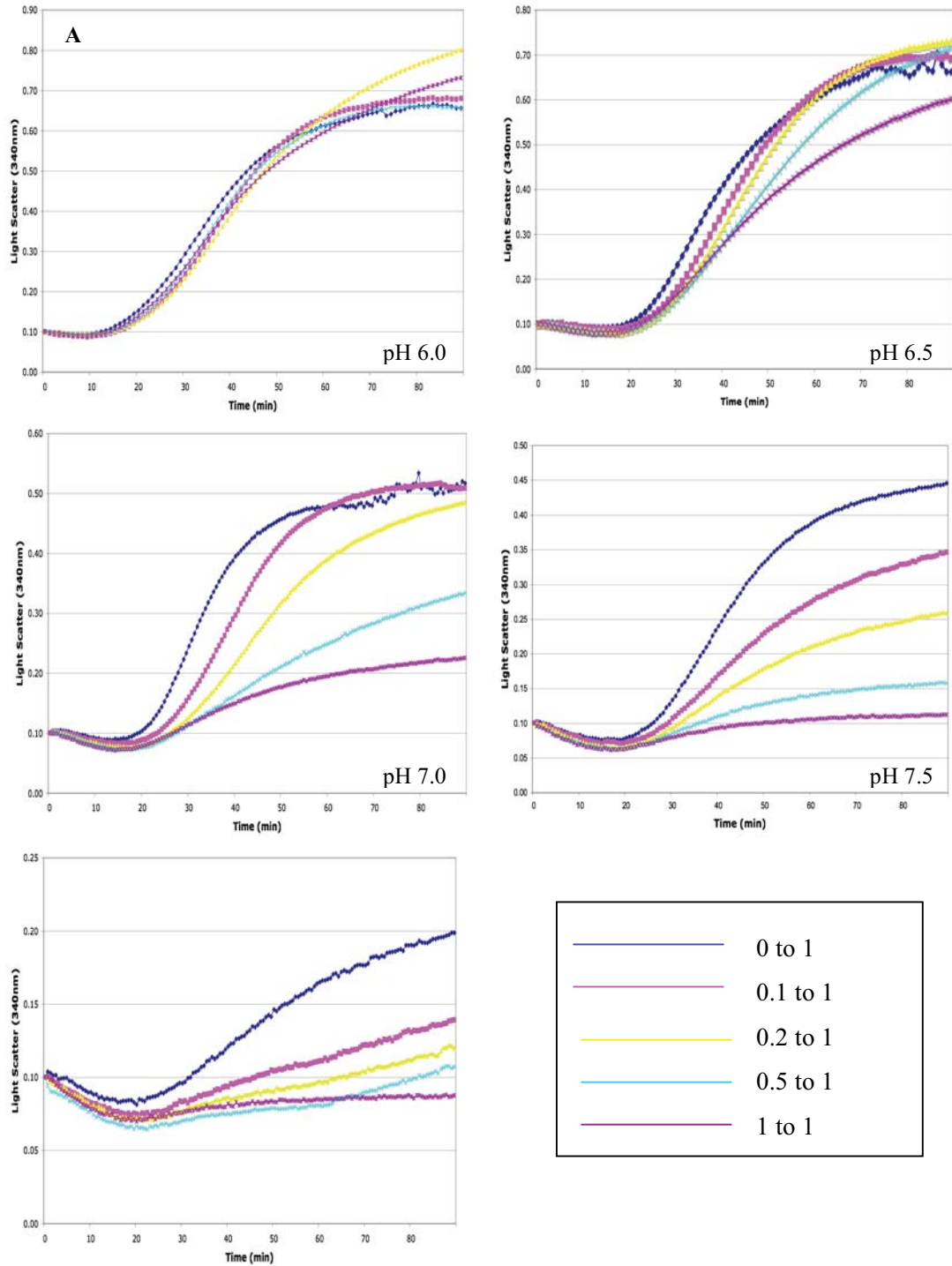**B.1 Explanation of Swiss-Prot entry names from Figure 7.4**

Entry name	Primary accession number	Protein name	Species of origin
CRYAA_TAMME	P02485	αA-crystallin	Mexican collared ant-eater
CRYAA_BRAVA	P02487	αA-crystallin	Brown-throated 3-fingered sloth
CRYAA_CHOHO	P02486	αA-crystallin	Hoffman's 2-fingered sloth
CRYAA_HUMAN	P02489	αA-crystallin	Human
CRYAA_MACMU	P02488	αA-crystallin	Rhesus macaque
CRYAA_MERUN	P68405	αA-crystallin	Mongolian gerbil
CRYAA_TUPGL	P68406	αA-crystallin	Tree shrew
CRYAA_CAVPO	P68281	αA-crystallin	Guinea pig
CRYAA_PEDCA	P68283	αA-crystallin	Springhaas
CRYAA_RABIT	P02493	αA-crystallin	Rabbit
CRYAA_HORSE	P02478	αA-crystallin	Horse
CRYAA_CERSI	P02479	αA-crystallin	White Rhinoceros
CRYAA_TAPIN	P02476	αA-crystallin	Asiatic tapir
CRYAA_BOVIN	P02470	αA-crystallin	Bovine
CRYAA_SHEEP	Q5ENZ0	αA-crystallin	Sheep
CRYAA_PIG	P02475	αA-crystallin	Pig
CRYAA_ARTJA	P02480	αA-crystallin	Jamaican fruit-eating bat
CRYAA_LOXAF	P02498	αA-crystallin	African elephant
CRYAA_PROCA	P02499	αA-crystallin	Cape hyrax
CRYAA_TUPTE	P02506	αA-crystallin	Common tegu
CRYAB-HUMAN	P02511	αB-crystallin	Human
CRYAB_PONPY	Q5R9KO	αB-crystallin	Bornean orangutan
CRYAB_MACFA	Q60HG8	αB-crystallin	Crab-eating macaque
CRYAB_RABIT	P41316	αB-crystallin	Rabbit
CRYAB_MESAU	P05811	αB-crystallin	Golden hamster
CRYAB_RAT	P23928	αB-crystallin	Rat
CRYAB_SPAJO	Q9EPF3	αB-crystallin	Blind subterranean mole rat
CRYAB_MOUSE	P23927	αB-crystallin	Mouse
CRYAB_SHEEP	Q589Y9	αB-crystallin	Sheep
CRYAB_BOVIN	P02510	αB-crystallin	Bovine
CRYAB_CHICK	Q05713	αB-crystallin	Chicken
CRYAB_ANAPL	Q05557	αB-crystallin	Domestic duck
CRYAB_RANCA	Q91312	αB-crystallin	Bullfrog
CRYAB_SQUAC	P02512	αB-crystallin	Spiny dogfish

## B.2 Explanation of Swiss-Prot entry names from Figure 7.5

Entry name	Primary accession number	Protein name
CRYAA_HUMAN	P02489	αA-crystallin
CRYAB_HUMAN	P02511	αB-crystallin
HSPB6_HUMAN	O14558	Small heat shock protein B6
HSPB1_HUMAN	P04792	Small heat shock protein B1
HSPB8_HUMAN	Q9UJY1	Small heat shock protein B8
HSPB2_HUMAN	Q16082	Small heat shock protein B2
HSPB3_HUMAN	Q12988	Small heat shock protein B3
HSPB7_HUMAN	Q9UBYN	Small heat shock protein B7
HSPB9_HUMAN	Q9BQ56	Small heat shock protein B9
ODFP1_HUMAN	Q14990	Outer dense fibre protein 1

Appendix C – Light scattering data from Section 3.2.1-2

C.1 – Light scattering assays of α_T-, αA- and αB-crystallin with thermally-stressed catalase
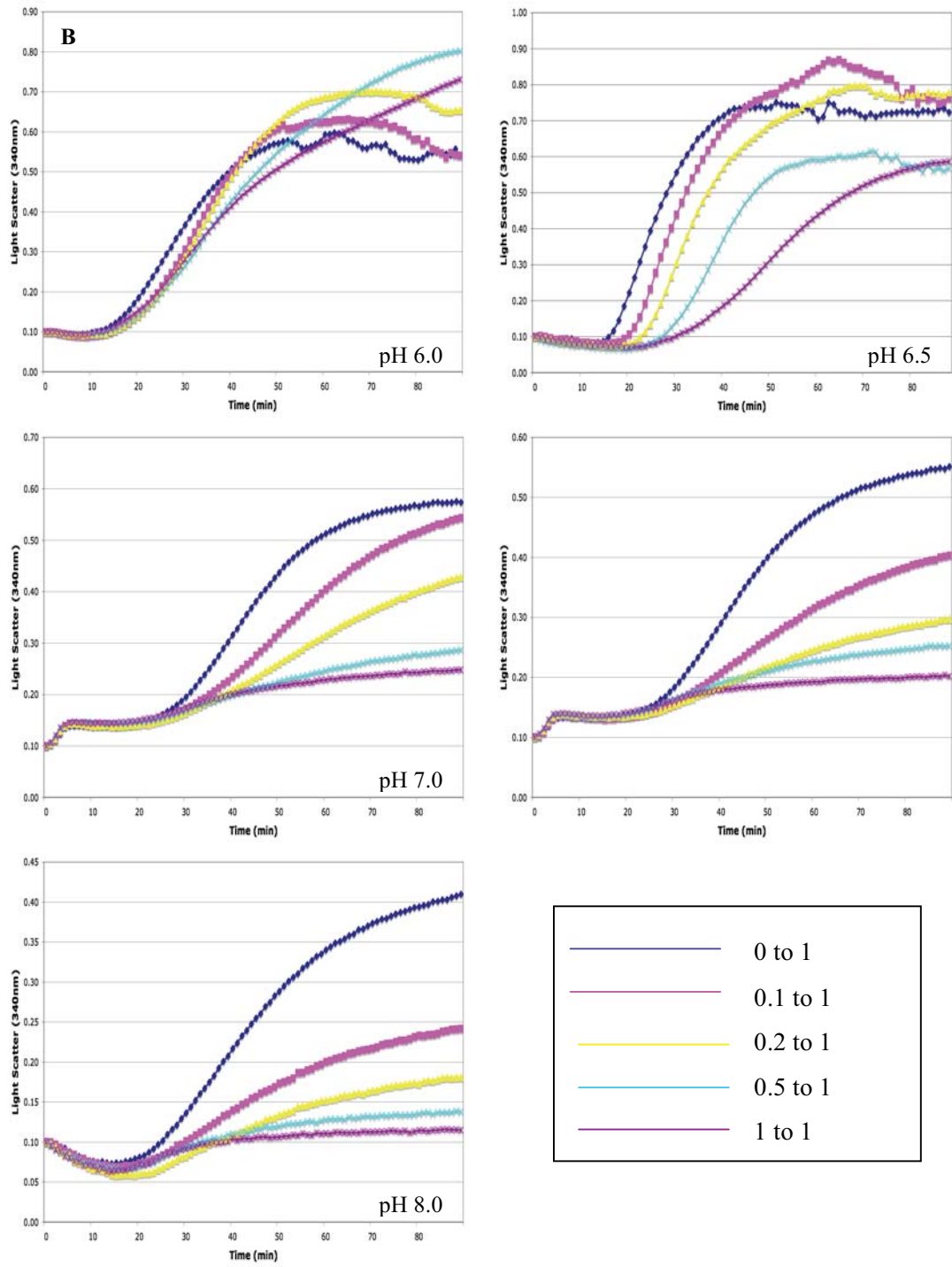
Appendix C
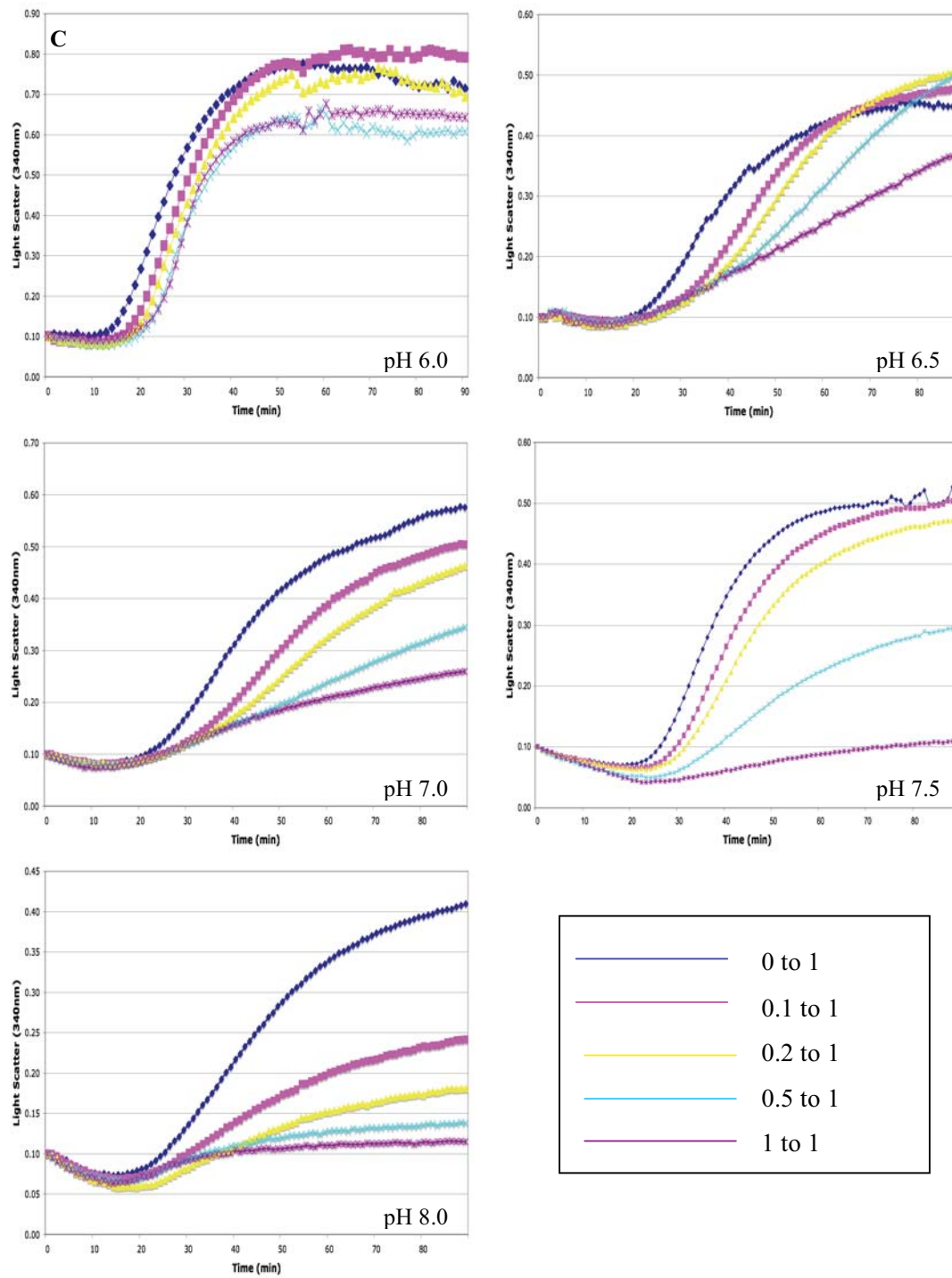
Figure C1 – Light scattering at 340nm (55°C) versus time of catalase with (a) α_T-crystallin, (b) αA-crystallin and (c) αB-crystallin

Appendix C

C.2 Light scattering assays of α_T-, αA- and αB-crystallin with thermally-stressed β_L-crystallin

Figure C3 – Light scattering at 340nm (60°C) versus time of β_L-crystallin with (a) α_T-crystallin, (b) αA-crystallin and (c) αB-crystallin

C.3 Light scattering assays of α_T-, αA- and αB-crystallin with reduction-stressed α-lactalbumin
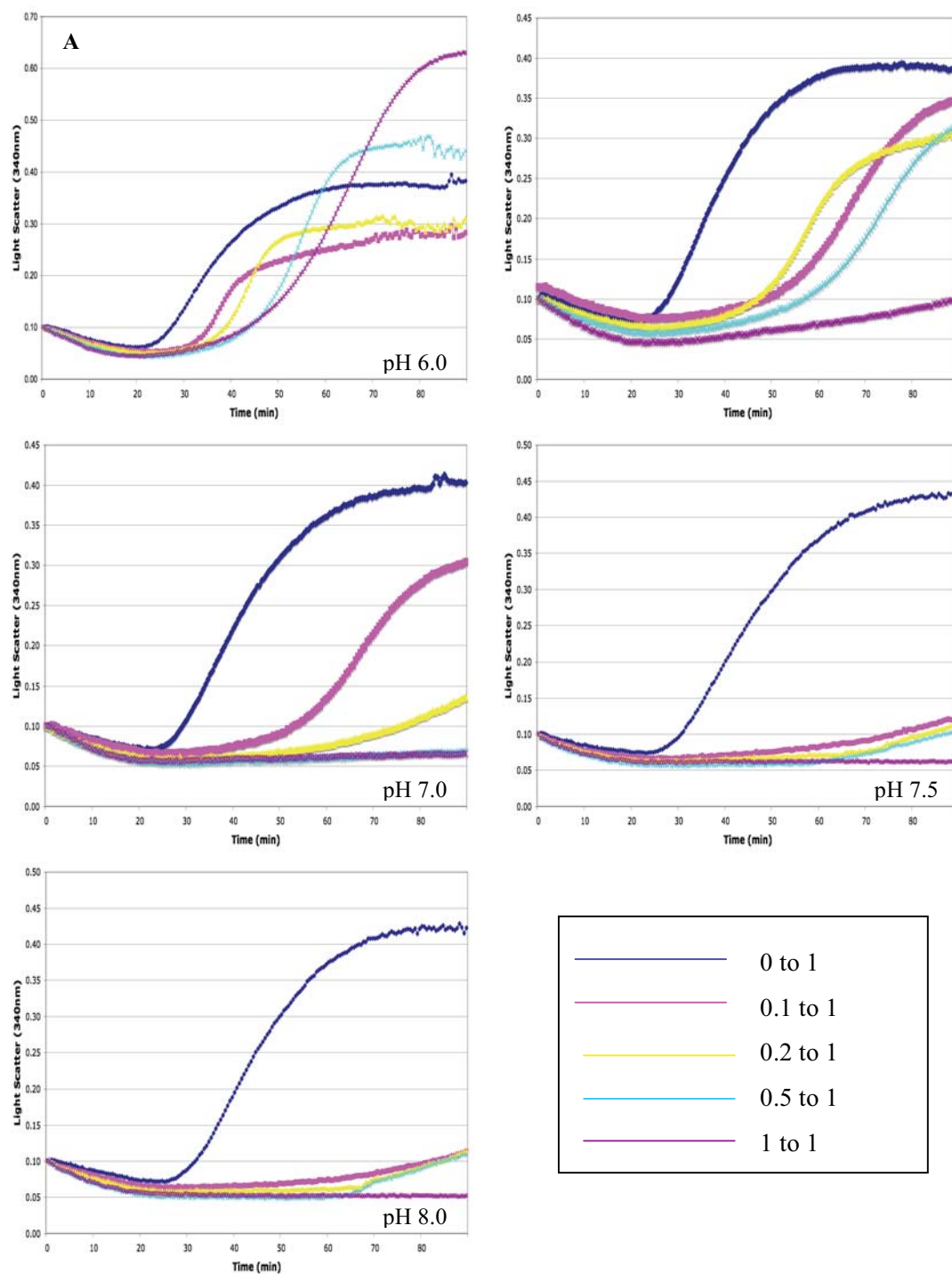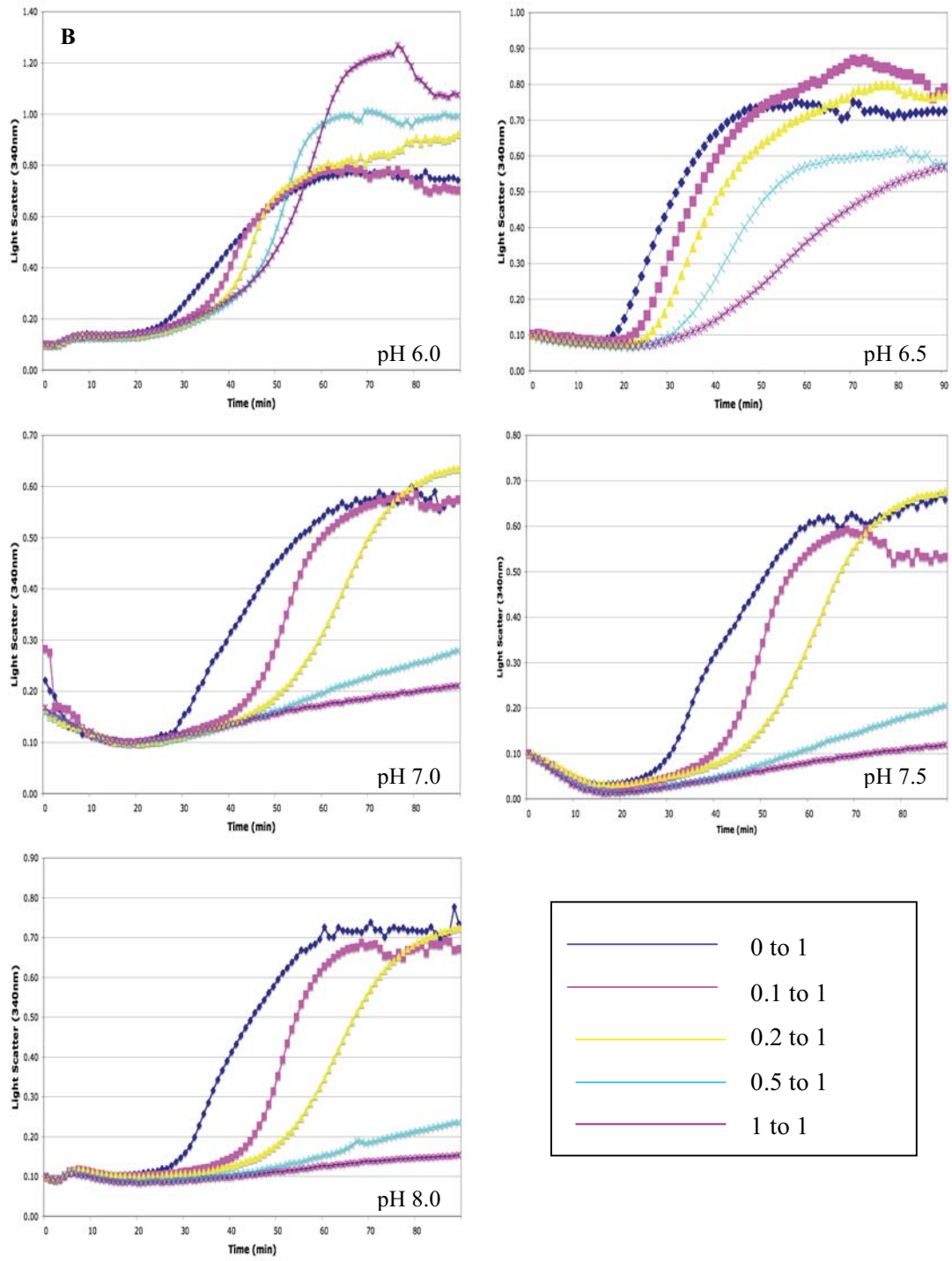
Appendix C

Appendix C
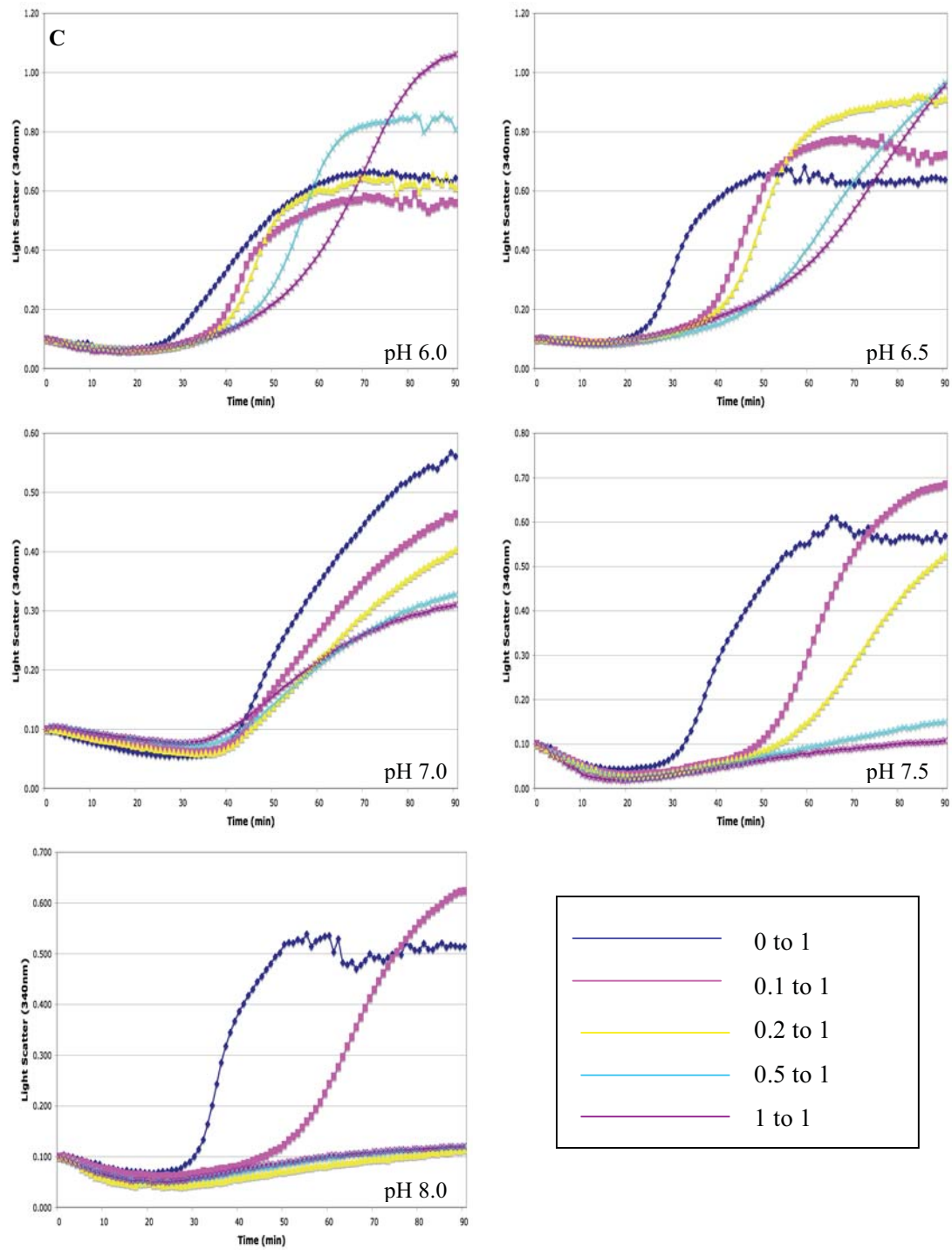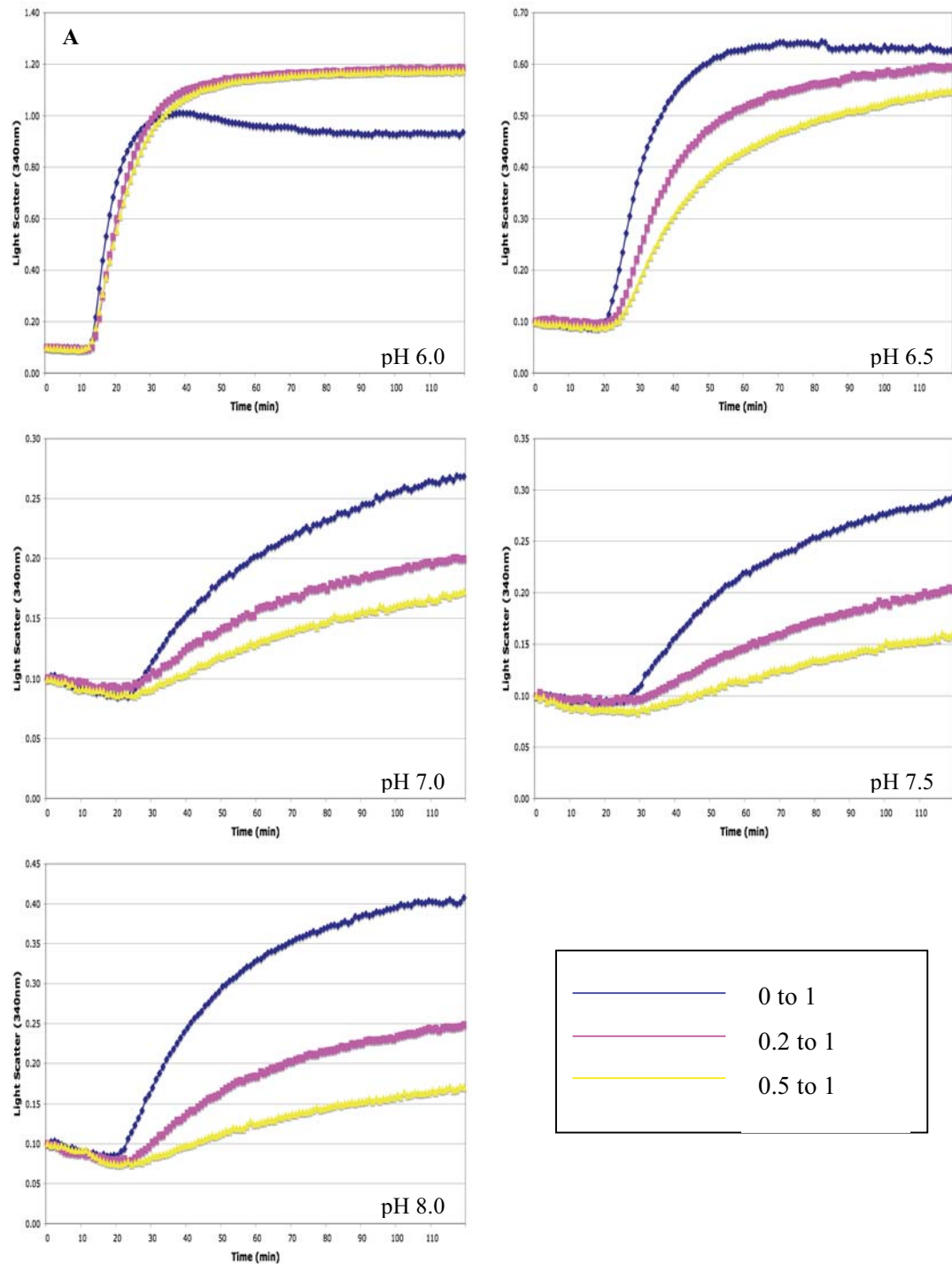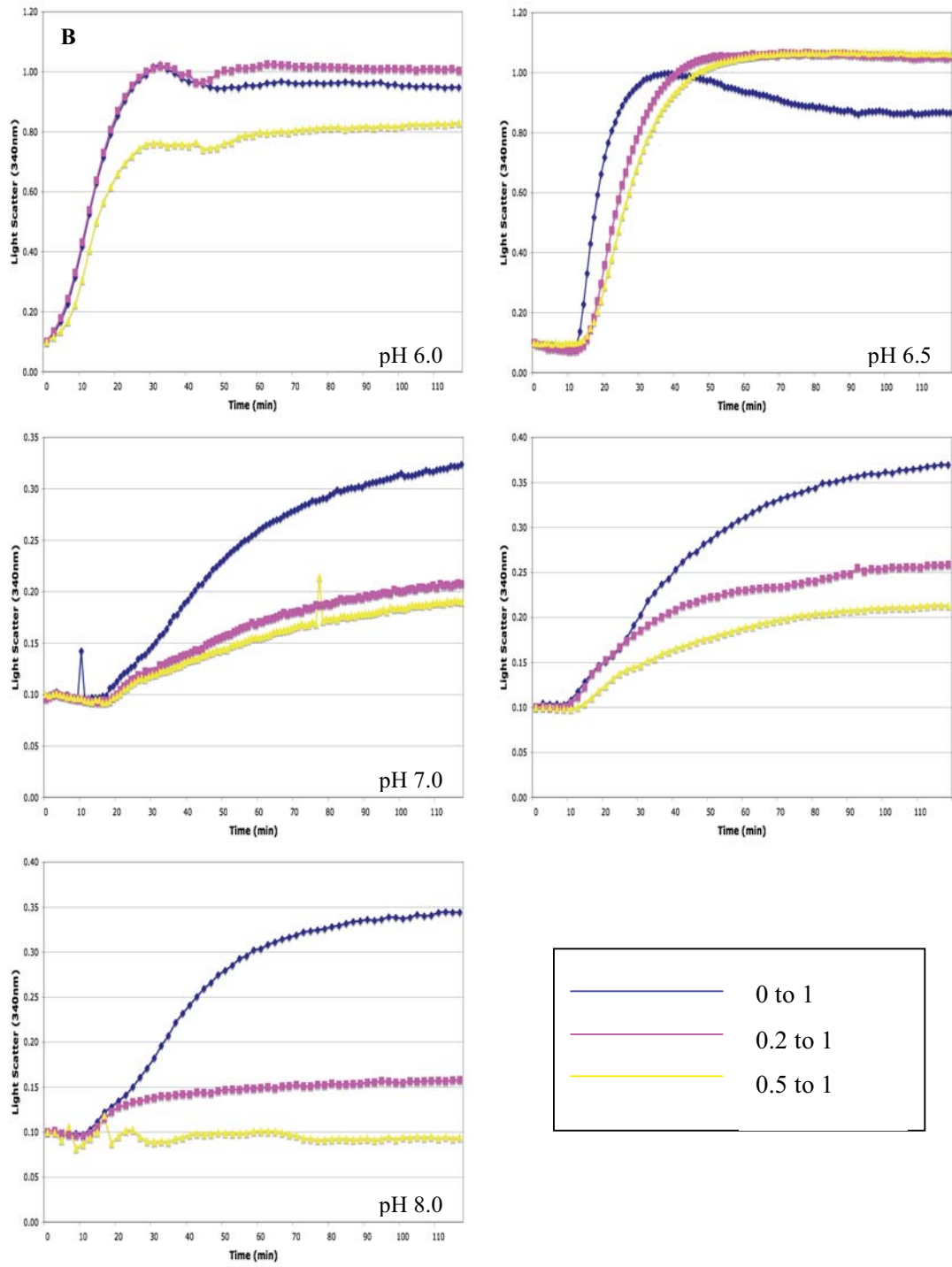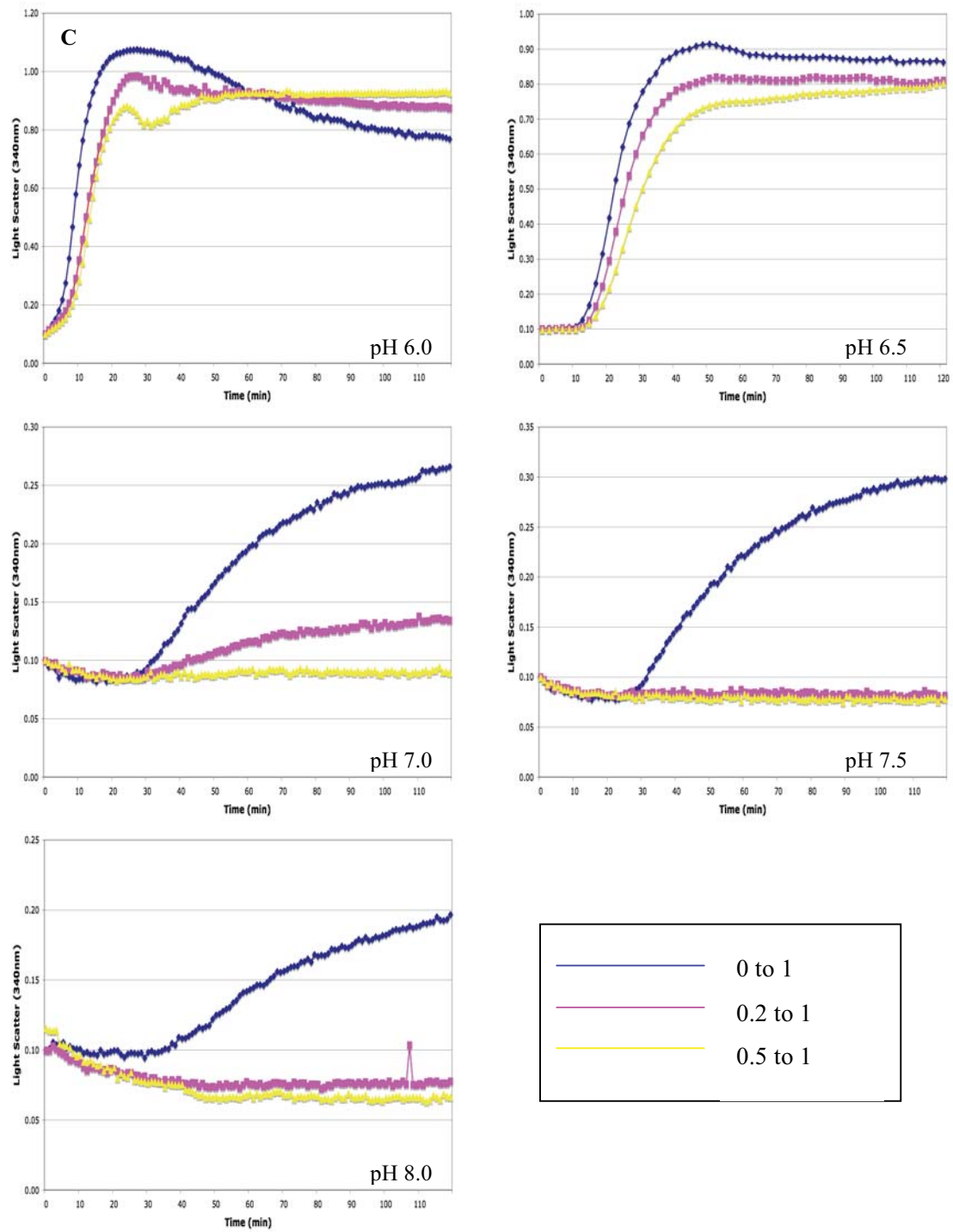

Figure C3 – Light scattering at 340nm (37°C) versus time of α-lactalbumin with
(a) α_T-crystallin, (b) αA-crystallin and (c) αB-crystallin

Appendix D

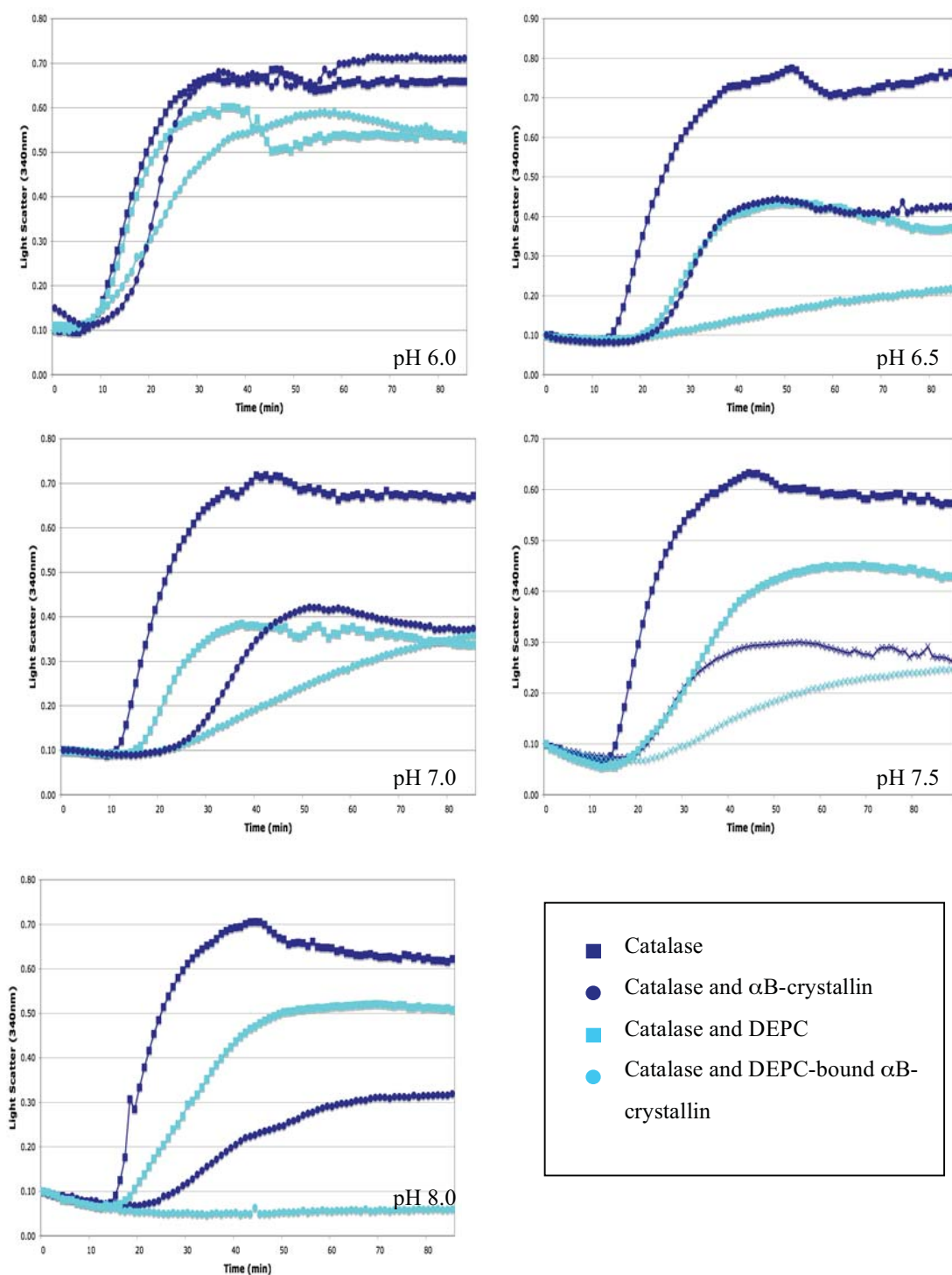## **Appendix D – Light scattering assays from Section 6.2.1**

Figure D1 – Light scattering assays of thermal-stress induced catalase aggregation in the presence of αB-crystallin, DEPC and DEPC-bound αB-crystallin.

BIBLIOGRAPHY

Chapter 10 - Bibliography

Aachmann, F.L., Otzen, D.E. Larsen, K.L. and Wimmer, R. (2003) Structural background of cyclodextrin-protein interactions. *Prot Eng.* **16:** 905-12.

Ahmad, M.F., Raman, B., Ramakrishna, T. and Rao, Ch.M. (2008) Effect of phosphorylation on αB-crystallin: differences in stability, subunit exchange and chaperone activity of homo and mixed oligomers of αB-crystallin and its phosphorylation-mimicking mutant. *J Mol Biol.* **375:** 1040-51.

Akiyoshi, K., Sasaki, Y. and Sunamoto, J. (1999) Molecular chaperone-like activity of hydrogel nanoparticles of hydrophobized pullulan: thermal stabilization with refolding of carbonic anhydrase B. *Bioconjug Chem.* **10:** 321-4.

Andley, U.P. (2007) Crystallins in the eye: Function and pathology. *Prog Retin Eye Res.* **26:** 78-98.

Anfinsen, C.B. (1973) Principles that govern the folding of protein chains. *Science.* **181:** 223-30.

Aquilina, J.A., Benesch, J.L., Ding, L.L., Yaron, O., Horwitz, J. and Robinson, C.V. (2004) Phosphorylation of αB-crystallin alters chaperone function through loss of dimeric substructure. *J Biol Chem.* **279:** 28675-80.

Aquilina, J.A., Benesch, J.L., Ding, L.L., Yaron, O., Horwitz, J. and Robinson, C.V. (2005) Subunit exchange of polydisperse proteins: mass spectrometry reveals consequences of αA-crystallin truncation. *J Biol Chem.* **280:** 14485-91.

Aquilina, J.A. and Watt, S.J. (2007) The N-terminal domain of αB-crystallin is protected from proteolysis by bound substrate. *Biochem Biophys Res Commun.* **353:** 1115-20.

Asayama, W., Sawada, S., Taguchi, H. and Akiyoshi, K. (2008) Comparison of refolding activities between nanogel artificial chaperone and GroEL systems. *Int J Biol Macromol.* **42:** 241-6.

Augusteyn, R.C. and Koretz, J.F. (1987) A possible structure for α-crystallin. *FEBS Lett.* **222:** 1-5.

Augusteyn, R.C., Ellerton, H.D., Putilina, T. and Stevens, A. (1988) Specific dissociation of αB subunits from α-crystallin. *Biochim Biophys Acta.* **957:** 192-201.

Augusteyn, R.C. (2004) α-crystallin: a review of its structure and function. *Clin Exp Optom.* **87:** 356-66.

Augusteyn, R.C. (2004) Dissociation is not required for α-crystallin's chaperone function. *Exp Eye Res.* **79:** 781-4.

Avilov, S.V., Aleksandrov, N.A. and Demchenko, A.P. (2004) Quaternary structure of α-crystallin is necessary for the binding of unfolded proteins: a surface plasmon resonance study. *Protein Pept Lett.* **11:** 41-8.

Bassnett, S. and Duncan, G. (1985) Direct measurement of pH in the rat lens by ion-sensitive microelectrodes. *Exp Eye Res*. **40:** 585-90.

Bassnett, S., Croghan, P.C. and Duncan, G. (1987) Diffusion of lactate and its role in determining intracellular pH in the lens of the eye. *Exp Eye Res.* **44:** 143-7.

Bassnett, S. and Beebe, D.C. (1992) Coincident loss of mitochondria and nuclei during lens fiber cell differentiation. *Dev Dyn.* **194:** 85-93.

Bauer, H.H., Aebi, U., Häner, M., Hermann, R., Müller, M. and Merkle, H.P. (1995) Architecture and polymorphism of fibrillar supramolecular assemblies produced by *in vitro* aggregation of human calcitonin. *J Struct Biol.* **115:** 1-15.

Beers, R.F. and Sizer, I.W. (1951) A spectrophotometric method for measuring the breakdown of hydrogen peroxide by catalase. *J Biol Chem.* **95:** 133–40.

Bennardini, F., Wrzosek, A. and Chiesi, M. (1992) αB-crystallin in cardiac tissue. Association with actin and desmin filaments. *Circulat Res.* **71:** 288–94.

Benedek, G.B., (1971). Theory of transparency of the eye. *Appl. Optics* **10:** 459–73.

Benedek, G.B., (1997). Cataract as a protein condensation disease. The Proctor Lecture. *Invest. Ophthalmol. Vis. Sci.* **38:** 1911–21.

Bera, S. and Ghosh, S.K. (1996) Histidine residues in α-crystallin are not all available for chemical modification and acid-base titration. *J Protein Chem.* **15:** 585-90.

Berke, S.J.S. and Paulson, H.L. (2003) Protein aggregation and the ubiquitin proteasome pathway: gaining the UPPer hand on neurodegeneration. *Curr Opin Genet Dev.* **13:** 253–261.

Bessems, G.J., Hoenders, H.J. and Wollensak, J. (1983) Variation in proportion and molecular weight of native crystallins from single human lenses upon aging and formation of nuclear cataract. *Exp Eye Res.* **37:** 627-37.

Bessems, G.J., De Man, B.M., Bours, J. and Hoenders, H.J. (1986) Age-related variations in the distribution of crystallins within the bovine lens. *Exp Eye Res.* **43:** 1019-30.

Bettelheim, F.A. and Ali, S. (1985) Light scattering of normal human lens. III. Relationship between forward and back scatter of whole excised lenses. *Exp Eye Res.* **41:** 1-9.

Bhat, S.P. and Nagineni, C.N. (1989) αB subunit of lens specific protein α-crystallin is present in other occular and non-occular tissues. *Biochem Biophys Res Commun.* **158:** 319–325.

Bhattacharyya, J. and Das, K.P. (1998) α-Crystallin does not require temperature activation for its chaperone-like activity. *Biochem Mol Biol Int.* **46:** 249-58.

Bhattacharyya, J., Padmanabha, Udupa, E.G., Wang, J. and Sharma, K.K. (2006) Mini-αB-crystallin: a functional element of αB-crystallin with chaperone-like activity. *Biochemistry.* **45:** 3069-76.

Blake, C.C. and Serpell, L.C. (1996) Synchrotron X-ray studies suggest that the core of the transthyretin amyloid fibril is a continuous β-sheet helix. *Structure.* **4:** 989-98.

Bloemendal, H. (1981) The lens proteins in Bloemendal, H. (ed.) *Molecular and cellular biology of the eye lens*, John Wiley and Sons, Canada

Bloemendal, H. and de Jong, W.W. (1991) Lens proteins and their genes. *Prog Nucleic Acid Res Mol Biol.* **41:** 259-81.

Bloemendal, H., de Jong, W., Jaenicke, R., Lubsen, N.H., Slingsby, C. and Tardieu, A. (2004) Ageing and vision: structure, stability and function of lens crystallins. *Prog Biophys Mol Biol*. **86:** 407-85.

Böde, C., Tölgyesi, F.G., Smeller, L., Heremans, K., Avilov, S.V. and Fidy, J. (2003) Chaperone-like activity of α-crystallin is enhanced by high-pressure treatment. *Biochem J.* **370:** 859-66.

Booth, D.R., Sunde, M., Bellotti, V., Robinson, C.V., Hutchinson, W.L., Fraser, P.E., Hawkins, P.N., Dobson, C.M., Radford, S.E., Blake, C.C. and Pepys, M.B. (1997) Instability, unfolding and aggregation of human lysozyme variants underlying amyloid fibrillogenesis. *Nature.* **385:** 787-93.

Bova, M.P., Ding, L.L., Horwitz, J. and Fung, B.K. (1997) Subunit exchange of αA-crystallin. *J Biol Chem.* **272:** 29511-7.

Bova, M.P., Yaron, O., Huang, Q., Ding, L., Haley, D.A., Stewart, P.L. and Horwitz, J. (1999) Mutation R120G in αB-crystallin, which is linked to a desmin-related myopathy, results in an irregular structure and defective chaperone-like function. *Proc Natl Acad Sci U S A.* **96:** 6137-42.

Bova, M.P., McHaourab, H.S., Han, Y. and Fung, B.K. (2000) Subunit exchange of small heat shock proteins. Analysis of oligomer formation of αA-crystallin and Hsp27 by fluorescence resonance energy transfer and site-directed truncations. *J Biol Chem.* **275:** 1035-42.

Boyle, D.L and Takemoto, L. (1996) EM immunolocalization of α-crystallins: association with the plasma membrane from normal and cataractous human lenses. *Curr Eye Res.* **15:** 577-82.

Bradbury, J. (2003) Chaperones: keeping a close eye on protein folding. *Lancet.* **361:** 1194–5.

Brady, J.P., Garland, D., Duglas-Tabor, Y., Robison, W.G. Jr., Groome, A. and Wawrousek, E.F. (1997) Targeted disruption of the mouse αA-crystallin gene induces cataract and cytoplasmic inclusion bodies containing the small heat shock protein αB-crystallin. *Proc Natl Acad Sci U S A.* **94:** 884-9.

Brady, J.P., Garland, D.L., Green, D.E., Tamm, E.R., Giblin, F.J. and Wawrousek, E.F. (2001) αB-crystallin in lens development and muscle integrity: a gene knockout approach. *Invest Ophthalmol Vis Sci.* **42:** 2924-34.

Bu, L., Yan, S., Jin, M., Jin, Y., Yu, C., Xiao, S., Xie, Q., Hu, L., Xie, Y., Solitang, Y., Liu, J., Zhao, G. and Kong, X. (2002) The γS-crystallin gene is mutated in autosomal recessive cataract in mouse. *Genomics.* **80:** 38-44.

Bucciantini, M., Giannoni, E., Chiti, F., Baroni, F., Formigli, L., Zurdo, J., Taddei, N., Ramponi, G., Dobson, C.M. and Stefani, M. (2002) Inherent toxicity of aggregates implies a common mechanism for protein misfolding diseases. *Nature.* **416:** 507-11.

Bukach, O.V., Seit-Nebi, A.S., Marston, S.B. and Gusev, N.B. (2004) Some properties of human small heat shock protein Hsp20 (HspB6). *Eur J Biochem.* **271:** 291-302.

Burgio, M.R., Kim, C.J., Dow, C.C. and Koretz, J.F. (2000) Correlation between the chaperone-like activity and aggregate size of α-crystallin with increasing temperature. *Biochem Biophys Res Commun.* **268:** 426-32.

Camilleri, P., Haskins, N.J. and Howlett, D.R. (1994) β-Cyclodextrin interacts with the Alzheimer amyloid β-A4 peptide. *FEBS Lett.* **341:** 256-8.

Carneiro, F.A., Stauffer, F., Lima, C.S., Juliano, M.A., Juliano, L. and Da Poian, A.T. (2003) Membrane fusion induced by vesicular stomatitis virus depends on histidine protonation. *J Biol Chem.* **278:** 13789-94.

Carver, J.A., Aquilina, J.A., Truscott, R.J. and Ralston, G.B. (1992) Identification by 1H NMR spectroscopy of flexible C-terminal extensions in bovine lens α-crystallin. *FEBS Lett.* **311:** 143-9.

Carver, J.A., Aquilina, J.A. and Truscott, R.J. (1994) A possible chaperone-like quaternary structure for α-crystallin. *Exp Eye Res.* **59:** 231-4.

Carver, J.A., Guerreiro, N., Nicholls, K.A. and Truscott, R.J. (1995) On the interaction of α-crystallin with unfolded proteins. *Biochim Biophys Acta*. **1252:** 251-60

Chapter 10 - Bibliography

Carver, J.A., Esposito, G., Schwedersky, G. and Gaestel, M. (1995) 1H NMR spectroscopy reveals that mouse Hsp25 has a flexible C-terminal extension of 18 amino acids. *FEBS Lett.* **369:** 305-10.

Carver, J.A., Nicholls, K.A., Aquilina, J.A. and Truscott, R.J. (1996) Age-related changes in bovine α-crystallin and high-molecular-weight protein. *Exp Eye Res.* **63:** 639-47.

Carver, J.A. and Lindner, R.A. (1998) NMR spectroscopy of α-crystallin. Insights into the structure, interactions and chaperone action of small heat-shock proteins. *Int J Biol Macromol.* **22:** 197-209.
Carver, J.A. (1999) Probing the structure and interactions of crystallin proteins by NMR spectroscopy. *Prog Retin Eye Res.* **18:** 431-62.

Carver, J.A., Lindner, R.A., Lyon, C., Canet, D., Hernandez, H., Dobson, C.M. and Redfield, C. (2002) The interaction of the molecular chaperone α-crystallin with unfolding α-lactalbumin: a structural and kinetic spectroscopic study. *J Mol Biol.* **318:** 815-27.

Carver, J.A., Rekas, A., Thorn, D.C. and Wilson, M.R. (2003) Small heat-shock proteins and clusterin: intra- and extracellular molecular chaperones with a common mechanism of action and function? *IUBMB Life.* **55:** 661-8.

Chaves, J.M., Srivastava, K., Gupta, R. and Srivastava, O.P. (2008) Structural and Functional Roles of Deamidation and/or Truncation of N- or C-Termini in Human α-crystallin. *Biochemistry.* Article in print.

Cherian, M. and Abraham, E.C. (1995) Diabetes affects α-crystallin chaperone function. *Biochem Biophys Res Commun.* **212:** 184-9.

Cherian, M. and Abraham, E.C. (1995) Decreased molecular chaperone property of α-crystallins due to posttranslational modifications. *Biochem Biophys Res Commun.* **208:** 675-9.

Chiti, F., Webster, P., Taddei, N., Clark, A., Stefani, M. and Ramponi, G. (1999) Designing conditions for *in vitro* formation of amyloid protofilaments and fibrils. *Proc. Natl. Acad. Sci. U.S.A.* **96:** 3590–3594.

Chiti, F., Bucciantini, M., Capanni, C., Taddei, N., Dobson, C.M. and Stefani, M. (2001) Solution conditions can promote formation of either amyloid protofilaments or mature fibrils from the HypF N-terminal domain. *Protein Sci.* **10:** 2541-7.

Chiti, F. and Dobson, C.M. (2006) Protein misfolding, functional amyloid, and human disease. *Annu Rev Biochem.* **75:** 333-66.

Chothia, C. (1974) Hydrophobic bonding and accessible surface area in proteins. *Nature.* **248:** 338-9.

Chothia, C. (1975) Structural invariants in ptotein folding. *Nature.* **254:** 304-8.

Clark, J.I. and Muchowski, P.J., (2000) Small heat-shock proteins and their potential role in human disease. *Curr Opin Struct Biol.* **10:** 52–59.

Cobb, B.A. and Petrash, J.M. (2000) Structural and functional changes in the αA-crystallin R116C mutant in hereditary cataracts. *Biochemistry.* **39:** 15791-8.

Cohen, F.E. and Kelly, J.W. (2003) Therapeutic approaches to protein misfolding diseases. *Nature.* **426:** 905–909.

Come, J.H., Fraser, P.E. and Lansbury, P.T. Jr. (1993) A kinetic model for amyloid formation in the prion diseases: importance of seeding. *Proc Natl Acad Sci U S A.* **90:** 5959-63.

Danielsson, J., Jarvet, J., Damberg, P. and Gräslund, A. (2004) Two-site binding of β-cyclodextrin to the Alzheimer Aβ(1-40) peptide measured with combined PFG-NMR diffusion and induced chemical shifts. *Biochemistry.* **43:** 6261-9.

Das, K.P. and Surewicz, W.K. (1995) Temperature-induced exposure of hydrophobic surfaces and its effect on the chaperone activity of α-crystallin. *FEBS Lett.* **369:** 321-5.

Das, K.P., Petrash, J.M. and Surewicz, W.K. (1996) Conformational properties of substrate proteins bound to a molecular chaperone α-crystallin. *J Biol Chem*. **271:** 10449-52.

Datta, S.A. and Rao, C.M. (1999) Differential temperature-dependent chaperone-like activity of αA- and αB-crystallin homoaggregates. *J Biol Chem.* **274:** 34773-8.

Daugherty, D.L., Rozema, D., Hanson, P.E. and Gellman, S.H. (1998) Artificial chaperone-assisted refolding of citrate synthase. *J Biol Chem.* **273:** 33961-71.

Derham, B.K. and Harding, J.J., (1999) α-Crystallin as a molecular chaperone. *Prog Retin Eye Res*. **18:** 463–509.

Desai, A., Lee, C., Sharma, L. and Sharma, A. (2006) Lysozyme refolding with cyclodextrins: structure-activity relationship. *Biochimie.* **88:** 1435-45.

Dietz, K.J., Canut, H. and Marigo, G. (1992) Identification of an essential histidine residue at the active site of the tonoplast malate carrier in Catharanthus roseus cells. *J Membr Biol.* **129:** 137-43.

Dobson, C.M. (1999) Protein misfolding, evolution and disease. *Trends Biochem. Sci.* **24:** 329–332.

Dobson, C.M. (2001) Protein folding and its links with human disease. *Biochem Soc Symp.* **68:** 1-26.

Dobson, C.M. (2006) Protein aggregation and its consequences for human disease. *Protein Pept Lett.* **13:** 219-27.

Chapter 10 - Bibliography

Dubin, R.A., Wawrousek, E.F. and Piatigorsky, J. (1989) Expression of the murine αB-crystallin is not restricted to the lens. *Mol. Cell Biol.* **9:** 1083–91.

Dunker, A.K., Brown, C.J., Lawson, J.D., Iakoucheva, L.M. and Obradović, Z. (2002) Intrinsic disorder and protein function. *Biochemistry.* **41:** 6573-82.

Easton, C.J. and Lincoln, S.F. (1999) *Modified cyclodextrins.* Imperial College Press, U.K.

Eckert, R. (2002) pH gating of lens fibre connexins. *Pflugers Arch.* **443:** 843-51.

Ecroyd, H., Meehan, S., Horwitz, J., Aquilina, J.A., Benesch, J.L., Robinson, C.V., Macphee, C.E. and Carver, J.A. (2007) Mimicking phosphorylation of αB-crystallin affects its chaperone activity. *Biochem J.* **401:** 129-41.

Ecroyd, H., Koudelka, T., Thorn, D.C., Williams, D.M., Devlin, G., Hoffmann, P. and Carver, J.A. (2008) Dissociation from the oligomeric state is the rate-limiting step in fibril formation by κ-casein. *J Biol Chem.* **283:** 9012-22.

Ecroyd, H. and Carver, J.A. (2008) The effect of small molecules in modulating the chaperone activity of αB-crystallin against ordered and disordered protein aggregation. *FEBS J.* **275:** 935-47.

Ehrnsperger, M., Graber, S., Gaestel, M. and Buchner, J. (1997) Binding of non-native protein to Hsp 25 during heat shock creates a reservoir of folding intermediates for reactivation. *EMBO J.* **16:** 221–229.

Ellis, R.J. and Hartl, F.U. (1996) Protein folding in the cell: competing models of chaperonin function. *FASEB J.* **10:** 20-6.

Estey, T., Kang, J., Schwendeman, S.P. and Carpenter, J.F. (2006) BSA degradation under acidic conditions; a model for protein instability during release from PLGA delivery systems. *J Pharm Sci.* **95:** 1626-39

Chapter 10 - Bibliography

Fändrich, M. and Dobson, C.M. (2002) The behaviour of polyamino acids reveals an inverse side chain effect in amyloid structure formation. *EMBO J.* **21:** 5682-90.

Farnsworth, P.N., Groth-Vasselli, B., Greenfield, N.J. and Singh, K. (1997) Effects of temperature and concentration on bovine lens α-crystallin secondary structure: a circular dichroism spectroscopic study. *Int J Biol Macromol.* **20:** 283-91.

Forno, L.S. (1996) Neuropathology of Parkinson's disease. *J Neuropathol Exp Neurol.* **55:** 259-72.

Freifelder, D. (1982) *Physical biochemistry.* W.H. Freeman and Co. U.S.A.

Fu, X., Zhang, X. and Chang, Z. (2005) 4,4'-Dianilino-1,1'-binaphthyl-5,5'-sulfonate, a novel molecule having chaperone-like activity. *Biochem Biophys Res Commun.* **329:** 1087-93.

Gazit, E. (2002). A possible role for π-stacking in the self-assembly of amyloid fibrils. *FASEB J.* **16:** 77–83.

Gesierich, U. and Pfeil, W. (1996) The conformational stability of α-crystallin is rather low: calorimetric results. *FEBS Lett.* **393:** 151-4.

Ghosh, J.G., Estrada, M.R. and Clark, J.I. (2005) Interactive domains for chaperone activity in the small heat shock protein, human αB crystallin. *Biochemistry.* **44:** 14854-69.

Ghosh, J.G. and Clark, J.I. (2005) Insights into the domains required for dimerization and assembly of human αB crystallin. *Protein Sci.* **14:** 684-95.

Ghosh, J.G., Houck, S.A. and Clark, J.I. (2008) Interactive sequences in the molecular chaperone, human αB crystallin modulate the fibrillation of amyloidogenic proteins. *Int J Biochem Cell Biol.* **40:** 954-67.

Giasson, B.I., Duda, J.E., Quinn, S.M., Zhang, B., Trojanowski, J.Q. and Lee, V.M. (2002) Neuronal α-synucleinopathy with severe movement disorder in mice expressing A53T human α-synuclein. *Neuron.* **34:** 521-33.

Gibbons, D.L. and Horowitz, P.M. (1995) Exposure of hydrophobic surfaces on the chaperonin GroEL oligomer by protonation or modification of His-401. *J Biol Chem.* **270:** 7335-40.

Goers, J., Permyakov, S.E., Permyakov, E.A., Uversky, V.N. and Fink, A.L. (2002) Conformational prerequisites for α-lactalbumin fibrillation. *Biochemistry.* **41:** 12546-51.

Goldsbury, C.S., Cooper, G.J., Goldie, K.N., Müller, S.A., Saafi, E.L., Gruijters, W.T., Misur, M.P., Engel, A., Aebi, U. and Kistler, J. (1997) Polymorphic fibrillar assembly of human amylin. *J Struct Biol.* **119:** 17-27.

Goldsbury, C.S., Wirtz, S., Müller, S.A., Sunderji, S., Wicki, P., Aebi, U. and Frey, P. (2000) Studies on the *in vitro* assembly of Aβ1-40: implications for the search for a β fibril formation inhibitors. *J Struct Bio.* **130:** 217-31.

Griffith, J.S. (1967) Self-replication and scrapie. *Nature.* **215:**1043-4.

Gupta, R. and Srivastava, O.P. (2004) Deamidation affects structural and functional properties of human αA-crystallin and its oligomerization with αB-crystallin. *J Biol Chem.* **279:** 44258-69.

Gupta, R. and Srivastava, O.P. (2004) Effect of deamidation of asparagine 146 on functional and structural properties of human lens αB-crystallin. *Invest Ophthalmol Vis Sci.* **45:** 206-14.

Hains, P.G. and Truscott, R.J. (2007) Post-translational modifications in the nuclear region of young, aged, and cataract human lenses. *J Proteome Res.* **6:** 3935-43.

Haley, D.A., Horwitz, J. and Stewart, P.L. (1998) The small heat-shock protein, αB-crystallin, has a variable quaternary structure. *J Mol Biol.* **277:** 27-35.

Hammond, C. and Helenius, A. (1995) Quality control in the secretory pathway. *Curr Opin Cell Biol.* **7:** 523–9.

Han, J.C. and Han, G.Y. (1994) A procedure for quantitative determination of tris(2-carboxyethyl)phosphine, an odorless reducing agent more stable and effective than dithiothreitol. *Anal Biochem.* **220:** 5-10.

Hanson, S.R., Hasan, A., Smith, D.L. and Smith, J.B. (2000) The major *in vivo* modifications of the human water-insoluble lens crystallins are disulfide bonds, deamidation, methionine oxidation and backbone cleavage. *Exp Eye Res.* **71:** 195-207.

Harper, J.D. and Lansbury, P.T. Jr. (1997) Models of amyloid seeding in Alzheimer's disease and scrapie: mechanistic truths and physiological consequences of the time-dependent solubility of amyloid proteins. *Annu Rev Biochem.* **66:** 385-407.

Hartl, F.U. and Hayer-Hartl, M. (2002) Molecular chaperones in the cytosol: from nascent chain to folded protein. *Science.* **295:** 1852-8.

Haslbeck, M., Franzmann, T., Weinfurtner, D. and Buchner, J. (2005) Some like it hot: the structure and function of small heat-shock proteins. *Nat Struct Mol Biol.* **12:** 842-6.

Hatters, D.M., Lindner, R.A., Carver, J.A and Howlett, G.J. (2001) The molecular chaperone, α-crystallin, inhibits amyloid formation by apolipoprotein C-II. *J Biol Chem.* **276:** 33755-61.

Hendriks, W., Weetink, H., Voorter, C.E.M., Sanders, J., Bloemendal, H. and de Jong, W.W. (1990) Structural equivalence of subunits in the rat α-crystallin aggregate. *Biochem Biophys Acta.* **1037:** 58-65.

Hoenders, H.J. and Bloemendal, H. (1983) Lens proteins and aging. *J Gerontol.* **38**: 278-86.

Horwitz, J. (1992) α-Crystallin can function as a molecular chaperone. *Proc Natl Acad Sci U S A*. **89:** 10449-53.

Horwitz, J. (2000) The function of α-crystallin in vision. *Semin Cell Dev Biol.* **11:** 53–60

Horwitz, J. (2003) α-Crystallin. *Exp Eye Res.* 2003 **76:** 145-53.

Huo, X. and Viola, R.E. (1996) Substrate specificity and identification of functional groups of homoserine kinase from Escherichia coli. *Biochemistry.* **35:** 16180-5.

Ignatova, Z. and Gierasch, L.M. (2005) Aggregation of a slow-folding mutant of a β-clam protein proceeds through a monomeric nucleus. *Biochemistry.* **44:** 7266-74.

Ikeda, K., Okada, T., Sawada, S., Akiyoshi, K. and Matsuzaki, K. (2006) Inhibition of the formation of amyloid β-protein fibrils using biocompatible nanogels as artificial chaperones. *FEBS Lett.* **580:** 6587-95.

Ito, H., Okamoto, K., Nakayama, H., Isobe, T. and Kato, K. (1997) Phosphorylation of αB-crystallin in response to various types of stress. *J Biol Chem.* **272:** 29934-41.

Ito, H., Kamei, K., Iwamoto, I., Inaguma, Y. and Kato, K. (2001) Regulation of the levels of small heat-shock proteins during differentiation of C2C12 cells. *Expt Cell Res.* **266:** 213–21.

Iwaki, T., Kume-Iwaki, A. and Goldman, J.E. (1990) Cellular distribution of αB-crystallin in non-lenticular tissues. *J Histochem Cytochem.* **38:** 31-9.

Jackson, M.R., Cohen-Doyle, M.F., Peterson, P.A. and Williams, D.B. (1994) Regulation of MHC class I transport by the molecular chaperone, calnexin (~88, lP90). *Science.* **263:** 384-87.

Jakob, M., Gaestel, U., Engel, K. and Buchner, J. (1993) Small heat-shock proteins are molecular chaperones. *J. Biol. Chem.* **268:** 1517–20.

Jarrett, J.T. and Lansbury, P.T. Jr. (1992) Amyloid fibril formation requires a chemically discriminating nucleation event: studies of an amyloidogenic sequence from the bacterial protein OsmB. *Biochemistry.* **31:** 12345-52.

Jarrett, J.T., Berger, E.P. and Lansbury, P.T. Jr. (1993) The carboxy terminus of the β amyloid protein is critical for the seeding of amyloid formation: implications for the pathogenesis of Alzheimer's disease. *Biochemistry.* **32:** 4693-7.

Jedziniak, J. A., Kinoshita, J. H., Yates, E. M., Hocker, L. O. and Benedek, G. B., (1973) On the presence and mechanism of formation of heavy molecular weight aggregates in human normal and cataractous lenses. *Exp. Eye Res.* **15:** 185–92.

Jedziniak, J.A., Kinoshita, J.H., Yates, E.M. and Benedek, G.B. (1975) The concentration and localization of heavy molecular weight aggregates in aging normal and cataractous human lenses. *Exp Eye Res.* **20:** 367-9.

Jiménez, J.L., Nettleton, E.J., Bouchard, M, Robinson, C.V., Dobson, C.M. and Saibil, H.R. (2002) The protofilament structure of insulin amyloid fibrils. *Proc Natl Acad Sci U S A*. **99:** 9196-201.

Jobby, M.K. and Sharma, Y. (2007) Calcium-binding to lens βB2- and βA3-crystallins suggests that all β-crystallins are calcium-binding proteins. *FEBS J.* **274:** 4135-47.

Jocelyn, P.C. (1987) Chemical reduction of disulfides. *Methods Enzymol.* **143:** 246-56.

Kamradt, M.C., Lu, M., Werner, M.E., Kwan, T., Chen, F., Strohecker, A., Oshita, S., Wilkinson, J.C., Yu, C., Oliver, P.G., Duckett, C.S., Buchsbaum, D.J., LoBuglio, A.F., Jordan, V.C. and Cryns, V.L. (2005) The small heat shock protein αB-crystallin is a novel inhibitor of TRAIL-induced apoptosis that suppresses the activation of caspase-3. *J Biol Chem.* **280:** 11059–66.

Kappe, G., Franck, E., Verschuure, P., Boelens, W.C., Leunissen, J.A.M. and de Jong, W.W. (2003) The human genome encodes 10 α-crystallin-related small heat shock proteins: HspB1-10. *Cell Stress Chap.* **8:** 53-61.

Karuppiah, N. and Sharma, A. (1995) Cyclodextrins as protein folding aids. *Biochem Biophys Res Commun.* **211:** 60-6.

Kato, K., Ito, H., Kamei, K., Inaguma, Y., Iwamoto, I. and Saga, S. (1998) Phosphorylation of αB-crystallin in mitotic cells and identification of enzymatic activities responsible for phosphorylation. *J Biol Chem.* **273:** 28346-54.

Kawai, C., Prado, F.M., Nunes, G.L., Di Mascio, P., Carmona-Ribeiro, A.M. and Nantes, I.L. (2005) pH-Dependent interaction of cytochrome c with mitochondrial mimetic membranes: the role of an array of positively charged amino acids. *J Biol Chem.* **280:** 34709-17.

Kelly, J.W. (1996) Alternative conformations of amyloidogenic proteins govern their behavior. *Curr Opin Struct Biol.* 6: 11–17.

Kelly, S.M., Jess, T.J. and Price, N.C. (2005) How to study proteins by circular dichroism. *Biochim Biophys Acta.* **1751:** 119-39.

Khandogin, J. and Brooks, C.L. 3rd. (2007) Linking folding with aggregation in Alzheimer's β-amyloid peptides. *Proc Natl Acad Sci U S A.* **104:** 16880-5.

Khurana, R., Coleman, C., Ionescu-Zanetti, C., Carter, S.A., Krishna, V., Grover, R.K., Roy, R. and Singh, S (2005). Mechanism of thioflavin T binding to amyloid fibrils. *J Struct Biol.* **151:** 229-38.

Kim, P.S. and Baldwin, R.L. (1982) Specific intermediates in the folding reactions of small proteins and the mechanism of protein folding. *Annu Rev Biochem.* **51:** 459-89.

Kim, K.K., Kim, R. and Kim, S.H. (1998) Crystal structure of a small heat-shock protein. *Nature.* **394:** 595-9.

Kim, Y. S., Randolph, T. W., Stevens, F .J. and Carpenter, J. F. (2002) Kinetics and energetics of assembly, nucleation and growth of aggregates and fibrils for an amyloidogenic protein. Insights into transition states from pressure, temperature and co-solute studies. *J Biol Chem.* **277:** 27240–27246.

Kim, H.J., Chatani, E., Goto, Y. and Paik, S.R. (2007) Seed-dependent accelerated fibrillation of α-synuclein induced by periodic ultrasonication treatment. *J Microbiol Biotechnol.* **17:** 2027-32.

Klemenz, R., Fröhli, E., Steiger, R.H., Schäfer, R. and Aoyama,A. (1991) αB-crystallin is a small heat shock protein. *Proc Natl Acad Sci U S A*. **88:** 3652-6.

Klimov, D.K. and Thirumalai, D. (2003) Dissecting the assembly of Aβ16-22 amyloid peptides into antiparallel β sheets. *Structure.* **11:** 295-307.

Koteiche, H.A. and McHaourab, H.S. (2003) Mechanism of chaperone function in small heat-shock proteins. Phosphorylation-induced activation of two-mode binding in αB-crystallin. *J Biol Chem.* **278:** 10361-7.

Koretz, J.F., Doss, E.W. and LaButti, J.N. (1998) Environmental factors influencing the chaperone-like activity of α-crystallin. *Int J Biol Macromol.* **22:** 283-94.

Kotzbauer, P.T., Giasson, B.I., Kravitz, A.V., Golbe, L.I., Mark, M.H., Trojanowski, J.Q. and Lee, V.M. (2004) Fibrillization of α-synuclein and tau in familial Parkinson's disease caused by the A53T α-synuclein mutation. *Exp Neurol.* **187:** 279-88.

Krüger, R., Kuhn, W., Müller, T., Woitalla, D., Graeber, M., Kösel, S., Przuntek, H., Epplen, J.T., Schöls, L. and Riess, O. (1998) Ala30Pro mutation in the gene encoding α-synuclein in Parkinson's disease. *Nat Genet.* **18:** 106-8.

Kumar, L.V., Ramakrishna, T. and Rao, C.M. (1999) Structural and functional consequences of the mutation of a conserved arginine residue in αA and αB crystallins. *J Biol Chem.* **274:** 24137-41.

Kumar, M.S., Kapoor, M., Sinha, S. and Reddy, G.B. (2005) Insights into hydrophobicity and the chaperone-like function of αA- and αB-crystallins: an isothermal titration calorimetric study. *J Biol Chem.* **280:** 21726-30.

Kumita, J.R., Poon, S., Caddy, G.L, Hagan, C.L., Dumoulin, M., Yerbury, J.J., Stewart, E.M., Robinson, C.V., Wilson, M.R. and Dobson, C.M. (2007) The extracellular chaperone clusterin potently inhibits human lysozyme amyloid formation by interacting with prefibrillar species. *J Mol Biol.* **369:** 157-67.

Kundu, M., Sen, P.C. and Das, K.P. (2007) Structure, stability, and chaperone function of αA-crystallin: role of N-terminal region. *Biopolymers.* **86:** 177-92.

Lai, Z., Colón, W. and Kelly, J.W. (1996) The acid-mediated denaturation pathway of transthyretin yields a conformational intermediate that can self-assemble into amyloid. *Biochemistry*. **35:** 6470-82.

Lavoie, J. N., Hickey, E., Weber, L. A. and Landry, J. (1993) Modulation of actin microfilament dynamics and fluid phase pinocytosis by phosphorylation of heat shock protein 27. *J Biol Chem.* **268:** 24210–14.

Lee, C.Y., Bagdasarian, M., Meng, M.H. and Zeikus, J.G. (1990) Catalytic mechanism of xylose (glucose) isomerase from Clostridium thermosulfurogenes. Characterization of the structural gene and function of active site histidine. *J Biol Chem.* **265:** 19082-90.

Lee, G. J., Pokala, N. and Vierling, E. (1995) Structure and *in vitro* molecular chaperone activity of cytosolic small heat shock proteins from pea. *J Biol Chem.* **270:** 10432–38.

Lee, G.J., Roseman, A.M., Saibil, H.R. and Vierling, E. (1997) A small heat shock protein stably binds heat-denatured model substrates and can maintain a substrate in a folding-competent state. *EMBO J.* **16:** 659-71.

Lee, J.S., Satoh, T., Shinoda, H., Samejima, T., Wu, S.H. and Chiou, S.H. (1997) Effect of heat-induced structural perturbation of secondary and tertiary structures on the chaperone activity of α-crystallin. *Biochem Biophys Res Commun.* **237:** 277-82.

Lee, G. J. and Vierling, E. (2000) A small heat shock protein cooperates with heat shock protein 70 systems to reactivate a heat-denatured protein. *Plant Physiol.* **122:** 189–98.

Lee, S., Carson, K., Rice-Ficht, A. and Good, T. (2006) Small heat shock proteins differentially affect Aβ aggregation and toxicity. *Biochem Biophys Res Commun.* **347:** 527-33.

Leroux, M.R., Melki, R., Gordon, B., Batelier, G. and Candido, E.P. (1997) Structure-function studies on small heat shock protein oligomeric assembly and interaction with unfolded polypeptides. *J Biol Chem.* **272:** 24646-56.

LeVine, H. 3rd (1999) Quantification of β-sheet amyloid fibril structures with thioflavin T. *Methods Enzymol.* **309:** 274-84.

Li, H., Li, C., Lu, Q., Su, T., Ke, T., Li, D.W., Yuan, M., Liu, J., Ren, X., Zhang, Z., Zeng, S., Wang, Q.K. and Liu, M. (2008) Cataract mutation P20S of αB-crystallin impairs chaperone activity of αA-crystallin and induces apoptosis of human lens epithelial cells. *Biochim Biophys Acta.* **1782:** 303-9.

Liang, J. and Rossi, M. (1989). Near-ultraviolet circular dichroism of bovine high molecular weight α-crystallin. *Invest Ophthal Vis Sci.* **30:** 2065-8.

Lin, J., Cassidy, C.S. and Frey, P.A. (1998) Correlations of the basicity of His 57 with transition state analogue binding, substrate reactivity, and the strength of the low-barrier hydrogen bond in chymotrypsin. *Biochemistry.* **37:** 11940-8.

Lin, S.Y., Li, M.J. and Ho, C.J. (1999) pH-dependent secondary conformation of bovine lens α-crystallin: ATR infrared spectroscopic study with second-derivative analysis. *Graefes Arch Clin Exp Ophthalmol.* **237:** 157-60.

Lindner, R.A., Kapur, A. and Carver, J.A. (1997) The interaction of the molecular chaperone, α-crystallin, with molten globule states of bovine α-lactalbumin. *J Biol Chem.* **272:** 27722-9.

Lindner, R.A., Treweek, T.M. and Carver, J.A. (2001) The molecular chaperone α-crystallin is in kinetic competition with aggregation to stabilize a monomeric molten-globule form of α-lactalbumin. *Biochem J.* **354:** 79-87.

Lindquist, S. (1986) The heat-shock response. *Annu Rev Biochem.* **55:** 1151-91.

Liu, Y., Choudhury, P., Cabral, C.M. and Sifers, R.N. (1999) Oligosaccharide modification in the early secretory pathway directs the selection of a misfolded glycoprotein for degradation by the proteasome. *J Biol Chem.* **274:** 5861-7.

Liu, L., Ghosh, J.G., Clark, J.I. and Jiang, S. (2006) Studies of αB-crystallin subunit dynamics by surface plasmon resonance. *Anal Biochem.* **350:** 186-95.

Chapter 10 - Bibliography

Liu, Y., Zhang, X., Luo, L., Wu, M., Zeng, R., Cheng, G., Hu, B., Liu, B., Liang, J.J. and Shang, F. (2006) A novel αB-crystallin mutation associated with autosomal dominant congenital lamellar cataract. *Invest Ophthalmol Vis Sci.* **47:** 1069-75.

Lodi, P.J. and Knowles, J.R. (1991) Neutral imidazole is the electrophile in the reaction catalyzed by triosephosphate isomerase: structural origins and catalytic implications. *Biochemistry.* **30:** 6948-56.

Lodi, P.J. and Knowles, J.R. (1993) Direct evidence for the exploitation of an α-helix in the catalytic mechanism of triosephosphate isomerase. *Biochemistry.* **32:** 4338-43.

Lomakin, A., Chung, D.S., Benedek, G.B., Kirschner, D.A. and Teplow, D.B. (1996) On the nucleation and growth of amyloid β-protein fibrils: detection of nuclei and quantitation of rate constants. *Proc Natl Acad Sci U S A.* **93:** 1125-9.

Lowe, J., Landon, M., Pike, I., Spendlove, I., McDermott, H. and Mayer, R.J. (1990) Dementia with β-amyloid deposition: involvement of αB-crystallin supports two main diseases. *Lancet* **336:** 515–516.

Lowe, J., McDermott, H., Pike, I., Spendlove, I., Landon, M. and Mayer, R.J. (1992) αB crystallin expression in non-lenticular tissues and selective presence in ubiquitinated inclusion bodies in human disease. *J Pathol.* **166:** 61-8.

Ma K., Clancy E. and Zhang Y. (1999) Residue specific pKa measurements of the β-peptide and mechanism of pH induced amyloid formation. *J American Chem. Soc.* **121:** 8698 – 706.

Magnuson, J.A., and Magnuson, N.S. (1971) A new NMR technique to study disulfide reduction: comparison of lysozyme and α-lactalbumin. *Biochem Biophys Res Commun.* **45:** 1513-7.

Maiti M, Kono M, Chakrabarti B. (1988) Heat-induced changes in the conformation of α- and β-crystallins: unique thermal stability of α-crystallin. *FEBS Lett.* **236:** 109-14.

Makin, O.S., Atkins, E., Sikorski, P., Johansson, J. and Serpell, L.C. (2005) Molecular basis for amyloid fibril formation and stability. *Proc Natl Acad Sci U S A.* **102:** 315-20.

Marcon, G., Plakoutsi, G., Canale, C., Relini, A., Taddei, N., Dobson, C.M., Ramponi, G. and Chiti, F. (2005) Amyloid formation from HypF-N under conditions in which the protein is initially in its native state. *J Mol Biol.* **347:** 323-35.

Mathias, R.T., Riquelme, G. and Rae, J.L. (1991) Cell to cell communication and pH in the frog lens. *J Gen Physiol.* **98:** 1085-103.

McFall-Ngai, M.J., Ding, L.L., Takemoto, L.J. and Horwitz, J. (1985) Spatial and temporal mapping of the age-related changes in human lens crystallins. *Exp Eye Res.* **41:** 745–58.

Meehan, S., Berry, Y., Luisi, B., Dobson, C.M., Carver, J.A. and MacPhee, C.E. (2004) Amyloid fibril formation by lens crystallin proteins and its implications for cataract formation *J. Biol. Chem.* **279:** 3413-3419.

Melkani, G.C., Zardeneta, G. and Mendoza, J.A. (2004) Oxidized GroEL can function as a chaperonin. *Front Biosci.* **9:** 724-31.

Miles, E.W (1977) Modification of histidyl residues in proteins by diethylpyrocarbonate. *Meth Enzymol.* **47:** 431–42.

Mizutani, T., Inose, T., Nakajima, S., Kakimi, S., Uchigata, M. and Ikeda, K. (1998) Familial parkinsonism and dementia with ballooned neurons, argyrophilic neuronal inclusions, atypical neurofibrillary tangles, tau-negative astrocytic fibrillary tangles, and Lewy bodies. *Acta Neuropathol (Berl).* **95:** 15–27.

Mornon, J.P., Halaby, D., Malfois, M., Durand, P., Callebaut, I. and Tardieu, A. (1998) α-Crystallin C-terminal domain: on the track of an Ig fold. *Int J Biol Macromol.* **22:** 219-27.

Mounier, N. and Arrigo, A.P. (2002) Actin cytoskeletin and small heat shock proteins: how do they interact? *Cell Stress Chap.* **7:** 167-76.

Muchowski, P.J. and Clark, J.I. (1998) ATP-enhanced molecular chaperone functions of the small heat shock protein human αB crystallin. *Proc Natl Acad Sci U S A*. **95:** 1004-9.

Murphy, R.M. and Kendrick, B.S. (2007) Protein misfolding and aggregation. *Biotechnol Prog.* **23:** 548-52.

Nelson, R., Sawaya, M.R., Balbirnie, M., Madsen, A.Ø., Riekel, C., Grothe, R. and Eisenberg, D. (2005) Structure of the cross-beta spine of amyloid-like fibrils. *Nature.* **435:** 773-8.

Nicholl, I.D. and Quinlan, R.A. (1994). Chaperone activity of α-crystallins modulates intermediate filament assembly. *EMBO J.* **13:** 945-53.

Nomura, Y., Ikeda, M., Yamaguchi, N., Aoyama, Y. and Akiyoshi, K. (2003) Protein refolding assisted by self-assembled nanogels as novel artificial molecular chaperone. *FEBS Lett.* **553:** 271-6.

Oh, I., Lee, M., Lee, Y., Shin, S. and Park, I. (1998) Spectroscopic characterization of ibuprofen/2-hydroxypropyl-β-cyclodextrin inclusion complex. *Int J Pharm.* **175:** 215-23.

Ono, K., Yoshiike, Y., Takashima, A., Hasegawa, K., Naiki, H. and Yamada, M. (2003) Potent anti-amyloidogenic and fibril-destabilizing effects of polyphenols in vitro: implications for the prevention and therapeutics of Alzheimer's disease. *J Neurochem.* **87:** 172-81.

Ono, K., Hasegawa K., Naiki H. and Yamada, M. (2004) Curcumin has potent anti-amyloidogenic effects for Alzheimer's β-amyloid fibrils in vitro. *J Neurosci Res*. **75:** 742– 750.

Otzen, D.E., Knudsen, B.R., Aachmann, F., Larsen, K.L. and Wimmer, R. (2002) Structural basis for cyclodextrins' suppression of human growth hormone aggregation. *Protein Sci.* **11:** 1779-87.

Ovádi, J. and Keleti, T. (1969) Effect of diethylpyrocarbonate on the conformation and enzymic activity of d-glyceraldehyde-3-phosphate dehydrogenase. *Acta Biochim Biophys Acad Sci Hung.* **4:** 365-78.

Pal, J. and Ghosh, S.K. (1998) Influence of chemical modification of cysteine and histidine side chains upon subunit reassembly of α-crystallin. *J Protein Chem.* **17:** 617-32.

Pawar, A.P., Dubay, K.F., Zurdo, J., Chiti, F., Vendruscolo, M. and Dobson, C.M. (2005) Prediction of "aggregation-prone" and "aggregation-susceptible" regions in proteins associated with neurodegenerative diseases. *J Mol Biol.* **350:** 379-92.

Pedersen, J.S., Dikov, D., Flink, J.L., Hjuler, H.A., Christiansen, G. and Otzen, D.E. (2006) The changing face of glucagon fibrillation: structural polymorphism and conformational imprinting. *J Mol Biol.* **355:** 501-23.

Pepys, M.B., Hawkins, P.N., Booth, D.R., Vigushin, D.M., Tennent, G.A, Soutar, A.K., Totty, N., Nguyen, O., Blake, C.C. and Terry, C.J. (1993) Human lysozyme gene mutations cause hereditary systemic amyloidosis. *Nature.* **362:** 553-7.

Pereira, P.C., Ramalho, J.S., Faro, C.J. and Mota, M.C. (1994) Age-related changes in normal and cataractous human lens crystallins, separated by fast-performance liquid chromatography. *Ophthalmic Res.* **26:** 149-57.

Perng, M.D., Cairns, L., van den IJssel, P., Prescott, A., Hutcheson, A.M. and Quinlan, R.A. (1999) Intermediate filament interactions can be altered by HSP27 and αB-crystallin. *J Cell Sci* **112:** 2099–112.

Perry, R.E., Swamy, M.S. and Abraham, E.C. (1987) Progressive changes in lens crystallin glycation and high-molecular-weight aggregate formation leading to cataract development in streptozotocin-diabetic rats. *Exp Eye Res.* **44:** 269-82.

Pind, S., Riordan, J.R. and Williams, D.B. (1994) Participation of the endoplasmic reticulum chaperone calnexin (p88, IP90) in the biogenesis of the cystic fibrosis transmembrane conductance regulator. *J Biol Chem.* **269:** 12784–88.

Plakoutsi, G., Taddei, N., Stefani, M. and Chiti, F. (2004) Aggregation of the acylphosphatase from *Sulfolobus solfataricus*: the folded and partially unfolded states can both be precursors for amyloid formation. *J Biol Chem.* **279:** 14111-9.

Plater, M.L., Goode, D. and Crabbe, M.J. (1996) Effects of site-directed mutations on the chaperone-like activity of αB-crystallin. *J. Biol. Chem.* **271:** 28558–566.

Plesofsky-Vig, N., Vig, J. and Brambl, R. (1992) Phylogeny of the α-crystallin-related heat-shock proteins. *J Mol Evol.* **35:** 537-45.

Polymeropoulos, M.H., Lavedan, C., Leroy, E., Ide, S.E., Dehejia, A., Dutra, A., Pike, B., Root, H., Rubenstein, J., Boyer, R., Stenroos, E.S., Chandrasekharappa, S., Athanassiadou, A., Papapetropoulos, T., Johnson, W.G., Lazzarini, A.M., Duvoisin, R.C., Di Iorio, G., Golbe, L.I. and Nussbaum RL. (1997) Mutation in the α-synuclein gene identified in families with Parkinson's disease. *Science.* **276:** 2045-7.

Ponce, A., Sorensen, C. and Takemoto, L. (2006) Role of short-range protein interactions in lens opacifications. *Mol Vis.* **12:** 879-84.

Poon, S., Rybchyn, M.S., Easterbrook-Smith, S.B., Carver, J.A., Pankhurst, G.J. and Wilson, M.R. (2002) Mildly acidic pH activates the extracellular molecular chaperone clusterin. *J Biol Chem.* **277:** 39532-40.

Porat, Y., Mazor, Y., Efrat, S. and Gazit, E. (2004) Inhibition of islet amyloid polypeptide fibril formation: a potential role for heteroaromatic interactions. *Biochemistry.* **43:** 14454-62.

Porat, Y., Abramowitz, A. and Gazit, E. (2006) Inhibition of amyloid fibril formation by polyphenols: structural similarity and aromatic interactions as a common inhibition mechanism. *Chem Biol Drug Des.* **67:** 27-37.

Powell, K. and Zeitlin, P.L. (2002) Therapeutic approaches to repair defects in DF508 CFTR cellular targeting. *Adv Drug Deliv Rev.* **54:** 1395–1408.

Prelli, F., Castano, E., Glenner, G.G. and Frangione, B. (1988). Differences between vascular and plaque core amyloid in Alzheimer's disease. *J. Neurochem.* **51:** 648-51.

Qin, X.R., Abe, H. and Nakanishi, H. (2002) NMR and CD studies on the interaction of Alzheimer β-amyloid peptide (12-28) with β-cyclodextrin. *Biochem Biophys Res Commun.* **297:** 1011-15.

Qin, Z., Hu, D., Han, S., Hong, D.P. and Fink, A.L. (2007) Role of different regions of α-synuclein in the assembly of fibrils. *Biochemistry.* **46:** 13322-30.

Rajan, S., Horn, C. and Abraham, E.C. (2006) Effect of oxidation of αA- and αB-crystallins on their structure, oligomerization and chaperone function. *Mol Cell Biochem.* **288:** 125-34.

Rajaraman, K., Raman, B., Ramakrishna, T. and Rao, C.M. (1998) The chaperone-like α-crystallin forms a complex only with the aggregation-prone molten globule state of α-lactalbumin. *Biochem Biophys Res Commun.* **249:** 917-21.

Rajini, B., Shridas, P., Sundari, C.S., Muralidhar, D., Chandani, S., Thomas, F. and Sharma, Y. (2001) Calcium binding properties of γ-crystallin: calcium ion binds at the Greek key β γ-crystallin fold. *J Biol Chem.* **276:** 38464-71.

Raman, B. and Rao, C.M. (1994) Chaperone-like activity and quaternary structure of α-crystallin. *J Biol Chem.* **269:** 27264-8.

Raman, B., Ramakrishna, T. and Rao, C.M. (1995) Temperature dependent chaperone-like activity of α-crystallin. *FEBS Lett.* **365:** 133-6.

Raman, B., Ban, T., Sakai, M., Pasta, S.Y., Ramakrishna, T., Naiki, H., Goto, Y. and Rao, C.M. (2005) αB-crystallin, a small heat-shock protein, prevents the amyloid fibril growth of an amyloid β-peptide and β2-microglobulin. *Biochem J.* **392:** 573-81.

Reddy, G.B., Das, K.P., Petrash, J.M. and Surewicz, W.K. (2000) Temperature-dependent chaperone activity and structural properties of human αA- and αB-crystallins. *J Biol Chem.* **275:** 4565-70.

Reddy, G.B., Kumar, P.A. and Kumar, M.S. (2006) Chaperone-like activity and hydrophobicity of α-crystallin. *IUBMB Life.* **58:** 632-41.

Rekas, A., Adda, C.G., Aquilina, J.A., Barnham, K.J., Sunde, M., Galatis, D., Williamson, N.A., Masters, C.L., Anders, R.F., Robinson, C.V., Cappai, R. and Carver, J.A. (2004) Interaction of the molecular chaperone αB-crystallin with α-synuclein: effects on amyloid fibril formation and chaperone activity. *J Mol Biol.* **340:** 1167-83.

Renkawek, K., de Jong, W.W., Merck, K.B., Frenken, C.W., van Workum, F.P. and Bosman, G.J. (1992) αB-crystallin is present in reactive glia in Creutzfeldt-Jakob disease. *Acta Neuropathol.* **83:** 324-7.

Renkawek, K., Voorter, C.E., Bosman, G.J., van Workum, F.P. and de Jong, W.W. (1994) Expression of αB-crystallin in Alzheimer's disease. *Acta Neuropathol.* **87:** 155-60.

Rossmann, M.G. and Argos, P. (1981) Protein folding. *Annu Rev Biochem.* **50:** 497-532.

Roy, D. and Spector, A. (1976) Absence of low-molecular-weight α-crystallin in the nuclear region of old human lenses. *Proc Nat Acad Sci USA.* **76:** 3484–7.

Rozema, D. and Gellman, S.H. (1996) Artificial chaperone-assisted refolding of denatured-reduced lysozyme: modulation of the competition between renaturation and aggregation. *Biochemistry.* **35:** 15760-71.

Rozema, D. and Gellman, S.H. (1996) Artificial chaperone-assisted refolding of carbonic anhydrase B. *J Biol Chem.* **27:** 3478-87.

Saha, S. and Das, K.P. (2004) Relationship between chaperone activity and oligomeric size of recombinant human αA- and αB-crystallin: a tryptic digestion study. *Proteins.* **57:** 610-7.

Saha, S. and Das, K.P. (2007) Unfolding and refolding of bovine α-crystallin in urea and its chaperone activity. *Protein J.* **26:** 315-26.

Santhoshkumar, P. and Sharma, K.K. (2001) Phe71 is essential for chaperone-like function in αA-crystallin. *J Biol Chem.* **276:** 47094-9.

Santhoshkumar, P. and Sharma, K.K. (2006) Conserved F84 and P86 residues in αB-crystallin are essential to effectively prevent the aggregation of substrate proteins. *Protein Sci.* **15:** 2488-98.

Sasahara, K., Yagi, H., Sakai, M., Naiki, H. and Goto, Y. (2008) Amyloid nucleation triggered by agitation of β2-microglobulin under acidic and neutral pH conditions. *Biochemistry.* **47:** 2650-60.

Serio, T.R., Cashikar, A.G., Kowal, A.S., Sawicki, G.J., Moslehi, J.J., Serpell, L., Arnsdorf, M.F. and Lindquist, S.L. (2000) Nucleated conformational conversion and the replication of conformational information by a prion determinant. *Science.* **289:** 1317-21.

Serpell, L.C., Sunde, M., Benson, M.D., Tennent, G.A., Pepys, M.B. and Fraser, P.E. (2000) The protofilament substructure of amyloid fibrils. *J. Mol. Biol.* **300:** 1033-39.

Sharma, L. and Sharma, A. (2001) Influence of cyclodextrin ring substituents on folding-related aggregation of bovine carbonic anhydrase. *Eur J Biochem.* **268:** 2456-63.

Sharma, K.K., Kumar, R.S., Kumar, G.S. and Quinn, P.T. (2000) Synthesis and characterization of a peptide identified as a functional element in αA-crystallin. *J Biol Chem.* **275:** 3767-71.

Shechter, Y., Patchornik, A. and Burstein, Y. (1973) Selective reduction of cystine I-VIII in α-lactalbumin of bovine milk. *Biochemistry* **12:** 3407-13

Sheluho, D. and Ackerman, S.H. (2001) An accessible hydrophobic surface is a key element of the molecular chaperone action of Atp11p. *J Biol Chem.* **276:** 39945-9.

Shinohara, H., Inaguma, Y., Goto, S., Inagaki, T., and Kato, K. (1993) αB crystallin and HSP28 are enhanced in the cerebral cortex of patients with Alzheimer's disease. *J. Neurol. Sci.* **119:** 203–8.

Shroff, N.P., Cherian-Shaw, M., Bera, S. and Abraham, E.C. (2000) Mutation of R116C results in highly oligomerized αA-crystallin with modified structure and defective chaperone-like function. *Biochemistry.* **39:** 1420-6.

Simon, S., Michiel, M., Skouri-Panet, F., Lechaire, J.P., Vicart, P. and Tardieu, A. (2007) Residue R120 is essential for the quaternary structure and functional integrity of human αB-crystallin. *Biochemistry.* **46:** 9605-14.

Singh, R. and Rao, Ch.M. (2002) Chaperone-like activity and surface hydrophobicity of 70S ribosome. *FEBS Lett.* **527:** 234-8.

Singh, D., Raman, B., Ramakrishna, T. and Rao, Ch.M. (2006) The cataract-causing mutation G98R in human αA-crystallin leads to folding defects and loss of chaperone activity. *Mol Vis.* **12:** 1372-9.

Sinha, D., Wyatt, M.K., Sarra, R., Jaworski, C., Slingsby, C., Thaung, C., Pannell, L., Robison, W.G., Favor, J., Lyon, M. and Wistow, G. (2001) A temperature-sensitive mutation of Cryγs in the murine Opj cataract. *J Biol Chem.* **276:** 9308–15.

Smith, C. C., Yu, Y.X., Kulka, M. and Aurelian, L. (2000) A novel human gene similar to the protein kinase (PK) coding domain of the large subunit of herpes simplex virus type 2 ribonucleotide reductase (ICP10) codes for a serine-threonine PK and is expressed in melanoma cells. *J. Biol Chem.* **275:** 25690-9.

Smulders, R.H., Merck, K.B., Aendekerk, J., Horwitz, J., Takemoto, L., Slingsby, C., Bloemendal, H. and de Jong, W.W. (1995) The mutation Asp69-->Ser affects the chaperone-like activity of αA-crystallin. *Eur J Biochem.* **232:** 834-8.

Smulders, R.H.P.H., Carver, J.A., Lindner, R.A., van Boekel, M.A.M., Bloemendal, H. and de Jong, W.W. (1996) Immobilization of the C-terminal extension of bovine αA-crystallin reduces chaperone-like activity *J Biol Chem.* **271:** 29060 – 66.

Spector, A., Li, L.K., Augusteyn, R.C., Schneider, A. and Freund, T. (1971) α-Crystallin. The isolation and characterization of distinct macromolecular fractions. *Biochem J.* **124:** 337-43.

Spillantini, M.G., Crowther, R.A., Jakes, R., Hasegawa, M. and Goedert, M. (1998) α-Synuclein in filamentous inclusions of Lewy bodies from Parkinson's disease and dementia with Lewy bodies. *Proc Natl Acad Sci USA.* **95:** 6469-73.

Sreelakshmi, Y., Santhoshkumar, P., Bhattacharyya, J. and Sharma, K. K. (2004) αA-crystallin interacting regions in the small heat shock protein, αB-crystallin. *Biochemistry.* **43:** 15785–95.

Srinivasan, A.N., Nagineni, C.N. and Bhat, S.P. (1992) αA-crystallin is expressed in non-ocular tissues. *J Biol Chem.* **267:** 23337-41.

Stauffer, J., Rothschild, C., Wandel, T. and Spector, A. (1974) Transformation of α-crystallin polypeptide chains with ageing. *Invest. Ophthalmol*. **13:** 135-46.

Stefani, M. and Dobson, C.M. (2003) Protein aggregation and aggregate toxicity: new insights into protein folding, misfolding diseases and biological evolution. *J Mol Med.* **81:** 678-99.

Stevens, A. and Augusteyn, R.C. (1993) Acid-induced dissociation of αA- and αB-crystallin homopolymers. *Biophys J.* **65:** 1648-55.

Stryer, L. (1995) *Biochemistry 4th edition.* W.H. Freeman and Company. USA.

Sun, Y and MacRae, T.H. (2005) Small heat shock proteins: molecular structure and chaperone function. *Cell Mol Life Sci.* **62:** 2460-76.

Sun, T.X., Das, B.K. and Liang, J.J. (1997) Conformational and functional differences between recombinant human lens αA- and αB-crystallin. *J Biol Chem.* **272:** 6220-5.

Sunde, M. and Blake, C. (1997) The structure of amyloid fibrils by electron microscopy and X-ray diffraction. *Adv Protein Chem.* **50:** 123-59.

Sunde, M., Serpell, L.C., Bartlam, M., Fraser, P.E., Pepys, M.B. and Blake, C.C. (1997) Common core structure of amyloid fibrils by synchrotron X-ray diffraction. *J Mol Biol.* **273:** 729-39.

Surewicz, W.K. and Olesen, P.R. (1995) On the thermal stability of α-crystallin: a new insight from infrared spectroscopy. *Biochemistry.* **34:** 9655-60.

Suzuki, A., Sugiyama, Y., Hayashi, Y., Nyu-i, N., Yoshida, M. and Nonaka, I. (1998) MKBP, a novel member of the small heat shock protein family, binds and activates the myotonic dystrophy protein kinase. *J Cell Biol.* **140:** 1113-24.

Swanton, E., High, S. and Woodman, P. (2003) Role of calnexin in the glycan-independent quality control of proteolipid protein. *EMBO J.* **22:** 2948-58.

Szejtli, J. (1998) Introduction and general overview of cyclodextrin chemistry. *Chem. Rev.* **98:** 1743-54.

Szejtli, J (1997) Utilization of cyclodextrins in industrial products and processes. *J Mater Chem.* **7:** 575-87.

Takemoto, L. and Boyle, D. (1994). Molecular properties of the high molecular weight aggregate from aged lens. *Curr Eye Res.* **13:** 35-44.

Takeuchi, N., Ouchida, A. and Kamei, A. (2004) C-terminal truncation of α-crystallin in hereditary cataractous rat lens. *Biol Pharm Bull.* **27:** 308-14.

Taniguchi, S., Suzuki, N., Masuda, M., Hisanaga, S., Iwatsubo, T., Goedert, M. and Hasegawa, M. (2005) Inhibition of heparin-induced tau filament formation by phenothiazines, polyphenols, and porphyrins. *J Biol Chem.* **280:** 7614-23.

Tardieu, A., Laporte, D., Licinio, P., Krop, B. and Delaye, M. (1986) Calf lens α-crystallin quaternary structure. A three-layer tetrahedral model. *J Mol Biol.* **192:** 711-24.

Tavornvipas, S., Tajiri, S., Hirayama, F., Arima, H. and Uekama, K. (2004) Effects of hydrophilic cyclodextrins on aggregation of recombinant human growth hormone. *Pharm Res.* **21:** 2369-76.

Tawfik, D.S. (1996) in Walker, J.M. (ed) *The protein protocols handbook*. Humana Press Inc. U.S.A

Taylor, R.P. and Benjamin, I.J. (2005) Small heat shock proteins: a new classification scheme in mammals. *J Mol Cell Card.* **38:** 433-44.

Thomson, J.A. and Augusteyn, R.C. (1988) On the structure of α-crystallin: the minimum molecular weight. *Curr Eye Res.* **7:** 563-9.

Thomson, J.A. and Augusteyn, R.C. (1989) On the structure of α-crystallin: construction of hybrid molecules and homopolymers. *Biochim Biophys Acta.* **994:** 246-52.

Thurston, G.M., Hayden, D.L., Burrows, P., Clark, J.I., Taret, V.G., Kandel, J., Courogen, M., Peetermans, J.A., Bowen, M.S., Miller, D.A., Sullivan, K.M., Storb, R., Stern, H. and Benedek, G.B., (1997). Quasi-elastic light scattering study of the living human lens as a function of age. *Curr. Eye. Res.* **16:** 197–207.

Tofaris, G.K. and Spillantini, M.G. (2005) α-Synuclein dysfunction in Lewy body diseases. *Mov Disord Suppl.* **12:** S37-44.

Tofaris, G.K. and Spillantini, M.G. (2007) Physiological and pathological properties of α-synuclein. *Cell Mol Life Sci.* **64:** 2194-201.

Treweek, T.M., Lindner, R.A., Mariani, M. and Carver, J.A. (2000) The small heat-shock chaperone protein, α-crystallin, does not recognize stable molten globule states of cytosolic proteins. *Biochim Biophys Acta.* **1481:** 175-88.

Treweek, T.M., Morris, A.M. and Carver, J.A (2003) Intracellular protein unfolding and aggregation: the role of small heat-shock chaperone proteins. *Aust J Chem.* **56:** 357-67.

Truscott, R.J. (2005) Age-related nuclear cataract-oxidation is the key. *Exp Eye Res.* **80:** 709-25.

van Boekel, M.A., Hoogakker, S.E., Harding, J.J. and de Jong, W.W. (1996) The influence of some post-translational modifications on the chaperone-like activity of α-crystallin. *Ophthalmic Res.* **28 Suppl 1:** 32-8.

van de Klundert, F.A., Smulders, R.H., Gijsen, M.L., Lindner, R.A., Jaenicke, R., Carver, J.A. and de Jong, W.W. (1998) The mammalian small heat-shock protein Hsp20 forms dimers and is a poor chaperone. *Eur J Biochem.* **258:** 1014-21.

van den Oetelaar, P.J., van Someren, P.F., Thomson, J.A., Siezen, R.J. and Hoenders, H.J. (1990) A dynamic quaternary structure of bovine α-crystallin as indicated from intermolecular exchange of subunits. *Biochemistry.* **29:** 3488-93.

van Montfort, R.L., Basha, E., Friedrich, K.L., Slingsby, C. and Vierling, E. (2001) Crystal structure and assembly of a eukaryotic small heat shock protein. *Nat Struct Biol.* **8:** 1025-30.

van Rijk, A.F. and Bloemendal, H. (2000) αB-crystallin in neuropathology. *Ophthalmologica.* **214:** 7-12.

Vanhoudt, J., Abgar, S., Aerts, T. and Clauwaert, J. (2000) Native quaternary structure of bovine α-crystallin. *Biochemistry.* **39:** 4483-92.

Velasco, P.T., Lukas, T.J., Murthy, S.N., Duglas-Tabor, Y., Garland, D.L. and Lorand, L. (1997) Hierarchy of lens proteins requiring protection against heat-induced precipitation by the α-crystallin chaperone. *Exp Eye Res.* **65:** 497-505.

Vicart, P., Caron, A., Guicheney, P., Li, Z., Prévost, M.C., Faure, A., Chateau, D., Chapon, F., Tomé, F., Dupret, J.M., Paulin, D. and Fardeau, M. (1998) A missense mutation in the αB-crystallin chaperone gene causes a desmin-related myopathy. *Nat Genet.* **20:** 92-5.

Wang, K., Ma, W. and Spector, A. (1995) Phosphorylation of α-crystallin in rat lenses is stimulated by H_2O_2 but phosphorylation has no effect on chaperone activity. *Exp Eye Res*. **61:** 115-24.

Wang, K. and Spector, A. (2000) α-Crystallin prevents irreversible protein denaturation and acts cooperatively with other heat-shock proteins to renature the stabilized partially denatured protein in an ATP-dependent manner. *Eur J Biochem.* **267:** 4705–12.

Wang, X., Garcia, C.M., Shui, Y.B. and Beebe, D.C. (2004) Expression and regulation of α-, β-, and γ-crystallins in mammalian lens epithelial cells. *Invest Ophthalmol Vis Sci.* **45:** 3608–19.

Weinreb, P.H., Zhen, W., Poon, A.W., Conway, K.A. and Lansbury, P.T. Jr. (1996) NACP, a protein implicated in Alzheimer's disease and learning, is natively unfolded. *Biochemistry.* **35:** 13709-15.

Welch, W.J. (2003) Role of quality control pathways in human diseases involving protein misfolding. *Semin Cell Dev Biol.* **15:** 31–8.

Wilhelmus, M.M., Boelens, W.C., Otte-Höller, I., Kamps, B., de Waal, R.M. and Verbeek, M.M. (2006) Small heat shock proteins inhibit amyloid-β protein aggregation and cerebrovascular amyloid-β protein toxicity. *Brain Res.* **1089:** 67-78.

Wistow, G. (1993) Possible tetramer-based quaternary structure for α-crystallins and small heat shock proteins. *Exp Eye Res.* **56:** 729-32.

Xia, C.H., Liu, H., Chang, B., Cheng, C., Cheung, D., Wang, M., Huang, Q., Horwitz, J. and Gong, X. (2006) Arginine 54 and Tyrosine 118 residues of αA-crystallin are crucial for lens formation and transparency. *Invest Ophthalmol Vis Sci.* **47:** 3004-10.

Yang, Z., Chamorro, M., Smith, D.L. and Smith, J.B. (1994) Identification of the major components of the high molecular weight crystallins from old human lens, *Curr Eye Res.* **13:** 415-21.

Yates, C.M., Butterworth, J., Tennant, M.C. and Gordon, A. (1990) Enzyme activities in relation to pH and lactate in postmortem brain in Alzheimer-type and other dementias. *J Neurochem.* **55:** 1624-30.

Yazdanparast, R., Khodarahmi, R. and Soori, E. (2005) Comparative studies of the artificial chaperone-assisted refolding of thermally denatured bovine carbonic anhydrase using different capturing ionic detergents and β-cyclodextrin. *Arch Biochem Biophys.* **437:** 178-85.

Young, J.C., Agashe, V.R., Siegers, K., and Hartl, F.U. (2004) Pathways of chaperone-mediated protein folding in the cytosol. *Nat Rev Mol Cell Biol.* **5:** 781–91.

Zahler, W.L. and Cleland, W.W. (1968) A specific and sensitive assay for disulfides.
J Biol Chem. **243:** 716-9

Zanuy, D., Porat, Y., Gazit, E. and Nussinov, R. (2004) Peptide sequence and amyloid formation; molecular simulations and experimental study of a human islet amyloid polypeptide fragment and its analogs. *Structure.* **12:** 439-55.